

ANISOTROPIC CONTINUUM THEORY OF LATTICE DEFECTS†

D. J. Bacon

Department of Metallurgy and Material Science,
University of Liverpool, Liverpool L69 3BX, England

D. M. Barnett

Department of Materials Science and Engineering,
Stanford University, Stanford, CA 94305, USA

and

R. O. Scattergood

Materials Science Division, Argonne National Laboratory,
Argonne, IL 60439, USA

(Submitted 24 May, 1978)

CONTENTS

LIST OF SYMBOLS	52
1. INTRODUCTION	53
1.1. <i>Aims of the Article</i>	53
1.2. <i>Survey of Methods Used Before 1967</i>	54
1.3. <i>Survey of Topics</i>	56
2. REVIEW OF ELASTICITY THEORY	58
2.1. <i>Notation and Other Relations</i>	59
2.2. <i>Basic Concepts</i>	62
2.2.1. <i>Stress and the equilibrium conditions</i>	63
2.2.2. <i>Strain</i>	65
2.2.3. <i>Work and energy</i>	66
2.3. <i>Hooke's Law and the Elastic Constants</i>	69
2.3.1. <i>General relations</i>	69
2.3.2. <i>Cubic symmetry and isotropy</i>	75
2.4. <i>The Green's Function Method</i>	77
2.4.1. <i>Solution of basic field equations</i>	78
2.4.2. <i>Integral solutions for the Green's function and its derivatives</i>	81
2.5. <i>Green's Function Representation for Dislocation Fields</i>	85
2.5.1. <i>General curvilinear dislocation fields—Volterra and Mura formulae</i>	86
2.5.2. <i>Infinite straight dislocation fields</i>	91
2.6. <i>Energies of and Forces on Dislocations</i>	94
2.6.1. <i>Energies</i>	94
2.6.2. <i>Forces</i>	100
2.7. <i>Green's Function Representation for Point Force Arrays</i>	106
2.7.1. <i>Multipole expansion formula and infinitesimal dipoles</i>	107
2.7.2. <i>Interaction energy</i>	111
2.7.3. <i>Continuous distributions of forces</i>	113
2.8. <i>Summary of Formulae</i>	116

† Work supported in part by the U.S. Department of Energy.

*3. THE FORMALISM FOR TWO-DIMENSIONAL (PLANE) ELASTIC PROBLEMS	118
3.1. <i>Statement of the Problem</i>	118
3.2. <i>The Sextic Formalism of Stroh</i>	119
3.3. <i>The Extended Sextic Formalism of Stroh</i>	122
3.4. <i>Orthogonality and Completeness Relations for the Stroh Eigenvectors</i>	123
3.5. <i>Invariance Relations for the Stroh Eigenvectors</i>	126
3.6. <i>The Integral Formalism</i>	131
3.7. <i>Uniform Motion (Dynamic) Problems</i>	135
4. DISLOCATIONS	138
4.1. <i>Infinite Straight Dislocations in Homogeneous Media</i>	138
*4.1.1. <i>Elastic fields of straight dislocations and lines of force</i>	141
4.1.1.1. The Stroh displacement field solution	141
4.1.1.2. The displacement gradients in the sextic and integral formalisms	143
4.1.1.3. The dislocation stress field and angular stress factors	144
4.1.1.4. The integral representation for the dislocation displacement field	146
4.1.1.5. The dislocation strain energy factor	146
4.1.1.6. Angular derivatives of the dislocation energy factor	148
4.1.1.7. Angular derivatives of the straight dislocation in-plane stress factors	151
4.1.1.8. Straight dislocations in uniform motion	152
4.1.2. <i>Summary of formulae for infinite straight dislocations</i>	154
4.1.2.1. General formulae	154
4.1.2.2. The elastic fields of infinite straight dislocations in the integral and sextic formalisms	155
4.1.3. <i>Field data for infinite straight dislocations</i>	158
4.2. <i>Dislocations of Arbitrary Shape in Homogeneous Infinite Media</i>	175
4.2.1. <i>Background to the Brown–Lothe–Indenbom–Orlov geometrical theorems</i>	175
4.2.2. <i>Brown's theorem for two dimensions</i>	177
4.2.3. <i>Extension to finite dislocation segments</i>	182
4.2.4. <i>Considerations in applying the two-dimensional formulae</i>	186
*4.2.5. <i>The Indenbom–Orlov formula for three-dimensions</i>	190
4.3. <i>Applications to Problems of Dislocations in Infinite, Homogeneous Media</i>	193
4.3.1. <i>Elastic energy of a rhombus shaped loop</i>	194
4.3.2. <i>Interactions between dislocations and either dislocations or other defects</i>	197
4.3.3. <i>Orowan mechanism in anisotropic crystals</i>	208
4.3.4. <i>Dislocation shear loops in anisotropic crystals</i>	213
4.3.5. <i>Stacking fault nodes in anisotropic crystals</i>	216
4.3.6. <i>Other problems</i>	219
4.4. <i>Straight Dislocations in Inhomogeneous Media</i>	221
4.4.1. <i>The straight dislocation parallel to a planar free surface</i>	222
4.4.2. <i>The interfacial dislocation</i>	223
4.4.3. <i>The image force theorem</i>	224
4.4.4. <i>The straight dislocation emergent at a planar free surface</i>	225
5. OTHER DEFECTS	227
5.1. <i>Point Defects</i>	227
5.2. <i>Inclusions</i>	234
5.3. <i>Fracture Mechanics</i>	243
5.4. <i>Line Force Solutions in Infinite Media</i>	247
5.5. <i>Two- and Three-Dimensional Surface Green's Functions</i>	250
APPENDIX: "A RECENT DEVELOPMENT IN THE THEORY OF THE SELF-FORCE ON A PLANE DISLOCATION LOOP"	252
ACKNOWLEDGEMENTS	259
REFERENCES	259

LIST OF IMPORTANT SYMBOLS

Symbol	Meaning
b	Burgers vector
C_{ijkl}	elastic stiffness

E	prelogarithmic factor in δ'
δ'	strain energy or interaction energy
ϵ'	strain energy per unit length of an infinite straight dislocation
e_{ij}	strain field
G_{ij}	Green's tensor for an infinite homogeneous body
n	unit normal to a plane
r_0	dislocation core radius
σ, τ	resolved shear stress
τ^L	self stress of a dislocation
t	unit tangent to a curve
σ_{ij}	stress field
Σ_{ij}	angular stress factor (orientation dependent part of infinite straight dislocation stress field)
u_i	displacement field
v	Poisson's ratio for an isotropic continuum
μ	shear modulus for an isotropic continuum

1. INTRODUCTION

1.1. Aims of the Article

The elastic fields of defects such as dislocations, inclusions and point defects can play an important part in determining the physical properties of crystalline materials. This article is concerned with the form of these fields and the ways in which they may be calculated. The continuum theory of crystal defects in the approximation of isotropic elasticity is well-established and has been extensively applied to the modelling of physical phenomena in crystals. Most crystals exhibit elastic anisotropy, however, and although the effects of anisotropy can be important, the complexity it can add to the theory has prevented the effects from being widely studied. Fortunately, significant advances have been made in this area in recent years and this provides the justification for presenting a review of the anisotropic continuum theory of crystal defects at the present time. The progress made has not had the effect of making the subject more complicated, but rather the reverse. We hope to demonstrate that the effort which has to be made to apply anisotropic elasticity theory to crystal defects, has been reduced to such an extent that the application is now no more difficult, in many cases, than that required for isotropic elasticity. Furthermore, as a result of studies already reported, we are now in a position to assess the effects of anisotropy in a number of areas.

The advances referred to have come about in two ways. Firstly, it has been shown that the elastic fields of dislocations of arbitrary shape can be constructed from the fields of infinite, straight dislocation lines. The significance of this lies in the fact that, once the field data for the infinite straight line have been computed, they can be applied to the more general problem in a very straightforward manner. Secondly, the recasting into a form more suitable for numerical evaluation of the equations for the fields of the infinite straight line and the widespread availability of fast digital computers means that the source data can be obtained fairly easily.

Although most of this article will be concerned with dislocations, we shall show that advances have also been achieved in the application of anisotropic elasticity theory to other crystal defects, for their fields can also be expressed in a form open to direct numerical evaluation.

A survey of the topics covered here is presented in Section 1.3, but in order to put the theory to be described into perspective, we first present a brief survey of the methods used up to about 1966, after which year the advances referred to above were made.

1.2. Survey of Methods Used Before 1967

The continuum theory discussed here is the linear elasticity theory, in which stress and strain components are proportional to one another. The relation between the two quantities is known as Hooke's law and it contains only two material constants for isotropic materials. Most materials are anisotropic to a certain extent and this increases the number of elastic constants required in Hooke's law. The number depends on the crystal symmetry of the material in question and is three for cubic media, five for hexagonal systems and so on. The complexity introduced by the inclusion of anisotropy precludes analytic solutions being obtained for many problems in anisotropic elasticity theory. Accordingly, resort has to be made to numerical methods or the approximation of isotropic elasticity (with suitably chosen elastic constants) has to be used. In the case of dislocation theory, the elastic field of an arbitrary dislocation is known from the work of Volterra⁽¹⁾ to be expressible as the integral over a surface bounded by the dislocation of the derivative of a function known as the Green's function of elasticity. This function, which represents the displacement due to a point force, can in general only be expressed in an analytic (as opposed to integral) form for the case of isotropic or hexagonal (transverse isotropic) media. Thus, until recently, most applications of the theory using the Green's elastic function have employed the isotropic approximation (for reviews see de Wit⁽²⁾, Mura⁽³⁾). The fields of other crystal defects can also be expressed in terms of the Green's function, but again isotropic theory was predominant in earlier studies. The Green's function method is at the centre of the approach to be used here.

Methods which do not use Green's functions for deriving the elastic fields associated with crystal defects, are available. They involve solving the equilibrium equations of elasticity subject to boundary conditions appropriate to the defect in question. The methods usually restrict the problems to those exhibiting a high degree of symmetry, and the use of stress function techniques for such problems in isotropic elasticity has been widespread. A class of problems which can be treated in anisotropic theory are particularly relevant to situations involving straight dislocations or cracks. They occur when the displacement and stress fields are invariant in one direction and this general form of plane strain can be treated using complex-variable methods.

The latter approach was first used for infinite, straight edge dislocations in anisotropic materials by Eshelby^(1,2) and for mixed dislocations by Eshelby *et al.*⁽⁴⁾; an alternative form was introduced by Stroh.⁽⁵⁾ The majority of the dislocation problems in anisotropic elasticity theory solved up to 1967 employed this method. A review to that time has been given by Hirth and Lothe,⁽⁶⁾ and a more recent comprehensive description of the method and its variants applied to numerous dislocation systems has been given by Steeds.⁽⁷⁾ In simple terms, the method of Eshelby *et al.* involves the following steps: (a) the crystal elastic constants are referred to a set of rectangular Cartesian axes parallel and normal to the dislocation line, (b) the roots of a sixth-order (sextic) polynomial involving these elastic constants are determined and (c) the roots and the Burgers vector components are used to determine the spatial-independent coefficients in the elastic displacement or stress field. The roots of the sextic can only be found analytically for special cases of symmetry—for example, when the dislocation is normal to a diad axis of the crystal—and numerical solution is generally required. Although this is not necessarily a disadvantage, the fact that it cannot be done simply has undoubtedly prevented many workers from incorporating anisotropic effects into their theories. Another difficulty arises from the fact that the transition from anisotropy to isotropy cannot be achieved easily, for the roots of the sextic polynomial are degenerate in the latter case. Thus, cases of isotropy and special symmetry, where root degeneracy occur, have to be treated differently from the general case and this can be computationally inconvenient. A more fundamental drawback of the method is that it only applies to straight dislocations of infinite length. This is clearly a gross simplification of most real situations and the errors introduced by its use can more than nullify the accuracy achieved by using anisotropy.

The methods to be described here for treating dislocations meet these criticisms. First and foremost, it is possible to construct the field of a dislocation of arbitrary shape from the corresponding field, and its angular derivatives, of an infinite straight dislocation. This result holds for arbitrary anisotropy. Thus, the problem is essentially reduced to obtaining the straight-line field data. Although this can be done by using more recent versions of the sextic formalism described above, we shall show that it is more efficient and straightforward to use a method producing solutions in the form of integrals, which are simple to evaluate numerically. In fact, this integral formalism has already been used to compute the source data for a number of cases and the values have been compiled in a form which is convenient to use. The incorporation of anisotropy into many dislocation problems, therefore, involves no more than a very simple calculation. The integral method for evaluating the derivatives of the Green's function is also directly applicable to other crystal defects. It provides, therefore, a unified approach to many defect problems.

1.3. Survey of Topics

In order to make the article self-contained, Chap. 2 contains a review of the basic relations which will be necessary for an understanding of the sections which follow. A summary of the notation to be used and an outline of the theory of linear, anisotropic elasticity is included. There follows a description of the Green's function of linear elasticity and a derivation of the integral form, from which it can be readily evaluated. Equations for the elastic fields of dislocations and point force arrays in terms of the Green's function are also derived. The concept of the force on a dislocation is also discussed in detail and a new derivation of the self force on a dislocation is given in the Appendix.

Chapter 3 contains an important theoretical part of the article, for it describes two ways of treating two-dimensional problems in anisotropic theory. These are the sextic and integral formalisms referred to above. The two approaches are intimately related and the elegant analysis of Lothe and co-workers, which enables the functions of the integral formalism to be related to the eigenvectors of the sextic formalism of Stroh^(5,8), are described. Extension of the theory to cases of uniform motion is also discussed.[†]

Dislocations are dealt with in Chap. 4. In the first section, the application of the theory of Chap. 3 to the straight dislocation of infinite length is considered. The equations for the displacement, strain and stress fields, and the energy factor are derived in terms of the integrals of Chap. 3. Expressions for the angular derivatives of these field quantities are also presented. Data for several dislocation systems in most of the common metals have already been computed and tables giving this data in simple form are described. The second part of the chapter treats dislocations of arbitrary shape in infinite, homogeneous media. The formulae due to Brown⁽⁹⁾ and Indenbom and Orlov,⁽¹⁰⁾ which express the field of a dislocation in terms of a line integral of the corresponding field and its angular derivative for infinite, straight lines, are derived. It is shown that the line integrals in Brown's theorem for two dimensions can be partially integrated for straight dislocation segments, and the resulting formulae assume a very simple form. The field of any dislocation configuration which consists of, or can be described by, straight segments, can, therefore, be obtained in a convenient manner. A similar result holds for three dimensions. The application of the formulae to some two-dimensional dislocation problems of a fairly complicated nature are described in Section 4.3. Other problems which have been treated by direct evaluation of the Green's function equations, as opposed to Brown's formula and its variants, are also reviewed. These applications enable an assessment of the effects of elastic anisotropy on a range of dislocation processes to be made. The

[†]*Note added in proof.* A recent review by Chadwick and Smith⁽¹⁷⁵⁾ deals with surface waves (and their relation to dislocations) in anisotropic materials in a more comprehensive way than the treatment given here.

bulk of the article is concerned with homogeneous media of infinite extent, but Chap. 4 closes with a review of the theory of straight dislocations in inhomogeneous media. We restrict attention to situations involving planar interfaces and show that many problems can be solved in terms of the field factors for straight dislocations in homogeneous media.

The infinite straight dislocation field data compiled in this chapter are sufficient to treat a rather wide range of two-dimensional (and some three-dimensional) problems. Although we do not recommend the use of strict "handbook" prescriptions, Section 4.1.3. is sufficiently self-contained that the reader who wishes to omit any theoretical discussion may refer directly to it to use the field data compiled in Table 4.3. This data gives the components of the traction vector acting in the glide plane of infinite straight dislocations in various slip systems in both cubic and hexagonal metals. This data by itself is useful for a number of dislocation problems, among which are included those problems that can be treated by anisotropic line-tension analysis; the traction data easily give values of the line tension $E + E''$ as functions of the Burgers vector orientation. The definition of angular stress factors and the sign convention discussed in Section 4.1.1.3 should be understood before using the tables. When planar, curvilinear dislocation field quantities are required, the data in Table 4.3. may be used in conjunction with Brown's geometric theorem (discussed in Section 4.2.2) to construct the fields. Infinitesimal segment expressions embodied in eqs. (4.2.19) and (4.2.24) can be used for this purpose, paying careful attention to the sign convention discussed at the end of the section. If a polygonal approximation to the curvilinear shape is sufficient, the finite straight segment formulae derived in Section 4.2.3 may be used; for example, eqs. (4.2.27) and (4.2.29) give the segment fields in terms of simple geometric constructions of the infinite straight dislocation fields. Section 4.2.4 explains how these segment formulae may be applied to certain three-dimensional problems as well. Finally, if the self force on a curvilinear, planar dislocation is required, for example, to compute the equilibrium configurations, the analysis discussed in Section 2.6.2 may be combined with the curvilinear field evaluation methods to obtain the proper self force or self stress acting on the dislocation. A specific application of this type is discussed in Section 4.3.3.

Chapter 5 contains applications of anisotropic elasticity theory to other crystal defects. These include point defects and inclusions, the latter being described by the now standard "transformation strain" technique of Eshelby.^(11,12) In other sections, we consider simple problems in fracture mechanics and the anisotropic solutions for lines of force in infinite media and point force loadings on surfaces. This chapter will again demonstrate how the Green's function method and the integral formalism can provide a direct solution to many problems.

We have concentrated on the Green's function and integral formalisms and have, thereby, attempted to present a unified and systematic approach

to the anisotropic elasticity theory of crystal defects. The papers reviewed here, therefore, fit into this framework and it has not been possible to describe all the recent papers concerned with anisotropy, particularly where the Eshelby *et al.* or Stroh methods have been used to study only straight dislocations. The article has been made comprehensive by including all the theory necessary for the derivation of the relevant equations and formulae. We recognize, however, that these detailed aspects may not be of interest to those who merely wish to apply the final equations or data. Sections which can be omitted on a first reading have therefore been indicated by an asterisk, thus *; these include all the sections of Chap. 3 and part of Section 4.1. The important and useful equations of these starred sections are summarized in special subsections which follow them.

2. REVIEW OF ELASTICITY THEORY

In this chapter we shall introduce much of the notation to be used throughout this article. We shall also briefly review the fundamentals of the linear theory of elasticity as it applies to anisotropic media. The Green's function method for the solution of the basic field equations will be introduced and we shall give representations of the elastic field of a general curvilinear dislocation in terms of the Green's tensor. The latter will serve as a useful starting point for the derivation of the Brown and Indenbom-Orlov theorems discussed in Chap. 4. We will also discuss here the energy of a dislocation and we treat, in some detail, the important concept of the force on a dislocation. Finally, we shall develop a Green's function representation for the elastic field due to an array of point forces since this is often a useful starting point for the development of continuum models for point defects. To complete the theoretical development we give a set of line integral solutions for the Green's tensor and its derivatives. These solutions are convenient for numerical evaluation purposes, because in the general anisotropic case an analytical solution for the Green's tensor cannot be found. In Chap. 4 and 5, we shall elaborate upon the straight dislocation field quantities and then review the results for dislocations, point defects, etc., which have been reported in the literature. It must be emphasized again that Chap. 3 contains an in-depth development of an alternative formalism from which the infinite straight dislocation field quantities may be obtained and in many respects that formalism gives a new and different insight into the nature of these quantities. For completeness, we give in this chapter a brief discussion of the straight dislocation field quantities as they are derived from the Green's function representation and some of these results are equivalent to those obtained in Chap. 3 and 4. Finally, we must point out that many of the results obtained in this and in subsequent chapters are expressed as integrals (integral formalism) and as such they are computationally convenient, because they

pass smoothly to the isotropic limit and they do not require a transformation to a local coordinate basis (e.g. dislocation coordinates).

2.1. Notation and Other Relations

All quantities are referred to a rectangular Cartesian frame of reference where \mathbf{x} denotes a general position vector. The reader is assumed to be familiar with the concept of tensors in Cartesian reference frames.^(13,14) The components of tensor quantities are indexed by subscripts, e.g. \mathbf{x} : (x_1, x_2, x_3) . A tensor field is a tensor quantity all of whose components are functions of position over all points of the domain in question.

Unless stated otherwise, we always use the summation convention: a repeated subscript, e.g. j , in any term implies summation with respect to that subscript over its range, e.g. $j = 1, 2, 3$. In addition, we use the indicial comma notation to indicate partial differentiation with respect to position: differentiation with respect to x_j is indicated by the subscript notation “ j ”. To illustrate,

$$A_{jn}B_n = A_{jk}B_k = \sum_{i=1}^3 A_{ji}B_i$$

and

$$\frac{\partial^2 A_{jk}}{\partial x_n \partial x_m} = A_{jk,mn}.$$

In some cases, partial differentiation will be written out in full, but frequent use of the comma notation to aid the writing of compact equations should cause no confusion.

We shall make use of the Kronecker delta tensor δ_{ij} and the epsilon, or permutation tensor ϵ_{ijk} . These are defined as

$$\delta_{ij} = 1 \text{ if } i = j \quad (2.1.1)$$

$$= 0 \text{ otherwise,}$$

$$\epsilon_{ijk} = 1 \text{ if } ijk \text{ is an even permutation of } 123 \quad (2.1.2)$$

$$\begin{aligned} &= -1 \text{ if } ijk \text{ is an odd permutation of } 123 \\ &= 0 \text{ otherwise.} \end{aligned}$$

These two tensors are connected by the identity

$$\epsilon_{ijk} \epsilon_{imn} = \delta_{jm} \delta_{kn} - \delta_{jn} \delta_{km}. \quad (2.1.3)$$

The tensor ϵ_{ijk} provides a convenient representation of the vector cross-product: if \mathbf{A} , \mathbf{B} and \mathbf{C} are vectors such that $\mathbf{C} = \mathbf{A} \wedge \mathbf{B}$, then $C_i = \epsilon_{ijk} A_j B_k$, or if $\mathbf{C} = \nabla \wedge \mathbf{A} = \text{curl}(\mathbf{A})$, then $C_i = \epsilon_{ijk} A_{k,j}$.

We invoke Gauss' theorem (also called the divergence theorem) and Stokes' theorem at various places throughout the text. These theorems allow volume integrals to be transformed into surface integrals (Gauss) and surface integrals into line integrals (Stokes). The theorems may be stated as follows:

$$\iiint_V A_{...i} dV = \oint_S A_{...} dS_i \quad (\text{Gauss}), \quad (2.1.4)$$

$$\iint_{S_0} \epsilon_{ijk} A_{...,j} dS_i = \oint_L A_{...} dx_k \quad (\text{Stokes}). \quad (2.1.5)$$

With the aid of eq. (2.1.3) Stokes' theorem can also be written

$$\iint_{S_0} (A_{...,k} dS_j - A_{...,j} dS_k) = \oint_L \epsilon_{ijk} A_{...} dx_i. \quad (2.1.6)$$

The quantity $A_{...}$ in the previous equations denotes a tensor field of any rank. In eq. (2.1.4) the volume V is bounded by the closed surface S , where n_i is the outward unit normal from V on S , dS is the area element and we define $dS_i = n_i dS$. In eqs (2.1.5) and (2.1.6) S_0 is any smooth orientable surface with unit normal n_i bounded by the closed curve L , where t_k is the unit tangent along L , ds is the arc length and $dx_k = t_k ds$. To orient S_0 , we assign a positive sense to the boundary curve L and then take the positive sense for n_i to be that of a right-handed screw advancing with respect to a positive traverse around L (right-hand rule). In applying these theorems, we assume that $A_{...}$ and all its required derivatives are continuous and single-valued everywhere within the integration domains. In eq. (2.1.4) V may be multiply-connected and S may include "cuts" or other barrier surfaces on which $A_{...}$ would otherwise be multivalued. We emphasize these restrictions on the integral theorems because, as will be seen later, care must be exercised when applying them to dislocation field quantities. Note that we use small circles through the integral signs to denote integration over closed domains; the absence of the circles denotes an open domain.

The generalized function $\delta = \delta(x)$ ^(15,16) known as the "delta function" (to be distinguished from the Kronecker delta tensor δ_{ij} and the notation δA used to indicate a vanishingly small variation in the quantity A), will be used in various mathematical manipulations throughout the text, particularly in this chapter. For scalar arguments, the delta function has the property that

$$\begin{aligned} \int_a^b \delta(x - x') h(x) dx &= h(x') \quad \text{if } a \leq x' \leq b \\ &= 0 \text{ otherwise,} \end{aligned} \quad (2.1.7)$$

where $h(\mathbf{x})$ is any arbitrary function with suitable properties, viz. continuous derivatives of all orders. With rectangular Cartesian reference frames, we may define a delta function for vector arguments as

$$\delta(\mathbf{x} - \mathbf{x}') = \delta(x_1 - x'_1) \delta(x_2 - x'_2) \delta(x_3 - x'_3) \quad (2.1.8)$$

and we therefore have

$$\iiint_V \delta(\mathbf{x} - \mathbf{x}') H(\mathbf{x}) dV = H(\mathbf{x}') \quad \text{if } \mathbf{x}' \text{ is in } V, \quad (2.1.9)$$

$$= 0 \text{ otherwise.}$$

where $H(\mathbf{x})$ is a suitable arbitrary function and the integration is to be carried out with respect to \mathbf{x} . The N -th derivative of the delta function is defined by the rule

$$\int_a^b \delta^{(N)}(x - x') h(x) dx = (-1)^N \int_a^b \delta(x - x') h^{(N)}(x) dx, \quad (2.1.10)$$

where the superscript N denotes the N -th derivative with respect to the argument; in other words, for differentiation of δ , the operation is interchanged with the test function in the manner indicated. Table 2.1 lists various useful properties of the delta function which can be derived from its definition. Note that the prime on δ denotes the first derivative with respect to the argument and the superscript N denotes the N -th derivative. Relations (1) through (4) give various representations of the delta function and these are often useful in deriving its properties. Relation (10) means that $\delta(\mathbf{x})$ can be viewed as a (positively) homogeneous function of degree -1 . It follows from eq. (2.1.8) that $\delta(\mathbf{x})$ can be viewed as homogeneous of degree -3 . A rigorous discussion of the delta function as a generalized function may be found in Gel'fand and Shilov.⁽¹⁶⁾ These authors also give many properties appropriate to the delta function as well as certain useful relations involving δ in domains of higher dimension. de Wit⁽¹⁷⁾ gives in an appendix a discussion of delta functions defined on surfaces and curves, as well as other relations.

In many applications dealing with physical problems, the delta function is used to provide a formal description of singular density functions, e.g. $f_j \delta(\mathbf{x} - \mathbf{x}')$ describes the \mathbf{x} dependence of a force density comprised of the single point force f_j applied at the fixed point \mathbf{x}' . The Green's function method discussed later in this chapter is based on such singular density functions.

Finally, we introduce a notation which will be used extensively here and in later chapters. Let A_i and B_m be certain unit vectors which depend on the particular problem at hand. We define the second-rank tensor AB

Table 2.1. Various relations involving the δ -function $\delta(x)$; in these formulae, x represents a scalar variable, while a is a constant; a' indicates the first derivative with respect to the argument, while the superscript N denotes the N^{th} derivative

1.	$\delta(x) = \lim_{A \rightarrow \infty} \frac{\sin(Ax)}{\pi x}$
2.	$\delta(x) = \frac{1}{2\pi} \int_{-\infty}^{\infty} e^{ikx} dk$
3.	$\delta(x) = \lim_{\epsilon \rightarrow 0} \frac{1}{\sqrt{\pi\epsilon}} e^{-x^2/\epsilon}$
4.	$\delta(x) = \lim_{\epsilon \rightarrow 0} \frac{e^{x/\epsilon}}{\epsilon(1 + e^{x/\epsilon})^2}$
5.	$\delta(x) = dH/dx, \text{ where } H(x) = 0 \text{ if } x < 0 \\ = 1 \text{ if } x > 0$
6.	$\delta(x - a) = \delta(a - x)$
7.	$\delta(x) = \delta(-x)$
8.	$\delta'(x) = -\delta'(-x)$
9.	$x\delta'(x) = -\delta(x)$
10.	$\delta(ax) = \delta(x)/ a $
11.	$\delta^{(N)}(ax) = \frac{\delta^{(N)}(x)}{ a ^{N+1}}$
12.	$\int_{-\infty}^{\infty} \delta(a - x) dx = 1$

by the contraction operation

$$(AB)_{jk} = A_i C_{ijkm} B_m, \quad (2.1.11)$$

where C_{ijkm} is the elastic stiffness tensor discussed in Section 2.3.

2.2. Basic Concepts

In this section, we give a brief review of the fundamentals of the continuum theory of elasticity as it applies to anisotropic bodies. The reader is referred to one of the many texts on the theory of elasticity for a more comprehensive account of the subject matter.^(14,13,18) Eshelby⁽¹⁹⁾ and de Wit⁽²⁾ give excellent reviews of the basic elements, especially as they apply to bodies containing defects. Fung⁽¹⁴⁾ gives a readable and quite comprehensive account of the fundamentals. Unless stated to the contrary, we shall always assume the body under consideration to be homogeneous and the material within the body to be characterized as a mathematical continuum of points.

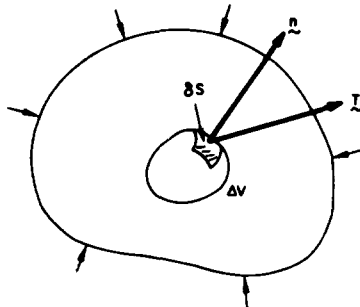


FIG. 2.1. Schematic diagram illustrating the definition of the traction vector T . The traction acts through the area element δS of ΔV where n is the surface unit normal to ΔV . The body itself is subjected to arbitrary loads (arrows).

2.2.1. Stress and the equilibrium conditions

The notion of stress is a fundamental concept in the theory of elasticity. If we apply forces to the surface of a body, these forces will be transmitted through it by the mutual interaction of its constituent parts. Imagine a small region ΔV in a body acted upon by some set of forces, as shown in Fig. 2.1, and let n be the unit normal to the surface enclosing ΔV such that the positive direction of n is from the inside to the outside of ΔV . On any vanishingly small element δS of this enclosing surface the material lying on the positive side (as determined by the positive direction of n) exerts a force per unit area T on the material lying on the negative side. In other words, T represents the action of the material outside of ΔV on the material inside. We call T the traction vector or simply the traction. By definition, the stress tensor σ_{ij} is a tensor field, which connects T to n at any point within the body, and we may write that

$$T_j = \sigma_{ij}n_i. \quad (2.2.1)$$

The stress σ_{ij} for $i = j$ (normal stress) gives the force component along the positive x_j axis acting through the area element having its normal along the same direction; the stresses for $i \neq j$ (shear stresses) give the two orthogonal force components acting in the same area element, with directions along the positive x_i axes, where $i \neq j$. Reversing the sense of the area element normal reverses the sense of the force components for the same signed σ_{ij} . With this sign convention for σ_{ij} , a purely hydrostatic pressure P acting on a body will give rise to the stress state $\sigma_{ij} = -P\delta_{ij}$. For an arbitrary stress state the quantity $\sigma_{kk}/3$ is called the "hydrostatic" part of the stress, for obvious reasons. $\sigma_{ij} - (\sigma_{kk}/3)\delta_{ij}$ is the "deviatoric" part of the stress.

The equations of equilibrium for the theory of elasticity can be derived from Newton's laws of motion applied to arbitrary volume elements of a body. Let ΔV be any volume element within a body subjected to the

stress σ_{ij} and the body force density f_j . The latter can be due to any force whose effect is proportional to the volume over which it acts, e.g. gravity. The total force acting on the material within ΔV is

$$F_j = \iiint_{\Delta V} f_j \, dV + \oint_{\Delta S} \sigma_{ij} \, dS_i, \quad (2.2.2)$$

where ΔS is the enclosing surface of ΔV . Gauss' theorem applied to the surface integral in eq. (2.2.2) gives

$$F_j = \iiint_{\Delta V} (f_j + \sigma_{ij,i}) \, dV. \quad (2.2.3)$$

We assume the body under consideration to be in static equilibrium and, therefore, Newton's laws of motion require $F_j = 0$. Equation (2.2.3) must hold for arbitrary ΔV and, thus, we arrive at the static equilibrium condition

$$f_j + \sigma_{ij,i} = 0. \quad (2.2.4)$$

The net moment with respect to the origin of the forces acting on ΔV is

$$M_j = \iiint_{\Delta V} \epsilon_{jik} x_i f_k \, dV + \oint_{\Delta S} \epsilon_{jik} x_i \sigma_{pk} \, dS_p. \quad (2.2.5)$$

Gauss' theorem applied to the surface integral reduces this to

$$M_j = \iiint_{\Delta V} [\epsilon_{jik} x_i (f_k + \sigma_{pk,p}) + \epsilon_{jpk} \sigma_{pk}] \, dV, \quad (2.2.6)$$

where we use the fact that $x_{i,p} = \delta_{ip}$. The first term in eq. (2.2.6) vanishes, because we assume static equilibrium, eq. (2.2.4). We assume, furthermore, that there are no body-torque densities or couple-stress gradients acting on the body, in which case Newton's laws of motion require $M_j = 0$. Equation (2.2.6) must hold for arbitrary ΔV and we have

$$\epsilon_{jpk} \sigma_{pk} = 0, \quad (2.2.7)$$

but, since the stress field is arbitrary, this is equivalent to

$$\sigma_{pk} = \sigma_{kp}; \quad (2.2.8)$$

hence, the stress tensor must be symmetric.

For simplicity, we have restricted the derivation of eqs (2.2.4) and (2.2.8) to the case of static equilibrium. The arguments follow in a rather similar fashion for the dynamical case,⁽¹⁴⁾ whereupon eq. (2.2.4) becomes

$$f_j + \sigma_{ij,i} = \rho a_j, \quad (2.2.9)$$

with ρ being the mass density and a_j the acceleration field. Equation (2.2.8) continues to hold in the dynamical case as long as body-torque densities and couple-stress gradients are absent. Equation (2.2.4), in conjunction with eq. (2.2.8), represents the basic field equation which must be satisfied for any stress field in a body in a state of static equilibrium; in this review, we generally deal with the static situation.

2.2.2. Strain

In addition to stress, the theory of elasticity is concerned with deformation, i.e. the changes in the size and shape of a body as a result of the forces acting on it. It should be clear that the description of deformation can be based on purely geometrical concepts. The displacement vector \mathbf{u} is defined as a vector field which maps every point of the body from its initial undeformed state into its final deformed state. We normally require \mathbf{u} to be a single-valued continuous function of position, but these conditions may have to be relaxed, as will be seen for the case of dislocations. We ignore for the moment any complications due to possible discontinuities in the displacement.

Although the displacement field \mathbf{u} completely characterizes the deformation, it is not a convenient description of the deformed state, because it does not easily distinguish rigid body motion from actual changes in size and shape. On the other hand, if we know the relative change in length between any two neighbouring points in the deformed body, then its deformed state can be completely characterized up to rigid body motions. The latter do not contribute to the true deformation. The strain tensor e_{ij} is normally used to provide a suitable measure of the deformation and we now derive the important strain-displacement relations. Let ds_0^2 be the square of the (infinitesimal) distance between two neighbouring points in the initial state of the body and let ds^2 be the value after deformation. If $d\mathbf{x}$ is the vector joining the neighbouring points, then the strain tensor e_{ij} is defined such that $ds^2 - ds_0^2 = 2e_{ij}dx_i dx_j$; the vector $d\mathbf{x}$ may be referred to embedded coordinates in either the initial or deformed state and the values of e_{ij} will differ for these two choices.⁽¹⁴⁾ After deformation, the point in the body originally at \mathbf{x} is at $\mathbf{x} + \mathbf{u}$, where \mathbf{u} must be regarded as a function of \mathbf{x} . Elementary differential geometry gives

$$ds_0^2 = dx_k dx_k = \delta_{ij} dx_i dx_j \quad (2.2.10)$$

and

$$\begin{aligned} ds^2 &= (\delta_{ki} + u_{k,i})(\delta_{kj} + u_{k,j})dx_i dx_j \\ &= (\delta_{ij} + u_{i,j} + u_{j,i} + u_{k,i}u_{k,j})dx_i dx_j, \end{aligned} \quad (2.2.11)$$

hence,

$$ds^2 - ds_0^2 = (u_{i,j} + u_{j,i} + u_{k,i}u_{k,j})dx_i dx_j,$$

so that

$$e_{ij} = \frac{1}{2}(u_{i,j} + u_{j,i} + u_{k,i}u_{k,j}). \quad (2.2.12)$$

When the spatial variation in u_j is sufficiently small, the products of derivatives in eq. (2.2.12) can be ignored and, by definition, this corresponds to the case of “infinitesimal” or “linear” strain. Throughout this review, we restrict all deformation to situations where the strains can be regarded as infinitesimal, whereupon the strain tensor becomes the symmetric tensor

$$e_{ij} = \frac{1}{2}(u_{i,j} + u_{j,i}). \quad (2.2.13)$$

When the strains are infinitesimal, the previously mentioned dependence of e_{ij} on the choice of reference vanishes. The displacement gradient tensor $u_{i,j}$ is called the “distortion” and eq. (2.2.13) shows that the infinitesimal strain tensor is the symmetric part of the distortion (the antisymmetric part of $u_{i,j}$ gives the infinitesimal rotation).

The strain tensor given in eq. (2.2.13) has the following geometric interpretation: the strain e_{ij} for $i = j$ (normal strain) gives the change in length per unit length of lines initially parallel to the x_j axis; the strains for $i \neq j$ (shear strains) give half the angular change between mutually orthogonal lines initially parallel to the x_i and x_j axes. The quantity $e_{kk} = e_{11} + e_{22} + e_{33}$ is called the “dilatation” and it equals the change in volume per unit volume associated with the strain field e_{ij} . We should remark that in engineering practice one often encounters the shear strains taken as $2e_{ij}$, but in this case the strains do not form a true tensor quantity.

Equation (2.2.13) can be viewed as six independent partial differential equations for the displacements u_j given the strains e_{ij} . Since there are only three independent components of displacement, an arbitrary choice of the strains does not, in general, allow the strain-displacement relation, eq. (2.2.13), to be integrated to obtain a continuous single-valued displacement. In general, if the strains are chosen arbitrarily, then a continuous single-valued displacement will not exist and a body subjected to these arbitrary strains must contain gaps or overlaps in its material. The strains will give rise to continuous single-valued displacements only if they satisfy the six independent “compatibility conditions,”⁽¹⁴⁾

$$\epsilon_{pmk}\epsilon_{qnj}\epsilon_{kj,nm} = 0. \quad (2.2.14)$$

These conditions apply to singly connected bodies. In the case of dislocations, where the displacements are required to be discontinuous, the situation is somewhat more complex and we shall return to this point in Section 2.5.

2.2.3. Work and energy

Consider a body subjected to tractions on its surface and body forces throughout its interior. When this body deforms, work must be done, and we wish to obtain a general expression for this work. Let ΔV be an arbitrary volume element in the body and let σ_{ij} and f be, respectively, the stress and body force density. Assume that ΔV is subjected to a small increment of displacement δu_j , which is applied in a quasi-static manner

so that equilibrium of the acting forces is always maintained. The work done δW on the element ΔV must be

$$\delta W = \oint_{\Delta S} \sigma_{ij} \delta u_j dS_i + \iiint_{\Delta V} f_j \delta u_j dV, \quad (2.2.15)$$

where ΔS is the enclosing surface of ΔV . Applying Gauss' theorem to the surface integral we obtain

$$\delta W = \iiint_{\Delta V} (\int_j \delta u_j + \sigma_{ij,i} \delta u_j + \sigma_{ij} \delta u_{j,i}) dV \quad (2.2.16)$$

and from the fact that static equilibrium is maintained, eq. (2.2.4), we have

$$\delta W = \iiint_{\Delta V} \sigma_{ij} \delta u_{j,i} dV. \quad (2.2.17)$$

Since σ_{ij} is symmetric, the antisymmetric part of $\delta u_{i,j}$ does not contribute to the sum under the integral sign in eq. (2.2.17). In addition, we can let ΔV shrink to an infinitesimal volume δV and then, with the restriction to infinitesimal strains, eq. (2.2.13), we obtain the work done per unit volume as

$$\delta W = \sigma_{ij} \delta e_{ij}. \quad (2.2.18)$$

Note that σ_{ij} and e_{ij} need not be related here; we require only that σ_{ij} satisfy static equilibrium and that e_{ij} correspond to infinitesimal strain.

We shall now make the fundamental requirement that all deformation be "elastic". Elastic deformation is, by definition, instantaneous deformation which is reversible in the thermodynamic sense. A body which deforms elastically has a unique thermodynamically stable state, to which it changes reversibly when a given set of external forces are applied, and a stable initial state, to which it returns when the external forces causing the deformation are removed. The strains accompanying the deformation are conveniently measured from this initial state. The entire work of deformation can be stored in the body as potential energy and can be released upon removal of the forces. Finally, when the deformation is elastic, the state of stress in the body must be a unique function of the strain and vice versa. In addition to "normal" elasticity, anelastic deformation can occur, for which there also exists a unique thermodynamically stable state for a given set of forces; however, this state is not achieved instantaneously and part of the work of deformation is dissipated by the material. We are concerned here only with normal, instantaneous elasticity. For crystalline materials, the most important deformation which is not elastic is called "plastic" and represents a permanent, irreversible change in the configuration of the body. This latter kind of deformation has been studied extensively in its own right.⁽²⁰⁾ We must point out here that the motion

of dislocations gives rise to plastic (shear) deformation; however, in this review we are concerned only with the elastic fields of stationary dislocations, not the deformations associated with their motion.

Consider a body which undergoes thermodynamically reversible changes, such that the only work performed is due to elastic deformation. We let T denote the temperature and du , df and ds the differential changes in, respectively, the density of internal energy, Helmholtz free energy, and entropy. Using eq. (2.2.18) to calculate the work and noting that the elastic strain e_{ij} may be taken as the independent variable because σ_{ij} must be uniquely determined by it, the first and second laws of thermodynamics combine to give, respectively,⁽¹⁴⁾

$$du = Tds + \sigma_{ij}de_{ij}, \quad (2.2.19)$$

$$df = -sdT + \sigma_{ij}de_{ij}. \quad (2.2.20)$$

Thus, for an adiabatic process

$$\sigma_{ij} = \left(\frac{\partial u}{\partial e_{ij}} \right)_s, \quad (2.2.21)$$

while for an isothermal process

$$\sigma_{ij} = \left(\frac{\partial f}{\partial e_{ij}} \right)_T. \quad (2.2.22)$$

In the formal theory of elasticity, it is often convenient to postulate the existence of a proper function of the strains $W = W(e_{ij})$ called the "strain energy density function", such that

$$\sigma_{ij} = \frac{\partial W}{\partial e_{ij}}. \quad (2.2.23)$$

From eqs (2.2.21) and (2.2.22) we see that dW may be identified with the change in either internal energy density for adiabatic processes or the Helmholtz free energy density for isothermal processes.⁽¹⁸⁾ In the initial undeformed state of a body, the internal energy or Helmholtz free energy must attain minimum values (depending on the type of process) since this is taken to be a stable state. It then follows that for arbitrary elastic deformations in the neighbourhood of this initial state W must be a positive definite function of the strains. In the theory of elasticity, we assume that the strains are small enough so that W always remains positive definite. When this is the case many important features follow, including the uniqueness of solutions to elasticity problems.⁽¹⁴⁾ Loss of positive definiteness of W is associated with instability or bifurcation behaviour.

If we are given a body with certain boundary conditions prescribed, such as tractions over its surface or body forces within its interior, eqs (2.2.4) and (2.2.14) represent 9 equations for the 15 unknown quantities u_j , σ_{ij} and e_{ij} . A solution is not possible without introducing further equations. The additional equations required are normally introduced by postulating a relation between stress and strain. Relations of this kind are known as constitutive laws and, since they will depend on the material in question, they introduce material properties into the theory. In the next section we discuss Hooke's law, which is the constitutive relation upon which the linear theory of elasticity is built.

2.3. Hooke's Law and the Elastic Constants

2.3.1. General relations

A consideration of the binding energy between atoms suggests that when sufficiently small forces are applied to a body the deformation will be elastic and, furthermore, the displacements will be proportional to the forces.⁽²¹⁾ Experience shows this to be true for a large class of materials over a range of deformation which is of practical importance. This proportional behaviour of elastic bodies provides the motivation for introducing into the theory of elasticity the well-known linear stress-strain relationship called Hooke's law. For the general anisotropic case, the stresses may be written in terms of the strains as

$$\sigma_{ij} = C_{ijkp}e_{kp} \quad (2.3.1)$$

and

$$e_{ij} = S_{ijkp}\sigma_{kp}, \quad (2.3.2)$$

where

$$C_{ijmn}S_{mnpq} = \frac{1}{2}(\delta_{ip}\delta_{jq} + \delta_{iq}\delta_{jp})$$

and the proportionality or elastic constants consist of the fourth-rank tensors C_{ijkp} and S_{ijkp} , called, respectively, the elastic stiffnesses and elastic compliances. The values of C_{ijkp} and S_{ijkp} depend upon the conditions (isothermal or adiabatic, the differences being negligible for most applications) and the particular material under consideration. The compliances can be inverted to obtain the stiffnesses and vice versa, and, therefore, in much of the discussion in this section we shall focus attention on the stiffnesses and merely point out analogous relations for the compliances. Hereafter, we assume that eqs (2.3.1) and (2.3.2) are valid, and, unless stated otherwise, that the body under consideration is homogeneous. The latter requirement means that C_{ijkp} and S_{ijkp} must be independent of position.

Equations (2.2.4), (2.2.13) and either (2.3.1) or (2.3.2) provide 15 independent equations for the 15 unknown quantities, u_j , σ_{ij} and e_{ij} ; hence, these equations form the basis for a determinable theory. In fact, these combined

equations with constant C_{ijkp} are the basic field equations for the linear theory of elasticity in homogenous anisotropic bodies, although, as we shall see later, they can be cast into a more compact form. Perhaps the deepest aspect of the linear theory is the property that various solutions can be superposed to yield another solution. The basis for the linearization of the theory rests in the linear stress-strain relation, eqs (2.3.1) or (2.3.2), and the linear form of the strain-displacement relation, eq. (2.2.13), which results when the restriction to infinitesimal strain is made. In the remainder of this section, we discuss various properties possessed by the elastic constants.

The 81 components of the fourth-rank tensors C_{ijkp} and S_{ijkp} are not all independent because σ_{ij} and e_{ij} are symmetric tensors. Since eqs (2.3.1) and (2.3.2) are assumed to hold for arbitrary states of stress or strain, we can, without loss of generality, assume that

$$C_{ijkp} = C_{jikp} = C_{ijpk}, \quad (2.3.3)$$

which follows from the symmetry of σ_{ij} and e_{ij} .⁽¹³⁾ A similar relation holds among the S_{ijkp} . These relations reduce the number of independent elastic constants to 36.

Thermodynamic requirements place additional restrictions on the elastic constants. Consider a body subjected to reversible processes in which the only work done is due to elastic deformation. Combining eqs (2.2.23) and (2.3.1) we have

$$\sigma_{ij} = C_{ijkp} e_{kp} = \frac{\partial W}{\partial e_{ij}}$$

and hence

$$C_{ijkp} = \frac{\partial^2 W}{\partial e_{ij} \partial e_{kp}}, \quad (2.3.4)$$

where W can be identified with internal energy density or Helmholtz free energy density, thus giving, respectively, the adiabatic or isothermal form of the elastic constants. W must be a state function and, therefore, the order of differentiation in eq. (2.3.4) is immaterial and we obtain

$$C_{ijkp} = C_{kpji} \quad (2.3.5)$$

with a similar relation holding for the compliances. Equations (2.3.3) and (2.3.5) reduce the number of independent elastic constants to 21 in the most general case.

For a material obeying Hooke's law, the basic field equations for the linear theory can be cast into a compact form. By combining eqs (2.2.4), (2.2.13) and (2.3.1), and using the symmetry of C_{ijkp} , eqs (2.3.3) and (2.3.5),

the basic field equations for static equilibrium become

$$C_{ijkp}u_{k,p} + f_i = 0, \quad (2.3.6)$$

where the right-hand side is to be replaced by ρa_i , as in eq. (2.2.9), for the dynamical case. Using the symmetry of C_{ijkp} the stresses follow from the distortions since

$$\sigma_{ij} = C_{ijkp}e_{kp} = C_{ijkp}u_{k,p}. \quad (2.3.7)$$

The solutions to problems in linear, anisotropic elasticity are, therefore, equivalent to solving boundary value problems involving the second order partial differential eqs (2.3.6) with constant coefficients C_{ijkp} ; we shall use this approach later when dealing with dislocation field quantities. In general, we solve directly for the displacements u_k from eq. (2.3.6) and since these solutions are normally given by single-valued continuous functions (the discontinuities required for dislocation displacements will be discussed in Section 2.5.1), compatibility will be satisfied.

The strain energy density function W , discussed previously, can be evaluated explicitly for Hookean materials. If we consider an elastic deformation, the work done dW per unit volume during the increment of strain de_{ij} is

$$dW = \sigma_{ij}de_{ij} \quad (2.3.8)$$

(here we write dW since for elastic deformation the work must be a perfect differential). Using eq. (2.3.1) we obtain

$$dW = C_{ijkp}e_{kp}de_{ij} \quad (2.3.9)$$

and this may be integrated to give an explicit form for the strain energy density W

$$\begin{aligned} W &= \frac{1}{2} C_{ijkp}e_{ij}e_{kp} \\ &= \frac{1}{2} \sigma_{ij}e_{ij}. \end{aligned} \quad (2.3.10)$$

The total elastic energy required to produce a given state of elastic deformation is obtained by integrating this expression for W over the volume of the body.

At this point, we wish to discuss the so-called "matrix notation", which is widely used in the theory of elasticity. The matrix notation introduced by Voigt⁽¹⁷³⁾ can be defined by a transformation which maps an index pair ij into a single index m according to the rule^(13,173)

$$\begin{array}{ccccccc} ij & = & 11 & 22 & 33 & 23,32 & 13,31 & 12,21 \\ m & = & 1 & 2 & 3 & 4 & 5 & 6 \end{array} \quad (2.3.11)$$

Using this transformation, we define symmetric 6×6 matrices C_{mn} and

S_{mn} for the stiffnesses and compliances, respectively, by the rules

$$C_{mn} = C_{ijkp} \text{ for } 1 \leq m, n \leq 6, \quad (2.3.12)$$

$$\begin{aligned} S_{mn} &= S_{ijkp} \text{ if both } m \text{ and } n = 1, 2, 3, \\ &= 2S_{ijkp} \text{ if either } m \text{ or } n \text{ (not both)} = 1, 2, 3, \\ &= 4S_{ijkp} \text{ if both } m \text{ and } n = 4, 5, 6, \end{aligned} \quad (2.3.13)$$

where m and n are the images, respectively, of ij and kp under the transformation (2.3.11). We also define 6×1 column or 1×6 row matrices for the stresses and strains according to the rules

$$\sigma_m = \sigma_{ij} \text{ for } 1 \leq m \leq 6, \quad (2.3.14)$$

$$\begin{aligned} e_m &= e_{ij} \text{ if } m = 1, 2, 3, \\ &= 2e_{ij} \text{ if } m = 4, 5, 6, \end{aligned} \quad (2.3.15)$$

where m is the image of ij under the transformation. Using this scheme, we have, for example

$$C_{11} = C_{1111}; C_{12} = C_{1122}; C_{44} = C_{2323};$$

$$S_{11} = S_{1111}; S_{16} = 2S_{1112}; S_{44} = 4S_{2323};$$

$$\sigma_1 = \sigma_{11}; \sigma_4 = \sigma_{23}; e_1 = e_{11}; e_4 = 2e_{23}; \text{etc.,}$$

and with matrix notation Hooke's law reads

$$\sigma_i = \sum_{j=1}^6 C_{ij} e_j \quad (2.3.16)$$

or

$$e_i = \sum_{j=1}^6 S_{ij} \sigma_j. \quad (2.3.17)$$

The work done is

$$dW = \sum_{j=1}^6 \sigma_j de_j, \quad (2.3.18)$$

which gives the strain energy density W as

$$W = \frac{1}{2} \sum_{j=1}^6 \sigma_j e_j = \frac{1}{2} \sum_{j=1}^6 C_{ij} e_i e_j = \frac{1}{2} \sum_{j=1}^6 S_{ij} \sigma_i \sigma_j. \quad (2.3.19)$$

It should be clear that eqs (2.3.16) through (2.3.19) can be viewed as matrix multiplication equations involving the 6×6 elastic constant matrices C_{mn}

or S_{mn} and the 6×1 column or 1×6 row matrices σ_m and e_m for the stress and strain. Some authors define an index transformation for degenerate 9×9 matrices for the elastic constants and degenerate 9×1 or 1×9 column or row matrices for the stress and strain.⁽⁶⁾ In this case, the form of the subsequent equations differs slightly from those described here. The 9×9 scheme is really a contracted notation for the full tensor equations and it is useful for transforming coordinates or determining invariants, but it does not readily facilitate matrix inversion because of the degeneracy. On the other hand, the 6×6 scheme outlined here results in non-degenerate elastic constant and stress and strain matrices; therefore, as we shall show, it permits easy matrix inversion, along with a simple derivation of certain other useful relations.

As already mentioned, the matrix notation facilitates the conversion of stiffnesses to compliances, etc. In the language of matrix algebra, C_{mn} is the inverse of S_{mn} and vice versa. Therefore, by standard matrix inversion methods, we can write⁽¹⁵⁾

$$S_{mn} = \frac{\text{Cof}(C_{mn})}{\|C_{mn}\|}, \quad (2.3.20)$$

where $\text{Cof}(C_{mn})$ denotes the cofactor matrix of C_{mn} and $\|C_{mn}\|$ is the determinant. A similar relation holds for the inversion of S_{mn} to C_{mn} . The inversion given in eq. (2.3.20) is valid as long as the determinant $\|C_{mn}\|$ is non-zero. This must be the case, however, since the strain energy density function given in eq. (2.3.19) is positive definite, and the necessary and sufficient conditions for this are that the eigenvalues of C_{mn} be positive definite or equivalently that all the determinants

$$\|C_{11}\|, \quad \begin{vmatrix} C_{11} & C_{12} \\ C_{21} & C_{22} \end{vmatrix}, \quad \begin{vmatrix} C_{11} & C_{12} & C_{13} \\ C_{21} & C_{22} & C_{23} \\ C_{31} & C_{32} & C_{33} \end{vmatrix}, \dots, \|C_{mn}\| \quad (2.3.21)$$

be greater than zero.⁽²²⁾ It should be clear that requiring non-zero values for all the determinants given in eq. (2.3.21) puts additional restrictions on the values of the elastic stiffnesses; we shall mention some of these later. Conditions analogous to those required in eq. (2.3.21) hold for the compliances.

We will often make use of the matrix notation for the elastic constants and the reader should be aware that this notation is quite commonly used in the literature. When the elastic constants are transformed between different reference frames, the full tensor notation is most convenient for carrying out the transformation. On the other hand, when converting stiffnesses to compliances or deriving conditions like those given in eq. (2.3.21), the non-degenerate matrix notation proves to be convenient.

In many important applications of the theory of elasticity we deal with crystalline bodies. The elastic properties of such bodies must display the symmetry elements of the crystal structure in question and, therefore, certain additional restrictions must be imposed on the elastic constants as a result of symmetry. Nye⁽¹³⁾ gives a complete discussion of the derivation of these restrictions and we shall not reproduce the detailed arguments here. When dealing with crystals, it is generally very useful to choose the coordinate reference frame to coincide with the native symmetry of the crystal under consideration. For example, with cubic crystals we would

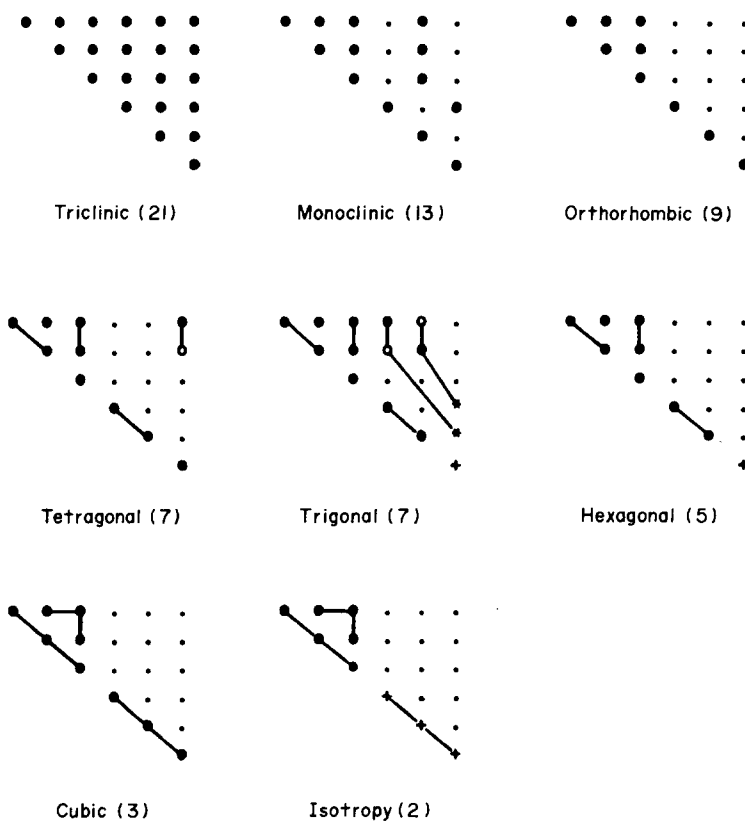


FIG. 2.2. Form of the symmetric elastic constant matrices C_{ij} and S_{ij} for the crystal symmetries shown.⁽¹³⁾ The numbers in parentheses give the number of independent elastic constants for each case. The coordinate axes are chosen according to standard crystallographic conventions, and alternate forms and/or classes exist for the monoclinic, tetragonal and trigonal cases.⁽¹³⁾ The meaning of the various matrix symbols is as follows: ● non-zero element, · zero element, —●— joined elements equal, —●—○ joined elements equal numerically but oppositely signed, * for S_{ij} equals twice the numerical value of joined element and for C_{ij} equals the numerical value of joined element, + for S_{ij} equals $2(S_{11} - S_{12})$ and for C_{ij} equals $\frac{1}{2}(C_{11} - C_{12})$.

choose the reference frame such that its axes lie along the cube directions. Following Nye,⁽¹³⁾ Fig. 2.2 shows in schematic form the C_{mn} (or S_{mn}) matrices for the various crystal classes. The most important effect of symmetry is that it reduces the number of independent elastic constants from 21 in the most general (triclinic) case to a smaller number, which is dependent on the symmetry. Cubic crystals possess three independent elastic constants, while hexagonal crystals have five. Since these latter two crystal classes are very important for the common metals and since the elastic fields of dislocations are an essential feature of the deformation behaviour of metals, we have given the detailed form of the C_{mn} matrices for these two cases in Fig. 2.3. The underlying symmetry elements are manifest in Fig. 2.3, e.g. the elastic properties of cubic crystals are invariant for 90° rotations about the cube axes, noting that the coordinate axes are chosen to coincide with the cube axes in this case.

2.3.2. Cubic symmetry and isotropy

Because of its particular importance for the common metals, we shall now discuss the pertinent relations among the elastic constants for cubic

$$(a)$$

$$\begin{bmatrix} c_{11} & c_{12} & c_{12} & 0 & 0 & 0 \\ c_{12} & c_{11} & c_{12} & 0 & 0 & 0 \\ c_{12} & c_{12} & c_{11} & 0 & 0 & 0 \\ 0 & 0 & 0 & c_{44} & 0 & 0 \\ 0 & 0 & 0 & 0 & c_{44} & 0 \\ 0 & 0 & 0 & 0 & 0 & c_{44} \end{bmatrix}$$

$$(b)$$

$$\begin{bmatrix} c_{11} & c_{12} & c_{13} & 0 & 0 & 0 \\ c_{12} & c_{11} & c_{13} & 0 & 0 & 0 \\ c_{13} & c_{13} & c_{33} & 0 & 0 & 0 \\ 0 & 0 & 0 & c_{44} & 0 & 0 \\ 0 & 0 & 0 & 0 & c_{44} & 0 \\ 0 & 0 & 0 & 0 & 0 & \frac{1}{2}(c_{11}-c_{12}) \end{bmatrix}$$

FIG. 2.3. The elastic constant matrices C_{ij} for (a) cubic symmetry and (b) hexagonal symmetry. For cubic symmetry, the coordinate axes lie along the cube directions. For hexagonal symmetry, two axes lie in the basal plane, while the third is normal to it. Note that hexagonal crystals are isotropic in the basal plane, i.e. the matrix is invariant with respect to orientation of the coordinate basis vectors in the basal plane.

symmetry. As already mentioned, for cubic symmetry the reference frame is chosen to coincide with the cube axes and the stiffness matrix C_{mn} appears as shown in Fig. 2.3. With this choice of reference frame the three independent elastic stiffness constants are C_{11} , C_{12} and C_{44} , while the three compliances are S_{11} , S_{12} and S_{44} . In terms of the full tensor notation, we have

$$C_{ijkp} = C_{12}\delta_{ij}\delta_{kp} + C_{44}(\delta_{ik}\delta_{jp} + \delta_{ip}\delta_{jk}) + (C_{11} - C_{12} - 2C_{44})\delta_{in}\delta_{jn}\delta_{kn}\delta_{pn}. \quad (2.3.22)$$

Therefore (no summation on repeated subscripts)

$$\begin{aligned} C_{jjjj} &= C_{11} \\ C_{iiji} &= C_{12} \text{ if } i \neq j, \\ C_{ijij} &= C_{44} \text{ if } i \neq j, \end{aligned}$$

with all other C_{ijkp} identically zero. The inversion of the stiffnesses to compliances and vice versa, follows from eq. (2.3.20)

$$\begin{aligned} C_{11} &= (S_{11} + S_{12})/S_0; \quad C_{12} = -S_{12}/S_0; \quad C_{44} = 1/S_{44}, \\ S_{11} &= (C_{11} + C_{12})/C_0; \quad S_{12} = -C_{12}/C_0; \quad S_{44} = 1/C_{44}, \end{aligned}$$

where

$$\begin{aligned} S_0 &= (S_{11} - S_{12})(S_{11} + 2S_{12}), \\ C_0 &= (C_{11} - C_{12})(C_{11} + 2C_{12}). \end{aligned} \quad (2.3.23)$$

The positive definiteness of the strain energy density function W requires

$$C_{44} > 0; \quad C_{11} > |C_{12}|; \quad C_{11} + 2C_{12} > 0. \quad (2.3.24)$$

There can be only three independent modes of elastic deformation for cubic crystals because of the three independent elastic constants.⁽²¹⁾ These modes can be taken as a hydrostatic mode (with bulk modulus $(C_{11} + 2C_{12})/3$), a shear mode on {100} cube planes in cube directions (with shear modulus C_{44}) and a shear mode on {110} diagonal planes in diagonal directions (with shear modulus $(C_{11} - C_{12})/2$). By definition, a body is "isotropic" if the elastic properties are completely independent of direction and, for cubic symmetry, a measure of the deviation from isotropy can be given by the anisotropy ratio

$$A = \frac{2C_{44}}{C_{11} - C_{12}}. \quad (2.3.25)$$

The anisotropy ratio $A = 1$ for isotropy, which makes evident the fact that all shear modes are equivalent in an isotropic body.

Although our primary concern in this review is with anisotropic bodies, for the sake of completeness we will mention the relations for the elastic constants in isotropic media. As was already mentioned, isotropy means

that the elastic properties are invariant with changes in direction and this requires that there be only two independent elastic constants. We may take these constants to be the shear modulus μ and the Poisson ratio v . The elastic stiffness tensor for an isotropic body then reads

$$C_{ijkp} = \mu \left(\delta_{ik} \delta_{jp} + \delta_{ip} \delta_{jk} + \frac{2v}{1 - 2v} \delta_{ij} \delta_{kp} \right). \quad (2.3.26)$$

In terms of μ and v we may write

$$\mu = C_{44} = \frac{1}{2}(C_{11} - C_{12}); \quad v = \frac{C_{12}}{C_{11} + C_{12}} = -\frac{S_{12}}{S_{11}}. \quad (2.3.27)$$

A useful way of summarizing the relations for an isotropic body is to consider it as having cubic symmetry along with the added relation

$$2C_{44} = C_{11} - C_{12}. \quad (2.3.28)$$

All previous relations discussed for cubic symmetry hold for isotropy and, furthermore, simplify when we include eq. (2.3.28). The positive definiteness of the strain energy density function requires that we have

$$\mu > 0; \quad -1 < v < \frac{1}{2}. \quad (2.3.29)$$

We should point out that in the literature the two independent elastic constants for isotropic bodies are expressed in many different forms.^(14,13) In addition to the pair μ, v used here, the Lamé constants μ, λ are commonly used, where

$$\lambda = \frac{2\mu v}{1 - 2v}. \quad (2.3.30)$$

Later in Table 4.2, we list the values of C_{mn} for some common cubic and hexagonal metals. Among the metals listed, aluminium, with an anisotropy ratio $A = 1.21$, most closely approaches isotropy; tungsten is the most isotropic of the cubic metals and in fact $A = 1.00$ for tungsten using the C_{mn} values given by Hirth and Lothe.⁽⁶⁾ The remaining cubic metals listed in Table 4.2 all deviate from isotropy by larger amounts; note that lithium is quite anisotropic with $A = 9.39$. We should repeat that the elastic behaviour of hexagonal crystals is actually isotropic in the basal plane, i.e. the C_{mn} are invariant to the choice of basis vectors in the basal plane.

2.4. The Green's Function Method

The Green's function method provides a convenient framework within which to display the elastic fields of dislocations and point force arrays in anisotropic media. The Green's function approach for the solution of boundary value problems is a device widely used throughout many areas of mathematical physics; the reader is referred elsewhere for a more complete discussion of the mathematical background.^(15,23) In this section,

we consider only linear elastic anisotropic bodies which are infinite in extent, homogeneous and everywhere in static equilibrium. Under these conditions, the time-independent Green's function approach can be applied to the solution of the basic field equations in a straightforward manner and a simple integral solution for the infinite-body Green's tensor can be developed. When the body is finite in extent or inhomogeneous in its elastic properties, the added difficulties are for the most part formidable. We should remark that a certain class of inhomogeneity problems, viz. ellipsoidal inclusions in an infinite matrix, can be solved in terms of the homogeneous Green's tensor discussed here and this is considered in Chap. 5 when we discuss Eshelby's ingenious transformation strain techniques. Chapter 5 also contains some discussion on methods to obtain the surface Green's tensor for elastic half spaces.

2.4.1. Solution of the basic field equations

Our Cartesian reference frame will be chosen as the one native to any symmetry possessed by the medium in question. This choice is usually convenient, although not necessary, and it is the reference frame in which the elastic constants are normally displayed. The Green's tensor $G_{ij}(\mathbf{x}, \mathbf{x}')$ is defined to be a tensor field which gives the displacement along the x_i axis at \mathbf{x} in response to a unit point force applied along the x_j axis at \mathbf{x}' . For an infinite homogeneous body the linear elastic behaviour must be translationally invariant, centrosymmetric⁽¹³⁾ and satisfy the Maxwell reciprocity condition.⁽¹⁴⁾ We then have that

$$G_{ij}(\mathbf{x}, \mathbf{x}') = G_{ij}(\mathbf{x} - \mathbf{x}') = G_{ij}(\mathbf{x}' - \mathbf{x}) = G_{ji}(\mathbf{x} - \mathbf{x}'),$$

hence

$$G_{ij,s}(\mathbf{x} - \mathbf{x}') = -G_{ij,s'}(\mathbf{x} - \mathbf{x}') = -G_{ij,s}(\mathbf{x}' - \mathbf{x}),$$

$$G_{ij,sk}(\mathbf{x} - \mathbf{x}') = G_{ij,s'k}(\mathbf{x} - \mathbf{x}') = G_{ij,sk}(\mathbf{x}' - \mathbf{x}), \quad (2.4.1)$$

where the unprimed subscripts denote partial differentiation with respect to \mathbf{x} and primed subscripts denote differentiation with respect to \mathbf{x}' ; hereafter we use this convention to distinguish differentiation with respect to \mathbf{x} or \mathbf{x}' . The latter two sets of relations in eq. (2.4.1) follow from the first set by the usual rules for differentiation. In what follows, our approach will be to start with the governing partial differential equation for G_{ij} and then show how the basic field equations can be solved using G_{ij} . For completeness, we then develop a method for the evaluation of G_{ij} and its derivatives in terms of integral solutions, which are easily evaluated by numerical methods; in general, an analytical solution cannot be found for G_{ij} in anisotropic media.

To derive the governing differential equation for G_{ij} we consider a point force \mathbf{F} acting at the position \mathbf{x}' . In view of the definition of G_{ij} the

displacement due to F is

$$u_i(\mathbf{x}) = G_{ij}(\mathbf{x} - \mathbf{x}')F_j,$$

hence

$$u_{i,m}(\mathbf{x}) = G_{ij,m}(\mathbf{x} - \mathbf{x}')F_j$$

and the associated stress field is

$$\sigma_{kp}(\mathbf{x}) = C_{kpim}G_{ij,m}(\mathbf{x} - \mathbf{x}')F_j.$$

For equilibrium, we must have

$$\begin{aligned} F_k &= - \oint_{\Delta S} \sigma_{kp}(\mathbf{x}) dS_p \\ &= - \oint_{\Delta S} C_{kpim}G_{ij,m}(\mathbf{x} - \mathbf{x}')F_j dS_p, \end{aligned}$$

so that an application of Gauss' theorem gives

$$F_k = - \iiint_{\Delta V} [C_{kpim}G_{ij,mp}(\mathbf{x} - \mathbf{x}') + \delta_{kj}\delta(\mathbf{x} - \mathbf{x}')]F_j dV,$$

where ΔS is an arbitrary surface enclosing \mathbf{x}' and ΔV is the volume contained within ΔS . The last relation may be written as

$$\iiint_{\Delta V} [C_{kpim}G_{ij,mp}(\mathbf{x} - \mathbf{x}') + \delta_{kj}\delta(\mathbf{x} - \mathbf{x}')]F_j dV = 0,$$

which holds for arbitrary ΔV and F_j , so that we obtain the desired governing equation for G_{ij}

$$C_{kpim}G_{ij,mp}(\mathbf{x} - \mathbf{x}') + \delta_{kj}\delta(\mathbf{x} - \mathbf{x}') = 0. \quad (2.4.2)$$

We shall now derive the general solution for displacements in terms of the Green's function G_{ij} . Using the relations given in eq. (2.4.1) we can write eq. (2.4.2) as

$$C_{kpim}G_{ij,m'p'}(\mathbf{x} - \mathbf{x}') + \delta_{kj}\delta(\mathbf{x} - \mathbf{x}') = 0. \quad (2.4.3)$$

The solution to all linear elasticity problems must give rise to displacement fields which satisfy the basic field equation (eq. (2.3.6))

$$C_{kpim}u_{i,m'p'}(\mathbf{x}') + f_k(\mathbf{x}') = 0, \quad (2.4.4)$$

where $f_k(\mathbf{x}')$ is the body force density. Let us multiply eqs (2.4.3) and (2.4.4) by $u_k(\mathbf{x}')$ and $G_{kj}(\mathbf{x} - \mathbf{x}')$, respectively, subtract and then integrate with respect to \mathbf{x}' over any volume V of the infinite body such that V contains \mathbf{x} . Let S denote the boundary surface of V and assume that the conditions outlined in Section 2.1 for Gauss' theorem hold throughout V . We obtain

the result

$$\begin{aligned} u_j(\mathbf{x}) = & \iiint_V G_{kj}(\mathbf{x} - \mathbf{x}') f_k(\mathbf{x}') dV' \\ & + \iiint_V C_{kpim} u_{i,m',p'}(\mathbf{x}') G_{kj}(\mathbf{x} - \mathbf{x}') dV' \\ & - \iiint_V C_{kpim} u_k(\mathbf{x}') G_{ij,m',p'}(\mathbf{x} - \mathbf{x}') dV', \end{aligned} \quad (2.4.5)$$

where $u_j(\mathbf{x})$ appears alone on the left-hand side because of the delta function in eq. (2.4.3). The symmetry $C_{kpim} = C_{imkp}$ permits the following identity to be established

$$\begin{aligned} C_{kpim} [u_{i,m',p'}(\mathbf{x}') G_{kj}(\mathbf{x} - \mathbf{x}') - u_k(\mathbf{x}') G_{ij,m',p'}(\mathbf{x} - \mathbf{x}')] \\ = C_{kpim} [u_{i,m'}(\mathbf{x}') G_{kj}(\mathbf{x} - \mathbf{x}') - u_k(\mathbf{x}') G_{ij,m'}(\mathbf{x} - \mathbf{x}')],_{p'}. \end{aligned} \quad (2.4.6)$$

If we substitute eq. (2.4.6) into eq. (2.4.5) for the last two terms and apply Gauss' theorem, we obtain

$$\begin{aligned} u_j(\mathbf{x}) = & \iiint_V G_{kj}(\mathbf{x} - \mathbf{x}') f_k(\mathbf{x}') dV' \\ & + \iint_S C_{kpim} u_{i,m'}(\mathbf{x}') G_{kj}(\mathbf{x} - \mathbf{x}') dS'_p \\ & - \iint_S C_{kpim} u_k(\mathbf{x}') G_{ij,m'}(\mathbf{x} - \mathbf{x}') dS'_p. \end{aligned} \quad (2.4.7)$$

Equation (2.4.7) represents the desired solution for the displacement field and its associated stresses and strains in terms of the Green's tensor G_{ij} . The surface S is arbitrary and in an infinite body S would normally be taken as a boundary at infinity, along with any cuts or other barrier surfaces required to remove discontinuities or singularities. In the event that the surface integrals vanish in eq. (2.4.7) we have

$$u_j(\mathbf{x}) = \iiint_{\infty} G_{jk}(\mathbf{x} - \mathbf{x}') f_k(\mathbf{x}') dV', \quad (2.4.8)$$

where we use the relations given in eq. (2.4.1) and the “ ∞ ” sign means that the integral is over all space. When eq. (2.4.7) is applied to dislocations, an interior surface cut must be introduced to avoid discontinuities in the displacement and, as will be discussed further in Section 2.5, the surface S in eq. (2.4.7) reduces to this interior surface. In summary, the essence of the Green's function method is captured in eqs (2.4.2) and (2.4.7); if we can find G_{ij} according to eq. (2.4.2), then we can construct solutions to elasticity problems by means of eq. (2.4.7).

Relation (10) in Table 2.1 shows that the delta function for vector arguments behaves as a homogeneous function of degree -3 , therefore, according to eq. (2.4.2), the second derivatives of G_{ij} must also have this property.

This implies that G_{ij} is itself homogeneous of degree -1 and we can write.

$$G_{ij}(\mathbf{x} - \mathbf{x}') = |\mathbf{x} - \mathbf{x}'|^{-1} g_{ij}, \quad (2.4.9)$$

where $|\mathbf{x} - \mathbf{x}'|$ denotes the magnitude of $\mathbf{x} - \mathbf{x}'$ and g_{ij} denotes the orientation dependent part of G_{ij} .

Although our concern in this section is with bodies of infinite extent, we should point out that with suitable modifications the Green's function method can be extended to finite bodies. Equation (2.4.2) is not appropriate for the finite body case, however, because static equilibrium with free surfaces could not be achieved under the action of a single point force. For finite bodies the Green's function can be defined as the response to a pair of antiparallel unit point forces, which are self equilibrated by means of a suitable compensating moment.^(23,12)

2.4.2. Integral solutions for the Green's function and its derivatives

For the Green's function method to have any practical significance, G_{ij} must be evaluated, i.e. we must obtain useful solutions to eq. (2.4.2). This can be done as we shall now show; however, G_{ij} has an exact analytical solution only in the case of isotropy or hexagonal symmetry and certain high symmetry situations associated with other crystal structures. Various schemes have been developed to evaluate G_{ij} . These include perturbation methods for weakly anisotropic media,⁽²⁴⁾ Fredholm's technique,^(25,26) and related procedures⁽²⁷⁾ which involve finding the roots of sextic equations, and the Fourier transform technique.^(28,29) Meissner⁽³⁰⁾ has reviewed several of these schemes. The Fourier transform method offers an advantage in the sense that a single line integral solution amenable to numerical evaluation can be obtained for G_{ij} and the derivatives of G_{ij} can be found by simple differentiation under the integral. Furthermore, in contrast to the sextic methods, the integral solutions pass smoothly into the isotropic limit. In the past, derivatives of G_{ij} have sometimes been found by differentiating truncated series expansions fitted to computed values of G_{ij} ,⁽²⁶⁾ but it should be clear that such procedures can lead to considerable error, as was demonstrated by Barnett.^{(29)†} In this section, we use a transform approach involving the Radon transform to develop the single line integral solution for G_{ij} . Compared to the Fourier transform, the Radon transform requires somewhat less mathematical manipulation, while leading to the same results.

Let $f(\mathbf{x})$ be a (scalar) function defined for \mathbf{x} ranging over all space. The Radon transform \hat{f} of f is defined as^(31,32)

$$\hat{f} = \hat{f}(\mathbf{z}, \alpha) = \iint_{\mathbf{z} \cdot \mathbf{x} = \mathbf{z}} f(\mathbf{x}) dS, \quad (2.4.10)$$

[†]It should not be assumed, however, that the same disadvantage applies to all series expansions. We have omitted here a description of the expansion of G_{ij} in spherical harmonics.^(165,166,25,167) It enables G_{ij} and its derivatives to be evaluated efficiently for each order of approximation and has been applied to point defect properties in metals^(168,169,170) and ionic crystals.⁽¹⁷¹⁾ A computer program for evaluation to the third order in cubic crystals has been given by Leutz and Bauer.⁽¹⁷²⁾

where z and α are the transform-space variables. \hat{f} is the integral of f over the infinite plane $z \cdot x = \alpha$ and we may, hereafter, assume that z is a unit vector. The inverse transform is given by the rule

$$f(x) = -\frac{1}{8\pi^2} \iint_{|z|=1} \left[\frac{\partial^2 \hat{f}(z, \alpha)}{\partial \alpha^2} \right]_{z \cdot x = \alpha} dS, \quad (2.4.11)$$

where the integration variable is z and the integration is taken over the surface of the unit sphere $|z| = 1$; the derivative under the integral sign is evaluated at $z \cdot x = \alpha$. Letting $(f(x))^\wedge = \hat{f}(z, \alpha)$ denote the Radon transform of $f(x)$, the following transforms can be obtained

$$\begin{aligned} (f(x - x'))^\wedge &= \hat{f}(z, \alpha - z \cdot x'), \\ (f_j(x))^\wedge &= z_j \frac{\partial \hat{f}(z, \alpha)}{\partial \alpha} \\ (\delta(x))^\wedge &= \delta(\alpha), \end{aligned} \quad (2.4.12)$$

where x' remains fixed. We then take the Radon transform of eq. (2.4.2), which, in view of eq. (2.4.12), reads

$$C_{kpim} z_m z_p \frac{\partial^2 \hat{G}_{ij}(z, \alpha - z \cdot x')}{\partial \alpha^2} + \delta_{kj} \delta(\alpha - z \cdot x') = 0. \quad (2.4.13)$$

The second rank symmetric tensor $(zz)_{ik}$ is defined as (see eq. (2.1.11))

$$(zz)_{ik} = C_{mikp} z_m z_p = C_{kpim} z_m z_p \quad (2.4.14)$$

and the inverse $(zz)_{ik}^{-1}$ of $(zz)_{ik}$ is defined by the property

$$(zz)_{ip}^{-1} (zz)_{pj} = (zz)_{ip} (zz)_{pj}^{-1} = \delta_{ij}. \quad (2.4.15)$$

We may multiply eq. (2.4.13) by $(zz)_{ik}^{-1}$ and apply eq. (2.4.15) to obtain

$$\frac{\partial^2 \hat{G}_{ij}(z, \alpha - z \cdot x')}{\partial \alpha^2} = -(zz)_{ij}^{-1} \delta(\alpha - z \cdot x'). \quad (2.4.16)$$

Equation (2.4.16) can be substituted into the inverse transform rule given by eq. (2.4.11) to yield

$$\begin{aligned} G_{ij}(x - x') &= \frac{1}{8\pi^2} \oint_{|z|=1} (zz)_{ij}^{-1} \delta[z \cdot (x - x')] dS \\ &= \frac{1}{8\pi^2 |x - x'|} \oint_{|z|=1} (zz)_{ij}^{-1} \delta(z \cdot T) dS, \end{aligned} \quad (2.4.17)$$

where here T is a unit vector along $x - x'$ (not to be confused with a traction vector) and the integration is with respect to z over the unit sphere $|z| = 1$. The second form of this equation follows using relation (10) in Table 2.1. Based on the definition of the delta function, eq. (2.4.17) reduces to (Gel'fand and Shilov⁽¹⁶⁾ p. 223),

$$G_{ij}(x - x') = \frac{1}{8\pi^2 |x - x'|} \oint_{|z|=1} (zz)_{ij}^{-1} ds, \quad (2.4.18)$$

where the integration contour is the unit circle $|z| = 1$ lying in the plane $\mathbf{z} \cdot \mathbf{T} = 0$, i.e. the $\delta(\mathbf{z} \cdot \mathbf{T})$ factor “extracts” the line integral from the surface integral.

Equation (2.4.18) reproduces the Fourier transform line integral solution for G_{ij} obtained by the authors already mentioned. This integral can be evaluated by standard numerical methods once C_{ijkp} is given. The inverse $(zz)_{ij}^{-1}$ can be obtained from $(zz)_{ij}$ by standard algebraic methods since $(zz)_{ij}$ is a positive definite form for $z \neq 0$. The general result is (see also eq. (4.1.17)),

$$(zz)_{ij}^{-1} = \frac{\epsilon_{ism}\epsilon_{jrw}(zz)_{sr}(zz)_{mw}}{2\epsilon_{pgn}(zz)_{1p}(zz)_{2g}(zz)_{3n}}. \quad (2.4.19)$$

We should point out here that in terms of the “integral formalism” discussed in Chap. 3, we have (compare eqs (3.6.4) and (2.4.18))

$$G_{ij}(\mathbf{x} - \mathbf{x}') = -\frac{1}{4\pi|\mathbf{x} - \mathbf{x}'|} Q_{ij}; \quad (2.4.20)$$

hence the quantity Q_{ij} in Chap. 3 is proportional to the orientation dependent part of G_{ij} , as defined in eq. (2.4.9).

If the medium under consideration is isotropic, G_{ij} reduces to an exact analytical solution after eq. (2.3.26) is used to evaluate $(zz)_{ij}^{-1}$. We simply reproduce the result here for an isotropic body:

$$G_{ij}(\mathbf{x} - \mathbf{x}') = \frac{1}{8\pi\mu|\mathbf{x} - \mathbf{x}'|} \left[2\delta_{ij} - \frac{\delta_{ij} - T_i T_j}{2(1-\nu)} \right], \quad (2.4.21)$$

where $\mathbf{x} - \mathbf{x}' = \mathbf{T}|\mathbf{x} - \mathbf{x}'|$ and the isotropic elastic constants are chosen as the shear modulus μ and Poisson ratio ν . The Green's function can also be obtained in analytic form for crystals of hexagonal symmetry. The solution, which is rather more cumbersome than that for isotropy, has been given by Kröner⁽¹⁶⁵⁾ and, with a minor correction, Willis.⁽³³⁾

As will be seen later, when dealing with dislocations and point force arrays, the derivatives of G_{ij} are necessary. Barnett⁽²⁹⁾ originally gave line integral expressions for the first two derivatives of G_{ij} . Willis⁽³⁴⁾ later reformulated the expressions and obtained a general result for all derivatives. We shall derive the general result starting from the first form of G_{ij} given in eq. (2.4.17), as does Willis.⁽³⁴⁾ We differentiate eq. (2.4.17) N times with respect to \mathbf{x} and again let $\mathbf{x} - \mathbf{x}' = \mathbf{T}|\mathbf{x} - \mathbf{x}'|$ to obtain

$$\begin{aligned} G_{ij,s_1s_2\dots s_N}(\mathbf{x} - \mathbf{x}') &= \frac{1}{8\pi^2} \oint \oint_{|z|=1} (zz)_{ij}^{-1} \delta_{s_1s_2\dots s_N} [\mathbf{z} \cdot (\mathbf{x} - \mathbf{x}')] dS \\ &= \frac{1}{8\pi^2} \frac{1}{|\mathbf{x} - \mathbf{x}'|^{N+1}} \oint \oint_{|z|=1} (zz)_{ij}^{-1} z_{s_1} z_{s_2} \dots z_{s_N} \delta^{(N)}[\mathbf{z} \cdot (\mathbf{x} - \mathbf{x}')] dS \\ &= \frac{1}{8\pi^2} \frac{1}{|\mathbf{x} - \mathbf{x}'|^{N+1}} \oint \oint_{|z|=1} (zz)_{ij}^{-1} z_{s_1} z_{s_2} \dots z_{s_N} \\ &\quad \times \delta^{(N)}(\mathbf{z} \cdot \mathbf{T}) dS, \end{aligned} \quad (2.4.22)$$

where the latter two expressions displayed in eq. (2.4.22) can be derived from a change in variables along with the homogeneity properties of the delta function (relation (11) of Table 2.1); the superscript N denotes the N -th derivative with respect to the argument. From the definition of the delta function and its derivatives, eq. (2.4.22) reduces to (Gel'fand and Shilov⁽¹⁶⁾ p. 230)

$$G_{ij,s_1s_2\dots s_N}(\mathbf{x} - \mathbf{x}') = \frac{(-1)^N}{8\pi^2 |\mathbf{x} - \mathbf{x}'|^{N+1}} \oint_{|z|=1} \frac{\partial^N}{\partial(z \cdot \mathbf{T})^N} \times [(zz)_{ij}^{-1} z_{s_1} z_{s_2} \dots z_{s_N}] ds, \quad (2.4.23)$$

where the integration contour is the unit circle $|z| = 1$ in the plane $z \cdot \mathbf{T} = 0$ and the derivative is evaluated at $z \cdot \mathbf{T} = 0$ in the direction of increasing θ . With reference to Fig. 2.4, we may write

$$z_j = \cos\theta T_j + \sin\theta M_j, \quad (2.4.24)$$

where $M_j = M_j(\phi)$ is the unit vector along the projection of z in $z \cdot \mathbf{T} = 0$ and ϕ gives its position in $z \cdot \mathbf{T} = 0$, relative to some fixed datum; all θ dependence is shown explicitly in eq. (2.4.24). From eq. (2.4.24) we have that

$$\left. \frac{\partial z_j}{\partial(z \cdot \mathbf{T})} \right|_{z \cdot \mathbf{T}=0} = \left. \frac{\partial z_j}{\partial \cos\theta} \right|_{\theta=(\pi/2)} = T_j. \quad (2.4.25)$$

Making a simple change of variables in eq. (2.4.23) and using eq. (2.4.25), we obtain the general relation for the derivatives of G_{ij}

$$G_{ij,s_1\dots s_N}(\mathbf{x} - \mathbf{x}') = \frac{(-1)^N T_{k_1} \dots T_{k_N}}{8\pi^2 |\mathbf{x} - \mathbf{x}'|^{N+1}} \oint_{|z|=1} \frac{\partial^N [(zz)_{ij}^{-1} z_{s_1} \dots z_{s_N}]}{\partial z_{k_1} \dots \partial z_{k_N}} ds. \quad (2.4.26)$$

This expression reproduces the original results of Willis⁽³⁴⁾ and one should note that eq. (2.4.18) is included for the case $N = 0$. We can evaluate

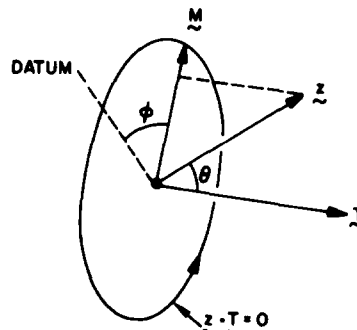


FIG. 2.4. Schematic diagram of the vector geometry discussed in the text. M lies in the plane containing the unit circle $z \cdot \mathbf{T} = 0$ and ϕ is the angle from a reference datum in the plane.

the derivatives required in eq. (2.4.26) by first differentiating eqs (2.4.14) and (2.4.15) with respect to z_p

$$\frac{\partial(zz)_{ij}^{-1}}{\partial z_p} = -(zz)_{ik}^{-1}(zz)_{qj}^{-1}C_{mkqn}(z_m\delta_{np} + z_n\delta_{mp}) \quad (2.4.27)$$

and the extension to higher order derivatives is obvious. The first two derivatives of G_{ij} read as follows, after combining eqs (2.4.26) and (2.4.27),

$$G_{ij,s}(\mathbf{x} - \mathbf{x}') = -\frac{1}{8\pi^2|\mathbf{x} - \mathbf{x}'|^2} \oint_{|z|=1} [T_s(zz)_{ij}^{-1} - z_s F_{ij}] ds, \quad (2.4.28)$$

$$G_{ij,sr}(\mathbf{x} - \mathbf{x}') = \frac{1}{8\pi^2|\mathbf{x} - \mathbf{x}'|^3} \oint_{|z|=1} [2T_s T_r(zz)_{ij}^{-1} - 2(z_s T_r + z_r T_s)F_{ij} \\ + z_s z_r E_{ij}] ds, \quad (2.4.29)$$

where using the notation of eq. (2.1.11) we have

$$F_{ij} = (zz)_{im}^{-1}(zz)_{kj}^{-1}[(zT)_{mk} + (Tz)_{mk}], \\ E_{ij} = [(zT)_{mk} + (Tz)_{mk}][F_{im}(zz)_{kj}^{-1} + (zz)_{im}^{-1}F_{kj}] \\ - 2(zz)_{im}^{-1}(zz)_{kj}^{-1}(TT)_{mk} \quad (2.4.30)$$

and these expressions are identical to the ones originally given by Barnett.⁽²⁹⁾

Despite the cumbersome appearance of these equations, they can be programmed for numerical evaluation in a completely straightforward manner, because the integrals are all well-behaved functions. Barnett⁽²⁹⁾ has given a useful coordinate system for z and T , which can be used to facilitate such numerical evaluations and he also gives the explicit components of $(zz)_{ij}^{-1}$ for cubic symmetry. As already mentioned, an advantage of the integral expressions given here is that they pass smoothly into the isotropic limit. This feature can be used to provide a useful check on the numerical computation procedure. In contrast, the methods mentioned earlier, which give G_{ij} and its derivatives as roots of sextic equations, generally display degeneracies which prevent passing smoothly to the isotropic limit. Finally, these integral expressions can be evaluated with C_{ijkp} referred to crystal coordinates, i.e. no coordinate transformation of the elastic constants is necessary.

2.5. Green's Function Representation for Dislocation Fields

In this section we shall develop the Green's function representation for the elastic fields associated with dislocations. Various aspects of the Green's function method applied to dislocations have been discussed by many authors.^(2,3,19,23,30,35) We shall derive integral expressions for the elastic field quantities of general curvilinear dislocations in terms of the

derivatives of G_{ij} . Starting from these results, the Indenbom-Orlov and Brown theorems may be derived in the manner shown in Chap. 4. As we have already noted, these theorems give the general curvilinear dislocation fields in terms of the fields due to infinite straight dislocations and convenient, easily evaluated integral expressions for the latter can be obtained. The results for infinite straight dislocations, in conjunction with the Indenbom-Orlov and Brown theorems, are the essential content of the contemporary theory of dislocation elastic field quantities in anisotropic media. Given a tractable means for obtaining the general curvilinear field quantities and a suitable energy evaluation and minimization procedure to yield the appropriate formulae for the forces on dislocations, a central problem of the elastostatic anisotropic dislocation theory may then be treated, viz. the static equilibrium configuration of an arbitrarily curved planar glide dislocation under prescribed boundary conditions (we consider the energy evaluation in the next section). Obtaining particular solutions to this central problem may of course require a considerable computational effort along with some ingenuity in devising appropriate numerical methods. In Chap. 4 we discuss such calculations.

We shall not deal extensively with the field quantities associated with infinite straight dislocations in this chapter. These quantities can be treated from an alternative point of view which also reveals the connection between the so-called "sextic" and "integral" formalisms for infinite straight dislocations. Chapters 3 and 4 contain the in-depth mathematical background for this alternative analysis and we feel it to be more fruitful to follow that general approach in detail, rather than a development based on the Green's function method. We shall, however, illustrate the use of the Green's function method here, but we give only the distortions and energy factors for infinite straight dislocations in anisotropic media, while in Chap. 4 we give these quantities (as well as displacements) and all the pertinent derivatives thereof.

2.5.1. General curvilinear dislocations—Volterra and Mura formulae

We assume the reader to be familiar with the concept of dislocations in crystals. For background, any of the standard texts may be consulted, e.g. Hirth and Lothe,⁽⁶⁾ Nabarro,⁽³⁶⁾ Friedel,⁽³⁷⁾ Cottrell.⁽³⁸⁾ We consider only the case of a dislocation in an infinite, homogeneous, anisotropic linear elastic continuum. A dislocation is a line defect characterized by certain discontinuities in its displacement field. Let the closed curve L shown in Fig. 2.5 represent a curvilinear dislocation loop of arbitrary shape in an infinite body and assign a positive direction to L , as indicated in the figure. Let $u_j(\mathbf{x})$ be the displacement field associated with L . By definition, L is a dislocation if for any closed circuit C (Fig. 2.5) we have

$$\oint_C u_{j,k}(\mathbf{x}) dx_k = b_j \text{ if } C \text{ irreducibly encloses } L, \\ = 0 \text{ otherwise,} \quad (2.5.1)$$

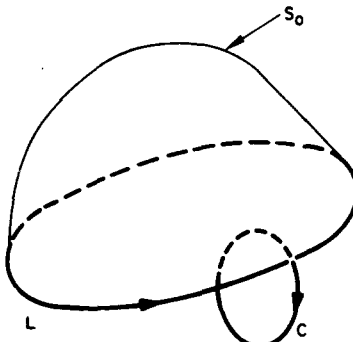


FIG. 2.5. Schematic diagram of a closed dislocation loop L and circuit C used for the Burgers vector determination. S_0 is an arbitrary surface bounded by L .

where $dx_k = t_k ds$ and t is the unit tangent vector to C . The positive sense for C is given by a right-hand screw rule with respect to the arbitrarily chosen positive sense for L , as shown in Fig. 2.5. The vector b is the Burgers vector and for a given dislocation L , b is required to be fixed, independent of the position of C . Some authors use the opposite sense for C and this reverses the sign of b . The sign convention for b adopted here is the same as that used by Bilby *et al.*,⁽³⁹⁾ de Wit⁽²⁾ and Hirth and Lothe,⁽⁶⁾ and the reverse of that used by Nabarro.⁽³⁶⁾ Note that reversing the sense of L is equivalent to reversing the sense of b .

In order to possess the property demanded by eq. (2.5.1), the displacement field u_j of a dislocation must be either discontinuous or multivalued (the two points of view are equivalent). Here, we formally remove the discontinuity by introducing a smooth, orientable, but otherwise arbitrary cut S_0 bounded by L , as is shown schematically in Fig. 2.5. The displacement u is considered to change discontinuously by the amount b when traversing opposite sides of S_0 . It is clear that the faces of the cut S_0 must be included in the boundary surfaces when quantities involving the dislocation displacements are used in Gauss' theorem. If we assign a unit normal n to the surface S_0 such that the positive sense of n is given by a right-hand screw rule with respect to the positive line direction of L , then from the definition of the Burgers vector, the material on the positive side of S_0 (as determined by the positive sense of n) must be displaced by $-b$ when the material on the negative side is held fixed.

The condition on the displacement required by eq. (2.5.1) means that the dislocation must be a source of internal strain since the distortions $u_{j,k}$ cannot be zero everywhere if the integral is to be non-vanishing. Operationally, we may produce the dislocation L shown in Fig. 2.5 by slitting the medium over the surface S_0 , displacing the slit faces by the constant translation vector b and then welding the faces together again, adding or removing material as required. Given the dislocation line direction as determined by the unit tangent vector t to L , the dislocation character is "edge" type if t is normal to b , whereas it is "screw" type if t and

b are parallel. For all other cases, the dislocation has a mixed character. Volterra⁽¹⁾ first analyzed the distinct types of dislocations produced by constant translation vectors b .

We have already mentioned in conjunction with eq. (2.2.14) that compatible elastic strains in singly connected bodies are the result of continuous, single-valued displacement fields. On the other hand, we have seen that the displacement field of a dislocation must be discontinuous (or multi-valued); however, compatibility can still be satisfied almost everywhere throughout the dislocated body and in particular everywhere that the internal strain can be treated as linear elastic. This latter fact follows from Weingarten's theorem:⁽¹⁷⁾ "If the body containing the dislocation L shown in Fig. 2.5 is rendered doubly-connected by removing a small core of material coaxial with L , then the compatibility eq. (2.2.14) can be satisfied everywhere within the doubly-connected region, and the resultant strains will be single-valued and continuous; furthermore, the cut S_0 is arbitrary and can be any open surface having L as its boundary." Thus, except for the small core of material coaxial with L , compatibility is satisfied everywhere in the dislocated body. The core of material must be "removed", at least in a mathematical sense, otherwise problems will arise in the mathematical development of the linear elastic field quantities, because L is the seat of a line singularity (also, because of this singular behaviour, linear elasticity could not be expected to hold near L , i.e. within the core region). The "incompatibility" associated with the core can be given a delta-function character and subsequently used as a source function in the so-called incompatibility theory of the (discrete) dislocation field quantities.⁽²⁾

We shall now derive the displacement field u_k for the dislocation L shown in Fig. 2.5 by applying eq. (2.4.7) along with suitable boundary conditions. In view of the previous discussion, a proper integration domain for eq. (2.4.7) can be made up of all space with a boundary at infinity and a surface "cap" surrounding L as shown schematically in Fig. 2.6. The cap consists of a toroidal or tubular surface of radius r_0 , which is coaxial with L , and a surface cut with sides S_0^+ and S_0^- , across which the displacements u_k change discontinuously by the Burgers vector b_k . The dashed surface S_0 shown in Fig. 2.6 is an oriented surface defining the cut. S_0 is bounded by L and has the unit normal n where the positive sense for n is determined by a right-hand rule with respect to the positive sense of L ; S_0^+ is the side of the cut on the positive side of S_0 , as given by the positive sense of n . This arrangement of boundary surfaces ensures that the displacements will be continuous within the integration domain, i.e. the cut excludes traversing directly across the discontinuity and, therefore, Gauss' theorem can be applied.

Since the dislocation is defined by displacement boundary conditions, we may set the body force $f_k = 0$ so that the volume integral term in eq. (2.4.7) makes no contribution. To obtain a vanishing contribution from

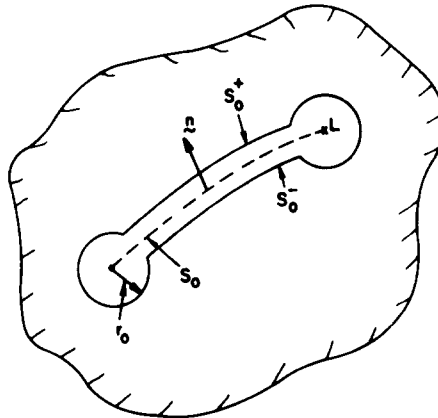


FIG. 2.6. Schematic diagram of the surface cap used to obtain the dislocation field quantities. The cap consists of the cut faces S_0^+ , S_0^- and a tubular surface of radius r_0 coaxial with the line L . The cut is defined by the oriented surface S_0 bounded by L (broken), where \mathbf{n} is the unit normal to S_0 as determined by a right-hand screw rule with respect to the sense of L .

the remaining surface integrals taken over the boundary at infinity and the tubular core surface in the limit $r_0 \rightarrow 0$, we evidently must require

$$|u(\mathbf{r})|/\|\mathbf{r}\| \rightarrow 0 \text{ as } |\mathbf{r}| \rightarrow 0 \text{ or } \infty, \quad (2.5.2)$$

where \mathbf{r} is a vector from a point on L to the boundary surface in question. We also require that the elastic field due to L be such that no net force is exerted by the tractions acting on any circuit surrounding L (no body-force distributed along the core). Note also that $G_{ij}(\mathbf{x})$ behaves like $|\mathbf{x}|^{-1}$ as $|\mathbf{x}| \rightarrow 0$. Boundary conditions for infinite straight dislocations are discussed in detail in Chap. 4.

In view of the conditions just stated, eq. (2.4.7) reduces to the two surface integrals taken over the sides S_0^+ and S_0^- of the cut. In order to evaluate the integrals, we let the two sides of the cut S_0^+ and S_0^- collapse onto the surface S_0 , taking account of the fact that the outward unit normal on S_0^- is \mathbf{n} and on S_0^+ it is $-\mathbf{n}$, where \mathbf{n} is the unit normal to S_0 . The first surface integral in eq. (2.4.7) makes no contribution since the integrand is continuous across S_0 and the integrals over S_0^+ and S_0^- exactly cancel. According to the definition of the Burgers vector given in eq. (2.5.1), the displacement u_k on S_0^+ is $-b_k$, when S_0^- is held fixed; therefore, the second surface integral in eq. (2.4.7) yields

$$\begin{aligned} u_j(\mathbf{x}) &= -C_{kpim} \left[\iint_{S_0} u_k(\mathbf{x}') G_{ij,m}(\mathbf{x} - \mathbf{x}') dS'_p \right. \\ &\quad \left. - \iint_{S_0^+} u_k(\mathbf{x}') G_{ij,m}(\mathbf{x} - \mathbf{x}') dS'_p \right] \\ &= -C_{kpim} b_k \iint_{S_0} G_{ij,m}(\mathbf{x} - \mathbf{x}') dS'_p, \end{aligned} \quad (2.5.3)$$

where $dS'_p = n_p dS'$. Equation (2.5.3) is called Volterra's displacement equation and, according to Weingarten's theorem, S_0 can be any oriented surface having L as its boundary. After a consideration of the appropriate boundary conditions, it turns out that Volterra's equation may also be applied to infinite straight dislocations.

The integrand of eq. (2.5.3) can be viewed as the displacement resulting from an infinitesimal dislocation loop subtending the area element dS'_p . The total displacement then results in an obvious fashion by integrating (superposing) the contribution of such elementary loops over the surface S_0 . Mutual cancellation of adjacent sides of the infinitesimal loops will occur and the resulting dislocation will be L , the boundary of S_0 . We can, thus, regard the integrand of eq. (2.5.3) as a source term in the sense that it represents the field due to a "displacement dipole", where the dipole produces the appropriate displacement shift b_k on opposite sides of dS'_p . As we shall discuss further in Section 2.7, a dislocation "source" is best formulated in terms of the appropriate displacement boundary conditions and not force boundary conditions as is generally the case for point defects.

The distortion field resulting from L may be obtained by differentiating eq. (2.5.3) with respect to x and the result reads

$$u_{j,s}(x) = b_k C_{kpim} \iint_{S_0} G_{ij,m's}(x - x') dS'_p. \quad (2.5.4)$$

In writing eq. (2.5.4) and in numerous other portions of the text, we have made use of the various symmetries for G_{ij} and its derivatives given in eq. (2.4.1); care must be exercised in applying Stokes' or Gauss' theorems so as to insure that all pertinent derivatives are taken with respect to the integration variable. We now apply Stokes' theorem in the form of eq. (2.1.6) along with eq. (2.4.2) in order to transform eq. (2.5.4) to a line integral. We obtain

$$u_{j,s}(x) = -b_k C_{kpim} \epsilon_{qps} \oint_L G_{ij,m}(x - x') dx'_q \quad (2.5.5)$$

and we have used the fact that S_0 is arbitrary, i.e. the integral of $\delta(x - x')$ with respect to x' over S_0 vanishes since one may always choose an S_0 which does not contain x . Equation (2.5.5) will diverge as x approaches points on L itself and this reflects the fact that L is a line singularity in the linear elastic representation. Of course, real crystal dislocations do not possess this singular behaviour.

Mura⁽⁴⁰⁾ appears to have been the first to obtain the line integral expression given in eq. (2.5.5) for the distortion field due to L . Indenbom and Orlov⁽¹⁰⁾ and later Asaro⁽⁴¹⁾ (although with what appears to be a sign error in his final result), derived an alternative line integral expression for $u_{j,s}(x)$, which will prove useful in Chap. 4. To derive this alternative

form, we first rewrite eq. (2.5.5) as

$$\begin{aligned} u_{j,s}(\mathbf{x}) &= -b_k C_{kpim} \epsilon_{qpr} \oint_L (x_r - x'_r) G_{ij,m}(\mathbf{x} - \mathbf{x}') d\mathbf{x}'_q \\ &= b_k C_{kpim} \epsilon_{qpr} \oint_L (x_r - x'_r) G_{ij,ms}(\mathbf{x} - \mathbf{x}') d\mathbf{x}'_q = I_{js}, \end{aligned}$$

where

$$I_{js} = b_k C_{kpim} \epsilon_{qpr} \oint_L [(x_r - x'_r) G_{ij,m}(\mathbf{x} - \mathbf{x}')]_s d\mathbf{x}'_q. \quad (2.5.6)$$

Applying Stokes' theorem in the form of eq. (2.1.6) to I_{js} gives

$$I_{js} = -b_j \iint_{S_0} [\delta_{ps} \delta(\mathbf{x} - \mathbf{x}') + (x_p - x'_p) \delta_{,s}(\mathbf{x} - \mathbf{x}')] dS'_p, \quad (2.5.7)$$

where we have used eq. (2.4.2) and the fact that G_{ij} is homogeneous of degree -1 , viz. Euler's relation in the form

$$(x_r - x'_r) G_{ij,ms}(\mathbf{x} - \mathbf{x}') = -2G_{ij,m}(\mathbf{x} - \mathbf{x}'). \quad (2.5.8)$$

In view of the definition of the derivative of the delta function, the two terms in eq. (2.5.7) cancel giving $I_{js} = 0$ (alternatively, we could use the fact that S_0 is arbitrary). We are left with the desired alternative form for the distortions due to L

$$u_{j,s}(\mathbf{x}) = b_k C_{kpim} \epsilon_{qpr} \oint_L (x_r - x'_r) G_{ij,ms}(\mathbf{x} - \mathbf{x}') d\mathbf{x}'_q. \quad (2.5.9)$$

2.5.2. Infinite straight dislocations

We shall now deal briefly with the elastic fields due to an infinite straight dislocation in an infinite, homogeneous anisotropic body. The distortions $u_{j,s}(\mathbf{x})$ at \mathbf{x} as a result of the infinite straight dislocation having line direction \mathbf{t} and Burgers vector \mathbf{b} can be obtained from eq. (2.5.5). The integration contour in eq. (2.5.5) is taken to be $x'_j = \lambda t_j$ with $-\infty \leq \lambda \leq \infty$, so that we obtain the result

$$u_{j,s}(\mathbf{x}) = -b_k C_{kpim} \epsilon_{qps} t_q \int_{-\infty}^{\infty} G_{ij,m}(\mathbf{x} - \lambda \mathbf{t}) d\lambda. \quad (2.5.10)$$

Substituting the second form of the derivative $G_{ij,m}$ given in eq. (2.4.22) into eq. (2.5.10), we have

$$u_{j,s}(\mathbf{x}) = -\frac{b_k C_{kpim} \epsilon_{qps} t_q}{8\pi^2} \iint_{|\mathbf{z}|=1} (zz)_{ij}^{-1} z_m \int_{-\infty}^{\infty} \delta'(\mathbf{z} \cdot \mathbf{x} - \mathbf{z} \cdot \mathbf{t}\lambda) d\lambda dS. \quad (2.5.11)$$

Using relation (2) in Table 2.1 to represent the δ -function, we may show that

$$\int_{-\infty}^{\infty} \delta'(a - c\lambda) d\lambda = \frac{-2\delta(c)}{a}, \quad (2.5.12)$$

where a and c are constants and we use the fact that

$$\int_{-\infty}^{\infty} \operatorname{sgn}(k) e^{ikx} dk = \frac{2i}{a} \quad (2.5.13)$$

where $\operatorname{sgn}(k)$ gives the sign of k .⁽¹⁶⁾ Equation (2.5.12) can be used to reduce the integration with respect to λ in eq. (2.5.11) and the result reads

$$u_{j,s}(x) = \frac{b_k C_{kpim} \epsilon_{qps} t_q}{4\pi^2} \oint_{|z|=1} \frac{(zz)_{ij}^{-1} z_m}{z \cdot x} \delta(z \cdot t) dS. \quad (2.5.14)$$

The $\delta(z \cdot t)$ factor in this equation reduces the integral over the unit sphere $|z| = 1$ to an integral over the unit circle $|z| = 1$ in the plane $z \cdot t = 0$ in the usual manner. We obtain the following result for the distortions, which is identical to that given by Barnett and Swanger⁽⁴²⁾

$$u_{j,s}(x) = \frac{b_k C_{kpim} \epsilon_{qps} t_q}{4\pi^2 \rho} \oint_{|z|=1} \frac{(zz)_{ij}^{-1} z_m}{z \cdot m} ds, \quad (2.5.15)$$

where ρ denotes the perpendicular distance from the dislocation line to the field point x and m is a unit vector along this perpendicular direction, i.e. $x = (x \cdot t)t + \rho m$. Equation (2.5.15) demonstrates that the distortions can be obtained as a single line integral around a unit circle normal to the line. Although simple in form eq. (2.5.15) is inconvenient for numerical evaluations because of the $z \cdot m$ factor in the denominator; the integral is a principal-value integral. Following the analysis due to Mura,⁽⁴³⁾ we may recast eq. (2.5.15) into a more convenient form. Take as a coordinate reference system the orthogonal triad of unit vectors t , m and n shown in Fig. 2.7. The vector $n = t \wedge m$ and z' lies in $z \cdot t = 0$ orthogonal to z as shown in the figure. With this choice of coordinates, we have

$$\begin{aligned} z_j &= -m_j \sin \omega + n_j \cos \omega, \\ z_j &= m_j \cos \omega + n_j \sin \omega, \\ z \cdot m &= z_j m_j = -\sin \omega, \end{aligned} \quad (2.5.16)$$

where ω is measured from the vector m in $z \cdot t = 0$ as shown in Fig. 2.7. The integral around the unit circle in eq. (2.5.15) reads

$$\oint_{|z|=1} \frac{(zz)_{ij}^{-1} z_m}{z \cdot m} ds = m_m \int_0^{2\pi} (zz)_{ij}^{-1} d\omega - n_m \int_0^{2\pi} \frac{\cos \omega}{\sin \omega} (zz)_{ij}^{-1} d\omega. \quad (2.5.17)$$

Using eqs (2.1.11), (2.4.15) and (2.5.16) the following identity may be

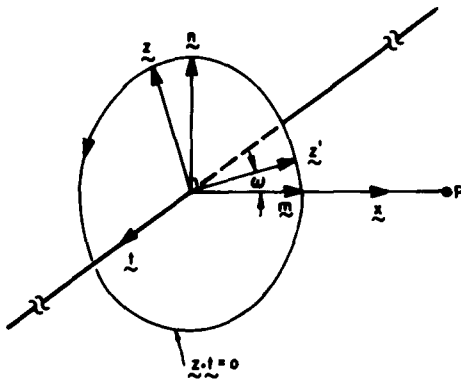


FIG. 2.7. Schematic diagram of the vector geometry used for infinite straight dislocations as discussed in the text. The field point P is at x , t is the line direction, m is a unit normal along x and $n = t \wedge m$. z is a unit vector which traverses the unit circle $z \cdot t = 0$ and z' is orthogonal to z as shown. The angle ω measured from the vector m in the plane containing $z \cdot t = 0$ gives the positions of z and z' .

verified⁽⁴³⁾

$$\begin{aligned} \frac{\cos \omega}{\sin \omega} (zz)_{ij}^{-1} &= (nn)_{ij}^{-1} \frac{\cos \omega}{\sin \omega} + (nn)_{ir}^{-1} (z'z)_{rw} (zz)_{wj}^{-1} \\ &\quad + (nn)_{ir}^{-1} (nm)_{rw} (zz)_{wj}^{-1}. \end{aligned} \quad (2.5.18)$$

Integrating eq. (2.5.18) over ω from 0 to 2π and noting that the tensors involving n and m are fixed with respect to ω integration reveals that the first term on the right vanishes. Now substitute the result into eq. (2.5.17) and combine with eq. (2.5.15) to obtain

$$\begin{aligned} u_{js}(x) &= \frac{b_k C_{kpim} \epsilon_{qps} t_q}{4\pi^2 \rho} \left\{ m_m \int_0^{2\pi} (zz)_{ij}^{-1} d\omega - n_m (nn)_{ir}^{-1} \right. \\ &\quad \times \left. \left[\int_0^{2\pi} (z'z)_{rw} (zz)_{wj}^{-1} d\omega + (nm)_{rw} \int_0^{2\pi} (zz)_{wj}^{-1} d\omega \right] \right\}. \end{aligned} \quad (2.5.19)$$

The result given in eq. (2.5.19) is equivalent to that originally derived by Asaro *et al.*⁽⁴⁴⁾ this follows from the symmetry of $(zz)_{ij}^{-1}$. We should point out that the integrals appearing in eq. (2.5.19) are of the same form as those which appear throughout Chap. 3 and 4 for the "integral formalism" (for clarity, we use z and z' here to denote those quantities to be integrated with respect to ω , whereas in Chap. 3 and 4 we use m and n for this purpose, as well as to denote the reference basis). We can rewrite eq. (2.5.19) in terms of the quantities Q_{ij} and S_{ij} defined, respectively, by eqs (3.6.4) and (3.6.6) in Chap. 3, along with the relation

$$\epsilon_{qps} t_q = m_p n_s - m_s n_p, \quad (2.5.20)$$

to obtain

$$\begin{aligned} u_{j,s}(x) = & \frac{b_k}{2\pi\rho} [-m_s S_{jk} - n_s(mn)_{ki} Q_{ij} + n_s(mn)_{ki}(nn)_{ir}^{-1} S_{jr} \\ & + n_s(mn)_{ki}(nn)_{ir}^{-1}(nm)_{rw} Q_{wj}] \end{aligned} \quad (2.5.21)$$

and we also use the fact that $(nm)_{ij} = (mn)_{ji}$. Equations (2.5.19) or (2.5.21) give the distortions in a convenient form, which involves only single integrals free of principal-value complications. Despite their appearance, equations like eq. (2.5.21) may be readily evaluated numerically. The tensors $(nm)_{ij}$, etc. are given from the geometry, while the integrals involve only straightforward numerical integration and there is no need to transform the C_{ijkm} to dislocation coordinates in order to carry out the evaluations.

2.6. Energies of, and Forces on, Dislocations

2.6.1. Energies

In order that we may discuss the forces acting on a dislocation, in this section we consider the various contributions to the total energy of a body containing a dislocation. For a body subjected to applied loading under isothermal conditions, the appropriate potential function is the Gibbs free energy and, therefore, we must take into account in the total energy both the stored elastic energy and the potential energy of the loading mechanism. This point is clearly made by Eshelby⁽¹⁹⁾ in his enlightening analysis of elastic bodies containing defects. Although we are normally concerned with the infinite-body case in this review, we shall consider finite-bodies here so that we may derive the image force on a dislocation.

Let a finite, anisotropic linear elastic body of volume V be bounded by the surface S and assume V to be in static equilibrium such that no body forces act within V . Let V contain the general curvilinear dislocation loop L , along with other sources of internal stress distinct from L , which are denoted by O , and let V be acted upon by tractions applied on S , which are denoted by A . In view of the linear elastic behaviour, the total displacement, stress and strain fields in V may be written as

$$\begin{aligned} u_i &= u_i^{L+I} + u_i^O + u_i^A, \\ \sigma_{ij} &= \sigma_{ij}^{L+I} + \sigma_{ij}^O + \sigma_{ij}^A, \\ e_{ij} &= e_{ij}^{L+I} + e_{ij}^O + e_{ij}^A \end{aligned} \quad (2.6.1)$$

where

$$\begin{aligned} u_i^{L+I} &= u_i^L + u_i^I, \\ \sigma_{ij}^{L+I} &= \sigma_{ij}^L + \sigma_{ij}^I \\ e_{ij}^{L+I} &= e_{ij}^L + e_{ij}^I. \end{aligned}$$

The contributions due to O and A are denoted by the respective superscripts. The contribution due to L is split into the infinite (unbounded) body field denoted by the superscript L and the image field associated with L , which is denoted by the superscript I . The image field when added to the infinite body field produces the finite body field $L + I$, which has zero traction acting through the boundary surface S , i.e. free surface boundary conditions. The image field is well-behaved in V and only u_i^I suffers the discontinuity b_i when crossing the cut S_0 (Fig. 2.5). Relative to the undeformed state, the total potential energy of the system is

$$\mathcal{E}^{TOT} = \frac{1}{2} \oint_V \sigma_{ij} e_{ij} dV - \oint_S \sigma_{ij}^A u_j dS_i, \quad (2.6.2)$$

where the first term represents the elastic strain energy stored in V and the second term accounts for the potential energy of the loading mechanism giving rise to the A field. Since the external surface S is subjected to pure traction boundary conditions, we have that

$$\sigma_{ij}^{L+I} \mathbf{n} = 0; \quad \sigma_{ij}^O \mathbf{n} = 0; \quad \sigma_{ij}^A \mathbf{n} = T_j^A \text{ on } S, \quad (2.6.3)$$

where \mathbf{n} is the outward unit normal on S and T_j^A denotes the prescribed surface tractions due to the loading mechanism. If we substitute eq. (2.6.1) into eq. (2.6.2), but retain only those terms depending on L , since we are ultimately interested in the forces on L , the result reads

$$\mathcal{E}^{TOT} = \mathcal{E}^{SELF} + \mathcal{E}^{L-O} + \mathcal{E}^{L-A} \quad (2.6.4)$$

where

$$\begin{aligned} \mathcal{E}^{SELF} &= \frac{1}{2} \oint_V \sigma_{ij}^{L+I} e_{ij}^{L+I} dV \\ &= \frac{1}{2} \oint_V \sigma_{ij}^{L+I} e_{ij}^L dV + \frac{1}{2} \oint_V \sigma_{ij}^{L+I} e_{ij}^I dV \\ &= \frac{1}{2} \oint_V (\sigma_{ij}^{L+I} u_j^L)_{,i} dV + \frac{1}{2} \oint_V (\sigma_{ij}^{L+I} u_j^I)_{,i} dV, \end{aligned} \quad (2.6.5)$$

$$\begin{aligned} \mathcal{E}^{L-O} &= \frac{1}{2} \oint_V (\sigma_{ij}^{L+I} e_{ij}^O + \sigma_{ij}^O e_{ij}^{L+I}) dV \\ &= \oint_V (\sigma_{ij}^O u_j^{L+I})_{,i} dV, \end{aligned} \quad (2.6.6)$$

$$\begin{aligned} \mathcal{E}^{L-A} &= \frac{1}{2} \oint_V (\sigma_{ij}^{L+I} e_{ij}^A + \sigma_{ij}^A e_{ij}^{L+I}) dV - \oint_S \sigma_{ij}^A u_j^{L+I} dS_i \\ &= \oint_V (\sigma_{ij}^A u_j^A)_{,i} dV - \oint_S \sigma_{ij}^A u_j^{L+I} dS_i. \end{aligned} \quad (2.6.7)$$

In deriving the final forms of eqs (2.6.5), (2.6.6) and (2.6.7), we have made use of the fact that each of the fields L , I , O and A satisfies eqs (2.2.4), (2.2.13) and (2.3.1). Note that any two fields A and B , which satisfy these latter three equations must also satisfy

$$\sigma_{ij}^A e_{ij}^B = (\sigma_{ij}^A u_j^B)_{,i} = \sigma_{ij}^B e_{ij}^A = (\sigma_{ij}^B u_j^A)_{,i} \quad (2.6.8)$$

and this relation has been applied to obtain the final result in eqs (2.6.5) (2.6.6) and (2.6.7). Equation (2.6.5) gives the elastic energy stored in V due to the field of L itself, while eqs (2.6.6) and (2.6.7) give, respectively, the interaction energy of L with O and A . The final forms retained in eqs (2.6.5), (2.6.6) and (2.6.7) are ones which facilitate further evaluation, as we shall discuss in the remainder of this section.

We consider first the interaction energy \mathcal{E}^{L-O} between the dislocation L and other sources O of internal strain. Equation (2.6.6) may be simplified by a judicious application of Gauss' theorem if we take V as the volume bounded by the external surface S and a surface cap surrounding L as is shown in Fig. 2.6. Within this region V , the integrand of eq. (2.6.6) is well-behaved since $\sigma_{ij}^O u_j^{L+I}$ is everywhere continuous and single-valued; note that the alternative expression $\sigma_{ij}^{L+I} u_j^O$ is not suitable since O is a source of internal strain and in V a well-behaved displacement field u_j^O cannot be assumed (e.g. surface cuts may be required around the source of O , just as with L). Applying Gauss' theorem to eq. (2.6.6) with this choice of boundaries for the integration domain V , we obtain

$$\begin{aligned} \mathcal{E}^{L-O} &= \iiint_V (\sigma_{ij}^O u_j^{L+I})_{,i} dV = \oint_{S + S_0^+ + S_0^- + TUBE} \sigma_{ij}^O u_j^{L+I} dS_i \\ &= \iint_{S_0^+ + S_0^-} \sigma_{ij}^O u_j^{L+I} dS_i = b_j \iint_{S_0} \sigma_{ij}^O dS_i. \end{aligned} \quad (2.6.9)$$

The surface integral over S vanishes because of eq. (2.6.3) and the integral over the tube surrounding L vanishes in the limit $r_0 \rightarrow 0$ because of the condition given in eq. (2.5.2). Just as in the case of eq. (2.5.3), we let S_0 be the oriented surface defining the cut (Fig. 2.6) such that the positive unit normal \mathbf{n} on S_0 is given by a right-hand screw rule taken with respect to the positive sense of L . The outward unit normal from V is \mathbf{n} on S_0^- and $-\mathbf{n}$ on S_0^+ . Since $\sigma_{ij}^O u_j^{L+I} = \sigma_{ij}^O u_j^L + \sigma_{ij}^O u_j^I$, the only contribution comes from the u_j^L term because u_j^L is continuous across the cut and the term involving $\sigma_{ij}^O u_j^I$ vanishes, when S_0^+ and S_0^- are collapsed into S_0 . From the definition of the Burgers vector, we can set $u_j^L(S_0^-) - u_j^L(S_0^+) = b_j$. Taking all these factors into account as the sides of the cut are collapsed into S_0 , we obtain the final integral over S_0 given in eq. (2.6.9).

We consider next the interaction energy \mathcal{E}^{L-A} between L and the surface tractions due to A . In view of eq. (2.6.3) and the fact that the A field

is well-behaved throughout V and in particular that $\sigma_{ij}^{L+I} u_j^A$ is continuous and single-valued across the cut, an application of Gauss' theorem in the manner just described shows that the volume integral term in eq. (2.6.7) vanishes; the tube integral vanishes because there can be no body force acting on L . The vanishing of this term is merely Eshelby's statement⁽¹⁹⁾ that there is no interaction strain energy between an external and an internal source of strain. \mathcal{E}^{L-A} is, therefore, given by the surface integral in eq. (2.6.7) and this represents potential energy of the loading mechanism giving rise to the A field. In order to evaluate this surface integral, we use eq. (2.6.8) to write

$$\oint\int\int_V (\sigma_{ij}^A u_j^{L+I})_{,i} dV = \oint\int\int_V (\sigma_{ij}^{L+I} u_j^A)_{,i} dV = 0 \quad (2.6.10)$$

and then apply Gauss' theorem to the first volume integral term in the manner already described, noting that eq. (2.5.2) implies the vanishing of the tube integral. We obtain

$$\oint\int_S \sigma_{ij}^A u_j^{L+I} dS_i = -b_j \int\int_{S_0} \sigma_{ij}^A dS_i. \quad (2.6.11)$$

Upon combining eqs (2.6.7), (2.6.10) and (2.6.11) we have

$$\mathcal{E}^{L-A} = b_j \int\int_{S_0} \sigma_{ij}^A dS_i. \quad (2.6.12)$$

The fact that the work done by the surface tractions acting on S exactly equals the work done over the cut (eq. (2.6.11)) is a consequence of the vanishing interaction strain energy between L and A . Although eqs (2.6.9) and (2.6.12) have the same form, the reader should note that \mathcal{E}^{L-O} is an interaction strain energy, while \mathcal{E}^{L-A} is interaction potential energy of the loading mechanism giving rise to the A field.

Finally, we consider the self energy \mathcal{E}^{SELF} of L as given by eq. (2.6.5). Since the image field I is well-behaved throughout V and $\sigma_{ij}^{L+I} u_j^I$ is continuous across the cut, an application of Gauss' theorem in conjunction with eq. (2.6.3) shows that the second volume integral term in eq. (2.6.5) vanishes. We next apply Gauss' theorem to the first term in eq. (2.6.5), noting that the surface integral over the outer boundary S vanishes because of eq. (2.6.3), and after splitting $\sigma_{ij}^{L+I} = \sigma_{ij}^L + \sigma_{ij}^I$ into its infinite-body and image components we have

$$\mathcal{E}^{SELF} = \mathcal{E}^L + \mathcal{E}^{L-I}, \quad (2.6.13)$$

where

$$\mathcal{E}^L = \frac{1}{2} \oint\oint_{S_0^+ + S_0^- + TUBE} \sigma_{ij}^L u_j^L dS_i, \quad (2.6.14)$$

$$\mathcal{E}^{L-I} = \frac{1}{2} \oint_{S_0^+ + S_0^- + TUBE} \sigma_{ij}^I u_j^L dS_i. \quad (2.6.15)$$

The term \mathcal{E}^L is just the infinite-body self energy of L , i.e. $\mathcal{E}^{SELF} = \mathcal{E}^L$ when the I field vanishes and the outer boundary S of V becomes a boundary at infinity (the contribution from the integral over this boundary can easily be shown to vanish). We identify \mathcal{E}^{L-I} as the image interaction strain energy, which is just the change in \mathcal{E}^{SELF} , relative to the infinite-body case, that results when a finite, free-surface boundary S is introduced. The image interaction energy can be written as

$$\mathcal{E}^{L-I} = \frac{1}{2} b_j \iint_{S_0} \sigma_{ij}^I dS_i \quad (2.6.16)$$

since eq. (2.5.3) implies the vanishing of the tube integral and the integrals over S_0^+ and S_0^- can be reduced to an integral over S_0 by the procedure given earlier. In contrast, the infinite-body self energy \mathcal{E}^L is more difficult to evaluate because σ_{ij}^L becomes infinite at points on L . We cannot take the limit $r_0 \rightarrow 0$ since \mathcal{E}^L would become infinite in that case, i.e. the strain energy density becomes infinite on L . To avoid this singular behaviour, we will exclude from the \mathcal{E}^L evaluation a core of material of radius r_0 coaxial with L (the material within the tube in Fig. 2.6). Noting also that the tube integral need not vanish in the limit $r_0 \rightarrow 0$, we obtain

$$\mathcal{E}^L = \frac{1}{2} b_j \iint_{S_0(r_0)} \sigma_{ij}^L dS_i + \frac{1}{2} \oint_{TUBE} \sigma_{ij}^L u_j^L dS_i. \quad (2.6.17)$$

The tube integral is retained in eq. (2.6.17), along with a finite value of r_0 , for the reasons mentioned, and we write $S_0(r_0)$ to emphasize the fact that the integral over the cut S_0 can be taken only to within a distance r_0 of L . In the linear elastic theory, the infinite-body self energy \mathcal{E}^L can only be obtained if some kind of cutoff procedure is invoked to avoid singular behaviour. The procedure adopted here, viz. excluding a core of material of radius r_0 surrounding the dislocation line L , is a common one and is probably the best choice that can be made, but it is not *a priori* self evident that other procedures cannot be used. The success of any particular procedure must ultimately rest in the agreement which can be achieved between the linear elastic theory and detailed atomistic calculations, i.e. for a suitable choice of the cutoff parameter r_0 , the linear elastic results should match the atomistic results. At present, however, atomistic calculations are intractable for the case of general curvilinear dislocations.

The parameter r_0 used here is called the core radius and we generally assume r_0 to be of the order of the Burgers vector magnitude b , but the precise value cannot be determined by linear elastic theory.⁽⁶⁾ The tube integral which appears in eq. (2.6.1) is known as the “core traction” term and this has been discussed by several authors.^(45,46) In practice, the tube

integral is difficult to evaluate and, therefore, is almost always neglected; however, one should be aware that by itself the first term in eq. (2.6.17) is not independent of the choice of S_0 .

In principle, the self energy \mathcal{E}^L of a general curvilinear dislocation L in an infinite body can be evaluated by combining eqs (2.5.5), (2.4.28) and (2.6.17). It should be clear that the resulting fourfold integration entails a great deal of computational effort and has actually been carried out in very few cases. In Chap. 4 we review calculations of this kind that have been made. As we shall see in the next section, the derivation of the infinite-body self force on a dislocation requires only eq. (2.6.17) and for many applications the actual self energy evaluation need not be made. We must point out that in the case of isotropy, the self energy evaluation is somewhat more tractable. Substituting eqs (2.4.21) and (2.5.5) into (2.6.17), and neglecting the tube integral, the isotropic result may be reduced by an application of Stokes' theorem to a double line integral over L and L' , where L' is a circuit in S_0 parallel to L and separated from it by r_0 .⁽²⁾ A similar double line integral expression has not been found for anisotropy.

We shall now digress briefly and demonstrate that the self energy \mathcal{E}' of an infinite straight dislocation L^∞ in an anisotropic body can be obtained as an expression involving single line integrals, which can be readily evaluated by numerical techniques. For the infinite straight dislocation, we need to use a finite integration volume per unit length of L' in order to obtain a bounded \mathcal{E}' . Figure 4.3 shows a suitable integration volume, which consists of a cylinder coaxial with L' , having inner and outer cutoff radii r_0 and R , respectively. As we shall show in Chap. 4, the displacement field of an infinite straight dislocation is such that the tube integrals over r_0 and R exactly cancel and, hence, the second term in eq. (2.6.17) vanishes so that the first term gives an exact result. To derive \mathcal{E}' for this case, let t be a unit vector along the positive direction of L' (Fig. 2.7) and take $S_0(r_0)$ to be the planar cut extending from r_0 to R as shown in Fig. 4.3. Substituting $\sigma_{ij}^L = C_{ijkl}u_{k,m}$ into eq. (2.6.17), where $u_{k,m}$ is given by eq. (2.5.21), and integrating per unit length of L' over $dS_i = n_i d\lambda$, $r_0 \leq \lambda \leq R$, we obtain for the self energy per unit length of an infinite straight dislocation

$$\mathcal{E}' = B_{kp} b_k b_p \ln \frac{R}{r_0} = E \ln \frac{R}{r_0}, \quad (2.6.18)$$

where E is defined as the prelogarithmic energy factor and

$$\begin{aligned} B_{kp} = \frac{1}{4\pi} & \{ - (nm)_{pj} S_{jk} - (nn)_{pj} (mm)_{ki} Q_{ij} \\ & + (nn)_{pj} (mn)_{ki} (nn)_{ir}^{-1} [S_{jr} + (nm)_{rw} Q_{wj}] \}. \end{aligned} \quad (2.6.19)$$

This expression for B_{kp} is an alternative to the one which is given in

Chap. 4. If we substitute eq. (2.6.19) into eq. (2.5.21), the distortions can be written as

$$u_{j,s} = \frac{b_k}{2\pi\rho} \left\{ -m_s S_{jk} + n_s(nn)_{jp}^{-1} [4\pi B_{kp} + (nm)_{pr} S_{rk}] \right\}, \quad (2.6.20)$$

which reproduces eq. (4.1.16). As was already mentioned, a complete discussion of the infinite straight dislocation field quantities is given in Chap. 4.

2.6.2. Forces

The force on a dislocation L is a generalized force in the thermodynamic sense. It is not the resolution of any actual interatomic forces, rather it is related to the variation of an appropriate potential function (e.g. Gibbs free energy) taken with respect to a virtual change in the configuration of L . It is convenient to classify the forces acting on L into two types. First, there are "external forces" due to stresses whose sources are distinct from L , e.g. other dislocations or applied loads. Second, there are "self forces", which are due to the stress field of L itself, and these forces will include contributions from both the image and infinite-body fields associated with L . The primary distinction to be made here is that at a given point P on L the external forces must be independent of the configuration of L (except for the local orientation of the line at P), whereas the self forces are not.

In order to derive an expression for the external forces, we consider a virtual displacement δx_p in the configuration of L . For the force due to another internal source of stress O , eq. (2.6.9) gives the energy change as

$$\begin{aligned} \delta\epsilon^{L-O} &= \epsilon_{j,p,q} b_i \oint_L \sigma_{ij}^O t_q \delta x_p ds + b_j \iint_{S_0} \delta\sigma_{ij}^O dS_i \\ &= \epsilon_{j,p,q} b_i \oint_L \sigma_{ij}^O t_q \delta x_p ds, \end{aligned} \quad (2.6.21)$$

where t_q is the local unit tangent vector to L at ds . The line integral term in eq. (2.6.21) gives the energy change due to the change in area δS_0 of S_0 , i.e. $n_j \delta S_0 = \epsilon_{j,p,q} \delta x_p t_q ds$, while the second term accounts for the change $\delta\sigma_{ij}^O$ in σ_{ij}^O . Since σ_{ij}^O is independent of L , $\delta\sigma_{ij}^O = 0$ and the second term vanishes. By definition, the distributed force F_p^O per unit length due to O must satisfy

$$\delta\epsilon^{L-O} = - \oint_L F_p^O \delta x_p ds; \quad (2.6.22)$$

hence by combining eqs (2.6.21) and (2.6.22) and recognizing that δx_p is arbitrary, the force per unit length at a given point P on L is

$$F_p^O = -\epsilon_{j,p,q} \sigma_{ij}^O b_i t_q, \quad (2.6.23)$$

which is the familiar Peach-Koehler formula.⁽⁴⁷⁾ The stress σ_{ij}^O and the tangent vector t_q are to be evaluated at the point P on L .

Crystal dislocations normally glide on specific planes and we are often interested in the glide component of the force. We can easily derive this component from the total force given by eq. (2.6.23). Let L be a planar dislocation loop lying in the plane with unit normal \mathbf{n} and let \mathbf{t} be the unit tangent to L at P ; recall that the positive sense for \mathbf{n} is determined by a right-hand screw rule with respect to the positive line direction of L . We assume that \mathbf{b} lies in the glide plane (conservative motion) and we confine all variations of L to be in this plane. Equation (2.6.23) immediately shows that the glide force acts along the in-plane normal $\mathbf{n} \wedge \mathbf{t}$ to L at P . The magnitude F^O of the glide force at P per unit length of dislocation is obtained by resolving \mathbf{F}^O along $\mathbf{n} \wedge \mathbf{t}$, and we obtain

$$F^O = -\epsilon_{jpr} \epsilon_{prs} \sigma_{ij}^O b_i t_q t_s n_r = \sigma_{ij}^O b_i n_j \equiv \tau^O b, \quad (2.6.24)$$

where we have used eq. (2.1.3) and τ^O is defined as indicated. τ^O is the resolved shear stress associated with σ_{ij}^O , i.e. the shear stress in the glide plane resolved along the Burgers vector direction (it is just this component of the stress which does work as the cut faces of the glide plane are displaced by \mathbf{b} and, hence, must determine the force). It is important to realize that eq. (2.6.24) gives F^O as a signed quantity, and if F^O is positive, then the force acts along $+\mathbf{n} \wedge \mathbf{t}$, whereas if it is negative, then it acts along $-\mathbf{n} \wedge \mathbf{t}$.

It should be clear that all of the previous derivations can be repeated starting with eq. (2.6.12) and we then obtain the forces on L due to the applied loads A . Equations (2.6.23) and (2.6.24) again hold, but with the superscripts O replaced by A . Thus, the Peach-Koehler formula is valid for any external force in the sense used here. The reader should notice that the forces due to internal stress sources (O -fields) are due to strain energy changes, whereas the forces due to applied loads (A -fields) are due to changes in the potential energy of the loading mechanism. We shall use the notation τ and σ for resolved shear stresses, which follows that given by Kocks *et al.*⁽⁴⁸⁾ for the purpose of distinguishing a glide resistance τ (strain energy change) from a driving force σ (load mechanism change). Thus, the resolved stress due to another internal defect is denoted by τ^O , while that due to the applied loads is σ^A .

We now wish to derive expressions for the self forces acting on L and we hasten to point out that in the literature one often finds either an incomplete or inconsistent treatment of these forces. Here, we outline a complete, self-consistent treatment. Starting from eq. (2.6.16), the change $\delta\mathcal{E}^{L-I}$ in the image interaction energy due to the variation δx_p in L reads

$$\delta\mathcal{E}^{L-I} = \frac{1}{2} \epsilon_{jpa} b_i \oint_L \sigma_{ij}^I t_q \delta x_p \, ds + \frac{1}{2} b_j \iint_{S_0} \delta \sigma_{ij}^I \, dS_i, \quad (2.6.25)$$

where the two terms have the same identification as in eq. (2.6.21). Since σ_{ij}^I depends on the configuration of L , the second term in eq. (2.6.25) does not vanish and the evaluation of this term is a crucial step in the analysis.

Gavazza and Barnett⁽⁴⁹⁾ have treated this in detail and they show that

$$\begin{aligned} b_j \iint_{S_0} \delta \sigma_{ij}^I dS_i &= b_j \iint_{\delta S_0} \sigma_{ij}^I dS_i \\ &= \epsilon_{jpk} b_i \oint_L \sigma_{ij}^I t_q \delta x_p ds, \end{aligned} \quad (2.6.26)$$

consequently eq. (2.6.25) reduces to

$$\delta \epsilon^{L-I} = \epsilon_{jpk} b_i \oint_L \sigma_{ij}^I t_q \delta x_p ds, \quad (2.6.27)$$

which has exactly the same form as eq. (2.6.21), albeit for different underlying reasons. The relation given in eq. (2.6.26) is by no means obvious and the reader is referred to the original derivation of Gavazza and Barnett for complete details. Equation (2.6.27) corresponds to a strain energy term, but the factor of $\frac{1}{2}$ in eq. (2.6.16) has disappeared because of eq. (2.6.26). The image force F'_p and glide force F^I follow in an obvious fashion from eqs (2.6.23) and (2.6.24), respectively, with the superscripts O replaced by I . The important feature to note here is that the image self force is given correctly with σ_{ij}^I inserted into the Peach-Koehler formula; prior to the derivation of Gavazza and Barnett⁽⁴⁹⁾ there does not appear to have been a rigorous justification of this fact in the literature.

We now consider the self force on L due to its own infinite-body stress field σ_{ij}^I . If for the present we neglect the tube integral, then the variation $\delta \epsilon^L$ of the surface-cut integral in eq. (2.6.17) is required. Although σ_{ij}^I and σ_{ij}^I both depend on L , the analysis for $\delta \epsilon^L$ is not the same as that for $\delta \epsilon^{L-I}$ since the surface integral in eq. (2.6.17) extends over $S_0(r_0)$ and not over S_0 as in eq. (2.6.16), i.e. for the infinite-body field, we can integrate only to within a distance r_0 of L for reasons already mentioned. The analysis for $\delta \epsilon^L$ is rather lengthy, and we have given it in the Appendix. For clarity, it is easiest to restrict the derivation to glide forces and this is what appears in the Appendix. If F^L denotes the glide component of the self force per unit length at some given point P on the planar dislocation L due to σ_{ij}^I , then we have (Appendix)

$$F^L = \bar{\sigma}_{ij}^I b_i n_j + \kappa E(t) \equiv b \tau^L,$$

where

$$\bar{\sigma}_{ij}^I = \frac{1}{2} [\sigma_{ij}^I|_{r_0} + \sigma_{ij}^I|_{-r_0}]. \quad (2.6.28)$$

In eq. (2.6.28), $E(t)$ is the prelogarithmic energy factor for an infinite straight dislocation lying along the tangent t to L at P and having the same Burgers vector as L , κ is the curvature at P (κ is always considered to be a positive number) and the remaining quantities have their usual meaning. The quantity τ^L defined by eq. (2.6.28) has the dimensions of stress and is called the "self stress" of the dislocation L .

The reader should recognize that although the term $\bar{\sigma}_{ij}^L b_i n_j$ in eq. (2.6.28) bears a formal resemblance to the term $\sigma_{ij}^X b_i n_j$, $X = A, O, I$, in the Peach-Koehler glide force formula, eq. (2.6.24), the former is not $\sigma_{ij}^L b_i n_j$ evaluated at P , as might be suggested by the Peach-Koehler analogy. Instead, $\bar{\sigma}_{ij}^L b_i n_j$ is the average in the glide plane of $\sigma_{ij}^L b_i n_j$ measured at points $\pm r_0$ away from P along the in-plane normal $n \wedge t$ to L at P . Some average of this type is required since σ_{ij}^L diverges as P is approached and $\sigma_{ij}^L b_i n_j$ would be infinite there. The particular form of F^L given in eq. (2.6.28) is a consequence of our method for calculating the self energy of L , viz. excluding a tube of material of radius r_0 surrounding L in order to avoid infinite self energy and this form is entirely self consistent in the sense of energy variations. The $\bar{\sigma}_{ij}^L b_i n_j$ term in eq. (2.6.28) was derived earlier by Brown⁽⁵⁰⁾ on the basis of a heuristic argument and this term alone is not self consistent; the $\kappa E(t)$ term removes the inconsistencies (see Appendix). The various signs which appear in eqs (2.6.24) and (2.6.28) are a result of our sign conventions for determining the force directions and we shall discuss this further later. In deriving the forces and sign conventions, we always relate the force to the negative of the energy variations, as is the common practice. The reader should also be aware that the self force F^L contains the arbitrary parameter r_0 and this parameter must always be carried through in linear elastic theory. For an infinite straight dislocation, the self force F^L vanishes since $\bar{\sigma}_{ij}^L$ in eq. (2.6.28) vanishes in this case. In deriving eq. (2.6.28), we have ignored the tube integral in eq. (2.6.17), and the effect of this on the self force is discussed in the Appendix.

If the planar dislocation loop L is to be in static equilibrium with respect to glide, then we must have that

$$\delta\epsilon^{TOT} = \delta\epsilon^{L-O} + \delta\epsilon^{L-A} + \delta\epsilon^{L-I} + \delta\epsilon^L = 0. \quad (2.6.29)$$

for arbitrary variations of L in its glide plane. In terms of the forces already discussed, we can write this as

$$F^O + F^A + F^I + F^L = 0$$

or

$$\tau^O b + \sigma^A b + \tau^I b + \tau^L b = 0, \quad (2.6.30)$$

which must hold at every point P on L which is free to vary. Although scalar terms appear in eq. (2.6.30), each force must be calculated as a signed quantity from the equations already given; then the direction of the force along the in-plane normal $n \wedge t$ to L must be determined, and the forces added vectorially. The sign conventions for the force directions are important for application purposes and we shall now outline these conventions.

Forces determined from the Peach-Koehler glide force, eq. (2.6.24), have been defined such that a positive force acts along $+n \wedge t$, while a negative force acts along $-n \wedge t$. Recall that t is the unit tangent to L with positive sense along the arbitrarily chosen positive line direction and n is the unit

normal to the glide plane with positive sense given by a right-hand screw rule taken with respect to the positive line direction. The direction of the self force F^L is given as follows: at a point P on L , let \mathbf{m} be the unit vector in the direction of the in-plane curvature vector $\boldsymbol{\kappa} = \kappa \mathbf{m} = d\mathbf{t}/ds$, where ds denotes the arc length along L and κ is always taken as a positive number. Note that \mathbf{m} lies in the glide plane and is directed along $\pm \mathbf{n} \wedge \mathbf{t}$. As discussed in the Appendix, if the sign of F^L determined from eq. (2.6.28) is positive, then the self force acts along $-\mathbf{m}$, whereas if the sign is negative, the force acts along $+\mathbf{m}$. As an example, consider the loop shown in Fig. A.1 of the Appendix. The vector $\mathbf{n} \wedge \mathbf{t}$ is the same at points A and B , whereas $\mathbf{m} = \mathbf{n} \wedge \mathbf{t}$ at A and $\mathbf{m} = -\mathbf{n} \wedge \mathbf{t}$ at B . Now suppose eq. (2.6.24) gives a force (due say to an applied stress) $F^A = +1$ at both points A and B , while eq. (2.6.28) gives $F^L = -1$ at both A and B . In this case our sign conventions show that the forces are balanced at B , but there is a net force of $+2$ acting along $\mathbf{n} \wedge \mathbf{t}$ at A . In other words, eq. (2.6.30) must be used as a vector equation for complex loop shapes in conjunction with the sign conventions already given. For convex planar loops we have that $\mathbf{m} = \mathbf{n} \wedge \mathbf{t}$ always and in this case we can use eq. (2.6.30) as a simple algebraic equation (we must in fact change $+F^L$ to $-F^L$ in eq. (2.6.30) so that positive forces are all directed along $+\mathbf{n} \wedge \mathbf{t}$).

At this point we wish to make a few remarks concerning the “line-tension approximation”, which is widely used in the literature for determining the dislocation self force. The line tension approximation rests upon the basic assumption that we can replace eq. (2.6.17) by

$$\mathcal{E}^L = \oint_L \mathcal{E}^\infty(\mathbf{t}) ds, \quad (2.6.31)$$

where $\mathcal{E}^\infty(\mathbf{t})$ is the energy per unit length of an infinite straight dislocation lying along the local tangent \mathbf{t} to L at ds and having the same Burgers vector as L . If we calculate $\delta\mathcal{E}^L$ from eq. (2.6.31) and define the force in the usual manner, we obtain the glide force at a point P on a planar loop $L^{(51,23)}$

$$F^L = -\kappa\Gamma \equiv \tau^L b, \quad (2.6.32)$$

where the “line tension” Γ is defined as

$$\begin{aligned} \Gamma &= \mathcal{E}^\infty(\theta) + \frac{d^2\mathcal{E}^\infty(\theta)}{d\theta^2} \\ &= \left[E(\theta) + \frac{d^2E(\theta)}{d\theta^2} \right] \ln \frac{R}{r_0} \end{aligned} \quad (2.6.33)$$

and θ is the angle between an arbitrary reference datum in the glide plane, e.g. the Burgers vector direction, and the tangent \mathbf{t} to L at P . κ is again the curvature at P (a positive number). If the force calculated from eq.

(2.6.32) is negative, then it acts along $+m$ and vice versa, just as in the case of eq. (2.6.28). In an isotropic body, the line tension is always positive (so that F^L acts along $+m$), but in an anisotropic body it can be negative, as will be discussed in Section 4.1.3.

The reader should recognize an important difference between eqs (2.6.28) and (2.6.32); viz. that the self force F^L computed from the latter depends only on the local geometric properties, i.e. curvature κ and tangent orientation θ at P , whereas the force given by eq. (2.6.28) depends on the entire configuration of L because for any given P , σ_{ij}^L must be obtained as a line integral over L . Consequently, when eq. (2.6.32) is combined with eq. (2.6.30), an ordinary differential equation governing static equilibrium results, but when eq. (2.6.28) is used, a complicated integro-differential equation results. The mathematical simplification offered by the line tension approximation is its chief advantage. As we show in the Appendix, the self force given by eq. (2.6.28) can be written in such a way that we can separate out an additive part $\kappa E(\theta) - \kappa [E(\theta) + d^2E(\theta)/d\theta^2]$ $\ln(8a/r_0)$, which depends only on the local geometry at P ; $a = \kappa^{-1}$ is the radius of curvature at P . Another additive term $J(L)$ also contributes and this must be obtained as an integral over the configuration of L (see eq. (A.8)). It is possible, therefore, that the self force obtained from eq. (2.6.28) behaves, in certain situations, like a line tension self force if the contribution proportional to $E(\theta) + d^2E(\theta)/d\theta^2$ happens to dominate. In this case the line tension approximation would be appropriate, but it is by no means obvious when such behaviour obtains and this must be investigated for each problem at hand. Also, when using the line tension self force, some value must be chosen for the outer cutoff radius R in eq. (2.6.33) and there is no unambiguous prescription for this.

When static equilibrium shapes of a planar glide dislocation are determined using eqs (2.6.28) and (2.6.30), we call the method the “self stress” method since it basically involves calculating the self stress τ^L as defined in eq. (2.6.28) and then finding the configuration L for which eq. (2.6.30) holds at every point P on L which is free to vary (not rigidly pinned by obstacles, etc.). In Chap. 4 we will discuss the geometrical theorems which, when combined with the straight dislocation field data, provide a computationally convenient method with which to numerically calculate E and σ_{ij}^L , and therefore τ^L , in media of arbitrary elastic anisotropy. In actually evaluating τ^L at some point P on L , the approach used by several investigators has been the following: the configuration L is represented by a set of finite dislocation segments such that the segment containing P is a circular arc (to approximate the curvature at P), while the remaining segments are straight (the field due to straight segments can be given in very simple form, as will be discussed in Section 4.2.3); expressions for the contributions from these finite segments can be obtained from the geometrical theorems and τ^L is obtained numerically as a summation over the segments. Once a method for evaluating τ^L has been developed,

it remains to develop a suitable computer-based algorithm to "relax" the dislocation L into the equilibrium configuration satisfying eq. (2.6.30) under the acting forces. Such an algorithm must be developed for each problem since, as yet, there is no general method for solution of the integro-differential static equilibrium equation. In Section 4.3, we review a number of dislocation theory problems which have been investigated using this approach.

In summary, we emphasize that eq. (2.6.28) gives the correct linear elastic self force acting on a dislocation L . The line tension approximation manifest in eq. (2.6.32) cannot be rigorously justified since there is no physical basis for eq. (2.6.31). In this context, the "self interactions" of a dislocation, i.e. the influence of its own elastic field on the determination of its configuration, can only be properly taken into account through the use of eq. (2.6.28). Furthermore, it is clear that the line tension approximation can only account for the self interactions insofar as they are determined at any point P on L by the local geometry at P , i.e. the curvature and tangent orientation. If the remainder of the configuration of L exerts an influence on P , as it certainly will if the more distant parts of L bend about such that they lie close to P , then only the self-stress method can properly capture the true interactions. When using the line tension analysis, one sometimes tries to account for the total self interaction by a judicious choice of the outer cutoff radius R , but any such choice can be made only in the sense that it seems intuitively to be physically reasonable. The rigorous selection of some interaction distance R can only be made by matching self-stress calculations to formulae deduced by line tension analysis, empirically fitting to obtain a value for R . Some of the problems discussed in Section 4.3 have been analyzed in this way. It is also important to note that with the methods discussed in Chap. 4 for the determination of σ_{ij}^L and E , a correct computation of τ^L can be made for the general anisotropic case with almost no more effort than for isotropy; hence, the self-stress method can easily be extended to include both the proper dislocation interactions and the elastic anisotropy. (For line tension calculations, anisotropy is also easily included by using the methods outlined in Section 4.1.3 for the evaluation of $E + d^2E/d\theta^2$.)

2.7. Green's Function Representation for Point Force Arrays

In this section we shall consider the Green's function representation of the displacement field due to an arbitrary arrangement of discrete point forces in an infinite, homogeneous anisotropic elastic body. As we shall see in Chap. 5, certain point force arrays can be used as models for point defects in crystals. We should mention here that a Green's function appropriate to a lattice of interacting atoms can be defined and in the harmonic approximation this finds wide use in constructing defect models

based on a discrete lattice. In this section, however, we consider only the elastic fields of point force arrays as they are obtained using the continuum Green's function discussed in Section 2.4. As might be expected, the continuum Green's function is the long-wavelength limit of the lattice Green's function.^(52,53)

2.7.1. Multipole expansion formula and infinitesimal force dipoles

Let $u_i(\mathbf{x})$ be the displacement at \mathbf{x} due to the array of point forces \mathbf{F}^q located at $\mathbf{x}' + \mathbf{a}^q$, $q = 1, 2, \dots, N$, as shown in Fig. 2.8. The centre of the point force array is assumed to be at \mathbf{x}' . From the definition of the Green's tensor G_{ij} , we can write that

$$u_i(\mathbf{x}) = \sum_{q=1}^N G_{ij}(\mathbf{x} - \mathbf{x}' - \mathbf{a}^q) F_j^q. \quad (2.7.1)$$

This equation may be evaluated numerically in the general anisotropic case using eq. (2.4.18) for G_{ij} . Stresses and strains may be obtained directly from the gradient of eq. (2.7.1) using the appropriate derivatives of G_{ij} and the latter may be evaluated using eq. (2.4.28). An alternative expression for $u_i(\mathbf{x})$ is possible in terms of a multipole expansion formula analogous to those used in electrostatics.⁽⁵⁴⁾ First, expand G_{ij} in a Taylor series around $\mathbf{x} - \mathbf{x}'$

$$G_{ij}(\mathbf{x} - \mathbf{x}' - \mathbf{a}^q) = \sum_{n=0}^{\infty} \frac{(-1)^n}{n!} G_{ij,s_1 \dots s_n}(\mathbf{x} - \mathbf{x}') a_{s_1}^q \dots a_{s_n}^q, \quad (2.7.2)$$

where there is to be no summation on repeated superscripts q unless shown explicitly. Now combine eqs (2.7.1) and (2.7.2) to obtain the multipole expansion formula given by Siems⁽⁵²⁾

$$u_i(\mathbf{x}) = \sum_{n=0}^{\infty} \frac{(-1)^n}{n!} P_{s_1 \dots s_n j} G_{ij,s_1 \dots s_n}(\mathbf{x} - \mathbf{x}'), \quad (2.7.3)$$

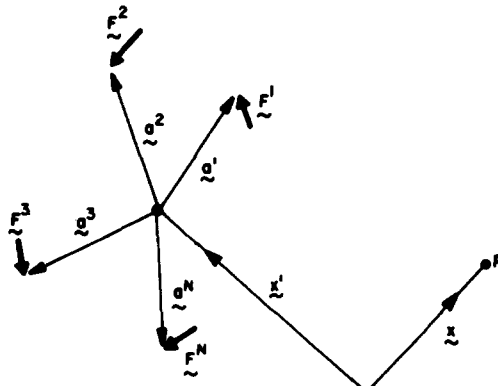


FIG. 2.8. Schematic diagram of a set of discrete point forces \mathbf{F}^q acting at positions \mathbf{a}^q relative to the array centre at \mathbf{x}' . The field point P is at \mathbf{x} as shown.

where

$$P_{s_1 \dots s_n j} = \sum_{q=1}^N F_j^q a_{s_1}^q \dots a_{s_n}^q.$$

The multipole tensors P_j , P_{sj} (dipole tensor), P_{srj} (quadrupole tensor), P_{srkj} (octopole tensor), etc. correspond to the various moments of the point force array, with P_j , P_{sj} , P_{srj} , ... being, respectively, the zeroth, first, second, ... moments. If the point force array produces no net force or moment within the containing body, static equilibrium requires that $P_j = 0$ and $P_{sj} = P_{js}$, and we shall, hereafter, assume this to always be the case. Furthermore, as will be seen in Section 5.1, models for point defects can be constructed using point forces which act at what would be the atom positions around the defect in the host crystal under consideration. In this case, the multipole tensors will, for a suitable choice of coordinates, display the symmetry of the defect in the host crystal. One should also note that since G_{ij} is homogeneous of degree -1 in $|x - x'|$, eq. (2.7.3) gives an expansion for $u_i(x)$ in powers of $|x - x'|^{-k}$, $k = 2, 3, 4, \dots$.

It is often convenient to consider a limiting case, in which the separation between the point forces becomes infinitesimal while the force magnitudes become arbitrarily large in such a manner that their products remain finite. For a single pair of antiparallel forces this limit gives the "infinitesimal force dipole", a limiting arrangement which finds frequent use as a basic element in simple models of point defects. Consider the pair of forces $\pm F\mathbf{n}$ acting at $x' \pm am$ as shown in Fig. 2.9, where \mathbf{n} and \mathbf{m} are unit vectors along the force direction and dipole axis, respectively. The multipole tensors for this force pair can be written as

$$P_{s_1 \dots s_k j} = 2Fa^k n_j m_{s_1} \dots m_{s_k} \text{ for even rank (odd } k) \quad (2.7.4)$$

$$= 0 \text{ for odd rank (even } k).$$

If the force pair in Fig. 2.9 is to produce no net moment, then \mathbf{n} and \mathbf{m} must be collinear (a single force pair within a force array could have

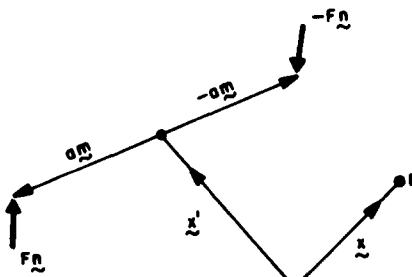


FIG. 2.9. Schematic diagram of a pair of antiparallel point forces $\pm F\mathbf{n}$ acting at $\pm am$ relative to the centre at x' . The field point P is at x as shown. The unit vector \mathbf{n} gives the force direction, while the unit vector \mathbf{m} gives the dipole axis. The unit vectors \mathbf{m} and \mathbf{n} need not be collinear in this geometry.

a net moment, but the array as a whole may not). We now take the limit $a \rightarrow 0$ such that the product Fa remains constant. In this limit, eq. (2.7.4) reduces to

$$P_{sj} = P n_j m_s, \quad (2.7.5)$$

where

$$P \equiv \lim_{a \rightarrow 0} (2Fa) \quad (2.7.6)$$

and all higher rank multipole tensors vanish, i.e. for $k > 1$ the products Fa^k vanish so that only the dipole tensor survives. The quantity P is called the "dipole strength". The displacement field for the infinitesimal force dipole is given by eq. (2.7.3)

$$u_i(x) = -PG_{ij,s}(x - x')n_j m_s. \quad (2.7.7)$$

It should be clear that in the limit of infinitesimal force separations, the displacement field of a point force array like that shown in Fig. 2.8 is determined exactly by the dipole tensor of the array. On the other hand, since G_{ij} is homogeneous of degree -1 in $|x - x'|$, the displacements at large distances $|x - x'|$ from a finitely-separated point force array, relative to the maximum distances $|a|$ between the forces in the array, are given to first order in $|a|/|x - x'|$ by the dipole tensor term in eq. (2.7.3), i.e. the far field of a point force array is dominated by the dipole terms.

Figure 2.10 shows a useful arrangement of infinitesimal force dipoles, in which there are three identical, orthogonal, moment-free dipoles. For convenience, we assume the dipoles to lie along the coordinate axes. With P given by eq. (2.7.6) the dipole tensor for the cubically symmetrical arrangement shown in Fig. 2.10 becomes

$$P_{sj} = \pm P \delta_{sj}; \quad (2.7.8)$$

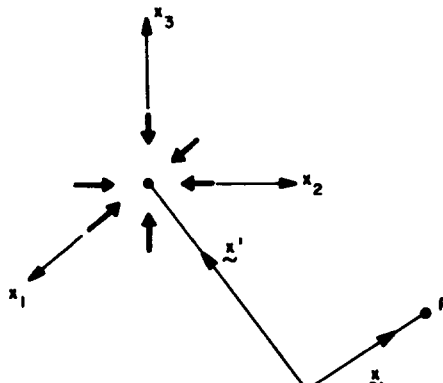


FIG. 2.10. Schematic diagram of three, identical, moment-free force dipoles centred at x' . The field point P is at x as shown. The dipoles are assumed to lie along the coordinate axes x_1, x_2, x_3 , and a centre of compression is shown.

hence

$$u_i(x) = \mp P G_{ij,s}(x - x'), \quad (2.7.9)$$

where the plus sign in eq. (2.7.8) holds for forces acting away from the array centre, while the minus sign holds when they act toward the centre (the converse holds for eq. (2.7.9)). When the forces act toward the centre, we have a “centre of compression”, whereas when they act away we have a “centre of dilatation”.⁽¹⁸⁾ For situations possessing cubic symmetry, centres of compression and dilatation are often used as elementary models for point defects, as will be discussed in Section 5.1.

Equation (2.7.7) demonstrates that $G_{ij,s}$ is directly related to the displacement field of an infinitesimal force dipole: $G_{ij,s}(x - x')$ gives the x_i component of the (negative) displacement at x due to a unit strength dipole at x' having forces along x_j and axis along x_s . Based on this, we might attempt to interpret some of the results derived earlier for dislocations in terms of force-dipole “sources” or “nuclei of strain”. As was already mentioned, the integrand of eq. (2.5.3) may be viewed as the displacement due to an infinitesimal dislocation loop or, in other words, an elementary “displacement dipole”, which produces the required displacement discontinuity b_k across dS_p . On the other hand, in view of the fact that $G_{ij,s}$ represents the displacement from a force dipole, we may consider the displacement from the infinitesimal loop dS_p , as represented by the integrand of eq. (2.5.3), to be the result of an appropriate combination of infinitesimal force dipoles, the strength of which is determined by the C_{kpim} factor. As a more specific example of this latter interpretation, consider a dislocation loop L with surface cut S_0 lying in the x_3 plane in an anisotropic body having cubic symmetry. If L is a pure edge loop, \mathbf{b} and \mathbf{n} lie along the x_3 axis and eqs (2.3.22) and (2.5.3) yield for the displacement field of L

$$\begin{aligned} u_j(x) = & \pm b \left[C_{12} \iint_{S_0} G_{jk,k}(x - x') dS' \right. \\ & \left. + (C_{11} - C_{12}) \iint_{S_0} G_{j3,3}(x - x') dS' \right], \end{aligned} \quad (2.7.10)$$

where here we use an unprimed subscript for the differentiation. Equations (2.7.7) and (2.7.9) show that we may consider the edge loop to be a result of a planar sheet S_0 of dilatation or compression centres (depending on the sense of \mathbf{b}) plus a sheet of single dipoles without moment aligned along the x_3 axis. If we apply the same rationale to a pure shear loop L , exactly as in the previous case except that now \mathbf{b} lies along the x_2 axis, we find the displacements to be

$$u_j(x) = \pm b C_{44} \iint [G_{j2,3}(x - x') + G_{j3,2}(x - x')] dS'. \quad (2.7.11)$$

The sources here are comprised of a planar sheet of two orthogonal dipoles

with moment, having forces along x_2 and axis along x_3 , and vice versa. Some care must be exercised when interpreting the dislocation field in terms of force dipole sources. For example, one might intuitively feel that the elastic field of a pure edge loop is identical with that of a sheet of coalesced vacancies or interstitials and that the vacancies or interstitials themselves should be represented in terms of force dipoles with the natural interpretation being that these point defects are to be considered as centres of compression or dilatation, respectively (Section 5.1). However, eq. (2.7.10) shows that the dislocation field is not simply the result of a sheet S_0 of dilatation or compression centres. As Groves and Bacon⁽⁵⁵⁾ have noted, a dislocation must be defined in terms of displacement boundary conditions or displacement dipole sources and, therefore, the interpretation in terms of force dipole sources may not have an obvious physical rationalization.

2.7.2. Interaction energy

The interaction energy between a point force array and other sources of stress is a quantity of physical interest. We shall treat the force array shown in Fig. 2.8 as a distribution of body force, recognizing that in the case of internal defects modelled by such arrays the potential energy of the mechanism responsible for the forces is actually internal energy, i.e. the defect forces exerted on the host medium by, say, a misfitting impurity atom are caused by the perturbed interatomic potential.

Consider a finite body of volume V bounded by the surface S and let the superscripts L , I , O and A denote, respectively, the infinite-body and image fields for the point force array L and the fields associated with an internal source of strain O or externally applied surface tractions A ; an image field to satisfy free surface conditions is possible in this case because we have assumed the force array to be internally self equilibrated ($P_j = 0$ and $P_{sj} = P_{js}$). The total displacement, stress and strain fields are given by eq. (2.6.1) where the superscript L now refers to the point force array. The total energy of the system is

$$\mathcal{E}^{TOT} = \frac{1}{2} \oint \int \int_V \sigma_{ij} e_{ij} dV - \oint \int \int_V f_i u_i dV - \oint \int_S \sigma_{ij}^A u_j dS_i, \quad (2.7.12)$$

where $f_i = -\sigma_{ij,j}^L$ is the body force density appropriate to the point force array L . The second term in this equation accounts for the potential energy of the mechanism giving rise to the forces f , while the remaining terms have the same identification as in eq. (2.6.2). For internal defects, the first two terms may be identified with strain energy, the second term being the internal work done by the forces f .

In contrast to dislocations, we are usually not interested in the elastic self energy of a point force array; therefore, we shall confine our attention to the interaction energy \mathcal{E}^{L-O} or \mathcal{E}^{L-A} between L and O or A , respectively. Using eq. (2.6.1) to expand eq. (2.7.12) and retaining only the relevant inter-

action (cross) terms, we obtain

$$\begin{aligned}\mathcal{E}^{L-O} &= \oint\int\int_V (\sigma_{ij}^O u_j^{L+I})_{,i} dV - \oint\int\int f_i u_i^O dV, \\ \mathcal{E}^{L-A} &= \oint\int\int_V (\sigma_{ij}^A u_j^{L+I})_{,i} dV - \oint\int\int f_i u_i^A dV - \oint\int_S \sigma_{ij}^A u_j^{L+I} dS_i,\end{aligned}$$

where the integrands in the leading volume integral terms have been reduced using eq. (2.6.8). Noting that u_j^{L+I} will be sufficiently well-behaved in V (although σ_{ij}^L may not), a straightforward application of Gauss' theorem shows that the first term in \mathcal{E}^{L-O} vanishes, since $\sigma_{ij}^O n_i = 0$ on S , while the first and third terms in \mathcal{E}^{L-A} cancel. For the general situation, the result reads

$$\mathcal{E}^{L-A} = - \oint\int\int_V f_i u_i^A dV \quad (2.7.13)$$

and for convenience we use the superscript A to denote either internal or external sources. The reader should note that if L is due to internal defect forces, then \mathcal{E}^{L-O} represents strain energy, whereas \mathcal{E}^{L-A} represents potential energy of the loading mechanism associated with A . In the latter case, the strain energy terms vanish because

$$\begin{aligned}& \oint\int\int_V (\sigma_{ij}^A u_j^{L+I})_{,i} dV - \oint\int\int_V f_i u_i^A dV \\ &= \oint\int\int_V \sigma_{ij}^{L+I} e_{ij}^A dV - \oint\int\int_V f_i u_i^A dV \\ &= \oint\int\int_V (\sigma_{ij}^{L+I} u_j^A)_{,i} dV - \oint\int\int_V (\sigma_{ij,j}^{L+I} + f_i) u_i^A dV \\ &= \oint\int_S \sigma_{ij}^{L+I} u_j^A dS_i - \oint\int\int_V (\sigma_{ij,j}^{L+I} + f_i) u_i^A dV = 0\end{aligned}$$

using $\sigma_{ij,j}^{L+I} = \sigma_{ij,j}^L = -f_i$ and $\sigma_{ij}^{L+I} n_i = 0$ on S (we have assumed σ_{ij}^L well-behaved in V , but the same result is reached if we surround each point force by a spherical interior surface with radius $\epsilon \rightarrow 0$).

For the discrete point force array shown in Fig. 2.8 we can write eq. (2.7.13) as

$$\begin{aligned}\mathcal{E}^{L-A} &= - \oint\int\int_V \sum_{q=1}^N F_q^q \delta(\mathbf{x} - \mathbf{x}' - \mathbf{a}^q) u_i^A(\mathbf{x}) dV, \\ &= - \sum_{q=1}^N F_q^q u_i^A(\mathbf{x}' + \mathbf{a}^q) \\ &= - \sum_{q=1}^N F_q^q \sum_{n=0}^{\infty} \frac{1}{n!} u_{i,s_1 \dots s_n}^A(\mathbf{x}') a_{s_1}^q \dots a_{s_n}^q \\ &= - \sum_{n=1}^{\infty} \frac{1}{n!} P_{s_1 \dots s_n} u_{i,s_1 \dots s_n}^A(\mathbf{x}),\end{aligned} \quad (2.7.14)$$

where the last two relations follow after expanding $u_i^A(\mathbf{x}' + \mathbf{a}^q)$ in a Taylor series around \mathbf{x}' and noting $P_i = 0$. If the force separations are taken to the infinitesimal limit mentioned earlier or the source A is sufficiently far from the point force array, or the A field is itself uniform (e.g. due to applied loads), then only the dipole term contributes to ϵ^{L-A} and we have

$$\epsilon^{L-A} = -P_{si}u_{i,s'}^A(\mathbf{x}') = -P_{si}e_{is'}^A(\mathbf{x}'), \quad (2.7.15)$$

where $e_{is'}^A(\mathbf{x}')$ is the strain due to A , evaluated at the array centre \mathbf{x}' . If A is a dislocation, we may calculate ϵ^{L-A} from eq. (2.7.15), in which case the dislocation displacement derivatives must be evaluated, or from eq. (2.6.12), in which case the roles of the superscripts L and A are interchanged and we must evaluate the stresses due to the point force array. It should be clear that these two alternatives are equivalent approaches (an explicit derivation of this equivalence will be given in Section 4.3.2). In Section 4.3.2 we discuss methods whereby dislocation-point defect interaction energies may be evaluated numerically for the general anisotropic case; eq. (2.7.15) has often been used for such evaluations.

If A and B are two point force arrays centred at \mathbf{x} and \mathbf{x}' , and if we let the superscripts A and B denote quantities associated with the respective arrays, then the mutual interaction energy ϵ^{A-B} between A and B is obtained by combining eqs (2.7.3) and (2.7.14). Using $P_i = 0$, the result reads

$$\epsilon^{A-B} = -\sum_{n=1}^{\infty} \sum_{m=1}^{\infty} \frac{(-1)^n}{n! m!} P_{s_1 \dots s_n j}^A P_{r_1 \dots r_m i}^B G_{ij, s_1 \dots s_n r_1 \dots r_m}(\mathbf{x} - \mathbf{x}'), \quad (2.7.16)$$

where $|\mathbf{x} - \mathbf{x}'|$ gives the distance between A and B . Siems⁽⁵²⁾ has used eq. (2.7.16) to rationalize the nature of the interaction between point defects, especially when comparing the results of continuum and lattice models, and we shall discuss this further in Section 5.1. The interaction forces are simply derived from the negative gradients of ϵ^{L-A} or ϵ^{A-B} .

2.7.3. Continuous distributions of forces

The whole of the discussion in this section has been focused on arrays of discrete point forces, but the reader should recognize the fact that the discussion can be carried over to continuous distributions of forces. In particular, the summation in eq. (2.7.1) can be replaced by an integration. Let the volume V in a homogeneous, infinite, anisotropic body contain the body force distribution f and let the boundary surface S of V be acted upon by the tractions T . The resulting displacement at \mathbf{x} must be

$$u_i(\mathbf{x}) = \iiint_V G_{ij}(\mathbf{x} - \mathbf{x}') f_j(\mathbf{x}') dV' + \oint_S G_{ij}(\mathbf{x} - \mathbf{x}') T_j(\mathbf{x}') dS', \quad (2.7.17)$$

which is an obvious analog of eq. (2.7.1) for the case of continuous force distributions. If we assume that the force distribution in eq. (2.7.17) results

from a self-equilibrated stress distribution σ_{ij}^T , then eq. (2.7.17) can be written as

$$u_i(x) = - \iiint_V G_{ij}(x - x') \sigma_{jk,k'}^T(x') dV' + \oint_S G_{ij}(x - x') \sigma_{jk}^T(x') dS'_k. \quad (2.7.18)$$

After transforming the surface integral by Gauss' theorem we obtain

$$u_i(x) = \iiint_V G_{ij,k'}(x - x') \sigma_{jk}^T(x') dV' \quad (2.7.19)$$

and the resulting distortions due to σ_{jk}^T are, therefore,

$$u_{i,s}(x) = - \iiint_V G_{ij,k's}(x - x') \sigma_{jk}^T(x') dV'. \quad (2.7.20)$$

We should point out here that eq. (2.7.20) may be combined with eq. (2.4.22) in order to obtain integral solutions for the distortion field due to σ_{jk}^T . Asaro and Barnett⁽⁵⁶⁾ used this form of eq. (2.7.20) as the starting point in their analysis of polynomial transformation strains in anisotropic bodies, and in Section 5.2 we discuss in detail the concept of transformation strain and its application to misfitting or inhomogeneous inclusions in anisotropic bodies. The reader is referred to that section for further discussion.

Finally, for the sake of completeness, we will outline a method of solution of eq. (2.7.20) for the case in which σ_{jk}^T is constant in V . This method is based on the Radon transform introduced in Section 2.4.2 and, for the case of uniform transformation strain in V ($\sigma_{jk}^T = C_{jki} e_{ip}^T$, where e_{ip}^T is the uniform transformation strain), it provides an alternative to the method developed by Asaro and Barnett⁽⁵⁶⁾ for the general case of polynomial transformation strain. The Radon transform method has the feature that it gives the resultant fields both inside and outside of V and this sometimes proves useful; the transformation strain results discussed in Section 5.2 deal only with interior fields. We discuss the Radon transform method here, rather than in Section 5.2, since it follows directly from our discussion on Green's function solutions in Section 2.4.2.

For uniform σ_{jk}^T , the distortion field given by eq. (2.7.20) may be written

$$\begin{aligned} u_{i,s}(x) &= -\sigma_{jk}^T \iiint_V G_{ij,k's}(x - x') dV' \\ &= -\sigma_{jk}^T \iiint_x h(x') G_{ij,k's}(x - x') dV', \end{aligned} \quad (2.7.21)$$

where $h(x')$ is the shape or characteristic function for V and is defined as

$$\begin{aligned} h(x') &= 1 \text{ if } x' \text{ is contained in } V, \\ &= 0 \text{ otherwise.} \end{aligned}$$

In order to reduce eq. (2.7.21) to a more useful form, we can use Plancherel's theorem in the form^(31,32)

$$\oint_{-\infty}^{\infty} g(x)f(x) dx = -\frac{1}{8\pi^2} \oint_{|z|=1} \left[\int_{-\infty}^{\infty} \hat{g} \frac{\partial^2 \hat{f}}{\partial p^2} dp \right] dS, \quad (2.7.22)$$

where $\hat{f} = \hat{f}(z, p)$ and $\hat{g} = \hat{g}(z, p)$ are the Radon transforms of the arbitrary functions $f(x)$ and $g(x)$, and z, p are the transform variables defined in Section 2.4.2. The surface integral in eq. (2.7.22) is taken over the unit sphere $|z| = 1$. Applying Plancherel's theorem to eq. (2.7.21) with $f(x) = h(x)$ we obtain

$$\begin{aligned} u_{i,s}(x) &= -\frac{\sigma_{jk}^T}{8\pi^2} \oint_{|z|=1} \left[\int_{-\infty}^{\infty} z_k z_s (zz)_{ij}^{-1} \delta(z \cdot x - p) \frac{\partial^2 \hat{h}(z, p)}{\partial p^2} dp \right] dS \\ &= -\frac{\sigma_{jk}^T}{8\pi^2} \oint_{|z|=1} z_k z_s (zz)_{ij}^{-1} \left[\frac{\partial^2 \hat{h}(z, p)}{\partial p^2} \right]_{p=x} dS, \end{aligned} \quad (2.7.23)$$

where $\alpha = z \cdot x$ and we have used eqs (2.4.12) and (2.4.16) to obtain

$$\begin{aligned} (G_{ij,k's}(x - x'))^* &= z_k z_s \frac{\partial^2 \hat{G}_{ij}(z, p - z \cdot x)}{\partial p^2} \\ &= -z_k z_s (zz)_{ij}^{-1} \delta(p - z \cdot x). \end{aligned}$$

Any further simplification requires the evaluation of the Radon transform $\hat{h}(z, p)$ of the characteristic function $h(x')$ for V , and this is facilitated by the fact that for a given x , \hat{h} is the area of intersection of the plane $z \cdot x = \alpha$ with V . To illustrate, for x contained within the interior of an ellipsoidal volume V , it can easily be shown that

$$\hat{h}(z, p) = \frac{\pi a_1 a_2 a_3 (a_k^2 z_k^2 - p^2)}{(a_k^2 z_k^2)^{3/2}}, \quad (2.7.24)$$

where a_1, a_2 and a_3 are the semi-major axes of the ellipse. We then have

$$\left[\frac{\partial^2 \hat{h}(z, p)}{\partial p^2} \right]_{p=x} = -\frac{2\pi a_1 a_2 a_3}{(a_k^2 z_k^2)^{3/2}}, \quad (2.7.25)$$

which is independent of α and, therefore, of x . Combining eqs (2.7.23) and (2.7.25), we see that for a uniform σ_{jk}^T imposed on an ellipsoidal volume V , the resulting interior field is also uniform (the ellipsoid is the most general shape possessing this property). This result provides an alternative derivation of eq. (5.2.9). For x not in V , i.e. the exterior field, eq. (2.7.23) still holds, but the transform \hat{h} is more complicated because not all planes $z \cdot x = \alpha$ will intersect V ; only those planes with unit normal z which both contain x and cut V will make a nonzero contribution to \hat{h} , the value of which is the area of intersection. For x outside of V , \hat{h} thus depends on x in a complicated but known fashion, and the exterior field can in

principle be obtained by this technique. Yoffe⁽³²⁾ has given the explicit evaluation for the case that V is a sphere. We shall not reproduce the details here, but simply remark that eq. (2.7.23) gives a useful result valid for both the interior and exterior field in media of arbitrary anisotropy.

2.8. Summary of Formulae

For convenience, we give in this section a brief summary of the most important equations derived in this chapter. The equation numbers in this section refer to the actual equation numbers in the text.

Traction vector:

$$T_j = \sigma_{ij} n_i. \quad (2.2.1)$$

Static equilibrium in terms of stress:

$$f_j + \sigma_{ij,i} = 0, \quad (2.2.4)$$

$$\sigma_{ij} = \sigma_{ji}. \quad (2.2.8)$$

Infinitesimal (linear) strain:

$$e_{ij} = \frac{1}{2}(u_{i,j} + u_{j,i}). \quad (2.2.13)$$

Hooke's law:

$$\sigma_{ij} = C_{ijkp} e_{kp}, \quad (2.3.1)$$

$$e_{ij} = S_{ijkp} \sigma_{kp}. \quad (2.3.2)$$

Elastic stiffness coefficients (symmetry relations):

$$C_{ijkp} = C_{jikp} = C_{ijpk} = C_{kpji}. \quad (2.3.3)$$

$$(2.3.5)$$

Basic field equation for displacements:

$$C_{ijkp} u_{k,pj} + f_i = 0. \quad (2.3.6)$$

Governing equation for Green's function G_{ij} in an infinite, homogeneous body:

$$C_{kpim} G_{ij,mp}(\mathbf{x} - \mathbf{x}') + \delta_{kj} \delta(\mathbf{x} - \mathbf{x}') = 0, \quad (2.4.2)$$

where G_{ij} has the following properties

$$G_{ij}(\mathbf{x} - \mathbf{x}') = G_{ij}(\mathbf{x}' - \mathbf{x}) = G_{ji}(\mathbf{x} - \mathbf{x}'), \quad (2.4.1)$$

$$G_{ij} = |\mathbf{x} - \mathbf{x}'|^{-1} g_{ij} \quad (2.4.9)$$

and g_{ij} depends only on the orientation of $\mathbf{x} - \mathbf{x}'$.

Solution for displacement field (eq. (2.3.6)) in terms of G_{ij} :

$$\begin{aligned} u_j(x) = & \oint\int_V G_{kj}(x - x') f_k(x') dV' \\ & + \oint\int_S C_{kpim} u_{i,m}(x') G_{kj}(x - x') dS'_p \\ & - \oint\int_S C_{kpim} u_k(x') G_{ij,m}(x - x') dS'_p, \end{aligned} \quad (2.4.7)$$

where V is any volume such that V contains x .

Integral solution for G_{ij} :

$$G_{ij}(x - x') = \frac{1}{8\pi^2 |x - x'|} \oint_{|z|=1} (zz)_{ij}^{-1} ds. \quad (2.4.18)$$

Integral solution for the derivatives of G_{ij} :

$$G_{ij,s_1 \dots s_N}(x - x') = \frac{(-1)^N T_{k_1} \dots T_{k_N}}{8\pi^2 |x - x'|^{N+1}} \oint_{|z|=1} \frac{\partial^N [(zz)_{ij}^{-1} z_{s_1} \dots z_{s_N}]}{\partial z_{k_1} \dots \partial z_{k_N}} ds; \quad (2.4.26)$$

where for eqs (2.4.18) and (2.4.26), $z \cdot T = 0$ and $x = x' = T|x - x'|$. Also see eqs (2.4.28) and (2.4.29).

Dislocation displacement field—Volterra equation:

$$u_j(x) = -b_k C_{kpim} \int \int_{S_0} G_{ij,m}(x - x') dS'_p, \quad (2.5.3)$$

where S_0 is an arbitrary oriented surface bounded by the dislocation line L .

Dislocation distortion field—Mura equation:

$$u_{j,s}(x) = -b_k C_{kpim} \epsilon_{qps} \oint_L G_{ij,m}(x - x') dx'_q \quad (2.5.5)$$

and an alternative form of the Mura equation is,

$$u_{j,s}(x) = b_k C_{kpim} \epsilon_{qpr} \oint_L (x_r - x'_r) G_{ij,ms}(x - x') dx'_q. \quad (2.5.9)$$

Force on a dislocation—Peach-Koehler formula:

$$F_p^X = -\epsilon_{jpr} \sigma_{ij}^X b_i t_q, \quad (2.6.23)$$

where $X = 0, A$ or I to denote another internal defect, applied load or the dislocation image field, respectively.

Glide force on a planar dislocation:

$$F^X = \sigma_{ij}^X b_i n_j, \quad (2.6.24)$$

where X follows from the previous equation.

Glide self-force on a planar (curvilinear) dislocation L :

$$F^L(P) = -\bar{\sigma}_{ij}^L b_i n_j + \kappa E(t), \quad (2.6.28)$$

where κ and t are, respectively, the curvature and tangent at a point P on L , $E(t)$ is the prelogarithmic energy factor of an infinite straight dislocation of orientation t and

$$\bar{\sigma}_{ij}^L = \frac{1}{2}[\sigma_{ij}^L|_{+r_0} + \sigma_{ij}^L|_{-r_0}],$$

where σ_{ij}^L represents the infinite-body dislocation stress field of L and $\bar{\sigma}_{ij}^L$ represents the in-plane average of σ_{ij} at points $\pm r_0$ away from P along the in-plane normal to L at P (see Section 2.6.2 for further discussion).

Displacement field due to infinitesimal force dipole (Fig. 2.9):

$$u_i(x) = -P G_{ij,s}(x - x') n_j m_s, \quad (2.7.7)$$

where

$$P = \lim_{a \rightarrow 0} (2Fa).$$

Displacement field due to three orthogonal infinitesimal force dipoles (Fig. 2.10):

$$u_i(x) = \mp P G_{ij,j}(x - x'). \quad (2.7.9)$$

*3. THE FORMALISM FOR TWO-DIMENSIONAL (PLANE) ELASTIC PROBLEMS

3.1. Statement of the Problem

Consider an infinite homogeneous anisotropic linear elastic solid with elastic constants C_{ijkl} relative to fixed crystal axes. Denote by x the position vector from the origin to a point in the medium and imbed a fixed triad of mutually orthogonal unit vectors m , n and t in the solid (Fig. 3.1) so that

$$m \cdot n = m \cdot t = n \cdot t = 0, \quad (3.1.1)$$

$$m = n \wedge t; n = t \wedge m; t = m \wedge n. \quad (3.1.2)$$

We seek displacement field solutions, u_k , to the equilibrium equations of elasticity which are independent of $t \cdot x$, i.e. we shall investigate a certain class of plane problems in which the elastic fields depend only on two

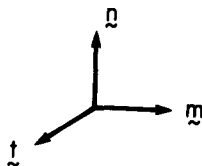


FIG. 3.1. The embedded triad of mutually orthogonal unit vectors m , n and t .

orthogonal coordinates $y_1 = \mathbf{m} \cdot \mathbf{x}$ and $y_2 = \mathbf{n} \cdot \mathbf{x}$ in the plane of \mathbf{m} and \mathbf{n} . Obviously problems involving infinite straight dislocations and lines of force in which the defect line is parallel to \mathbf{t} are members of this class.

3.2. The Sextic Formalism of Stroh

Following Stroh^(5,8) we assume a displacement field solution of the form

$$u_k = A_k f(\mathbf{m} \cdot \mathbf{x} + p\mathbf{n} \cdot \mathbf{x}), \quad (3.2.1)$$

where A is a constant complex vector, p is a complex constant and f is an analytic function of its argument. We seek conditions A and p must satisfy to ensure that the form (3.2.1) is an admissible solution to the static elastic equilibrium equations (eq. (2.3.6)),

$$C_{ijkm} u_{k,mi} = 0 \quad (3.2.2)$$

in the absence of body forces. Letting

$$\lambda = \mathbf{m} \cdot \mathbf{x} + p\mathbf{n} \cdot \mathbf{x} = m_s x_s + p n_s x_s \quad (3.2.3)$$

so that

$$\frac{\partial}{\partial x_s} = \frac{\partial \lambda}{\partial x_s} \frac{d}{d\lambda} = (m_s + p n_s) \frac{d}{d\lambda}, \quad (3.2.4)$$

it is apparent that eq. (3.2.1) satisfies eq. (3.2.2) if

$$C_{ijkm} (m_i + p n_i) (m_m + p n_m) A_k \frac{d^2 f}{d\lambda^2} = 0. \quad (3.2.5)$$

Hence, if we choose A_k and p so that

$$C_{ijkm} (m_i + p n_i) (m_m + p n_m) A_k = 0, \quad (3.2.6)$$

then u_k as given by eq. (3.2.1) is an admissible displacement field for *any* analytic function f .

The three equations represented by eq. (3.2.6) are linear homogeneous algebraic equations for the three A_k and it is well-known that a non-trivial (non-zero) solution A exists provided that

$$\| C_{ijkm} (m_i + p n_i) (m_m + p n_m) \| = 0, \quad (3.2.7)$$

where “ $\| \cdot \|$ ” means “determinant of”. The left side of eq. (3.2.7) is a polynomial of the sixth-degree in p whose six roots $p_\alpha (\alpha = 1, 2, \dots, 6)$ occur in complex conjugate pairs, since the polynomial coefficients are real. Furthermore, none of the six p_α can be purely real for then eq. (3.2.7) would violate the condition of elastic stability given by eq. (3.3.11). Assuming for the moment that the six roots are distinct, corresponding to each p_α is a distinct “eigenvector” $A_{k\alpha}$. We can always arrange to order the eigen-

values p_α so that p_α has a positive imaginary part for $\alpha = 1, 2, 3$ and a negative imaginary part for $\alpha = 4, 5, 6$ with

$$\left. \begin{array}{l} p_{\alpha+3} = p_\alpha^* \\ A_{k,\alpha+3} = A_{k\alpha}^* \end{array} \right\} \alpha = 1, 2, 3, \quad (3.2.8)$$

where * indicates complex conjugation. For a given function f , the most general solution which can be built from the form (3.2.1) is a linear combination of solutions corresponding to each p_α , i.e.

$$u_k = \sum_{\alpha=1}^6 A_{k\alpha} D_\alpha f(\mathbf{m} \cdot \mathbf{x} + p_\alpha \mathbf{n} \cdot \mathbf{x}), \quad (3.2.9)$$

where the D_α are constants, which must be determined by the boundary conditions of the elastic problem under consideration.

Following Stroh we introduce the associated vector \mathbf{L} through the definition⁽⁵⁷⁾

$$L_{j\alpha} = -n_i C_{ijk\alpha}(m_m + p_\alpha n_m) A_{k\alpha} \quad (\text{no sum on } \alpha). \quad (3.2.10)$$

Equation (3.2.6) implies that the alternate definition

$$L_{j\alpha} = \frac{1}{p_\alpha} m_i C_{ijk\alpha}(m_m + p_\alpha n_m) A_{k\alpha} \quad (\text{no sum on } \alpha) \quad (3.2.11)$$

is also valid. Since $A_{k\alpha}$ (and hence $L_{j\alpha}$) are determined only to within an arbitrary complex multiplicative constant, we shall render $A_{k\alpha}$ and $L_{j\alpha}$ unique by the normalization condition

$$2 A_{k\alpha} L_{k\alpha} = 1 \quad (\text{no sum on } \alpha). \quad (3.2.12)$$

The stresses associated with the displacement field given by eq. (3.2.9) are

$$\begin{aligned} \sigma_{ij} &= C_{ijk\alpha} u_{k,m} \\ &= \sum_{\alpha=1}^6 C_{ijk\alpha}(m_m + p_\alpha n_m) A_{k\alpha} D_\alpha \frac{df}{d\lambda_\alpha}, \end{aligned} \quad (3.2.13)$$

where

$$\lambda_\alpha = \mathbf{m} \cdot \mathbf{x} + p_\alpha \mathbf{n} \cdot \mathbf{x} = m_s x_s + p_\alpha n_s x_s.$$

Thus, using the definitions of $L_{j\alpha}$ in eqs (3.2.10) and (3.2.11)

$$\sigma_{ij} n_i = - \sum_{\alpha=1}^6 L_{j\alpha} D_\alpha \frac{df}{d\lambda_\alpha}, \quad (3.2.14)$$

$$\sigma_{ij} m_i = \sum_{\alpha=1}^6 p_\alpha L_{j\alpha} D_\alpha \frac{df}{d\lambda_\alpha}. \quad (3.2.15)$$

Now consider the function

$$\varphi_j = \sum_{\alpha=1}^6 L_{j\alpha} D_\alpha f(\mathbf{m} \cdot \mathbf{x} + p_\alpha \mathbf{n} \cdot \mathbf{x}). \quad (3.2.16)$$

Clearly

$$\varphi_{j,i} = \sum_{x=1}^6 L_{jx} D_x (m_i + p_x n_i) \frac{df}{d\lambda_x}, \quad (3.2.17)$$

so that

$$\sigma_{ij} n_i = -m_i \varphi_{j,i}; \quad \sigma_{ij} m_i = n_i \varphi_{j,i}. \quad (3.2.18)$$

The functions φ_j are the (vector) Airy stress functions for this class of plane anisotropic problems corresponding to the displacement field given by eq. (3.2.9).

Now consider the integral

$$T_j = \oint_C \sigma_{ij} N_i ds,$$

where C is any closed curve in the plane of \mathbf{m} and \mathbf{n} whose unit outer normal at an elemental arc ds is \mathbf{N} . T represents the integrated net traction over C . Since

$$N_i = m_i \cos(\mathbf{N}, \mathbf{m}) + n_i \sin(\mathbf{N}, \mathbf{m}), \quad (3.2.19)$$

where (\mathbf{N}, \mathbf{m}) is the angle between \mathbf{N} and \mathbf{m} measured counter-clockwise from \mathbf{m} , using eq. (3.2.18)

$$T_j = \oint_C \varphi_{j,i} [n_i \cos(\mathbf{N}, \mathbf{m}) - m_i \sin(\mathbf{N}, \mathbf{m})] ds. \quad (3.2.20)$$

However, the tangent to the curve C at ds is merely

$$dx_i = ds [\cos(\mathbf{N}, \mathbf{m}) - \sin(\mathbf{N}, \mathbf{m})]$$

and thus,

$$T_j = \oint_C \varphi_{j,i} dx_i = \oint_C d\varphi_j. \quad (3.2.21)$$

Integration yields

$$T_j = \Delta \varphi_j = \varphi_j(\text{final}) - \varphi_j(\text{initial}). \quad (3.2.22)$$

Hence, if no net body forces (line forces) are present inside C ,

$$\Delta \varphi_j = 0. \quad (3.2.23)$$

If a net line force of strength f_j exists within C , then

$$\Delta \varphi_j = -f_j, \quad (3.2.24)$$

since the material within C must be in force equilibrium. Eqs (3.2.23) and (3.2.24) will serve as boundary conditions for the dislocation and line force solutions to be generated.

3.3. The Extended Sextic Formalism of Stroh

In his 1962 paper, Stroh extended the three-dimensional formalism of Section 3.2 to a six-dimensional framework, from which further important properties of the eigenvectors A_{kx} and L_{jx} may be derived. The present section develops this extension using the notation introduced by Malén and Lothe.⁽⁵⁷⁾ Summation over repeated Latin indices from 1 to 3 is implied; summation over repeated Greek indices will always be indicated explicitly.

The two eqs (3.2.10) and (3.2.11) may be rewritten in the form

$$(nm)_{jk} A_{kx} + L_{jx} = -p_x(nn)_{jk} A_{kx}, \quad (3.3.1)$$

$$(mm)_{jk} A_{kx} = -p_x(mn)_{jk} A_{kx} + p_x L_{jx}, \quad (3.3.2)$$

where we now use the notation defined in eq. (2.1.11)

$$(ab)_{jk} = a_i C_{ijkm} b_m. \quad (3.3.3)$$

Equations (3.3.1) and (3.3.2) contain the equilibrium condition eq. (3.2.6) and may be rewritten using block notation in a six-dimensional framework as

$$\begin{Bmatrix} (nm) & \mathbf{I} \\ (mm) & \mathbf{O} \end{Bmatrix} \begin{Bmatrix} \mathbf{A}_x \\ \mathbf{L}_x \end{Bmatrix} = p_x \begin{Bmatrix} -(nn) & \mathbf{O} \\ -(mn) & \mathbf{I} \end{Bmatrix} \begin{Bmatrix} \mathbf{A}_x \\ \mathbf{L}_x \end{Bmatrix}, \quad (3.3.4)$$

where the six-component column vector

$$\begin{Bmatrix} \mathbf{A}_x \\ \mathbf{L}_x \end{Bmatrix} = \begin{Bmatrix} A_{kx} \\ L_{kx} \end{Bmatrix} = \begin{Bmatrix} A_{1x} \\ A_{2x} \\ A_{3x} \\ L_{1x} \\ L_{2x} \\ L_{3x} \end{Bmatrix} \quad (3.3.5)$$

and \mathbf{I} is the 3×3 unit matrix, i.e. $I_{jk} = \delta_{jk}$.

Premultiplying both sides of eq. (3.3.4) by

$$\begin{Bmatrix} (nn)^{-1} & \mathbf{O} \\ (mn)(nn)^{-1} & -\mathbf{I} \end{Bmatrix}$$

and noting that

$$\begin{Bmatrix} (nn)^{-1} & \mathbf{O} \\ (mn)(nn)^{-1} & -\mathbf{I} \end{Bmatrix} \begin{Bmatrix} -(nn) & \mathbf{O} \\ -(mn) & \mathbf{I} \end{Bmatrix} = -\begin{Bmatrix} \mathbf{I} & \mathbf{O} \\ \mathbf{O} & \mathbf{I} \end{Bmatrix} \quad (3.3.6)$$

we obtain

$$\mathbf{N} \begin{Bmatrix} \mathbf{A}_x \\ \mathbf{L}_x \end{Bmatrix} = p_x \begin{Bmatrix} \mathbf{A}_x \\ \mathbf{L}_x \end{Bmatrix}, \quad (3.3.7)$$

where, in block notation, the 6×6 real matrix N is

$$N = - \begin{Bmatrix} (nn)^{-1}(nm) & (nn)^{-1} \\ (mn)(nn)^{-1}(nm) - (mm) & (mn)(nn)^{-1} \end{Bmatrix}. \quad (3.3.8)$$

Equation (3.3.7) is a standard six-dimensional eigenvalue problem. The eigenvalues p_z are determined from the sextic algebraic equation

$$\|N - p_z I\| = 0. \quad (3.3.9)$$

Corresponding to each eigenvalue p_z is a six-dimensional eigenvector

$$\zeta_z = \begin{Bmatrix} A_z \\ L_z \end{Bmatrix}. \quad (3.3.10)$$

Since N is real the six p_z and the six ζ_z each occur in three complex conjugate pairs, and if the six p_z are distinct (as they are in the general case) then the six ζ_z form a complete set of distinct eigenvectors. There do exist degenerate cases in which the p_z are not distinct; in isotropic media $p_\alpha = i$ ($\alpha = 1, 2, 3$) and $p_\alpha = -i$ ($\alpha = 4, 5, 6$) so that one must employ a mathematical extension in order to construct the appropriate complete set of eigenvectors ζ_z . Such degeneracies shall not concern us here; we merely remark that these special cases may be treated by the limiting process described by Nishioka and Lothe⁽⁵⁸⁾. In fact, in Section 3.5 we shall develop an alternative formalism (the integral formalism) in which such degeneracies never appear.

We digress briefly to point out that construction of the matrix N in eq. (3.3.8) involves the matrix $(nn)^{-1}$. For elastic stability one requires that the strain energy of a deformed solid relative to its undeformed state be positive (Section 2.2.3), so that

$$a_i b_j C_{ijkl} b_k a_l > 0 \quad (3.3.11)$$

for all real non-zero vectors a and b . Thus, the matrix (aa) must always be positive definite, i.e. its three eigenvalues and its determinant are always positive. Taking $a = n$, the existence of $(nn)^{-1}$ is guaranteed.

3.4. Orthogonality and Completeness Relations for the Stroh Eigenvectors

Let us return to the eigenvalue problem, eq. (3.3.7), in order to deduce an important relation involving the eigenvectors A_{kz} and L_{kz} . Consider the eigenvalue problem for two distinct eigenvalues p_z and p_β ($\alpha \neq \beta$), i.e.

$$N \begin{Bmatrix} A_z \\ L_z \end{Bmatrix} = p_z \begin{Bmatrix} A_z \\ L_z \end{Bmatrix} \quad (3.4.1)$$

and

$$N \begin{Bmatrix} A_\beta \\ L_\beta \end{Bmatrix} = p_\beta \begin{Bmatrix} A_\beta \\ L_\beta \end{Bmatrix}. \quad (3.4.2)$$

Premultiplying eq. (3.4.1) by the 1×6 row matrix $\{L_\beta A_\beta\}$ and premultiplying eq. (3.4.2) by $\{L_x A_x\}$ and subtracting we obtain

$$p_x \{L_\beta A_\beta\} \begin{Bmatrix} A_x \\ L_x \end{Bmatrix} - p_\beta \{L_x A_x\} \begin{Bmatrix} A_\beta \\ L_\beta \end{Bmatrix} = \{L_\beta A_\beta\} N \begin{Bmatrix} A_x \\ L_x \end{Bmatrix} - \{L_x A_x\} N \begin{Bmatrix} A_\beta \\ L_\beta \end{Bmatrix}. \quad (3.4.3)$$

But

$$\{L_\beta A_\beta\} \begin{Bmatrix} A_x \\ L_x \end{Bmatrix} = L_{i\beta} A_{ix} + A_{i\beta} L_{ix} \quad (3.4.4)$$

and

$$\{L_x A_x\} \begin{Bmatrix} A_\beta \\ L_\beta \end{Bmatrix} = L_{ix} A_{i\beta} + A_{ix} L_{i\beta}, \quad (3.4.5)$$

where i runs from 1 to 3, so that the left side of eq. (3.4.3) is merely

$$(p_x - p_\beta)(A_{ix} L_{i\beta} + A_{i\beta} L_{ix}).$$

Now the symmetry of the elastic constant tensor guarantees that

$$(mn)_{jk} = (nm)_{kj}; (mm)_{jk} = (mm)_{kj}, \quad (3.4.6)$$

so that if

$$R_{ij} = (nn)_{ik}^{-1} (nm)_{kj}, \quad (3.4.7)$$

then

$$R_{ji} = (nn)_{jk}^{-1} (nm)_{ki} = (mn)_{ik} (nn)_{kj}^{-1}. \quad (3.4.8)$$

Examining eq. (3.3.8), in block notation we can write the 6×6 matrix N in the form

$$N = - \begin{Bmatrix} R_{ij} & H_{ij} \\ F_{ij} & R_{ji} \end{Bmatrix}, \quad (3.4.9)$$

where $H_{ij} = H_{ji}$ and $F_{ij} = F_{ji}$, i.e. the upper right and lower left blocks of N are symmetric, and the upper left and lower right blocks are transposes of each other. Thus,

$$\begin{aligned} - \{L_\beta A_\beta\} N \begin{Bmatrix} A_x \\ L_x \end{Bmatrix} &= \{L_{i\beta} A_{i\beta}\} \begin{Bmatrix} R_{ij} A_{jx} + H_{ij} L_{jx} \\ F_{ij} A_{jx} + R_{ji} L_{jx} \end{Bmatrix} \\ &= L_{i\beta} R_{ij} A_{jx} + L_{i\beta} H_{ij} L_{jx} \\ &\quad + A_{i\beta} F_{ij} A_{jx} + A_{i\beta} R_{ji} L_{jx}. \end{aligned} \quad (3.4.10)$$

Similarly

$$-\{L_x A_x\} N \begin{Bmatrix} A_\beta \\ L_\beta \end{Bmatrix} = L_{ix} R_{ij} A_{j\beta} + L_{ix} H_{ij} L_{j\beta} + A_{ix} F_{ij} A_{j\beta} + A_{ix} R_{ji} L_{j\beta}. \quad (3.4.11)$$

Interchanging i and j in eq. (3.4.11) shows that eqs (3.4.10) and (3.4.11) are identical due to the fact that H and F are symmetric matrices. Hence, eq. (3.4.3) reduces to

$$(p_x - p_\beta)(A_{ix} L_{i\beta} + A_{i\beta} L_{ix}) = 0. \quad (3.4.12)$$

Thus, if $\alpha \neq \beta$ and $p_x \neq p_\beta$,

$$A_{ix} L_{i\beta} + A_{i\beta} L_{ix} = 0. \quad (3.4.13)$$

If we normalize A_x and L_x according to eq. (3.2.12), the following orthogonality relation (first derived by Stroh) is valid:

$$A_{ix} L_{i\beta} + A_{i\beta} L_{ix} = \delta_{x\beta}. \quad (3.4.14)$$

The eigenvectors A_x and L_x , when normalized according to eq. (3.4.14), satisfy certain completeness relations which may be derived in the following fashion. Consider the following set of equations to be solved for an unknown complex vector D_x ($x = 1, 2, \dots, 6$):

$$\sum_{x=1}^6 A_{ix} D_x = b_i \quad (3.4.15)$$

and

$$\sum_{x=1}^6 L_{ix} D_x = f_i, \quad (3.4.16)$$

where b_i and f_i are components of two arbitrary vectors. Multiplying eqs (3.4.15) and (3.4.16) by $L_{i\beta}$ and $A_{i\beta}$, respectively, adding, and using the orthogonality relation eq. (3.4.14) yields

$$D_\beta = L_{i\beta} b_i + A_{i\beta} f_i. \quad (3.4.17)$$

If this relation is substituted into eqs (3.4.15) and (3.4.16) we obtain

$$\left(\sum_{x=1}^6 A_{ix} L_{sx} \right) b_s + \left(\sum_{x=1}^6 A_{ix} A_{sx} \right) f_s = b_i, \quad (3.4.18)$$

$$\left(\sum_{x=1}^6 L_{ix} L_{sx} \right) b_s + \left(\sum_{x=1}^6 L_{ix} A_{sx} \right) f_s = f_i. \quad (3.4.19)$$

Since b and f are arbitrary vectors, the following completeness relations⁽⁸⁾ must then hold:

$$\sum_{x=1}^6 A_{ix} A_{sx} = 0, \quad (3.4.20)$$

$$\sum_{\alpha=1}^6 L_{i\alpha} L_{s\alpha} = 0, \quad (3.4.21)$$

$$\sum_{\alpha=1}^6 A_{i\alpha} L_{s\alpha} = \delta_{is}. \quad (3.4.22)$$

The completeness relations imply that certain combinations of $A_{i\alpha}$ and $L_{s\alpha}$ yield purely 3×3 matrices. For instance, since

$$\sum_{\alpha=4}^6 A_{i\alpha} A_{s\alpha} = \sum_{\alpha=1}^3 A_{i\alpha}^* A_{s\alpha}^*, \quad (3.4.23)$$

eq. (3.4.20) requires that the matrix

$$Q_{is} = Q_{si} = i \sum_{\alpha=1}^6 \pm A_{i\alpha} A_{s\alpha} \quad (3.4.24)$$

is purely real (the upper sign is used for $\alpha = 1, 2, 3$ and the lower sign for $\alpha = 4, 5, 6$). Similarly two real matrices B and S may be defined by

$$B_{si} = B_{is} = -\frac{1}{4\pi i} \sum_{\alpha=1}^6 \pm L_{i\alpha} L_{s\alpha}, \quad (3.4.25)$$

$$S_{is} = i \sum_{\alpha=1}^6 \pm A_{i\alpha} L_{s\alpha}. \quad (3.4.26)$$

Furthermore,

$$\sum_{\alpha=1}^3 A_{i\alpha} L_{s\alpha} = \frac{1}{2} \{\delta_{is} - i S_{is}\}. \quad (3.4.27)$$

We shall show in Section 3.6 that the matrices Q , B , and S may be calculated in a very simple way using numerical integration. It will turn out that most of the elastic solutions of interest to us can be determined solely from a knowledge of Q , B and S , so that we may entirely circumvent the need for solving the sextic eigenvalue problem originally posed by Stroh.^(5,8) The method of circumvention is termed “the integral formalism” in order to distinguish it from Stroh’s technique; this alternative formalism is the subject of the following two sections.

3.5. Invariance Relations for the Stroh Eigenvectors

Because the matrix N given in eq. (3.3.8) depends on the choice of the plane basis \mathbf{m} and \mathbf{n} , in general one would expect that A_α , L_α and p_α depend on the choice of \mathbf{m} and \mathbf{n} . In order to determine this dependence let us define a plane basis (\mathbf{m}, \mathbf{n}) by the angle ω between \mathbf{m} and some fixed datum in the plane (Fig. 3.2), so that

$$\frac{\partial \mathbf{m}}{\partial \omega} = \mathbf{n}; \quad \frac{\partial \mathbf{n}}{\partial \omega} = -\mathbf{m}. \quad (3.5.1)$$

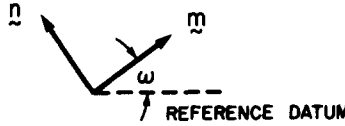


FIG. 3.2. The angle ω defining m and n relative to a fixed datum in the plane normal to t .

We wish to examine

$$\frac{\partial A_{iz}}{\partial \omega}, \quad \frac{\partial L_{iz}}{\partial \omega} \quad \text{and} \quad \frac{\partial p_z}{\partial \omega}.$$

Following Barnett and Lothe^(59,60) we begin with the Stroh eigenvalue problem

$$N\zeta_x = p_x\zeta_x, \quad (3.5.2)$$

which, when differentiated with respect to ω , yields

$$\frac{\partial N}{\partial \omega} \zeta_x + N \frac{\partial \zeta_x}{\partial \omega} = \frac{\partial p_x}{\partial \omega} \zeta_x + p_x \frac{\partial \zeta_x}{\partial \omega}. \quad (3.5.3)$$

But using eq. (3.5.1)

$$\frac{\partial}{\partial \omega} (mm) = (nm) + (mn), \quad (3.5.4)$$

$$\frac{\partial}{\partial \omega} (nn) = -(mn) - (nm), \quad (3.5.5)$$

$$\frac{\partial}{\partial \omega} (mn) = (nn) - (mm), \quad (3.5.6)$$

$$\frac{\partial}{\partial \omega} (nm) = -(mm) + (nn). \quad (3.5.7)$$

Furthermore, by differentiating the relation

$$(nn)(nn)^{-1} = I \quad (3.5.8)$$

with respect to ω , one obtains

$$\frac{\partial}{\partial \omega} (nn)^{-1} = (nn)^{-1} [(mn) + (nm)](nn)^{-1}. \quad (3.5.9)$$

Using eqs (3.3.8) and (3.5.4)–(3.5.9),

$$\begin{aligned} & \frac{\partial}{\partial \omega} N = \\ & - \left\{ \begin{array}{ll} I + (nn)^{-1}[(mn) + (nm)](nn)^{-1}(nm) & (nn)^{-1}[(mn) + (nm)](nn)^{-1} \\ -(nn)^{-1}(mm) & \\ \hline (mm)(nm)^{-1}(nm) & I - (mm)(nn)^{-1} \\ -(mn)(nn)^{-1}(mm) & \\ +(mn)(nn)^{-1}[(mm) + (nm)] & + (mn)(nn)^{-1}[(mn) + (nm)](nn)^{-1} \\ \times (nn)^{-1}(nm) & \end{array} \right\}, \end{aligned} \quad (3.5.10)$$

which is equivalent to

$$\frac{\partial}{\partial \omega} N = -\{I + N^2\}, \quad (3.5.11)$$

where I is the 6×6 unit matrix. Thus, eq. (3.5.3) reduces to

$$-(I + N^2)\zeta_x + N \frac{\partial \zeta_x}{\partial \omega} = \frac{\partial p_x}{\partial \omega} \zeta_x + p_x \frac{\partial \zeta_x}{\partial \omega}. \quad (3.5.12)$$

Premultiplying eq. (3.5.2) by N yields

$$N^2 \zeta_x = p_x^2 \zeta_x, \quad (3.5.13)$$

so that eq. (3.5.12) reduces to

$$-(1 + p_x^2)\zeta_x + N \frac{\partial \zeta_x}{\partial \omega} = \frac{\partial p_x}{\partial \omega} \zeta_x + p_x \frac{\partial \zeta_x}{\partial \omega}. \quad (3.5.14)$$

At this point we must digress to derive several relationships of importance. If we take the transpose of the eigenvalue problem given by eq. (3.5.2) we obtain

$$\zeta_x^T N^T = p_x \zeta_x^T, \quad (3.5.15)$$

where the superscript T indicates transposition and ζ_x^T is the row vector

$$\zeta_x^T = \{A_x L_x\}. \quad (3.5.16)$$

Using eq. (3.4.9) and block notation

$$N^T = \begin{Bmatrix} R^T & F \\ H & R \end{Bmatrix}, \quad (3.5.17)$$

due to the fact that $H = H^T$ and $F = F^T$. Now define the 6×6 matrix J in block notation by

$$J = \begin{Bmatrix} O & I \\ I & O \end{Bmatrix} = J^T \quad (3.5.18)$$

so that

$$JJ = I. \quad (3.5.19)$$

One may verify that

$$J N^T J = \begin{Bmatrix} R & H \\ F & R^T \end{Bmatrix} = N, \quad (3.5.20)$$

from which it follows that

$$J N J = N^T. \quad (3.5.21)$$

Finally, postmultiplying eq. (3.5.15) by J and noting that

$$\begin{aligned} \zeta_x^T N^T J &= (\zeta_x^T J)(J N^T J) \\ &= \zeta_x^T J N, \end{aligned} \quad (3.5.22)$$

we find that

$$\zeta_x^T \mathbf{J} \mathbf{N} = p_x \zeta_x^T \mathbf{J}. \quad (3.5.23)$$

Returning to eq. (3.5.14), premultiplying that equation by $\zeta_x^T \mathbf{J}$ yields

$$-(1 + p_x^2) \zeta_x^T \mathbf{J} \zeta_x + p_x \zeta_x^T \mathbf{J} \frac{\partial \zeta_x}{\partial \omega} = \frac{\hat{p}_x}{\hat{\omega}} \zeta_x^T \mathbf{J} \zeta_x + p_x \zeta_x^T \mathbf{J} \frac{\partial \zeta_x}{\partial \omega}, \quad (3.5.24)$$

so that

$$\frac{\hat{p}_x}{\hat{\omega}} \zeta_x^T \mathbf{J} \zeta_x = -(1 + p_x^2) \zeta_x^T \mathbf{J} \zeta_x. \quad (3.5.25)$$

But by direct matrix multiplication one sees that

$$\zeta_x^T \mathbf{J} \zeta_x = A_{ix} L_{ix} + A_{ix} L_{ix} = 1 \quad (3.5.26)$$

due to the normalization we have chosen, so that

$$\frac{\hat{p}_x}{\hat{\omega}} = -(1 + p_x^2), \quad (3.5.27)$$

a relation first deduced by Barnett and Lothe.⁽⁵⁹⁾

Substituting eq. (3.5.27) in eq. (3.5.14) requires that

$$\mathbf{N} \frac{\partial \zeta_x}{\partial \omega} = p_x \frac{\partial \zeta_x}{\partial \omega}. \quad (3.5.28)$$

For distinct p_x , a comparison of eq. (3.5.28) with the original eigenvalue problem eq. (3.5.2) shows that eq. (3.5.28) is satisfied if and only if

$$\frac{\partial \zeta_x}{\partial \omega} = K(\omega) \zeta_x, \quad (3.5.29)$$

where $K(\omega)$ is a complex scalar function of ω . Premultiplying eq. (3.5.29) by $\zeta_x^T \mathbf{J}$ and using eq. (3.5.26) yields

$$\begin{aligned} K(\omega) &= \zeta_x^T \mathbf{J} \frac{\partial \zeta_x}{\partial \omega} \\ &= L_{ix} \frac{\hat{A}_{ix}}{\hat{\omega}} + \frac{\hat{L}_{ix}}{\hat{\omega}} A_{ix}. \end{aligned} \quad (3.5.30)$$

But differentiating the normalization condition

$$2 A_{ix} L_{ix} = 1$$

with respect to ω shows that

$$A_{ix} \frac{\hat{L}_{ix}}{\hat{\omega}} + L_{ix} \frac{\hat{A}_{ix}}{\hat{\omega}} = 0 \quad (3.5.31)$$

so that

$$\left. \begin{aligned} K(\omega) &= 0 \\ \text{and} \\ \frac{\partial \zeta_x}{\partial \omega} &= 0 \end{aligned} \right\}. \quad (3.5.32)$$

We have, thus, arrived at the invariance relations for the Stroh eigenvectors deduced by Barnett and Lothe,⁽⁵⁹⁾ namely that

$$\frac{\partial A_{iz}}{\partial \omega} = 0; \quad \frac{\partial L_{iz}}{\partial \omega} = 0; \quad (3.5.33)$$

i.e. the eigenvectors A_x and L_x depend only on the normal t to the plane of the elastic problem and the elastic constants C_{ijkl} , but they do not depend on the choice of plane basis (m, n) used to solve the Stroh eigenvalue problem, eq. (3.5.2). This result is somewhat unexpected since the eigenvalues p_x are not independent of ω (see eq. (3.5.27)). As we shall see the invariance of the Stroh eigenvectors to rotations ω in the plane will have important physical consequences with regard to dislocation solutions.

The eq. (3.5.27) is a differential equation for $p_x(\omega)$, which is easily solved to yield

$$p_x(\omega) = \tan(\psi_x - \omega), \text{ if } p_x \neq \pm i, \quad (3.5.34)$$

where ψ_x is a complex constant such that $p_x(\omega = 0) = \tan \psi_x$. A bit of manipulation shows that $\mathcal{I}(p_x)$, the imaginary part of p_x , is proportional to

$$\sinh\{2\mathcal{I}(\psi_x)\}$$

for all real ω , where the constant of proportionality is positive. Hence, the sign of $\mathcal{I}(p_x)$ is the same as that of $\mathcal{I}(\psi_x)$, and our ordering of the eigenvalues of p_x according to the sign of $\mathcal{I}(p_x)$ is independent of ω . If $p_x = \pm i$ (as is the case for isotropy) then $\partial p_x / \partial \omega = 0$ and all higher derivatives of p_x also vanish; thus, if $p_x = \pm i$ for any ω , then $p_x = \pm i$ for all ω , $0 \leq \omega \leq 2\pi$.

Although the p_x are not invariant under rotations in the plane, we can show that

$$\int_0^{2\pi} p_x d\omega = \pm 2\pi i, \quad (3.5.35)$$

where, as usual, the upper and lower signs go with $\alpha = 1, 2, 3$ and $\alpha = 4, 5, 6$, respectively. Consider

$$\int_0^{2\pi} p_x d\omega = -i \int_0^{2\pi} d\omega \frac{1 - \exp[-i2(\psi_x - \omega)]}{1 + \exp[-i2(\psi_x - \omega)]}. \quad (3.5.36)$$

Let $\alpha = 4, 5, 6$ so that $\mathcal{I}(\psi_x) < 0$. The integrand in eq. (3.5.36) has poles at $\omega = \psi_x + (m + \frac{1}{2})\pi$, where m is an integer. If we consider

$$I = -i \int_C d\omega \frac{1 - \exp[-i2(\psi_x - \omega)]}{1 + \exp[-i2(\psi_x - \omega)]}, \quad (3.5.37)$$

where C is the rectangle in the complex ω plane with vertices at $0, 2\pi, 2\pi + iR, iR$, then for $R > 0$ the integrand in eq. (3.5.37) has no poles within C for $\alpha = 4, 5, 6$ (i.e. $\mathcal{I}(\psi_x) < 0$). Furthermore, the integrals on $[2\pi, 2\pi + iR]$ and $[iR, 0]$ cancel due to periodicity of the integrand so that the residue theorem yields

$$\int_0^{2\pi} p_x d\omega = i \int_{2\pi+iR}^{iR} d\omega \frac{1 - \exp[-i2(\psi_x - \omega)]}{1 + \exp[-i2(\psi_x - \omega)]}. \quad (3.5.38)$$

As $R \rightarrow \infty$, on $[2\pi + iR, iR]$ $\exp(i2\omega) \rightarrow 0$ so that the integrand on the right side of eq. (3.5.38) tends to unity. Thus

$$\int_0^{2\pi} p_x d\omega = -2\pi i \quad (\alpha = 4, 5, 6). \quad (3.5.39)$$

For $\alpha = 1, 2, 3$ we perform a similar integration over a rectangular contour in the lower half of the complex ω plane to obtain

$$\int_0^{2\pi} p_x d\omega = 2\pi i \quad (\alpha = 1, 2, 3), \quad (3.5.40)$$

so that eq. (3.5.35) is verified. Hence, although the p_x are not rotationally invariant, the angular average of the p_x yields the isotropic result, namely

$$\frac{1}{2\pi} \int_0^{2\pi} p_x d\omega = \pm i. \quad (3.5.41)$$

3.6. The Integral Formalism

Consider the definition of L_{jx} given in eq. (3.2.10), i.e.

$$L_{jx} = -(nm)_{jk} A_{kx} - p_x (nn)_{jk} A_{kx}. \quad (3.6.1)$$

Multiplying by A_{sx} and summing over α from 1 to 6 yields

$$\sum_{x=1}^6 A_{sx} L_{jx} = -(nm)_{jk} \sum_{x=1}^6 A_{sx} A_{kx} - (nn)_{jk} \sum_{x=1}^6 p_x A_{sx} A_{kx}, \quad (3.6.2)$$

which, using the completeness relations eqs (3.4.20) and (3.4.21), reduces to

$$-(nn)_{jk} \sum_{x=1}^6 p_x A_{sx} A_{kx} = \delta_{sj}$$

or

$$\sum_{x=1}^6 p_x A_{sx} A_{kx} = -(nn)_{sk}^{-1}. \quad (3.6.3)$$

Equation (3.6.3) is a sum rule which must hold for any choice of plane basis (\mathbf{m}, \mathbf{n}) , i.e. any angle ω . If we integrate eq. (3.6.3) over ω from 0 to 2π and use the invariance relations eqs (3.5.33) and (3.5.35), we obtain

$$Q_{sk} = i \sum_{x=1}^6 \pm A_{sx} A_{kx} = - \frac{1}{2\pi} \int_0^{2\pi} (nn)_{sk}^{-1} d\omega. \quad (3.6.4)$$

As noted in eq. (3.4.24), the matrix \mathbf{Q} is real and symmetric; the integral on the right side of eq. (3.6.4) is clearly independent of plane basis (\mathbf{m}, \mathbf{n}) so that \mathbf{Q} depends only on \mathbf{t} and C_{ijkm} . Reference to eq. (2.4.18) shows that $-Q_{ij}/4\pi$ is also the angular part of the elastic Green's tensor $G_{ij}(\mathbf{x} - \mathbf{x}')$.

If we multiply eq. (3.6.1) by L_{sx} , sum over x from 1 to 6, and use the completeness relations eqs (3.4.21) and (3.4.22) we obtain the sum rule

$$(nn)_{jk} \sum_{x=1}^6 p_x A_{kx} L_{sx} = -(nm)_{js}$$

or

$$\sum_{x=1}^6 p_x A_{kx} L_{sx} = -(nn)_{kj}^{-1} (nm)_{js}. \quad (3.6.5)$$

Integration of eq. (3.6.5) over ω from 0 to 2π coupled with the invariance relations, eqs (3.5.33) and (3.5.35), yields

$$S_{ks} = i \sum_{x=1}^6 \pm A_{kx} L_{sx} = - \frac{1}{2\pi} \int_0^{2\pi} (nn)_{kj}^{-1} (nm)_{js} d\omega. \quad (3.6.6)$$

Like \mathbf{Q} , the real matrix \mathbf{S} depends only upon \mathbf{t} and C_{ijkm} . The normalization condition eq. (3.2.12) ensures that $S_{kk} = 0$, i.e. the trace of \mathbf{S} vanishes.

Using the alternative definition of L_{jx} given by eq. (3.2.11), namely

$$p_x L_{jx} = (mm)_{jk} A_{kx} + (mn)_{jk} p_x A_{kx}, \quad (3.6.7)$$

multiplication by L_{sx} , summation over x from 1 to 6, and use of the completeness relations of eqs (3.4.21) and (3.4.22) establishes the sum rule

$$\sum_{x=1}^6 p_x L_{sx} L_{jx} = (mm)_{js} + (mn)_{jk} \sum_{x=1}^6 p_x A_{kx} L_{sx}. \quad (3.6.8)$$

Substituting eq. (3.6.5) into eq. (3.6.8) and integrating over ω from 0 to 2π allows us to define the real symmetric matrix \mathbf{B} by

$$\begin{aligned} B_{js} &= - \frac{1}{4\pi i} \sum_{x=1}^6 \pm L_{jx} L_{sx} \\ &= \frac{1}{8\pi^2} \int_0^{2\pi} [(mm)_{js} - (mn)_{jr} (nn)_{rk}^{-1} (nm)_{ks}] d\omega. \end{aligned} \quad (3.6.9)$$

\mathbf{B} depends only on \mathbf{t} and C_{ijkm} .

It should be noted that the “integral” formulae eqs (3.6.4), (3.6.6) and

(3.6.9) for \mathbf{Q} , \mathbf{S} and \mathbf{B} may be reduced to integrals from 0 to π , since it can be easily shown that the integrands are periodic in ω with period π , i.e. in eqs (3.6.4), (3.6.6) and (3.6.9)

$$\int_0^{2\pi} \dots d\omega = 2 \int_0^\pi \dots d\omega.$$

This is obviously an important time-saving when computing such integrals by numerical integration.

We note that reversing the sense of \mathbf{t} (i.e. $\mathbf{t} \rightarrow -\mathbf{t}$) in the integral formulae for \mathbf{B} , \mathbf{S} and \mathbf{Q} is equivalent to letting $\mathbf{n} \rightarrow -\mathbf{n}$ and leaving \mathbf{m} unchanged. Thus, we can deduce that

$$\begin{aligned}\mathbf{Q}(\mathbf{t}) &= \mathbf{Q}(-\mathbf{t}), \\ \mathbf{B}(\mathbf{t}) &= \mathbf{B}(-\mathbf{t}), \\ \mathbf{S}(\mathbf{t}) &= -\mathbf{S}(-\mathbf{t}).\end{aligned}$$

Equations (3.6.4), (3.6.6) and (3.6.9) allow one to calculate the matrices \mathbf{Q} , \mathbf{B} and \mathbf{S} by real numerical integration without ever solving for the eigenvectors A_{kx} and L_{jx} of the Stroh eigenvalue problem. Furthermore, these integral representations for \mathbf{Q} , \mathbf{B} and \mathbf{S} are valid in the isotropic limit, even though the Stroh eigenvalue problem is highly degenerate in this instance. It will turn out that the elastic fields of straight dislocations and lines of force and force multipoles can be expressed solely in terms of these three real matrices, so that we have introduced a formalism which allows one to circumvent solution of the Stroh eigenvalue problem. Following Barnett and Lothe,⁽⁵⁹⁾ we refer to this method as the “integral formalism” in order to distinguish it from the Stroh “sextic formalism”.

For isotropic media

$$C_{ijkl} = \lambda \delta_{ij} \delta_{km} + \mu (\delta_{ik} \delta_{jm} + \delta_{im} \delta_{jk}), \quad (3.6.10)$$

where λ and μ are Lamé's constants. Furthermore,

$$(nn)_{jk} = \mu \left\{ \delta_{jk} + \frac{\lambda + \mu}{\mu} n_j n_k \right\}, \quad (3.6.11)$$

$$(nn)_{jk}^{-1} = \frac{1}{\mu} \left\{ \delta_{jk} - \frac{\lambda + \mu}{\lambda + 2\mu} n_j n_k \right\}, \quad (3.6.12)$$

$$(nm)_{jk} = (mn)_{kj} = \lambda n_j m_k + \mu n_k m_j. \quad (3.6.13)$$

Integration of eqs (3.6.4), (3.6.6) and (3.6.9) is most easily performed by fixing two orthogonal unit vectors \mathbf{M} and \mathbf{N} normal to \mathbf{t} so that

$$m_i = M_i \cos \omega + N_i \sin \omega,$$

$$n_i = -M_i \sin \omega + N_i \cos \omega.$$

Direct integration and use of these relations shows that for an isotropic

medium

$$Q_{jk} = -\frac{1}{2\mu(\lambda+2\mu)} \{(\lambda+3\mu)\delta_{jk} + (\lambda+\mu)t_j t_k\}, \quad (3.6.14)$$

which with eq. (2.4.20) can be shown to yield the result for G_{ij} given in eq. (2.4.21).

Similarly, for isotropic media with the x_3 -axis along t , the only non-vanishing components of the matrices S and B are

$$S_{12} = -S_{21} = -\frac{(1-2\nu)}{2(1-\nu)}, \quad (3.6.15)$$

$$B_{11} = B_{22} = \frac{\mu}{4\pi(1-\nu)}; \quad B_{33} = \frac{\mu}{4\pi}, \quad (3.6.16)$$

where ν is Poisson's ratio.

There exist additional relationships between the matrices Q , S and B . Consider

$$\begin{aligned} B_{ij}S_{jk} + S_{ji}B_{jk} &= -\frac{1}{4\pi} \sum_{\alpha=1}^6 \pm L_{i\alpha} L_{j\alpha} \sum_{\beta=1}^6 \pm A_{j\beta} L_{k\beta} \\ &\quad - \frac{1}{4\pi} \sum_{\alpha=1}^6 \pm A_{j\alpha} L_{i\alpha} \sum_{\alpha=1}^6 \pm L_{j\beta} L_{k\beta}. \end{aligned} \quad (3.6.17)$$

The right side of eq. (3.6.17) is equivalent to

$$-\frac{1}{4\pi} \sum_{\alpha=1}^6 \sum_{\beta=1}^6 (\pm L_{i\alpha})(\pm L_{k\beta}) \{L_{j\alpha} A_{j\beta} + A_{j\alpha} L_{j\beta}\},$$

which, using the orthogonality relation eq. (3.4.14), is merely

$$-\frac{1}{4\pi} \sum_{\alpha=1}^6 \sum_{\beta=1}^6 (\pm L_{i\alpha})(\pm L_{k\beta}) \delta_{\alpha\beta} = -\frac{1}{4\pi} \sum_{\alpha=1}^6 L_{i\alpha} L_{k\alpha} = 0$$

by virtue of eq. (3.4.21). Hence,

$$B_{ij}S_{jk} + S_{ji}B_{jk} = 0 \quad (3.6.18)$$

or in matrix notation

$$BS + S^T B = 0. \quad (3.6.19)$$

In the same manner one may deduce that

$$QS^T + S^T Q = 0; \quad Q_{ij}S_{kj} + S_{ij}Q_{jk} = 0; \quad (3.6.20)$$

$$4\pi B Q + S^T S^T = -I; \quad 4\pi B_{ij}Q_{jk} + S_{ji}S_{kj} = -\delta_{ik}. \quad (3.6.21)$$

Since (nn) and $(nn)^{-1}$ are positive definite for any stable elastic medium, eq. (3.6.4) implies that Q is negative definite so that $\|Q\| < 0$. From eq. (3.6.20) we immediately deduce that

$$\|S^T\| = -\|S\|$$

or

$$\| \mathbf{S} \| = 0, \quad (3.6.22)$$

a result which holds for any anisotropy.

There are many additional "sum rules" involving the Stroh eigenvectors which may be derived; a partial list is given in Nishioka and Lothe.⁽⁵⁸⁾ Certain sum rules will prove useful when discussing dislocation, line force and line force dipole solutions. We shall derive one such rule and merely list the remainder, since these can be derived by the same method. Consider multiplying both sides of eq. (3.6.1) by $\pm L_{sx}$ (upper sign $\alpha = 1, 2, 3$; lower sign $\alpha = 4, 5, 6$) and summing over α from 1 to 6. One obtains

$$(nn)_{jk} \sum_{\alpha=1}^6 \pm p_{\alpha} A_{k\alpha} L_{sx} = -(nm)_{jk} \sum_{\alpha=1}^6 \pm A_{k\alpha} L_{sx} - \sum_{\alpha=1}^6 \pm L_{j\alpha} L_{sx} \quad (3.6.23)$$

or

$$\sum_{\alpha=1}^6 \pm p_{\alpha} A_{r\alpha} L_{sx} = i(nn)_{rj}^{-1} \{ 4\pi B_{js} + (nm)_{jk} S_{ks} \}, \quad (3.6.24)$$

a relation first derived by Barnett and Lothe⁽⁵⁹⁾ by a different method. In a similar manner one may show that

$$\sum_{\alpha=1}^6 \pm p_{\alpha} A_{r\alpha} A_{s\alpha} = i(nn)_{rj}^{-1} \{ S_{sj} + (nm)_{jk} Q_{ks} \}, \quad (3.6.25)$$

$$\sum_{\alpha=1}^6 \pm p_{\alpha} L_{j\alpha} L_{s\alpha} = -i(mm)_{jk} S_{ks} + (mn)_{jk} \sum_{\alpha=1}^6 \pm p_{\alpha} A_{k\alpha} L_{s\alpha}, \quad (3.6.26)$$

$$\sum_{\alpha=1}^6 \pm p_{\alpha} L_{j\alpha} A_{s\alpha} = -i(mm)_{jk} Q_{ks} + (mn)_{jk} \sum_{\alpha=1}^6 \pm p_{\alpha} A_{k\alpha} A_{s\alpha}. \quad (3.6.27)$$

Sum rules involving $\pm (p_{\alpha})^2$ and higher powers may be derived by differentiating eqs (3.6.24)–(3.6.27) with respect to ω using eqs (3.5.4)–(3.5.9) and (3.5.27). Many of these rules are listed in Asaro *et al.*⁽⁴⁴⁾

The utility of the sum rules eqs (3.6.24)–(3.6.27) will become apparent when we discuss dislocation and line force solutions in the following sections of this article. Essentially these sum rules allow one to express quantities involving p_{α} , $A_{k\alpha}$ and $L_{j\alpha}$ solely in terms of the matrices \mathbf{Q} , \mathbf{S} and \mathbf{B} , which may be computed by real numerical integration, and the matrices (mm) , (nn) , $(nn)^{-1}$ and (mn) , which are known *explicitly* for any anisotropy.

3.7. Uniform Motion (Dynamic) Problems

The previous six sections have dealt with two formalisms capable of treating plane anisotropic static problems, in which the elastic equilibrium equations are

$$C_{ijk\mathbf{m}} u_{k,\mathbf{m}\mathbf{i}} = 0. \quad (3.7.1)$$

In the dynamic case the equilibrium equations take the form (eq. (2.2.9))

$$C_{ijkm} u_{k,mi} = \rho \frac{\partial^2 u_j}{\partial t^2}, \quad (3.7.2)$$

where ρ is the mass density of the medium and t is time (not to be confused with the vector $\mathbf{t} = \mathbf{m} \wedge \mathbf{n}$). If we restrict our attention to uniform motion solutions of the form

$$\mathbf{u} = \mathbf{u}(\mathbf{x} - \mathbf{v} t),$$

where \mathbf{v} is a constant velocity vector in the plane normal to \mathbf{t} , then if

$$\mathbf{R} = \mathbf{x} - \mathbf{v} t; R_j = x_j - v_j t, \quad (3.7.3)$$

$$\frac{\partial}{\partial x_m} = \frac{\partial}{\partial R_m}, \quad (3.7.4)$$

$$\frac{\partial}{\partial t} = -v_j \frac{\partial}{\partial R_j}, \quad (3.7.5)$$

so that we may rewrite eq. (3.7.2) as

$$C'_{ijkm} \frac{\partial^2 u_k}{\partial R_i \partial R_m} = 0, \quad (3.7.6)$$

where

$$C'_{ijkm} = C_{ijkm} - \rho v_i v_m \delta_{jk}. \quad (3.7.7)$$

Equation (3.7.6) is of the same form as the static case with \mathbf{x} replaced by \mathbf{R} and with usual static elastic constants replaced by the “effective dynamic elastic constants” given by eq. (3.7.7). The effect of uniform motion is merely to endow the medium with a “different anisotropy”. Hence, *every* result of the previous six sections (the static case) will remain valid if we replace C_{ijkm} *everywhere* by C'_{ijkm} , e.g.

$$(ab)_{jk} = a_i C'_{ijkm} b_m \quad (3.7.8)$$

and if we consider velocities such that the operator $C'_{ijkm} \partial^2 / \partial R_i \partial R_m$ remains elliptic so that the six p_α are always complex. The condition of ellipticity is equivalent to the condition that the matrix (rr) be positive definite (i.e. its three eigenvalues must be positive) for all real unit vectors \mathbf{r} normal to \mathbf{t} . The three eigenvalues $\lambda_\beta (\beta = 1, 2, 3)$ of (rr) are determined by solving

$$\| r_i C_{ijkm} r_m - \{ \rho(v \cdot r)^2 + \lambda \} \delta_{jk} \| = 0. \quad (3.7.9)$$

Now the three sonic velocities corresponding to plane wave propagation in the direction \mathbf{r} are determined from

$$\| r_i C_{ijkm} r_m - \rho c^2 \delta_{jk} \| = 0. \quad (3.7.10)$$

If c_1^2 is the smallest of the three roots of eq. (3.7.10), i.e. the slowest sonic

velocity corresponding to \mathbf{r} , the condition of ellipticity is that

$$\frac{1}{(\mathbf{v} \cdot \mathbf{r})^2} > \frac{1}{c_1^2} \quad (3.7.11)$$

for all directions \mathbf{r} normal to \mathbf{t} . Equation (3.7.11) is obviously satisfied at $v = 0$. There exists a limiting velocity v_L above which eq. (3.7.11) ceases to be satisfied. For $0 \leq v \leq v_L$, the six p_x are always complex. v_L will turn out to be the lowest velocity at which the strain energy of a uniformly moving straight dislocation becomes infinite, so that v_L is a "limiting velocity" in a certain sense.

Malén⁽⁶¹⁾ has given a simple geometrical interpretation of v_L in terms of slowness surfaces (Fig. 3.3). If we draw a horizontal axis along the direction of \mathbf{v} in the plane normal to \mathbf{t} and call ω the angle measured counter-clockwise from \mathbf{v} to \mathbf{r} , then we may solve eq. (3.7.10) for $c_1(\omega)$, the smallest root of eq. (3.7.10) corresponding to the direction \mathbf{r} . A polar plot of $1/c_1(\omega)$ vs. ω is a closed curve which is called a slowness surface. A vertical line of distance $1/v$ from the origin will first become tangent to this slowness surface at an angle $\omega = \omega_o$ such that

$$\frac{1}{v_L^2 \cos^2 \omega_o} = \frac{1}{c_1^2(\omega_o)}. \quad (3.7.12)$$

At $v = v_L$ at least two of the roots p_x are real and equal and are given by⁽⁶²⁾

$$p_x = \tan \omega_o. \quad (3.7.13)$$

For $v > v_L$ at least two p_x are always real. Every intersection of the vertical line $1/v$ with the three slowness surfaces $1/c_\beta(\omega)$ corresponds to the existence of a real root, p_x , of the Stroh sextic eq. (3.2.7) with C_{ijkm} replaced by C'_{ijkm} . In this review paper we shall not concern ourselves with the supersonic cases $v \geq v_L$. The Stroh and the integral formalisms may be extended to treat these cases, but at the present it is not known if super-

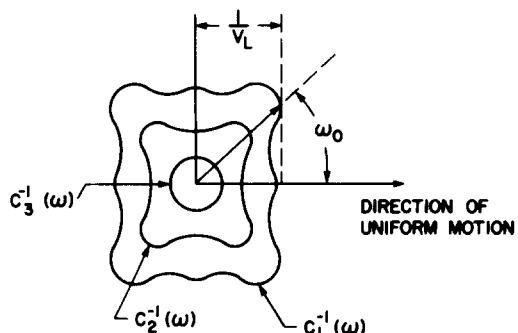


FIG. 3.3. Geometric interpretation of the limiting velocity v_L in terms of slowness surfaces.

sonic dislocation motion is a physical phenomenon which may really occur.

For the sake of completeness we list the non-zero components of the matrices B , Q and S for uniform motion in isotropic media. We choose the x_3 axis along t and the x_1 axis along v . The shear wave velocity V_1 and the dilatational wave velocity V_3 are given by

$$V_1^2 = \frac{\mu}{\rho}; \quad V_3^2 = \frac{\lambda + 2\mu}{\rho},$$

where λ and μ are Lamé's constants, and we define the non-dimensional variables h_1 and h_3 by

$$h_1 = \left(\frac{v}{V_1} \right)^2; \quad h_3 = \left(\frac{v}{V_3} \right)^2.$$

Then, for the non-vanishing elements of B , Q and S one obtains

$$B_{11} = \frac{\mu}{4\pi} h_1^{-1} (1 - h_1)^{-1/2} \{ 4(1 - h_3)^{1/2} (1 - h_1)^{1/2} - (2 - h_1)^2 \},$$

$$B_{22} = \frac{\mu}{4\pi} h_1^{-1} (1 - h_3)^{-1/2} \{ 4(1 - h_3)^{1/2} (1 - h_1)^{1/2} - (2 - h_1)^2 \},$$

$$B_{33} = \frac{\mu}{4\pi} (1 - h_1)^{1/2},$$

$$Q_{11} = \frac{1}{\mu} h_1^{-1} \{ (1 - h_1)^{1/2} - (1 - h_3)^{-1/2} \},$$

$$Q_{22} = \frac{1}{\mu} h_1^{-1} \{ (1 - h_3)^{1/2} - (1 - h_1)^{-1/2} \},$$

$$Q_{33} = -\frac{1}{\mu} (1 - h_1)^{-1/2}$$

$$S_{12} = h_1^{-1} (1 - h_3)^{-1/2} \{ 2(1 - h_3)^{1/2} (1 - h_1)^{1/2} - (2 - h_1) \},$$

$$S_{21} = -h_1^{-1} (1 - h_1)^{-1/2} \{ 2(1 - h_3)^{1/2} (1 - h_1)^{1/2} - (2 - h_1) \}.$$

4. DISLOCATIONS

4.1. Infinite Straight Dislocations in Homogeneous Media

The first parts of this chapter are confined to the elastic properties of an infinitely-long, straight dislocation in a homogeneous medium. Physical reasoning demonstrates that none of the elastic-field quantities can

vary with the coordinate directed along the axis parallel to the line and so this is an example of the plane problem discussed in Chap. 3. The analysis of that chapter can, therefore, be brought to bear on this defect. We shall show in Section 4.1.1 that all the field quantities of interest can be expressed in terms of integrals, which can be written explicitly in terms of the elastic constants (referred conveniently to the crystal axes) and vectors describing the dislocation geometry and Burgers vector. The computational effort required for their evaluation is, therefore, minimal.

An analysis which can only be applied to the infinite, straight line has, of course, a rather restricted usefulness, particularly since the anisotropic-elastic properties of this dislocation have already been studied by numerous workers using the original analyses of Eshelby *et al.*⁽⁴⁾ and Stroh.⁽⁵⁾ Thus, although the equations to be derived here can be evaluated more easily than those of the earlier analyses, our primary purpose in presenting them is not that they should be applied solely to that particular problem. We shall show in Section 4.2 how they can be used for the general problem of the determination of the elastic field of a dislocation of arbitrary shape in an anisotropic, homogeneous medium: this is their main utility and the main reason why they should be computationally simple to handle. The relationships between the fields of curved and polygonal dislocations and those of infinite, straight dislocations are described by some simple, geometrical formulae due originally to Brown, Lothe, and Indenbom and Orlov. Their derivation, and various extensions of them, are presented in Section 4.2. It will be seen that if field data for infinite, straight lines are available or can be readily obtained, most problems associated with dislocations in a homogeneous medium can be solved in the anisotropic case with almost as much ease as in the isotropic approximation. Straight-line field data for a class of two-dimensional problems have already been computed and compiled for the common cubic and hexagonal metals, and they are discussed in Section 4.1.3.

We review in Section 4.3 a number of dislocation problems which have been analyzed and solved within the framework of anisotropic elasticity theory. These applications have used either the geometric formulae and straight-line data described here or methods which require the solution of sextic equations, but are still closely related to the theme of this article. These problems show the extent to which dislocation calculations have already utilized the theoretical developments discussed here and, furthermore, give an indication of the effects of anisotropy in a number of interesting situations.

Most of this chapter is concerned with the homogeneous elastic continuum, but there are a number of situations involving dislocations in inhomogeneous elastic media for which the formulae of Chap. 3 and Section 4.1.1 can be applied directly, namely, when the dislocation is infinitely-long and straight and either lies in or runs parallel to the interface between two anisotropic, semi-infinite media. We describe in Section 4.4 how the

resulting field quantities and, in the latter case, the image force on the dislocation can be expressed directly in terms of the field quantities of the dislocation in an homogeneous medium. The force acting on a straight dislocation intersecting a free surface is also discussed and numerical results are presented for equilibrium orientations for a number of crystals.

We caution the reader on several points regarding the notation used in this chapter, especially with regard to the dislocation field quantities discussed in Section 4.1.1. As is common practice in the literature, the unit vector \mathbf{t} specifies some arbitrary direction for which the basic matrices $\mathbf{Q}(\mathbf{t})$, $\mathbf{S}(\mathbf{t})$ and $\mathbf{B}(\mathbf{t})$ discussed in Chap. 3 must be calculated; the matrices depend only on \mathbf{t} and the elastic constants C_{ijkp} . To derive these matrices, we have already introduced in Chap. 3 the orthonormal basis vectors \mathbf{m} , \mathbf{n} , \mathbf{t} , where the vector pair (\mathbf{m}, \mathbf{n}) may be oriented at an arbitrary position in the plane normal to \mathbf{t} , as given by the angle ω measured from some arbitrary in-plane reference datum (Figs 3.1 and 3.2). The quantities \mathbf{Q} , \mathbf{S} and \mathbf{B} are obtained in the integral formalism as integrals over ω , i.e. \mathbf{m} and \mathbf{n} rotate in a positive sense about \mathbf{t} , and the components of \mathbf{m} and \mathbf{n} as they appear in matrix form in the integrands of the formulae for \mathbf{Q} , \mathbf{S} and \mathbf{B} play the role of integration variables (e.g. eq. (4.1.39)). In treating the derivatives with respect to the orientation \mathbf{t} of \mathbf{Q} , \mathbf{S} and \mathbf{B} , and for related quantities such as angular stress factors, we fix a plane containing \mathbf{t} with unit normal \mathbf{N} , and then compute derivatives with respect to the angle θ between \mathbf{t} and an arbitrary in-plane reference datum (Fig. 4.4). For a given value of θ , the orthogonal vectors \mathbf{t} , \mathbf{N} and $\partial\mathbf{t}/\partial\theta$ appearing in the derivative formulae are fixed with respect to ω integration; (\mathbf{m}, \mathbf{n}) are again rotating integration vectors (e.g. eq. (4.1.44)).

When dealing with the infinite, straight, dislocation field quantities such as distortions and stresses, it is necessary to choose a coordinate system to describe the dislocation geometry. We choose a system where \mathbf{t} is the dislocation line direction and the vectors \mathbf{m} and \mathbf{n} are fixed vectors such that $\mathbf{x} = |\mathbf{x}| \mathbf{m}$, $\mathbf{n} \cdot \mathbf{x} = 0$, where \mathbf{x} is the perpendicular from the line to a field point (Fig. 4.2). The formulae for distortions and stresses are, thus, given in terms of the matrices $\mathbf{Q}(\mathbf{t})$, $\mathbf{S}(\mathbf{t})$ and $\mathbf{B}(\mathbf{t})$, and the components of \mathbf{m} and \mathbf{n} in matrix form (e.g. eq. (4.1.18)); the latter are known quantities, directly evaluated from the dislocation geometry. The distinction between the vector pair (\mathbf{m}, \mathbf{n}) used as functions of ω , i.e. rotating integration vectors, and used as fixed dislocation coordinates should be clear from the context. We retain the (\mathbf{m}, \mathbf{n}) notation for both purposes since, as can be seen in Chap. 3, the basic matrix and dislocation field formulae have common origins; the former make use of the fact that certain quantities are independent of the orientation ω of (\mathbf{m}, \mathbf{n}) , whereas the latter require a specific choice for (\mathbf{m}, \mathbf{n}) . Throughout, the elastic constants C_{ijkp} may be referred to crystal axes and this is a convenient computational feature.

We hasten to point out that in some instances, the symbols m and n appear in tensor subscripts, as well as representing components of \mathbf{m}

and \mathbf{n} . The different meanings should again be clear from the context. The reader will also notice that the vector pair (z, z') used for the infinite straight field quantities discussed in Chap. 2 plays the same role as the rotating integration vectors (\mathbf{m}, \mathbf{n}) here. The vectors (\mathbf{m}, \mathbf{n}) in Chap. 2 refer to the fixed dislocation coordinates (Fig. 2.7). Finally, we remark that the dislocation coordinates used in Section 4.1.3 for the traction data are the orthonormal vectors \mathbf{M}, \mathbf{N} and $\mathbf{b}/|\mathbf{b}|$, where \mathbf{b} is the Burgers vector, \mathbf{N} is the glide plane normal and $\mathbf{M} = \mathbf{N} \wedge \mathbf{b}/|\mathbf{b}|$.

*4.1.1. Elastic fields of straight dislocations and lines of force

4.1.1.1. *The Stroh displacement field solution*—Consider the displacement field given by

$$u_i = \frac{1}{2\pi i} \sum_{x=1}^6 A_{ix} D_x \ln(\mathbf{m} \cdot \mathbf{x} + p_x \mathbf{n} \cdot \mathbf{x}) \quad (4.1.1)$$

corresponding to the vector Airy stress functions

$$\varphi_i = \frac{1}{2\pi i} \sum_{x=1}^6 L_{ix} D_x \ln(\mathbf{m} \cdot \mathbf{x} + p_x \mathbf{n} \cdot \mathbf{x}). \quad (4.1.2)$$

We wish to show that if the constants D_x are chosen appropriately, then eq. (4.1.1) will correspond to the solution for an infinite straight dislocation line and/or a line of force parallel to \mathbf{t} and passing through the origin $\mathbf{x} = 0$. \mathbf{m} and \mathbf{n} are two mutually orthogonal unit vectors normal to \mathbf{t} (Fig. 3.1). The results of Chap. 3 show that eq. (4.1.1) is an admissible solution to the elastic equilibrium equations if p_x , A_{ix} and L_{ix} are determined by the Stroh prescriptions; the elastic fields due to eq. (4.1.1) are independent of $\mathbf{t} \cdot \mathbf{x}$, i.e. the fields represent the solution to a plane elastostatic problem. Hence, we may consider only those vectors \mathbf{x} in the plane of \mathbf{m} and \mathbf{n} , and we note that the stresses associated with eq. (4.1.1) will vary as $|\mathbf{x}|^{-1}$. In order to verify that the above solution can correspond to a dislocation or a line of force, we must examine the multi-valued behaviour of the logarithmic function.

Let us render the logarithmic function single-valued by a branch cut extending from $\mathbf{x} = 0$ to $\mathbf{m} \cdot \mathbf{x} \rightarrow \infty$ along the line $\mathbf{n} \cdot \mathbf{m} = 0$ (Fig. 4.1). Our convention is such that for $\mathbf{m} \cdot \mathbf{x} > 0$ along the cut

$$\ln(\mathbf{m} \cdot \mathbf{x} + p_x \mathbf{n} \cdot \mathbf{x}) \rightarrow \ln(\mathbf{m} \cdot \mathbf{x}) \pm i0 \text{ as } \mathbf{n} \cdot \mathbf{x} \rightarrow 0^+, \quad (4.1.3)$$

$$\rightarrow \ln(\mathbf{m} \cdot \mathbf{x}) \pm i2\pi \text{ as } \mathbf{n} \cdot \mathbf{x} \rightarrow 0^-, \quad (4.1.4)$$

where the upper sign is for $x = 1, 2, 3$ and the lower sign is for $x = 4, 5, 6$, i.e. the argument of the logarithm changes by $\pm 2\pi$ across the cut. In this sense the complex variable $\mathbf{m} \cdot \mathbf{x} + p_x \mathbf{n} \cdot \mathbf{x}$ is no different from the usual complex variable $\mathbf{m} \cdot \mathbf{x} + i \mathbf{n} \cdot \mathbf{x}$; in fact, points in the complex $\mathbf{m} \cdot \mathbf{x} + p_x \mathbf{n} \cdot \mathbf{x}$ plane are related one-to-one to points in the familiar $\mathbf{m} \cdot \mathbf{x} + i \mathbf{n} \cdot \mathbf{x}$ plane by a simple stretching and shear transformation.

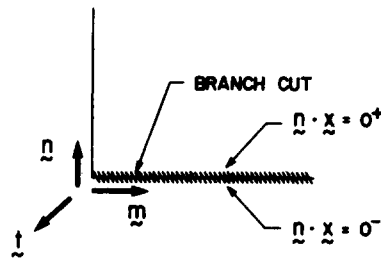


FIG. 4.1 The branch cut rendering the logarithmic function of the Stroh formalism single-valued.

The discontinuities across the cut in u_i and ϕ_i given by eqs (4.1.1) and (4.1.2) are

$$\begin{aligned}\Delta u_i &= u_i(\mathbf{m} \cdot \mathbf{x} > 0; \mathbf{n} \cdot \mathbf{x} = 0^-) - u_i(\mathbf{m} \cdot \mathbf{x} > 0; \mathbf{n} \cdot \mathbf{x} = 0^+) \\ &= \sum_{z=1}^6 \pm A_{iz} D_z,\end{aligned}\quad (4.1.5)$$

$$\begin{aligned}\Delta \phi_i &= \phi_i(\mathbf{m} \cdot \mathbf{x} > 0; \mathbf{n} \cdot \mathbf{x} = 0^-) - \phi_i(\mathbf{m} \cdot \mathbf{x} > 0; \mathbf{n} \cdot \mathbf{x} = 0^+) \\ &= \sum_{z=1}^6 \pm L_{iz} D_z.\end{aligned}\quad (4.1.6)$$

If we desire the solution for a line of force of constant strength f per unit length coincident with a straight dislocation of Burgers vector b and line direction t , then we must require that

$$\Delta u_i = b_i, \quad (4.1.7)$$

$$\Delta \phi_i = -f_i, \quad (4.1.8)$$

i.e. we must choose the D_z such that

$$\sum_{z=1}^6 \pm A_{iz} D_z = b_i \quad (4.1.9)$$

$$\sum_{z=1}^6 \pm L_{iz} D_z = -f_i. \quad (4.1.10)$$

Equation (4.1.7) is the usual Burgers condition for a dislocation; eq. (4.1.8) follows from eq. (3.2.24), i.e. force equilibrium of the material within any closed curve C encircling the origin. Equations (4.1.9) and (4.1.10) are identical in form to eqs (3.4.15) and (3.4.16) so that the solution for D_z is merely

$$D_z = \pm L_{sz} b_s \mp A_{sz} f_s, \quad (4.1.11)$$

where, as usual, the upper (lower) signs are used for $\alpha = 1, 2, 3$ (4, 5, 6).

Hence, the displacement field solution for a pure dislocation ($f_s = 0$) is

$$u_i = \frac{1}{2\pi i} \sum_{z=1}^6 \pm A_{iz} L_{sz} b_s \ln(\mathbf{m} \cdot \mathbf{x} + p_z \mathbf{n} \cdot \mathbf{x}). \quad (4.1.12)$$

The solution for a pure line of force ($b_s = 0$) is

$$u_i = -\frac{1}{2\pi i} \sum_{z=1}^6 \pm A_{iz} A_{sz} f_s \ln(\mathbf{m} \cdot \mathbf{x} + p_z \mathbf{n} \cdot \mathbf{x}). \quad (4.1.13)$$

These forms of the dislocation and line force solutions were first given by Stroh.⁽⁸⁾

4.1.1.2. The dislocation displacement gradients in the sextic and integral formalisms—Let us consider the pure dislocation solution. We wish to express the dislocation displacement gradients in both the sextic and the integral representations discussed in Chap. 3. The dislocation displacement gradients obtained by direct differentiation of eq. (4.1.12) are

$$u_{i,p} = \frac{1}{2\pi i} \sum_{z=1}^6 \pm A_{iz} L_{sz} b_s \frac{m_p + p_z n_p}{\mathbf{m} \cdot \mathbf{x} + p_z \mathbf{n} \cdot \mathbf{x}}. \quad (4.1.14)$$

Equation (4.1.14) allows one to evaluate the dislocation displacement gradients once the Stroh eigenvalue problem has been solved. The displacement gradients are continuous everywhere and are independent of the branch cut used to render the logarithmic function single-valued.

It is possible to develop an expression for $u_{i,p}$ which does not rely on the solution to the Stroh eigenvalue problem for its evaluation. We note that eq. (4.1.14) is valid for any choice of base vectors (\mathbf{m}, \mathbf{n}) normal to \mathbf{t} and that the results of Chap. 3 show that A_{iz} and L_{iz} are independent of the choice of (\mathbf{m}, \mathbf{n}) . Following Barnett and Lothe,⁽⁵⁹⁾ we may choose \mathbf{m} and \mathbf{n} such that $\mathbf{m} \cdot \mathbf{x} = |\mathbf{x}|$ and $\mathbf{n} \cdot \mathbf{x} = 0$ (Fig. 4.2), i.e. we choose \mathbf{m} along \mathbf{x} . Then

$$u_{i,p} = (2\pi i |\mathbf{x}|)^{-1} \left\{ m_p b_s \sum_{z=1}^6 \pm A_{iz} L_{sz} + n_p b_s \sum_{z=1}^6 \pm p_z A_{iz} L_{sz} \right\}. \quad (4.1.15)$$

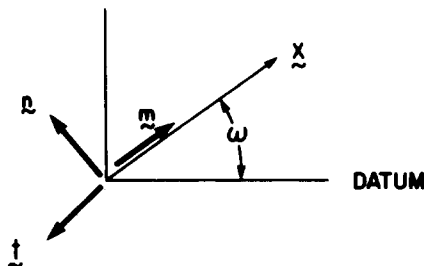


FIG. 4.2. The choice of plane basis (\mathbf{m}, \mathbf{n}) for which $\mathbf{m} \cdot \mathbf{x} = |\mathbf{x}|$, $\mathbf{n} \cdot \mathbf{x} = 0$.

Using eq. (3.6.6) and the sum rule eq. (3.6.24), we find that

$$\begin{aligned} u_{i,p} = & (2\pi|\mathbf{x}|)^{-1} b_s \{ -m_p S_{is} \\ & + n_p (nn)_{ik}^{-1} \{ 4\pi B_{ks} + (nm)_{kr} S_{rs} \} \}. \end{aligned} \quad (4.1.16)$$

Clearly eq. (4.1.16) is an expression for the dislocation displacement gradients which involves only real variables and does not require solving the Stroh eigenvalue problem for its evaluation. The constant matrices B and S depend only on t and C_{ijkm} and may be evaluated by simple numerical integration according to the formulae of eqs (3.6.6) and (3.6.9). The matrices $(nn)^{-1}$ and (nm) are known *explicitly* for any direction \mathbf{m} parallel to \mathbf{x} , the point at which the elastic field is evaluated. The elements of $(nn)^{-1}$ may be computed from

$$(nn)_{ij}^{-1} = \frac{\epsilon_{ism}\epsilon_{jrw}(nn)_{sr}(nn)_{mw}}{2\epsilon_{pgn}(nn)_{1p}(nn)_{2g}(nn)_{3n}}, \quad (4.1.17)$$

where ϵ_{ism} is the alternating tensor. All computations involving eq. (4.1.16) may be performed with reference to a crystal coordinate system in which the C_{ijkm} exhibit their simplest form, i.e. there is no need to use dislocation coordinates or to calculate the C_{ijkm} in a coordinate system rotated with respect to the crystal coordinate system.

4.1.1.3. The dislocation stress field and angular stress factors—The dislocation stress field σ_{mn}^x for an infinite straight line may be obtained from eq. (4.1.16) using Hooke's law

$$\sigma_{mn}^x = C_{mnip} u_{i,p}$$

so that for $\mathbf{m} \cdot \mathbf{x} = |\mathbf{x}|$, $\mathbf{n} \cdot \mathbf{x} = 0$

$$\begin{aligned} \sigma_{mn}^x = & (2\pi|\mathbf{x}|)^{-1} C_{mnip} b_s \{ -m_p S_{is} \\ & + n_p (nn)_{ik}^{-1} \{ 4\pi B_{ks} + (nm)_{kr} S_{rs} \} \}. \end{aligned} \quad (4.1.18)$$

Thus, for any infinite straight dislocation the stress field at any point $\mathbf{x} = |\mathbf{x}| \mathbf{m}$ is always of the form

$$\sigma_{mn}^x(\mathbf{x} = |\mathbf{x}| \mathbf{m}) = \frac{1}{|\mathbf{x}|} \Sigma_{mn}(\mathbf{m}; t, \mathbf{b}). \quad (4.1.19)$$

Σ_{mn} is the so-called straight dislocation angular stress factor and is given by

$$\Sigma_{mn} = \frac{1}{2\pi} C_{mnip} b_s \{ -m_p S_{is} + n_p (nn)_{ik}^{-1} \{ 4\pi B_{ks} + (nm)_{kr} S_{rs} \} \}. \quad (4.1.20)$$

The sense t of the tangent to the dislocation line is arbitrary, since one could have chosen $-t$ instead. It is well-known that reversing the sense of t is equivalent to reversing the sense of \mathbf{b} , i.e. $\mathbf{b} \rightarrow -\mathbf{b}$, so that the vector pair (t, \mathbf{b}) is always uniquely defined. Keeping \mathbf{m} fixed, the results

of Chap. 3 have shown that under the transformation $\mathbf{t} \rightarrow -\mathbf{t}$

$$\begin{aligned}\mathbf{n} &= \mathbf{t} \times \mathbf{m} \rightarrow -\mathbf{n}, \\ \mathbf{B}(\mathbf{t}) &= \mathbf{B}(-\mathbf{t}), \\ \mathbf{S}(\mathbf{t}) &= -\mathbf{S}(-\mathbf{t}).\end{aligned}$$

so that from eq. (4.1.20) we deduce that

$$\Sigma_{mn}(\mathbf{m}; \mathbf{t}) = \Sigma_{mn}(\mathbf{m}; -\mathbf{t}). \quad (4.1.21)$$

We shall later see that Σ_{mn} and certain of its angular derivatives are the quantities required to construct the in-plane elastic fields of plane curvilinear loops of dislocations. Equation (4.1.21) indicates if one defines the vector pair (\mathbf{t}, \mathbf{b}) correctly (as discussed in Section 2.5.1), then Σ_{mn} is invariant under a reversal of the sense of \mathbf{t} . On the other hand, reversing the sense of \mathbf{b} with \mathbf{t} , \mathbf{m} and \mathbf{n} held fixed, i.e. reversing the sign of the dislocation, changes the sign of Σ_{mn} as indicated by eq. (4.1.20). Thus, the sign of the dislocation field components is given unambiguously by the above equations and a proper application of the sign convention for \mathbf{b} discussed in Section 2.5.1. Asaro *et al.*⁽⁴⁴⁾ have given an alternative expression for Σ_{mn} in terms of the matrices \mathbf{Q} and \mathbf{S} .

Taking the dot product of eq. (4.1.18) with n_m and m_m , respectively, leads to the formulae:

$$\left. \begin{aligned}\sigma'_{mn}(\mathbf{x} = |\mathbf{x}| \mathbf{m}) n_m &= \frac{2}{|\mathbf{x}|} B_{ns} b_s, \\ \sigma'_{mn}(\mathbf{x} = |\mathbf{x}| \mathbf{m}) m_m &= (2\pi |\mathbf{x}|)^{-1} b_s \{ -(mm)_{ni} S_{is} \\ &\quad + (mn)_{ni} (nn)_{ik}^{-1} [4\pi B_{ks} + (nm)_{kr} S_{rs}] \} \end{aligned} \right\}. \quad (4.1.22)$$

These two formulae could have been obtained by differentiating the stress functions φ_j and using the same reasoning which led to eq. (4.1.16).

The components of the dislocation tractions \mathbf{T}' in the plane whose normal is \mathbf{n} are given by the first part of eq. (4.1.22) since

$$T'_n = \sigma'_{mn} n_m = \frac{2}{|\mathbf{x}|} B_{ns} b_s.$$

The components of \mathbf{T}' along \mathbf{n} , \mathbf{m} and \mathbf{t} , respectively, are merely $T'_n n_n$, $T'_n m_n$ and $T'_n t_n$, and these three (scalar) quantities may be computed in the laboratory frame used to compute \mathbf{B} without transforming to dislocation coordinates. The six independent components of the dislocation stress tensor referred to dislocation coordinates $(\mathbf{m}, \mathbf{n}, \mathbf{t})$ are merely

$$m_n \sigma'_{mn} n_m, n_n \sigma'_{mn} n_m, t_n \sigma'_{mn} n_m, m_n \sigma'_{mn} m_n, t_n \sigma'_{mn} m_n \text{ and } t_n \sigma'_{mn} t_m.$$

The first five listed quantities may be computed using eq. (4.1.22) without explicitly transforming to dislocation coordinates. The component $t_n \sigma'_{mn} t_m$

is obtained by using the fact that

$$t_i e_{ij} t_j = t_i t_j S_{ijmn} \sigma_{mn}^x = 0,$$

where the S_{ijmn} are the elastic compliances.

4.1.1.4. The integral representation for the dislocation displacement field—

Even the displacement field of the dislocation has a representation in the integral formalism. An examination of Fig. 4.2 shows that choosing \mathbf{m} in the direction of \mathbf{x} so that $\mathbf{m} \cdot \mathbf{x} = |\mathbf{x}|$, $\mathbf{n} \cdot \mathbf{x} = 0$ implies that

$$m_p \frac{\partial u_i}{\partial x_p} = \frac{\partial u_i}{\partial |\mathbf{x}|}; \quad n_p \frac{\partial u_i}{\partial x_p} = \frac{1}{|\mathbf{x}|} \frac{\partial u_i}{\partial \omega},$$

where ω is the angle measured counter-clockwise from a fixed datum in the plane to \mathbf{x} (or \mathbf{m}). Using eq. (4.1.16) we obtain

$$\frac{\partial u_i}{\partial |\mathbf{x}|} = -(2\pi |\mathbf{x}|)^{-1} b_s S_{is} \quad (4.1.23)$$

$$\frac{\partial u_i}{\partial \omega} = \frac{1}{2\pi} (nn)_{ik}^{-1} \{4\pi B_{ks} + (nm)_{kr} S_{rs}\} b_s, \quad (4.1.24)$$

which may be integrated to yield

$$u_i(|\mathbf{x}|, \omega) = \frac{1}{2\pi} b_s \left\{ -S_{is} \ln |\mathbf{x}| + 4\pi B_{ks} \int_0^\omega (nn)_{ik}^{-1} d\omega \right. \\ \left. + S_{rs} \int_0^\omega (nn)_{ik}^{-1} (nm)_{kr} d\omega \right\}. \quad (4.1.25)$$

Using the integral definitions of \mathbf{Q} and \mathbf{S} given in eqs (3.6.4) and (3.6.6) and the relation of eq. (3.6.21) shows that

$$u_i(|\mathbf{x}|, 2\pi) - u_i(|\mathbf{x}|, 0) = b_i, \quad (4.1.26)$$

i.e. the integral representation for u_i produces the correct discontinuity in the dislocation displacement field.

4.1.1.5. The dislocation strain energy and energy factor—Because the dislocation is a source of pure internal stress, the total mechanical energy associated with it is merely its strain energy, i.e.

$$\mathcal{E} = \frac{1}{2} \iiint_V \sigma_{ij} u_{j,i} dV. \quad (4.1.27)$$

Because the solution for the infinite straight dislocation is independent of $\mathbf{t} \cdot \mathbf{x}$, we shall compute \mathcal{E}^* , the strain energy per unit length of dislocation line. Applying the divergence theorem to eq. (4.1.27) for the region in the plane normal to \mathbf{t} which is bounded by two circles of radii r_0 and

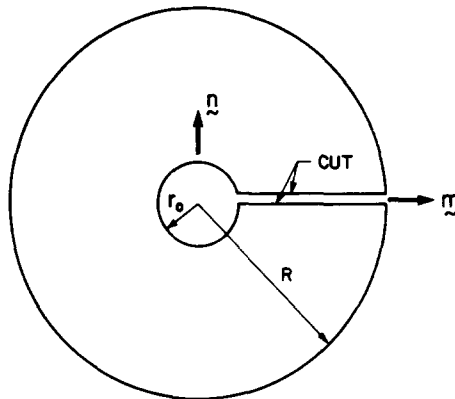


FIG. 4.3. The region of integration used to evaluate the self-energy of a straight dislocation via the divergence theorem.

R (Fig. 4.3) centred about the dislocation we find that

$$\begin{aligned} \mathcal{E}^\infty &= \frac{1}{2} \int_{|x|=r_0}^{|x|=R} \sigma_{ij}' b_j n_i d|x| + \frac{1}{2} \oint_{|x|=R} \sigma_{ij}' u_j N_i ds \\ &\quad - \frac{1}{2} \oint_{|x|=r_0} \sigma_{ij}' u_j N_i ds. \end{aligned} \quad (4.1.28)$$

N is the unit outer normal at a point on the circles $|x| = r_0$ or R ; for the calculation of \mathcal{E}^∞ we have chosen m and n so that m is along the cut, over which u_i is discontinuous and $n = t \wedge m$. Using the following reasoning one may deduce that only the first integral on the right side of eq. (4.1.28) contributes to \mathcal{E}^∞ . From eq. (4.1.25) we note that on any circle $|x| = \text{constant}$ the displacement field is of the form

$$u_j = C_j \ln|x| + R_j(\omega)$$

and

$$\sigma_{ij}' ds = |x| \sigma_{ij}' d\omega = \Sigma_{ij}(\omega) d\omega$$

since the stresses vary as $|x|^{-1}$. Furthermore,

$$\oint_C \sigma_{ij}' N_i ds = 0$$

for any closed curve C since there is no line force associated with the dislocation. These results are sufficient to reduce eq. (4.1.28) to

$$\mathcal{E}^\infty = \frac{1}{2} \int_{r_0}^R \sigma_{ij}' b_j n_i d|x| \quad (4.1.29)$$

or, using eq. (4.1.22),

$$\mathcal{E}' = B_{js} b_j b_s \int_{r_0}^R \frac{d|x|}{|x|}. \quad (4.1.30)$$

Integration yields

$$\mathcal{E}' = E \ln \frac{R}{r_0}, \quad (4.1.31)$$

where

$$E = B_{js} b_j b_s. \quad (4.1.32)$$

We cannot pass formally to the limit $R \rightarrow \infty$ and $r_0 \rightarrow 0$, so that the inner and outer “cutoff radii”, r_0 and R , are not unambiguously defined; it is customary to choose $r_0 \simeq |\mathbf{b}|$. Nevertheless, E , the “pre-logarithmic energy factor” is uniquely determined by \mathbf{B} and \mathbf{b} . Since \mathcal{E}' must always be positive for any stable elastic medium, the matrix \mathbf{B} is always positive definite, i.e. its three eigenvalues and its determinant are always positive. We further note that E depends only on \mathbf{b} , \mathbf{t} and C_{ijkm} , but E does not depend on the sense of \mathbf{t} or on the choice of (\mathbf{m}, \mathbf{n}) or the cut used to render the logarithmic function in eq. (4.1.1) single-valued. We shall see that E and certain of its angular derivatives play a central role in performing computations involving curvilinear dislocation lines.

The pre-logarithmic energy factor may be computed easily using crystal coordinates and numerical integration to evaluate \mathbf{B} from eq. (3.6.9). It is now clear that every elastic field quantity associated with an infinite straight dislocation may be expressed in terms of \mathbf{B} , \mathbf{Q} , \mathbf{S} and matrices which are known explicitly, so that one is not required to solve the Stroh eigenvalue problem to compute dislocation fields. Ultimately, of course, the method of computation one chooses is a matter of individual taste.

4.1.1.6. Angular derivatives of the dislocation energy factor—As we shall see, it proves convenient to have available formulae for the first two angular derivatives of E , the dislocation pre-logarithmic energy factor, in a given plane. These formulae allow one to compute the self-stresses associated with plane curvilinear dislocation loops. Consider a plane whose unit normal is \mathbf{N} and a straight dislocation in this plane whose line direction is \mathbf{t} and whose Burgers vector is \mathbf{b} . Obviously, \mathbf{t} is normal to \mathbf{N} . Let the angle measured counter-clockwise from a fixed datum in the plane to \mathbf{t} be θ . We wish to develop expressions for $E(\theta)$, $\partial E / \partial \theta$ and $\partial^2 E / \partial \theta^2$ for a fixed \mathbf{b} .

The geometry needed to develop these formulae is shown in Fig. 4.4. We note that

$$\frac{\partial \mathbf{t}}{\partial \theta} = \mathbf{N} \wedge \mathbf{t}; \quad \frac{\partial t_i}{\partial \theta} = \epsilon_{ijk} N_j t_k \quad (4.1.33)$$

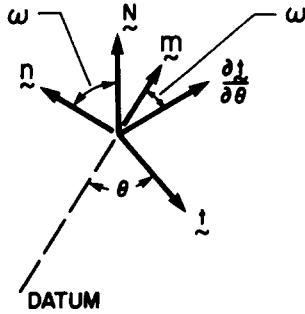


FIG. 4.4. The geometry used to compute angular derivatives of the dislocation stress and energy factors in a plane whose unit normal is N .

is normal to both N and t . In the plane containing N and $\partial t/\partial\theta$ we define the orthogonal unit vectors m and n by

$$m = \frac{\partial t}{\partial\theta} \cos\omega + N \sin\omega, \quad (4.1.34)$$

$$n = -\frac{\partial t}{\partial\theta} \sin\omega + N \cos\omega. \quad (4.1.35)$$

Since

$$\frac{\partial^2 t}{\partial\theta^2} = -t, \quad (4.1.36)$$

we also note that

$$\frac{\partial m}{\partial\theta} = -t \cos\omega; \quad \frac{\partial n}{\partial\theta} = t \sin\omega. \quad (4.1.37)$$

The quantity $E(\theta)$ is merely

$$E(\theta) = B_{ij} b_i b_j, \quad (4.1.38)$$

where

$$B_{ij} = \frac{1}{8\pi^2} \int_0^{2\pi} \{(mm)_{ij} - (mn)_{ir}(mn)_{rk}^{-1}(nm)_{kj}\} d\omega \quad (4.1.39)$$

with m and n given by eqs (4.1.34) and (4.1.35). Now

$$\frac{\partial E(\theta)}{\partial\theta} = b_i b_j \frac{\partial B_{ij}}{\partial\theta}, \quad (4.1.40)$$

and

$$\begin{aligned} \frac{\partial}{\partial\theta} (nn)_{rk}^{-1} &= -(nn)_{rs}^{-1} \left\{ \frac{\partial}{\partial\theta} (nn)_{sp} \right\} (nn)_{pk}^{-1} \\ &= -(nn)_{rs}^{-1} \{(nt)_{sp} + (tn)_{sp}\} (nn)_{pk}^{-1} \sin\omega \\ &= -F_{rk} \sin\omega. \end{aligned} \quad (4.1.41)$$

where $F_{rk} = F_{kr}$. Thus, using eq. (4.1.37) we obtain

$$\begin{aligned}\frac{\partial B_{ij}}{\partial \theta} &= \frac{1}{8\pi^2} \int_0^{2\pi} \{ -[(mt)_{ij} + tm] \cos \omega + (mn)_{ir} F_{rk} (nm)_{kj} \sin \omega \\ &\quad + [(tn)_{ir} \cos \omega - (mt)_{ir} \sin \omega] (nn)_{rk}^{-1} (nm)_{kj} \\ &\quad - (mn)_{ir} (nn)_{rk}^{-1} [(tm)_{kj} \sin \omega - (nt)_{kj} \cos \omega] \} d\omega. \quad (4.1.42)\end{aligned}$$

The quantity

$$\frac{\partial^2 E}{\partial \theta^2} = b_i b_j \frac{\partial^2 B_{ij}}{\partial \theta^2} \quad (4.1.43)$$

may be obtained by differentiating eq. (4.1.42). Differentiation yields

$$\begin{aligned}\frac{\partial^2 B_{ij}}{\partial \theta^2} &= \frac{1}{8\pi^2} \int_0^{2\pi} \left\{ - \left[\left(m \frac{\partial t}{\partial \theta} \right)_{ij} + \left(\frac{\partial t}{\partial \theta} m \right)_{ij} \right] \cos \omega + 2(tt)_{ij} \cos^2 \omega \right. \\ &\quad - 2[(tn)_{ir} \cos \omega - (mt)_{ir} \sin \omega] F_{rk} (nm)_{kj} \sin \omega \\ &\quad + 2(mn)_{ir} F_{rk} [(tm)_{kj} \sin \omega - (nt)_{kj} \cos \omega] \sin \omega \\ &\quad + 2[(tn)_{ir} \cos \omega - (mt)_{ir} \sin \omega] (nn)_{rk}^{-1} [(tm)_{kj} \sin \omega - (nt)_{kj} \cos \omega] \\ &\quad + \left[\left(\frac{\partial t}{\partial \theta} n \right)_{ir} \cos \omega - \left(m \frac{\partial t}{\partial \theta} \right)_{ir} \sin \omega + 2(tt)_{ir} \sin \omega \cos \omega \right] \\ &\quad \times (nn)_{rk}^{-1} (nm)_{kj} - (mn)_{ir} (nn)_{rk}^{-1} \\ &\quad \times \left[\left(\frac{\partial t}{\partial \theta} m \right)_{kj} \sin \omega - \left(n \frac{\partial t}{\partial \theta} \right)_{kj} \cos \omega - 2(tt)_{kj} \sin \omega \cos \omega \right] \\ &\quad \left. + (mn)_{ir} H_{rk} (nm)_{kj} \sin \omega \right\} d\omega, \quad (4.1.44)\end{aligned}$$

where

$$\begin{aligned}H_{rk} &= \frac{\partial F_{rk}}{\partial \theta} \\ &= -F_{rs} \{(nt)_{sp} + (tn)_{sp}\} (nn)_{pk}^{-1} \sin \omega \\ &\quad - (nn)_{rs}^{-1} \{(nt)_{sp} + (tn)_{sp}\} F_{pk} \sin \omega \\ &\quad + (nn)_{rs}^{-1} \left\{ \left(n \frac{\partial t}{\partial \theta} \right)_{sp} + \left(\frac{\partial t}{\partial \theta} n \right)_{sp} + 2(tt)_{sp} \sin \omega \right\} (nn)_{pk}^{-1}. \quad (4.1.45)\end{aligned}$$

Admittedly, the formulae for the first two angular derivatives of \mathbf{B} appear unwieldy, but they are easily evaluated using numerical integration. When \mathbf{b} lies in the plane normal to \mathbf{N} , Barnett *et al.*⁽⁶³⁾ have derived similar formulae for E , $\partial E/\partial \theta$ and $E + \partial^2 E/\partial \theta^2$ based upon an integral representation of E given by Barnett and Swanger.⁽⁴²⁾ The corresponding formulae for the angular derivatives of E in the Stroh sextic representation have been derived by Malén and Lothe.⁽⁵⁷⁾

Because of its utility we shall give the following formula for $E(\theta) + \partial^2 E / \partial \theta^2$ derived by Barnett *et al.*⁽⁶³⁾ for a dislocation whose Burgers vector \mathbf{b} lies in the plane whose normal is N . For convenience we choose the datum to lie along \mathbf{b} ; hence, $\theta = 0$ corresponds to a pure screw dislocation. In terms of the notation of the present work the formula deduced by Barnett *et al.*⁽⁶³⁾ (their equation (23)) may be written as

$$E(\theta) + \partial^2 E / \partial \theta^2 = A_{jsir} \left\{ - \left(2 \frac{\partial t_j}{\partial \theta} t_s + t_j \frac{\partial t_s}{\partial \theta} \right) \int_0^\pi (m)_i^{-1} d\omega \right. \\ \left. + 2 \int_0^\pi \left\{ \frac{\partial t_j}{\partial \theta} n_s + t_j t_s \sin \omega \right\} F_{ir} d\omega + t_j \int_0^\pi n_s H_{ir} d\omega \right\},$$

where

$$A_{jsir} = \frac{1}{4\pi^2} b_m b_g N_n \epsilon_{pjw} C_{ngip} C_{wmrs}$$

and F_{ir} and H_{ir} are given by eqs (4.1.41) and (4.1.45).

4.1.1.7. *Angular derivatives of the straight dislocation in-plane stress factors*—The dislocation stress factors Σ_{mn} have been given in eq. (4.1.20). Consider a straight dislocation (Burgers vector \mathbf{b}), whose line direction \mathbf{t} lies in a plane whose unit normal is N . Using the geometry of Fig. 4.4 and replacing \mathbf{n} and \mathbf{m} in eq. (4.1.20) by N and $\partial \mathbf{t} / \partial \theta$, respectively, the angular stress factors in the plane whose unit normal is N may be written as

$$\Sigma_{mn} = \frac{1}{2\pi} C_{mni_p} b_s \left\{ - \frac{\partial t_p}{\partial \theta} S_{is} + N_p (NN)_{ik}^{-1} \left[4\pi B_{ks} + \left(N \frac{\partial t}{\partial \theta} \right)_{kr} S_{rs} \right] \right\}. \quad (4.1.46)$$

We wish to develop expressions for $\partial \Sigma_{mn} / \partial \theta$ and $\partial^2 \Sigma_{mn} / \partial \theta^2$, where θ is the angle measured counter-clockwise from a fixed datum in the plane to \mathbf{t} . Since N is constant

$$\frac{\partial \Sigma_{mn}}{\partial \theta} = \frac{1}{2\pi} C_{mni_p} b_s \left\{ t_p S_{is} - \frac{\partial t_p}{\partial \theta} \frac{\partial S_{is}}{\partial \theta} \right. \\ \left. + N_p (NN)_{ik}^{-1} \left[4\pi \frac{\partial B_{ks}}{\partial \theta} + \left(N \frac{\partial t}{\partial \theta} \right)_{kr} \frac{\partial S_{rs}}{\partial \theta} - (Nt)_{kr} S_{rs} \right] \right\}. \quad (4.1.47)$$

Similarly

$$\frac{\partial^2 \Sigma_{mn}}{\partial \theta^2} = \frac{1}{2\pi} C_{mni_p} b_s \left\{ 2t_p \frac{\partial S_{is}}{\partial \theta} + \frac{\partial t_p}{\partial \theta} \left(S_{is} - \frac{\partial^2 S_{is}}{\partial \theta^2} \right) \right. \\ \left. + N_p (NN)_{ik}^{-1} \left[4\pi \frac{\partial^2 B_{ks}}{\partial \theta^2} - 2(Nt)_{kr} \frac{\partial S_{rs}}{\partial \theta} - \left(N \frac{\partial t}{\partial \theta} \right)_{kr} \right. \right. \\ \left. \left. \times \left(S_{rs} - \frac{\partial^2 S_{rs}}{\partial \theta^2} \right) \right] \right\}. \quad (4.1.48)$$

Adding eq. (4.1.46) and eq. (4.1.48) yields

$$\begin{aligned} \Sigma_{mn} + \frac{\partial^2 \Sigma_{mn}}{\partial \theta^2} = & \frac{1}{2\pi} C_{mni_p} b_s \left\{ 2t_p \frac{\partial S_{is}}{\partial \theta} - \frac{\partial t_p}{\partial \theta} \frac{\partial^2 S_{is}}{\partial \theta^2} \right. \\ & + N_p(NN)_{ik}^{-1} \left[4\pi \left(B_{ks} + \frac{\partial^2 B_{ks}}{\partial \theta^2} \right) + \left(N \frac{\partial t}{\partial \theta} \right)_{kr} \frac{\partial^2 S_{rs}}{\partial \theta^2} \right. \\ & \left. \left. - 2(Nt)_{kr} \frac{\partial S_{rs}}{\partial \theta} \right] \right\}, \end{aligned} \quad (4.1.49)$$

which is a quantity of some utility in curvilinear dislocation problems.

We already have available formulae for \mathbf{B} and its first two angular derivatives. The angular derivatives of Σ_{mn} can be considered known once we have expressions for \mathbf{S} and its first two angular derivatives. With \mathbf{m} and \mathbf{n} given by eqs (4.1.34) and (4.1.35), respectively, \mathbf{S} has the integral representation

$$S_{ks} = - \frac{1}{2\pi} \int_0^{2\pi} (nn)_{kj}^{-1} (nm)_{js} d\omega.$$

Using the geometry of Fig. 4.4

$$\begin{aligned} \frac{\partial S_{ks}}{\partial \theta} = & - \frac{1}{2\pi} \int_0^{2\pi} \{ -F_{kj}(nm)_{js} \sin \omega \\ & + (nn)_{kj}^{-1} [(tm)_{js} \sin \omega - (nt)_{js} \cos \omega] \} d\omega, \end{aligned} \quad (4.1.50)$$

where $F_{kj} = F_{jk}$ is as defined in eq. (4.1.41).

Differentiation of eq. (4.1.50) with respect to θ yields

$$\begin{aligned} \frac{\partial^2 S_{ks}}{\partial \theta^2} = & - \frac{1}{2\pi} \int_0^{2\pi} \left\{ -2F_{kj} [(tm)_{js} \sin \omega - (nt)_{js} \cos \omega] \sin \omega \right. \\ & + (nn)_{kj}^{-1} \left[\left(\frac{\partial t}{\partial \theta} m \right)_{js} \sin \omega - \left(n \frac{\partial t}{\partial \theta} \right)_{js} \cos \omega - 2(tt)_{js} \sin \omega \cos \omega \right] \\ & \left. - H_{kj}(nm)_{js} \sin \omega \right\} d\omega, \end{aligned} \quad (4.1.51)$$

where $H_{kj} = H_{jk}$ is given by eq. (4.1.45).

Asaro and Barnett⁽⁶⁴⁾ have also given integral representations for the angular derivatives of Σ_{mn} , which involve the matrices \mathbf{Q} , \mathbf{S} and their angular derivatives.

4.1.1.8. Straight dislocations in uniform motion—As noted in Chap. 3, the Stroh and the integral formalisms used to solve the elastostatic straight dislocation problem are easily extended to include straight dis-

locations in uniform motion.[†] We need merely replace the static elastic constants C_{ijkm} everywhere by their “dynamic counterparts” C'_{ijkm} defined by eq. (3.7.7), i.e.

$$C'_{ijkm} = C_{ijkm} - \rho v_i v_m \delta_{jk};$$

ρ is the mass density of the medium and v is the uniform velocity normal to the dislocation line. We note that there is one exception to this rule of replacing C_{ijkm} by C'_{ijkm} ; we *always* compute the stresses from the displacement gradients using Hooke’s law in the form

$$\sigma_{ij} = C_{ijkm} u_{k,m}.$$

The Lagrangian, \mathcal{L} , for a uniformly moving dislocation is the difference between its kinetic energy, T , and its strain energy, \mathcal{E}' , i.e.

$$\mathcal{L} = T - \mathcal{E}'. \quad (4.1.52)$$

Thus,

$$\mathcal{L} = \frac{1}{2} \oint \int \int_V \{ \rho \dot{u}_k \dot{u}_k - C_{ijkm} u_{j,i} u_{k,m} \} dV, \quad (4.1.53)$$

where ‘ indicates time derivative. For problems of uniform motion (see Chap. 3.)

$$\dot{u}_k = -v_m u_{k,m}$$

and

$$\begin{aligned} \mathcal{L} &= \frac{1}{2} \oint \int \int_V \{ \rho v_i v_m \delta_{jk} - C_{ijkm} \} u_{j,i} u_{k,m} dV \\ &= -\frac{1}{2} \oint \int \int_V C'_{ijkm} u_{j,i} u_{k,m} dV. \end{aligned} \quad (4.1.54)$$

In the static case we obtained eq. (4.1.32)

$$\begin{aligned} \mathcal{E}' &= \frac{1}{2} \oint \int \int_V C_{ijkm} u_{j,i} u_{k,m} dV \\ &= B_{ij} b_i b_j \ln \frac{R}{r_0} \quad (\text{per unit length of dislocation}). \end{aligned}$$

Thus, for a dislocation in uniform motion,

$$\mathcal{L} = -B_{ij} b_i b_j \ln \frac{R}{r_0} \quad (\text{per unit length of dislocation}), \quad (4.1.55)$$

where B is computed from eq. (3.6.9) using C'_{ijkm} .

[†]This problem was first treated in the two-dimensional case by Bullough and Bilby,⁽¹⁷⁸⁾ who extended the analysis for static dislocations by Eshelby *et al.*⁽⁴⁾ the general case has been treated by Sáenz.⁽¹⁷⁹⁾

Beltz *et al.*⁽⁶⁵⁾ have shown that for a uniformly moving straight dislocation

$$\frac{\partial \mathcal{L}}{\partial v} = \frac{2T}{v} > 0 \quad (4.1.56)$$

so that⁽⁶⁶⁾

$$\frac{\partial \mathbf{B}}{\partial v} \text{ is a negative definite matrix.}$$

For velocities below the Rayleigh velocity \mathbf{B} is always a positive definite matrix;⁽⁶⁶⁾ at the Rayleigh velocity two eigenvalues of \mathbf{B} vanish simultaneously.

4.1.2. Summary of formulae derived in Chapters 3 and 4

For the convenience of those readers who wish to omit the mathematical details of the previous sections and for general reference purposes, we give in this section a summary of the most important two-dimensional formulae derived in this review, with strong emphasis on the infinite straight dislocation field formulae derived in Section 4.1.1. The integral forms of the formulae given here are, in the authors' view, the most suitable ones for making actual numerical computations. In particular, these forms provide a good basis on which to prepare the straight dislocation field data tabulations required in the geometric theorems to be discussed in the following sections. The equation numbers in this section refer to the actual equation numbers in the text.

4.1.2.1. *General formulae*—In the equations in this section we refer to a set of mutually orthogonal unit vectors \mathbf{m} , \mathbf{n} , \mathbf{t} as shown in Fig. 4.2. The vectors \mathbf{m} and \mathbf{n} rotate in a positive sense (right-hand screw rule) about \mathbf{t} through the angle ω measured from an arbitrary reference datum in the (\mathbf{m}, \mathbf{n}) plane; consequently, the components of the vectors \mathbf{m} and \mathbf{n} as they appear in matrix form in the integrands of the expressions for $Q(\mathbf{t})$, etc. play the role of integration variables. We emphasize again that the basic matrices $Q(\mathbf{t})$, $S(\mathbf{t})$ and $B(\mathbf{t})$ depend only on the direction \mathbf{t} and the elastic constants C_{ijkl} . The latter may be referred to an arbitrary set of axes, and these may conveniently be chosen as the crystal axes, for which C_{ijkl} display their simplest form.

$$(nm)_{jk} = n_i C_{ijkp} m_p, \quad (3.3.3)$$

$$Q_{sk} = Q_{ks} = -\frac{1}{\pi} \int_0^\pi (nn)_{sk}^{-1} d\omega \quad (\text{integral}) \quad (3.6.4)$$

$$= i \sum_{x=1}^6 \pm A_{sx} A_{kx} \quad (\text{sextic}), \quad (3.6.4)$$

$$S_{ks} = -\frac{1}{\pi} \int_0^\pi (nn)_{kj}^{-1} (nm)_{js} d\omega \quad (\text{integral}) \quad (3.6.6)$$

$$= i \sum_{z=1}^6 \pm A_{kz} L_{sz} \quad (\text{sextic}), \quad (3.6.6)$$

$$B_{ks} = B_{sk} = \frac{1}{4\pi^2} \int_0^\pi \{(mm)_{ks} - (mn)_{kr}(nn)_{rj}^{-1}(nm)_{js}\} d\omega \quad (\text{integral}) \quad (3.6.9)$$

$$= -\frac{1}{4\pi i} \sum_{z=1}^6 \pm L_{kz} L_{sz} \quad (\text{sextic}), \quad (3.6.9)$$

$$(nn)_{ij}^{-1} = \frac{\epsilon_{ism}\epsilon_{jrw}(nn)_{sr}(nn)_{mw}}{2\epsilon_{pgn}(nn)_{1p}(nn)_{2g}(nn)_{3n}} = (nn)_{ji}^{-1} \quad (\text{general symmetry}). \quad (4.1.17)$$

For a medium of cubic symmetry

$$(nn)_{11}^{-1} = \frac{e(e+f) - efn_1^2 + (f^2-1)(n_2 n_3)^2}{(C_{12} + C_{44})D},$$

$$(nn)_{12}^{-1} = -\frac{n_1 n_2 [(f-1)n_3^2 + e]}{(C_{12} + C_{44})D}.$$

The remaining components of $(nn)^{-1}$ are obtained by cyclic permutation of indices, i.e. $1 \rightarrow 2$, $2 \rightarrow 3$ and $3 \rightarrow 1$.

$$\begin{aligned} D &= e^2(e+f) + e(f^2-1)(n_1^2 n_2^2 + n_1^2 n_3^2 + n_2^2 n_3^2) \\ &\quad + (f-1)^2(f+2)(n_1 n_2 n_3)^2, \end{aligned}$$

$$e = \frac{C_{44}}{C_{12} + C_{44}}; \quad f = \frac{C_{11} - C_{44}}{C_{12} + C_{44}}.$$

Note that n_1 , n_2 and n_3 are the components of \mathbf{n} relative to the cube axes. If $f=1$, the isotropic case is recovered.

4.1.2.2. The elastic fields of infinite straight dislocations in the integral and the sextic formalisms—For the equations in this section, \mathbf{m} , \mathbf{n} , \mathbf{t} form an orthogonal set of unit vectors and the components of the vectors \mathbf{m} , \mathbf{n} play the role of integration variables when they appear in the integrands, just as in the previous section. On the other hand, when the components of \mathbf{m} , \mathbf{n} do not appear within integrands, they play the role of dislocation coordinates chosen such that \mathbf{t} is the positive line direction, $\mathbf{x} = |\mathbf{x}| \mathbf{m}$ and $\mathbf{n} \cdot \mathbf{x} = 0$ where \mathbf{x} is the perpendicular vector from the line to the field point in question. In other cases, e.g. the angular derivatives of the basic matrices $Q(\mathbf{t})$, etc. we are interested in taking derivatives with respect to the orientation of \mathbf{t} ; here we let \mathbf{N} be a unit vector normal to a plane containing \mathbf{t} , and we take derivatives with respect to θ , the

angle between t and an arbitrary in-plane reference datum. Also note that in the latter case, N , t and $\partial t/\partial\theta = N \wedge t$ form an orthogonal set of unit vectors, fixed for any given θ , and the rotating vector pair m , n defining the integration variables lies in the plane containing N and $\partial t/\partial\theta$ (Fig. 4.4).

Integral formulae.

(i) Displacement

$$\begin{aligned} u_i(|x|, \omega) = & \frac{1}{2\pi} b_s \left\{ -S_{is} \ln |x| + 4\pi B_{ks} \int_0^\omega (nn)_{ik}^{-1} d\omega \right. \\ & \left. + S_{rs} \int_0^\omega (nn)_{ik}^{-1} (nm)_{kr} d\omega \right\}. \end{aligned} \quad (4.1.25)$$

(ii) Displacement gradient

$$\begin{aligned} u_{i,p}(x = |x| m) = & (2\pi|x|)^{-1} b_s \{ -m_p S_{is} \\ & + n_p (nn)_{ik}^{-1} [4\pi B_{ks} + (nm)_{kr} S_{rs}] \}. \end{aligned} \quad (4.1.16)$$

(iii) Stress

$$\begin{aligned} \sigma_{mn}^x(x = |x| m) = & C_{mnip} u_{i,p} \\ = & |x|^{-1} \Sigma_{mn}(m; t, b). \end{aligned} \quad (4.1.18)-(4.1.20)$$

(iv) Energy

$$\mathcal{E}^x = E \ln \frac{R}{r_0}, \text{ self-energy per unit length}; \quad (4.1.32)$$

$$E = B_{js} b_j b_s, \text{ energy factor}. \quad (4.1.32)$$

(v) Angular derivatives of basic matrices, stress factors and energy factors (see Fig. 4.4)

$$\begin{aligned} \frac{\partial}{\partial\theta} B_{ij} = & \frac{1}{8\pi^2} \int_0^{2\pi} \{ -[(mt)_{ij} + (tm)_{ij}] \cos\omega + (mn)_{ir} F_{rk} (nm)_{kj} \sin\omega \\ & + [(tn)_{ir} \cos\omega - (mt)_{ir} \sin\omega] (nn)_{rk}^{-1} (nm)_{kj} \\ & - (mn)_{ir} (nn)_{rk}^{-1} [(tm)_{kj} \sin\omega - (nt)_{kj} \cos\omega] \} d\omega. \end{aligned} \quad (4.1.42)$$

$$\begin{aligned} \frac{\partial^2}{\partial\theta^2} B_{ij} = & \frac{1}{8\pi^2} \int_0^{2\pi} \left\{ - \left[\left(m \frac{\partial t}{\partial\theta} \right)_{ij} + \left(\frac{\partial t}{\partial\theta} m \right)_{ij} \right] \cos\omega + 2(tt)_{ij} \cos^2\omega \right. \\ & - 2[(tn)_{ir} \cos\omega - (mt)_{ir} \sin\omega] F_{rk} (nm)_{kj} \sin\omega \\ & + 2(mn)_{ir} F_{rk} [(tm)_{kj} \sin\omega - (nt)_{kj} \cos\omega] \sin\omega \\ & \left. + 2[(tn)_{ir} \cos\omega - (mt)_{ir} \sin\omega] (nn)_{rk}^{-1} [(tm)_{kj} \sin\omega - (nt)_{kj} \cos\omega] \right\} d\omega. \end{aligned}$$

$$\begin{aligned}
& + \left[\left(\frac{\partial t}{\partial \theta} n \right)_{ir} \cos \omega - \left(m \frac{\partial t}{\partial \theta} \right)_{ir} \sin \omega + 2(tt)_{ir} \sin \omega \cos \omega \right] \\
& \times (nn)_{rk}^{-1} (nm)_{kj} - (mn)_{ir} (nn)_{rk}^{-1} \\
& \times \left[\left(\frac{\partial t}{\partial \theta} m \right)_{kj} \sin \omega - \left(n \frac{\partial t}{\partial \theta} \right)_{kj} \cos \omega - 2(tt)_{kj} \sin \omega \cos \omega \right] \\
& + (mn)_{ir} H_{rk} (nm)_{kj} \sin \omega \Big\} d\omega. \tag{4.1.44}
\end{aligned}$$

$$\frac{\partial^2 S_{ks}}{\partial \theta^2} = - \frac{1}{2\pi} \int_0^{2\pi} \{ -F_{kj}(nm)_{js} \sin \omega + (nn)_{kj}^{-1} [(tm)_{js} \sin \omega - (nt)_{js} \cos \omega] \} d\omega. \tag{4.1.50}$$

$$\begin{aligned}
\frac{\partial^2 S_{ks}}{\partial \theta^2} = & - \frac{1}{2\pi} \int_0^{2\pi} \left\{ -2F_{kj} [(tm)_{js} \sin \omega - (nt)_{js} \cos \omega] \sin \omega \right. \\
& + (nn)_{kj}^{-1} \left[\left(\frac{\partial t}{\partial \theta} m \right)_{js} \sin \omega - \left(n \frac{\partial t}{\partial \theta} \right)_{js} \cos \omega - 2(tt)_{js} \sin \omega \cos \omega \right] \\
& \left. - H_{kj} (nm)_{js} \sin \omega \right\} d\omega. \tag{4.1.51}
\end{aligned}$$

$$\Sigma_{mn} = \frac{1}{2\pi} C_{mnp} b_s \left\{ - \frac{\partial t_p}{\partial \theta} S_{is} + N_p (NN)_{ik}^{-1} \left[4\pi B_{ks} + \left(N \frac{\partial t}{\partial \theta} \right)_{kr} S_{rs} \right] \right\}. \tag{4.1.46}$$

$$\begin{aligned}
\frac{\partial}{\partial \theta} \Sigma_{mn} = & \frac{1}{2} C_{mnp} b_s \left\{ t_p S_{is} - \frac{\partial t_p}{\partial \theta} \frac{\partial S_{is}}{\partial \theta} \right. \\
& \left. + N_p (NN)_{ik}^{-1} \left[4\pi \frac{\partial B_{ks}}{\partial \theta} + \left(N \frac{\partial t}{\partial \theta} \right)_{kr} \frac{\partial S_{rs}}{\partial \theta} - (Nt)_{kr} S_{rs} \right] \right\}. \tag{4.1.47}
\end{aligned}$$

$$\begin{aligned}
\Sigma_{mn} + \frac{\partial^2 \Sigma_{mn}}{\partial \theta^2} = & \frac{1}{2\pi} C_{mnp} b_s \left\{ 2t_p \frac{\partial S_{is}}{\partial \theta} - \frac{\partial t_p}{\partial \theta} \frac{\partial^2 S_{is}}{\partial \theta^2} \right. \\
& + N_p (NN)_{ik}^{-1} \left[4\pi \left(B_{ks} + \frac{\partial^2 B_{ks}}{\partial \theta^2} \right) + \left(N \frac{\partial t}{\partial \theta} \right)_{kr} \frac{\partial^2 S_{rs}}{\partial \theta^2} \right. \\
& \left. \left. - 2(Nt)_{kr} \frac{\partial S_{rs}}{\partial \theta} \right] \right\}. \tag{4.1.49}
\end{aligned}$$

$$\frac{\partial E(\theta)}{\partial \theta} = b_i b_j \frac{\partial B_{ij}}{\partial \theta}. \tag{4.1.40}$$

The glide plane line tension factor is

$$\begin{aligned} E(\theta) + \frac{\partial^2}{\partial \theta^2} E(\theta) = A_{jsir} \left\{ - \left(2 \frac{\partial t_j}{\partial \theta} t_s + t_j \frac{\partial t_s}{\partial \theta} \right) \int_0^\pi (nn)_{ir}^{-1} d\omega \right. \\ \left. + 2 \int_0^\pi \left(\frac{\partial t_j}{\partial \theta} n_s + t_j t_s \sin \omega \right) F_{ir} d\omega \right. \\ \left. + t_j \int_0^\pi n_s H_{ir} \right\} d\omega, \end{aligned}$$

where

$$A_{jsir} = \frac{1}{4\pi^2} b_m b_g N_n \epsilon_{pjw} C_{ngip} C_{wmrs}$$

and F_{ir} and H_{ir} are given by eqs (4.1.41) and (4.1.45).

Sextic formulae.

(i) Displacement

$$u_i(x) = \frac{1}{2\pi i} \sum_{z=1}^6 \pm A_{iz} L_{sz} b_s \ln(m \cdot x + p_z n \cdot x). \quad (4.1.12)$$

(ii) Displacement gradient

$$u_{i,p}(x) = \frac{1}{2\pi i} \sum_{z=1}^6 \pm A_{iz} L_{sz} b_s \frac{m_p + p_z n_p}{m \cdot x + p_z n \cdot x}. \quad (4.1.14)$$

(iii) Stress

$$\sigma_{mn}^x(x) = C_{mnp} u_{i,p}(x).$$

4.1.3. Field data for infinite, straight dislocations

The formulae summarized in the preceding section for the elastic field of an infinite, straight dislocation in an homogeneous medium are of value in two respects. Firstly, they enable the field quantities to be evaluated in a reasonably straightforward manner for any problem in which the straight-line description of the dislocation is a valid approximation. Although formulae for evaluating displacement, stress and self-energy have been available from the work of Eshelby *et al.*⁽⁴⁾ and Stroh,⁽⁵⁾ the integral forms presented in Section 4.1.2 are more useful for numerical analysis. All components are referred to arbitrary axes and degeneracy problems inherent in the sextic method are avoided. Secondly, the equations derived show how the derivatives of the field quantities with respect to line orientation can be expressed in a convenient form for numerical evaluation. This is a particularly important aspect, for the data so obtained can be used in the formulae of Brown⁽⁹⁾ and Indenbom and Orlov⁽¹⁰⁾ to compute the fields of dislocations of arbitrary shape. The derivation of these formulae, and their application in several problems involving curved dislocations, will be described in Sections 4.2 and 4.3. The remainder of the present section will be concerned with the data for the infinite, straight line, which have already been obtained. It will be seen that they can be presented in a form which is very convenient for general use.

Equation (4.1.38) for the energy factor $E(\theta)$ was first programmed by Barnett and Swanger⁽⁴²⁾ and applied to perfect dislocations in copper, lithium and niobium. Equations (4.1.38), (4.1.40) and (4.1.43) for $E(\theta)$, $E'(\theta)$ and $E(\theta) + E''(\theta)$, respectively, were used by Barnett *et al.*⁽⁶³⁾ to evaluate these quantities for some dislocation systems in copper, nickel, iron, lithium and niobium, and the data were presented in tabular form (accurate to 4 figures) as well as graphically. Integral expressions for the three stress components acting on the plane defined by an infinite, straight line and its Burgers vector were derived by Asaro and Hirth⁽⁶⁷⁾ (see Section 4.1.1.3). The first angular derivatives were also given, and the integrals were evaluated for the $\frac{1}{2}\langle 111 \rangle\{111\}$ dislocation in iron; the data were presented in graphical form and were applied to the study of equilibrium node configurations in iron. These papers demonstrated the value of the integral form for the field quantities, but they did not provide data in a form which could be used generally. For this to be achieved, two criteria must be satisfied. First, the data should be accurate to a reasonable (and specified) accuracy. Second, they should be presented in a form which is as convenient to use as their isotropic counterparts. (The latter criterion was not satisfied in the tables of Barnett *et al.*⁽⁶³⁾) These two conditions were met in the data compilations of Bacon and Scattergood,^(68,69) and an outline of the results of their second paper, which was confined to the common fcc and bcc metals, will now be described. In addition, results for the fcc metals iridium, palladium and platinum and the common hcp metals will be presented for the first time.

Bacon and Scattergood⁽⁶⁹⁾ evaluated the three components of stress—one normal and two shear—acting in the plane containing an infinite, straight line and its Burgers vector; the first angular derivatives with respect to line orientation of these three tractions were also determined. The three tractions specified in this two-dimensional situation are sufficient to solve many dislocation-dislocation interaction problems. The stress components are most conveniently referred to the mutually orthogonal vectors b° , M and N , where b° is the unit vector in the Burgers vector direction ($b = |b|b^\circ$), N is the unit vector normal to the plane and $M = N \wedge b^\circ$. The orientation θ of the dislocation line is defined such that if the unit vector in the positive line direction is t , then $b^\circ \wedge t = N \sin \theta$, i.e. θ is to be measured modulo 2π from b to t in the positive sense given by a right-hand screw rule with respect to N (see Fig. 4.5). The three traction components acting in the plane in the directions b , M and N at a field point at $(N \wedge t)d$ with respect to a point on the line will be denoted by $T_i'(d, \theta)$, where $i = 1, 2, 3$ refer to the directions of b , M and N , respectively. (Tractions are related to stresses by $T_i' = \sigma_{ij}' N_j$, eq. (2.2.1).) The quantities computed by Bacon and Scattergood⁽⁶⁹⁾ were the orientation-dependent factors $T_i(\theta)$, where

$$T_i'(d, \theta) = \frac{2T_i(\theta)}{d}. \quad (4.1.57)$$

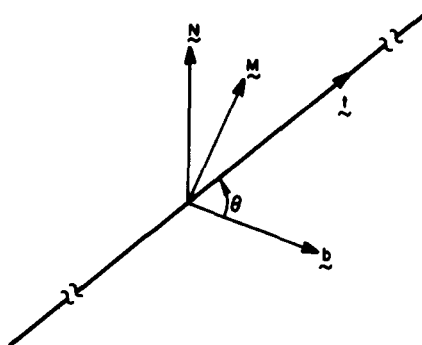


FIG. 4.5. The dislocation geometry used in the text to define the in-plane tractions.

(We shall take d to be a positive quantity, so the sign of $T_i^\infty(d, \theta)$ is reversed when evaluated at a point $-(N \wedge t)d$.) These components have the following simple form for an isotropic medium:

$$T_1 = K(2 - v - v \cos 2\theta), \quad T_2 = K(-v \sin 2\theta), \quad T_3 = 0, \quad (4.1.58)$$

where $K = \mu b / 8\pi(1 - v)$, μ is the shear modulus and v is Poisson's ratio. With the coordinate frame used here, reference to eq. (4.1.22) shows that in the general case

$$\begin{aligned} T_1(\theta) &= \frac{1}{2} \sum_{pq} N_p b_q^0 = \frac{1}{|\mathbf{b}|} B_{pq} b_p b_q = \frac{E(\theta)}{|\mathbf{b}|}, \\ T_2(\theta) &= \frac{1}{2} \sum_{pq} N_p M_q = B_{pq} b_p M_q, \\ T_3(\theta) &= \frac{1}{2} \sum_{pq} N_p N_q = B_{pq} b_p N_q, \end{aligned} \quad (4.1.59)$$

where Σ_{pq} is the angular part of the stress field of an infinite straight line as defined by eq. (4.1.19). The relation between T_1 and the prelogarithmic energy factor E follows from eq. (4.1.32).

It can be seen from eq. (4.1.58) that the functions $T_i(\theta)$ for isotropic media are the expansions to first-order harmonics of the Fourier series representation of even or odd functions. The tractions for anisotropic media are also periodic in θ with period π , although they are not necessarily even, odd or identically zero, and the Fourier series is, therefore, a natural way to represent the anisotropic data. The number of terms required in the series to represent $T_i(\theta)$ to a given accuracy over one period in θ will be a measure of the deviation of the material from isotropic behaviour.

The slip systems considered here and the notation used to describe them are given in Table 4.1. The metals for which data have been obtained and the room-temperature elastic constants which were used in the computations, are listed in Table 4.2. The tractions $T_i(\theta)$ and their first derivatives $T'_i(\theta)$ were computed to a relative accuracy of 10^{-6} using eqs (4.1.59) and

Table 4.1. The Slip Planes and Burgers Vectors for the Crystal Structures Which Are Considered Here: the Designations Shown Are Used to Identify These Systems in Table 4.3

Crystal structure	Slip plane normal	Burgers vector	Designation
fcc	[111]	1/2[110]	fcc1
fcc	[111]	1/6[112]	fcc2
bcc	[110]	1/2[111]	bcc1
bcc	[112]	1/2[111]	bcc2
hcp	[1100]	1/3[1120]	hcp1

(4.1.42) for $\theta = 0(2^\circ)90^\circ$ for the fcc1, fcc2, hcp1 and bcc2 systems and $\theta = 0(2^\circ)180^\circ$ for the bcc1 system. Fourier coefficients were fitted to the computed data such that the maximum percentage deviation between the fitted and computed values was less than 0.5%. This deviation is defined as

$$D_N = 100 \max_{0 < \theta < \pi} \left| \frac{f(\theta) - f_N(\theta)}{f_{\max}} \right|, \quad (4.1.60)$$

where $f(\theta)$ is the function of interest, i.e. T_i or T'_i , $f_N(\theta)$ is the value obtained from the Fourier series retaining N harmonics and f_{\max} is the maximum absolute value of $f(\theta)$ in the range $\theta = 0(2^\circ)180^\circ$; the quantity $f_N(\theta)$ can be written as

$$f_N(\theta) = A_0 + \sum_{n=1}^N (A_n \cos 2n\theta + B_n \sin 2n\theta). \quad (4.1.61)$$

The data to be presented here are the coefficients A_n and B_n for each $T_i(\theta)$; the coefficients for $T'_i(\theta)$ can be obtained from these by differentiation of eq. (4.1.61), giving $A'_0 = 0$, $A'_n = 2nB_n$ and $B'_n = -2nA_n$. The coefficients for the second derivatives $T''_i(\theta)$ could also be obtained from A_n and B_n , but the values for T'_i so obtained are unlikely to be as accurate as the 0.5% deviation specified for T_i and T'_i .

Values of the $T_i(\theta)$ coefficients A_n and B_n for the metals listed in Table 4.2 are presented in Table 4.3. The columns labelled A and B give the values A_n and B_n for each $T_i(\theta)$ in the order $n = 0, 1, \dots, N$, and a blank entry denotes zero. $E \pm X$ means multiply by $10^{\pm X}$ and the units are $a \times 10^{11}$ dyne cm $^{-2}$, where a is the lattice parameter. The convenience of the Fourier series representation is demonstrated by considering a specific example: the stresses in the fcc2 system of aluminium are given to an accuracy of better than 0.5% by

$$\begin{aligned} T_1(\theta) &= 0.107597 - 0.023567 \cos 2\theta, \\ T_2(\theta) &= -0.023567 \sin 2\theta, \\ T_3(\theta) &= (0.015016 - 19.3798 \cos 2\theta - 5.2054 \cos 4\theta) \times 10^{-4}. \end{aligned} \quad (4.1.62)$$

Table 4.2. The Elastic Stiffness Constants Used for the Data Compilation of Table 4.3 (the Units Are 10^{11} d.cm $^{-2}$ = 10^{10} Nm $^{-2}$); many of the Values Were Taken From the Table Compiled by Hirth and Lothe⁽⁶⁾ [reference (a)] and More Recently Obtained Values for Some of These Metals May Be Found in the Handbook by Simmons and Wang⁽¹⁴⁸⁾ Listed as Reference (k) below.

Element	Structure	Reference	C_{11}	C_{12}	C_{44}
Ag	fcc	(a)	12.40	9.34	4.61
Al	fcc	(a)	10.82	6.13	2.85
Au	fcc	(a)	18.60	15.70	4.20
Cr	bcc	(a)	35.00	5.78	10.10
Cu	fcc	(a)	16.84	12.14	7.54
Fe	bcc	(a)	24.20	14.65	11.20
Ir	fcc	(b)	58.00	24.20	25.60
Li	bcc	(c)	1.48	1.25	1.08
Mo	bcc	(a)	46.00	17.60	11.00
Nb	bcc	(a)	24.60	13.40	2.87
Ni	fcc	(a)	24.65	14.73	12.47
Pb	fcc	(a)	4.66	3.92	1.44
Pd	fcc	(d)	22.71	17.60	7.17
Pt	fcc	(e)	34.67	25.07	7.65
Ta	bcc	(a)	26.70	16.10	8.25
V	bcc	(a)	22.80	11.90	4.26

Element	Structure	Reference	C_{11}	C_{12}	C_{13}	C_{33}	C_{44}
Be	hcp	(f)	29.23	2.67	1.40	33.64	16.25
Cd	hcp	(g)	11.38	3.92	4.00	5.06	2.00
Hf	hcp	(h)	18.11	7.72	6.61	19.69	5.57
Mg	hcp	(i)	5.95	2.61	2.18	6.16	1.64
Ti	hcp	(h)	16.24	9.20	6.90	18.07	4.67
Zn	hcp	(j)	16.37	3.64	5.30	6.35	3.88
Zr	hcp	(h)	14.34	7.28	6.53	16.48	3.20

References:

- (a) Hirth and Lothe⁽⁶⁾
- (b) MacFarlane *et al.*⁽¹⁴⁹⁾
- (c) Nash and Smith⁽¹⁵⁰⁾
- (d) Rayne⁽¹⁵¹⁾
- (e) MacFarlane *et al.*⁽¹⁵²⁾
- (f) Smith and Arbogast⁽¹⁵³⁾
- (g) Garland and Silverman⁽¹⁵⁴⁾
- (h) Fisher and Renken⁽¹⁵⁵⁾
- (i) Wazzan and Robinson⁽¹⁵⁶⁾
- (j) Alers and Neighbours⁽¹⁵⁷⁾
- (k) Simmons and Wang⁽¹⁴⁸⁾

Aluminium is not very anisotropic and only a small number of terms are required in the series. For most of the metals considered, however, the data can be fitted to an accuracy of better than 0.5% with expansions to only 4th or 5th harmonic and these expansions are, therefore, almost as easy to use as their isotropic counterparts, eq. (4.1.58). To cite a simple example, consider the dissociation into two Shockley partials of an infinite straight line with Burgers vector $\frac{1}{2}\langle 110 \rangle$ in fcc metals. If ϕ is the angle

Table 4.3. The Fourier Coefficients A_n and B_n for the Three Traction Components in the Planes Listed in Table 4.1. T_1 , T_2 and T_3 Give the Stresses Acting in the Direction of \mathbf{b} , \mathbf{M} and \mathbf{N} , Respectively, on the Plane With Normal \mathbf{N} . Inclusion of All the Terms Gives $T_i(\theta)$ and $T'_i(\theta)$ With a Maximum Deviation of Less Than 0.5%*, Except for the Cases Marked * or ** Which Have Only Been Fitted to 1% or 2%*, Respectively

	T_1	T_2	T_3	
	A	B	A	
Ag fcc 1	0.213341 -0.60420E-01 -0.220125E-02 -0.547931E-03 -0.727600E-03 -0.318760E-04		-0.604195E-01 0.220115E-02 0.174782E-06 -0.727239E-03	0.213468E-01 0.601578E-02 0.586594E-08 -0.621703E-03
Ag fcc 2	0.123171 -0.348838E-01 0.127061E-02 0.315996E-03 0.41967E-03 -0.183561E-04		0.113335E-05 -0.348824E-01 -0.127111E-02 -0.143246E-07 0.419979E-03	0.123249E-01 -0.347338E-02 -0.857077E-07 0.358959E-03
Al fcc 1	0.186364 -0.408191E-01		-0.408191E-01	0.335603E-02 0.901428E-03
Al fcc 2	0.107597 -0.235669E-01		-0.235668E-01 -0.520537E-03	0.150158E-05 -0.193798E-02
Au fcc 1	0.210702 -0.684969E-01 -0.226572E-02 -0.263109E-03 -0.801263E-03 0.413967E-04		-0.684968E-01 0.226548E-02 -0.141709E-06 -0.801214E-03	0.163721E-01 0.635155E-02 -0.200499E-06 0.671452E-03 0.640868E-04

Table 4.3. Continued

	<i>A</i>	<i>T</i> ₁	<i>B</i>	<i>A</i>	<i>T</i> ₂	<i>B</i>	<i>A</i>	<i>T</i> ₃	<i>B</i>
Au fcc 2	0.121648 -0.395474E-01 0.30818E-02 0.151932E-03 0.462695E-03 -0.238758E-04				-0.395459E-01 -0.130845E-02 -0.124571E-07 0.462706E-03 0.369802E-04		0.182769E-05 -0.945288E-02 -0.366726E-02 0.159476E-07 -0.387735E-03		
Be hcp 1	1.16296 0.694259E-02 -0.173743E-02 0.898953E-03 -0.618742E-04				-0.414801E-01 -0.620694E-02 0.117231E-02				
Cd hcp 1	0.304902 -0.924780E-01 0.298902E-02 0.159753E-02 0.315970E-03				-0.531448E-01 0.419034E-03 0.798137E-03 0.181819E-03				
Cr bcc 1	0.924431 -0.521170E-01 0.106332E-01 0.177551E-02 -0.236361E-04			-0.520686E-02 0.792744E-03 0.48161E-02 -0.145653E-03	-0.297434E-01 0.249848E-01 0.656197E-02 -0.166099E-02		-0.124638E-02 0.238544E-02 0.193192E-02		
Cr bcc 2	0.924844 -0.526912E-01 0.108163E-01 0.172303E-02				-0.124401 0.233928E-02 0.177367E-02		-0.216831E-01 0.163589E-01 -0.150543E-03		
Cu fcc 1	0.331488 -0.886658E-01 -0.367916E-02 -0.111383E-02 -0.117177E-02 -0.503659E-04					-0.886657E-01 0.367882E-02 0.211846E-06 -0.117117E-02 -0.387562E-04	0.379591E-01 0.950847E-02 -0.150758E-06 -0.105950E-02		

Table 4.3. *Continued*

	T_1			T_2			T_3		
	A	B	A	B	A	B	A	B	A
Cu fcc 2*	0.191390 -0.511829E-01		0.106107E-01 0.131060E-02		0.558564E-01 -0.187070E-01		0.256680E-04 -0.219282E-01		
	0.211524E-02 0.640687E-03		-0.368055E-02 -0.317933E-03		-0.272455E-02 0.298298E-04		-0.548915E-02 0.316247E-05		
	0.677478E-03		-0.127010E-03		0.116592E-03		-0.616730E-03 -0.232754E-04		
							-0.213919E-05 -0.245414E-05		
Fe bcc 1	0.647876 -0.189365		0.106107E-01 0.131060E-02		0.399937E-01 -0.187070E-01		0.724948E-01 -0.793755E-02		
	-0.235101E-01 -0.403877E-02		-0.368055E-02 -0.317933E-03		-0.272455E-02 0.298298E-04		-0.385452E-02 0.116592E-03		
	-0.547095E-04 -0.124796E-03								
Fe bcc 2	0.653383 0.197462		0.106107E-01 0.131060E-02		0.399937E-01 -0.187070E-01		0.335046E-01 -0.214342E-01		
	-0.202966E-01 -0.496138E-02		-0.368055E-02 -0.338638E-03		-0.272455E-02 0.298298E-03		-0.555296E-02 -0.569466E-02		
	-0.273661E-03						-0.101321E-01 0.116178E-02		
							-0.589518E-03 0.189710E-03		
							-0.132691E-03 -0.446466E-04		
Hf hcp 1	0.512277 -0.802922E-01		0.766909E-01 -0.149431E-02						
	0.343063E-02 -0.487260E-03		-0.558143E-03						
Ir fcc 1	0.139639E+01 -0.223665						-0.223660 0.108774E-02		
	-0.108780E-02 -0.717332E-03						0.198215E-05 -0.508277E-03		
	-0.511165E-03							0.680171E-01 0.139059E-01	
								-0.196728E-05 -0.127688E-03	

Table 4.3. Continued

	<i>A</i>	<i>T</i> ₁	<i>B</i>	<i>A</i>	<i>T</i> ₂	<i>B</i>	<i>A</i>	<i>T</i> ₃	<i>B</i>
Ir fcc 2	0.806208 -0.129131 0.628740E-03 0.416090E-03 0.294405E-03				-0.129129 -0.631103E-03 -0.475966E-06 0.294365E-03		0.110346E-04 -0.392739E-01 -0.803155E-02 -0.690795E-07 -0.750775E-04		
Li bcc 1**	0.368304E-01 -0.154915E-01 -0.407894E-02 -0.515008E-03 0.165536E-04 -0.166050E-03	0.258765E-02 -0.779335E-03 -0.323397E-03 0.304601E-04 0.189625E-04		0.102365E-01 0.555700E-02 -0.440421E-02 -0.110405E-03 0.313292E-04 -0.194078E-03	0.114022E-02 -0.266922E-02 -0.158311E-03 0.129274E-03 -0.108086E-04 0.301398E-05		-0.354015E-03 -0.790049E-03 -0.115551E-02 0.407325E-03 -0.136527E-03 0.163966E-04	0.509024E-02 -0.273964E-02 -0.110025E-02 -0.545482E-03 -0.444066E-03 0.115242E-03 -0.992035E-04 0.195826E-04 0.125524E-05 -0.657561E-05	
Li bcc 2**	0.405293E-01 -0.208423E-01 -0.221787E-02 -0.713649E-03 0.517166E-04 -0.249975E-03			0.405293E-01 -0.208423E-01 -0.221787E-02 -0.713649E-03 0.517166E-04 -0.249975E-03	0.405293E-01 -0.208423E-01 -0.221787E-02 -0.713649E-03 0.517166E-04 -0.249975E-03		-0.354015E-03 -0.790049E-03 -0.115551E-02 0.407325E-03 -0.136527E-03 0.163966E-04	0.509024E-02 -0.273964E-02 -0.110025E-02 -0.545482E-03 -0.444066E-03 0.115242E-03 -0.992035E-04 0.195826E-04 0.125524E-05 -0.657561E-05	
Mg hcp 1	0.162713 -0.295152E-01 -0.141760E-02 -0.312987E-03						-0.238387E-01 -0.251314E-03 -0.324040E-03		
Mo bcc 1	0.103563E+01 -0.149649 0.886311E-02 0.195049E-02						-0.215282E-01 0.175122E-01 0.564032E-02 -0.165979E-02		

Table 4.3. *Continued*

	<i>A</i>	<i>T</i> ₁	<i>B</i>	<i>A</i>	<i>T</i> ₂	<i>B</i>	<i>A</i>	<i>T</i> ₃	<i>B</i>	
Mo bcc 2	0.103604E+01 -0.150267	0.105009E-01 -0.913380E-02 0.184161E-02		0.200528 0.205555E-02 0.184307E-02		-0.164705E-01 -0.132281E-01 -0.174158E-02	0.144770E-01 0.03331E-01 0.429679E-02			
Nb bcc 1	0.354497 -0.585009E-01 0.722375E-02 0.221472E-02 0.145214E-03 -0.356556E-04	0.219104E-02 -0.776827E-03 0.166642E-02 -0.151239E-03 -0.154755E-03		-0.164705E-01 0.132281E-01 0.504898E-02 0.189757E-02 -0.604042E-04 0.161640E-03		-0.966903E-01 -0.123743E-02 -0.956338E-04 0.322310E-04	0.100331E-01 0.629449E-02 0.417664E-02 0.392874E-03 -0.656379E-04 0.145839E-04			
Nb bcc 2	0.355584 -0.603030E-01 0.830879E-02 0.165778E-02 0.101579E-03 -0.891333E-04				-0.964794E-01 0.190608E-02 0.1754776E-02 0.213468E-03	0.190608E-02 0.1754776E-02 0.213468E-03	0.124408 0.328387E-02 0.390621E-06 -0.114284E-02	0.629449E-02 0.417664E-02 0.392874E-03 -0.656379E-04 0.145839E-04		
Ni fcc 1	0.572800 -0.124406 -0.328393E-02 0.143771E-02 -0.114338E-02					-0.124408 0.328387E-02 0.390621E-06 -0.114284E-02	0.583816E-01 0.128798E-01 0.297355E-06 -0.761887E-03 0.842900E-04			
Ni fcc 2*	0.330676 -0.71828E-01 0.190156E-02 0.835681E-03 0.665078E-03						0.249342E-04 -0.337120E-01 0.744110E-02 0.422184E-05 0.443550E-03 0.516438E-04			

Table 4.3. Continued

	<i>A</i>	<i>T</i> ₁	<i>B</i>	<i>A</i>	<i>T</i> ₂	<i>B</i>	<i>A</i>	<i>T</i> ₃	<i>B</i>
Pb fcc 1	0.635745E-01 -0.208315E-01 -0.112427E-02 -0.181543E-03 -0.357423E-03 -0.274571E-04 0.247024E-04	-0.208316E-01 0.112415E-02 0.408470E-07 -0.357450E-03 0.274701E-04 0.353167E-07 -0.410108E-05	0.690763E-02 0.223575E-02 0.820456E-07 -0.394132E-03 0.202839E-04 0.353167E-07 -0.410108E-05						
Pb fcc 2	0.367044E-01 -0.120273E-01 0.649010E-03 0.104767E-03 0.206374E-03 -0.158737E-04 0.142864E-04	-0.120269E-01 -0.649258E-03 -0.515521E-07 0.206396E-03 0.158718E-04 0.444875E-08 0.235393E-05	0.632347E-06 -0.398829E-02 -0.129083E-02 -0.338037E-07 -0.227582E-03 0.117224E-04 0.444875E-08	-0.102039 0.322472E-02 0.278051E-06 -0.110552E-02	-0.102039 0.322472E-02 0.278051E-06 -0.110552E-02	0.305484E-01 0.952647E-02 -0.363769E-06 -0.881581E-03			
Pd fcc 1	0.347848 -0.102039 -0.322468E-02 -0.672238E-03 -0.110586E-02	-0.589112E-01 -0.186224E-02 -0.926014E-08 0.638392E-03	-0.589112E-01 -0.186224E-02 -0.926014E-08 0.638392E-03	0.176310E-05 -0.176363E-01 -0.550028E-02 -0.264181E-06 0.183122E-04	-0.176310E-05 -0.176363E-01 -0.550028E-02 -0.264181E-06 0.183122E-04	0.173874E-01 0.608314E-02 -0.241702E-07 -0.105055E-03			
Pd fcc 2	0.200928 -0.589132E-01 0.186141E-02 0.387870E-03 0.638425E-03	-0.589112E-01 -0.186224E-02 -0.926014E-08 0.638392E-03	-0.589112E-01 -0.186224E-02 -0.926014E-08 0.638392E-03	0.176310E-05 -0.176363E-01 -0.550028E-02 -0.264181E-06 0.183122E-04	-0.126960 -0.777761E-03 -0.165277E-03 -0.323611E-03	-0.126960 -0.778210E-03 0.156690E-06 -0.323652E-03	0.173874E-01 0.608314E-02 -0.241702E-07 -0.105055E-03		
Pt fcc 1	0.469207 -0.126961 -0.777761E-03 -0.165277E-03 -0.323611E-03	-0.126960 -0.778210E-03 0.156690E-06 -0.323652E-03	-0.126960 -0.778210E-03 0.156690E-06 -0.323652E-03	-0.126960 -0.778210E-03 0.156690E-06 -0.323652E-03	-0.126960 -0.778210E-03 0.156690E-06 -0.323652E-03	0.173874E-01 0.608314E-02 -0.241702E-07 -0.105055E-03			

Table 4.3. C continued

	T_1	B	A	T_2	B	A	T_3	B
Pt fcc 2	0.270897 -0.733016E-01 0.449032E-03 0.954519E-04 0.186869E-03	0.378651E-02 0.116476E-02 -0.180129E-02	0.238051E-01 -0.174511E-01 0.799395E-02 0.159475E-02	-0.104916 -0.306948E-02 -0.207654E-02	0.733007E 01 -0.449532E-03 0.784256E-08 0.186868E-03	0.388800E-05 -0.100396E-01 0.351228E-02 -0.449272E-07 -0.606128E-04		
Ta bcc 1	0.589767 -0.155614 -0.104265E-01 -0.211235E-02	0.378651E-02 0.116476E-02 -0.180129E-02	0.238051E-01 -0.174511E-01 0.799395E-02 0.159475E-02	-0.104916 -0.306948E-02 -0.207654E-02	0.141305E-01 -0.260250E-02 -0.254299E-02 0.178877E-03	-0.105073 -0.260250E-02 -0.254299E-02 0.178877E-03	-0.876680E-02 0.491501E-02 0.299605E-03 -0.132669E-03	
Ta bcc 2	0.591014 -0.157508 -0.955361E-02 -0.243686E-02							0.145673E-04
Ti hop 1	0.385503 -0.580293E-01 -0.477425E-02							
V bcc 1	0.420688 -0.796875E-01 0.354079E-02 0.900572E-03	-0.122837E-02 -0.355051E-03 0.711423E-03	0.808779E-02 0.636337E-02 0.246029E-02 -0.749459E-03	-0.981220E 01 0.851291E-03 0.908145E-03	-0.684767E-01 -0.464900E-02	-0.981070E-01 0.897981E-03 0.826524E-03	0.325668E-02 0.183708E-02 -0.617209E-04	-0.154173E-04
V bcc 2	0.420887 -0.800016E-01 0.370483E-02 0.825517E-03							

Table 4.3. Continued

	T_1	B	A	T_2	B	A	T_3	B
Zn hcp 1	0.491123 -0.119491	0.146048E-01 0.760808E-02 0.154394E-02		-0.924281E-01 -0.238349E-02 0.291330E-02 0.899774E-03 0.906065E-04				
Zr hcp 1	0.349355 -0.766233E-01 -0.383587E-02 -0.136925E-02			-0.572597E-01 0.101259E-02 -0.142977E-02 0.400654E-04				

between this vector and the line direction, the repulsive force per unit length on one partial due to the other is

$$\begin{aligned} F &= (b/d) [T_1(\phi - 30^\circ) - \sqrt{3}T_2(\phi - 30^\circ)] \\ &= (b/d) [T_1(\phi + 30^\circ) + \sqrt{3}T_2(\phi + 30^\circ)], \end{aligned} \quad (4.1.63)$$

where b is the magnitude of the Shockley partial Burgers vector, d is the perpendicular distance between the partials, and T_1 and T_2 are given by the data for the fcc2 system in Table 4.3. It is clear that the use of this data, of which eq. (4.1.62) is an example, in eq. (4.1.63) is very straightforward.

The variation of the three components $T_i(\theta)$ and their derivatives $T'_i(\theta)$ with θ for the moderately anisotropic metals copper and α -iron are shown in Figs 4.6a-d. The departure from the isotropic form, eq. (4.1.58), is apparent, particularly for the derivatives.

A notable feature of the data in Table 4.3 is that the normal traction $T_3(\theta)$ on the slip plane is only identically zero for the bcc1 and hcp1 systems. This has important consequences for the other systems for the interaction between one dislocation and another in the same plane which has a non-zero component of its Burgers vector normal to the plane. Taking another simple example, which will again demonstrate the power of the Fourier series representation, consider the interaction energy between an infinite, straight dislocation on the (111) plane of an fcc metal and a small dislocation loop of area α lying on the same plane. If the perpendicular distance d from the loop to the line is large compared with the loop dimensions, the interaction energy between the line and loop is given by, see eq. (2.6.9),

$$\mathcal{E}^I = \pm (2\alpha/d)T_i b_i, \quad (4.1.64)$$

where b_i ($i = 1, 2, 3$) are the components of the Burgers vector of the loop referred to the axes \mathbf{b} , \mathbf{M} and \mathbf{N} of the line. (The + or - sign in eq. (4.1.64) is used according to whether the positive normal to the loop, as defined by the sign convention of Section 2.5.1, is parallel or anti-parallel to \mathbf{n} , respectively.) Thus, if the line has Burgers vector $\frac{1}{2}[1\bar{1}0]$ and the loop has Burgers vector $1/3[111]$, the interaction energy is

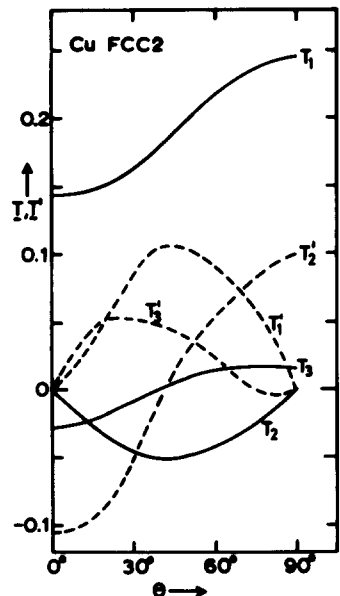
$$\mathcal{E}^I = \pm (2\alpha a / \sqrt{3d}) T_3(\theta), \quad (4.1.65)$$

and if the loop has Burgers vector $\frac{1}{2}[110]$, then

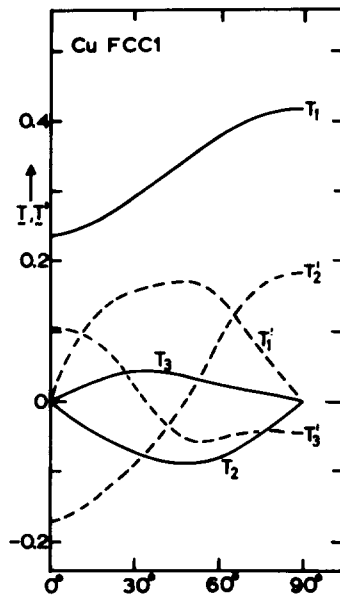
$$\mathcal{E}^I = \pm (2\alpha a / \sqrt{6d}) [T_2(\theta) + \sqrt{2}T_3(\theta)]; \quad (4.1.66)$$

T_2 and T_3 in these equations refer to the fcc1 system of the metal in question.

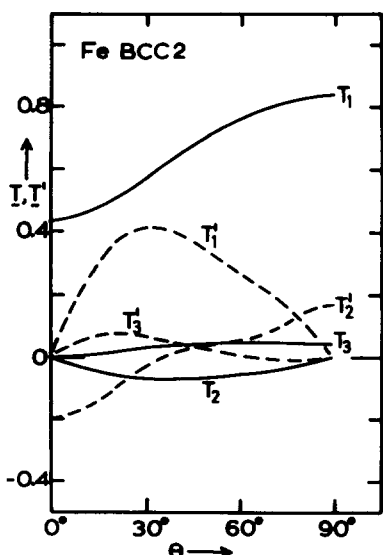
In an earlier paper, in which three systems in the cubic and two in the hcp metals were considered, Bacon and Scattergood⁽⁶⁸⁾ presented data for the energy factor $E(\theta)$ and its derivatives $E'(\theta)$ and $E''(\theta)$. These are



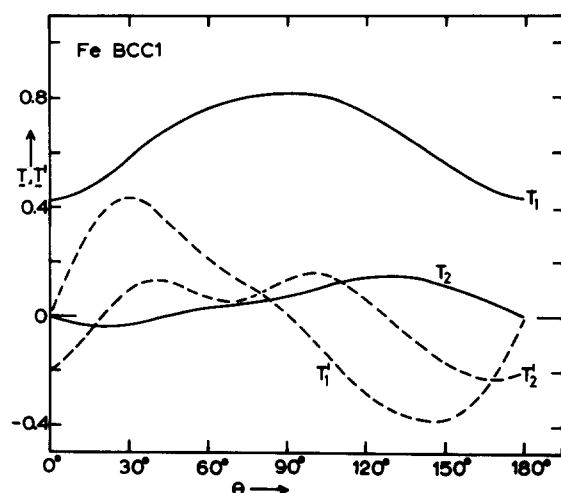
(a)



(b)



(c)



(d)

FIG. 4.6. The variation of T_1 , T'_1 , T_2 , T'_2 , T_3 and T'_3 with θ for (a) the fcc2 system of copper, (b) the fcc1 system of copper, (c) the bcc2 system of iron and (d) the bcc1 system of iron, for which T_3 and T'_3 are identically zero.⁽⁶⁹⁾

related to the data for the traction components $T_1(\theta)$, $T'_1(\theta)$ and $T''_1(\theta)$ since $E(\theta) = bT_1(\theta)$. The Fourier coefficients in that paper were obtained by fitting to the computed data for $E(\theta) + E''(\theta)$ to a prescribed maximum deviation. They, therefore, give more accurate values of $E''(\theta)$ than would the ones presented here when used with a twice-differentiated Fourier series. (The change in the accuracy of the fit with N , the number of harmonics retained, was discussed in detail for the E data by Bacon and Scattergood.⁽⁶⁸⁾) Nevertheless, the coefficients presented here give an accuracy in $E''(\theta)$ which is sufficient for most graphical purposes. Apart from its use in Brown's formula for the stress field of a planar dislocation of arbitrary shape (Section 4.2.2), $E''(\theta)$ is of interest because of its relation to the line-tension model of a dislocation. As was discussed in Section 2.6.2, the basic assumption is made that the energy per unit length at a point on a dislocation of arbitrary shape is equal to the energy per unit length of an infinite straight dislocation tangent to the line at the point.⁽⁵¹⁾ This leads to the result that the radius of curvature at a point on the line in equilibrium with a shear stress τ acting in the slip plane in the direction of the Burgers vector is proportional to $[E(\theta) + E''(\theta)]/\tau b$, where θ is the angle between the tangent to the line and the Burgers vector. $E + E''$ is, therefore, a measure of the "stiffness" of the dislocation in a given orientation and is known as the "line tension". Because of the importance of this quantity in many dislocation processes, we close this section with an assessment of the influence elastic anisotropy has on its character.

The Fourier coefficients, eq. (4.1.61), for $E(\theta) + E''(\theta)$ are given in terms of those for $T_1(\theta)$ such that

$$E(\theta) + E''(\theta) = b A_0 + \sum_n (1 - 4n^2)(A_n \cos 2n\theta + B_n \sin 2n\theta).$$

From the coefficients presented in Table 4.3, it is found that the variation of $E(\theta) + E''(\theta)$ with θ for the systems quoted tends to fall into one of five broad classes of behaviour. Typical examples are shown in Fig. 4.7, where the anisotropic cases are labelled I–IV and the other class is the isotropic curve for $v = 1/3$. The distinguishing feature of the anisotropic curves is the appearance of maxima and minima for values of θ between 0 and 90° . The classification of the line tension for a given metal is not always straightforward, particularly for the cases which are not symmetric about $0 = 90^\circ$ (bcc1), but within reasonable bounds, the following classification is possible. The metals with class I behavior are Cd, Cr, Mo, Nb, V (both slip systems in each case) and Zn, and those with class II behavior are Fe, Li and Ta (both systems). The metals Ag, Au, Cu, Ni, Pb and Pd exhibit class III behaviour for the fcc1 system and class IV behaviour for the fcc2 system. In the case of the fcc metals Al, Ir and Pt (both systems) and hcp metals Be, Hf, Mg, Ti and Zr, the behaviour is more analogous to isotropic behaviour with a suitable choice of Poisson's ratio.

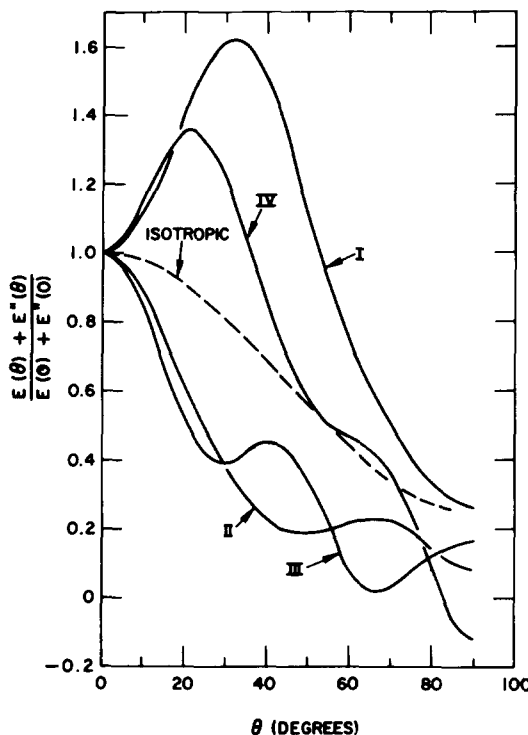


FIG. 4.7. The main classes of line-tension behaviour for the metals and systems listed in Table 4.3. The line tension is normalized to the value for the screw orientation, and the curves shown are: I. Nb(bcc2); II. Fe(bcc2); III. Pb(fcc1); IV. Au(fcc2); the isotropic curve is for Poisson's ratio equal to 1/3.

(The line-tension variation for the $1/3\langle 11\bar{2}0 \rangle\{1\bar{1}01\}$ system of the hcp metals is very similar to that for the $1/3\langle 11\bar{2}0 \rangle\{1\bar{1}00\}$ system.⁽⁶⁸⁾) The effect of anisotropy on the line tension in some metals is more extreme than is suggested by Fig. 4.7; for example, Zn has a maximum in the line tension which is approximately four times its value at $\theta = 0^\circ$, whereas the minima for Li are so deep that the line tension falls to approximately -0.3 on the normalized scale used in Fig. 4.7. It can be seen that $(E + E'')$ also becomes negative close to the edge orientation for the $1/6\langle 112 \rangle\{111\}$ system of the fcc metals of class IV. It can be expected that the marked differences between the line-tension behaviour of the various classes will manifest themselves in the shapes of dislocations bowing under an applied stress. For example, a dislocation should have a relatively low curvature in orientations where the line tension is high. Furthermore, it should not be stable in orientations where it is negative and this is in fact observed to be the case for perfect dislocations in beta-brass,^(70,176) near-edge Shockley partials in copper-aluminium alloys of very low stacking-fault energy⁽⁷¹⁾ and dissociated dislocations in an ordered Fe_3Al alloy. The line-

tension model is only an approximation, however, for it ignores the forces a dislocation segment on a line experiences due to other parts of the line and other sources of internal stress. It also ignores the force associated with the stacking fault in the fcc2 system. The influence these factors can have on the equilibrium form of dislocations will be discussed and assessed by way of examples in Section 4.3.

4.2. Dislocations of Arbitrary Shape in Homogeneous Infinite Media

4.2.1 Background to the Brown–Lothe–Indenbom–Orlov geometrical theorems

The theory and data of Section 4.1 refer to straight dislocation lines of infinite length and they can obviously be applied directly to problems, for which the assumption that dislocations have this form is a valid one. There are cases for which this may be so—for example, parallel interacting dislocations forming pile-ups or dipoles—but they are probably few in number. In many situations of interest, dislocations may have a geometry which prevents them from adopting a straight-line form, e.g. prismatic loops, or they may interact with obstacles to slip such that they change shape under the combined influence of internal and external stresses. In fact, it is these deviations from the straight-line geometry which give dislocations many of their most interesting and important properties.

It has been customary to employ two approximations in order to make treatment of the elastic field of curved and polygonal dislocations tractable. First, the isotropic approximation has been used. This enables the distortion fields of polygonal dislocations and curvilinear dislocations of simple shape to be written in closed analytic form as a single line integral over the dislocation configuration, a result which arises from the fact that the Green's function in the line integral for the field, eq. (2.5.5), has a simple analytic form for elastic isotropy, viz. eq. (2.4.21). Many of the solutions derived by this approach are reviewed in the texts by Hirth and Lothe⁽⁶⁾ and Nabarro.⁽³⁶⁾ The second approximation arises from the nature of the self-forces acting on a dislocation. If we consider a dislocation in equilibrium with respect to glide forces in a slip plane, then, as was discussed in Section 2.6.2, the glide force per unit length must be zero at all points on the dislocation line L ; this may be expressed as

$$b\sigma + b\tau^O(s) + b\tau^L(s) = 0, \quad (4.2.1)$$

where σ is the applied stress, τ^O is the stress due to other dislocations or sources of internal stress, τ^L is a properly-defined “self stress” contribution arising from the stress field of the line itself (see Section 2.6.2 and the Appendix) and s is a parameter describing the position on the line where the stresses are evaluated. (All stresses in eq. (4.2.1) are components resolved on the slip plane in the direction of the Burgers vector b as

is demanded by eq. (2.6.24).) It is clear from eq. (2.6.28) that even for the case of isotropy, the self-stress τ^L is related to a line integral taken over the line and there are only a few special shapes, for which this can be integrated analytically. The solution of eq. (4.2.1) for the equilibrium line shape, therefore, requires numerical integration. As was mentioned in Section 2.6.2, to avoid this complication, τ^L can be approximated by using the line-tension model, wherein the line experiences a force per unit length which depends on the local curvature and line orientation, but which is independent of the configuration of the remainder of the line. The force acts towards the centre of curvature and has a magnitude per unit length given by

$$b\tau^L = -\kappa\Gamma(\theta), \quad (4.2.2)$$

where κ is the curvature of the line and θ is the angle between the tangent to the line and the Burgers vector at the point under consideration; $\Gamma(\theta)$ is called the line tension and, as has already been mentioned, is proportional to $[E(\theta) + E''(\theta)]$.^(51,72,164) Even at this level of approximation, τ^L has a rather complicated dependence on θ (see Section 4.1.3) and the solution of eq. (4.2.1) is generally a non-trivial problem. Most calculations involving the line-tension model have, therefore, used the additional approximation that $E(\theta)$ is a constant independent of θ . With this assumption $\Gamma(\theta)$ is a constant and bowing segments form the arcs of circles, independent of line orientation. This is equivalent to putting $v = 0$ in the isotropic continuum and then Γ is simply proportional to μb^2 . This approach has formed the basis of numerous theories of deformation processes, e.g. the Frank–Read source,⁽⁷³⁾ strengthening associated with dispersed particles, solute atoms, precipitates and other dislocations^(74,6,48,75,36) and computer simulation of dislocation motion through random arrays of obstacles.^(76,77,78)

Despite the apparent successes of the isotropic-elasticity and constant-line-tension models, it is known that the effects of anisotropy and configuration-dependent self-stress need not be second-order ones for situations in which dislocations are not infinitely long and straight. This will be demonstrated by way of examples in Section 4.3. Thus, it is desirable to have recourse to an approach which enables the elastic fields of dislocations of arbitrary shape in anisotropic media to be computed as readily as those of dislocations in the isotropic case. Such an approach is now available, for it has been shown by a number of geometrical theorems that the fields of dislocations of arbitrary shape can be expressed in terms of the fields of infinite, straight dislocations for media of arbitrary anisotropy. The straight-line fields were shown in Section 4.1 to be readily available and we describe in the remainder of Section 4.2 the geometrical formulae in which they can be used.

The theorems originated with the derivation by Lothe⁽⁷⁹⁾ of an expression for the force exerted at a point on one arm of an angular disloca-

tion in an anisotropic continuum due to the stress field of the other arm. The force was found to be inversely proportional to the distance from the apex and to have an angular dependence, which is a function only of the angle between the arms and the energy factor and its first derivative for an infinite, straight dislocation with the same Burgers vector. Brown⁽⁹⁾ gave a proof of Lothe's result and in so doing developed a formula for decomposing the field of a dislocation loop of arbitrary shape in a plane into a line integral of a function of the field of an infinite, straight dislocation on the same plane. The field point is restricted to lie in the plane of the loop; a generalized three-dimensional form of the geometrical theorem was given by Indenbom and Orlov.⁽¹⁰⁾ In the following, we derive Brown's result using essentially the analysis he presented. The formula can be derived from Indenbom and Orlov's three-dimensional equation, but the physical meaning behind the geometrical theorem is more transparent in the two-dimensional formalism. For an arbitrary line, the field will be seen to be a function of the zeroth and second derivatives of the field of an infinite, straight line, but for certain configurations, Brown's formula can be partially integrated to yield expressions which do not contain the second derivative; for some cases, even the first derivative is not required. Such expressions are presented for straight segments, angular dislocations and planar, polygonal loops in Section 4.2.3. We then discuss in Section 4.2.4 how the two-dimensional formulae can be applied to three-dimensional problems. We shall also refer to the field equations for infinite lines and finite segments derived by Willis;⁽⁸⁰⁾ they require the solution of sextic equations, but are completely explicit and have been used in a number of applications. For completeness, a derivation of the Indenbom–Orlov formula is presented at the end of this section; the derivation is not the same as that originally given by Indenbom and Orlov,⁽¹⁰⁾ but is perhaps easier to follow.

4.2.2. Brown's theorem for two dimensions

The starting point for the derivation is eq. (2.5.9), which is one of the line-integral forms for the distortion field due to a dislocation. The field at \mathbf{x} due to the general curvilinear planar dislocation loop L shown in Fig. 4.8a is given by:

$$u_{m,n}(\mathbf{x}) = \epsilon_{qjp} b_i C_{ijkl} \oint_L (x_p - x'_p) G_{km,ln}(\mathbf{x} - \mathbf{x}') d\mathbf{x}'_q. \quad (4.2.3)$$

The integrand of this expression is simply the field at \mathbf{x} due to an infinitesimal segment $d\mathbf{x}'$ of L at \mathbf{x}' , so that if we drop the integral sign from eq. (4.2.3), set $\mathbf{x}' = 0$, $|\mathbf{x}| = r$ and $d\mathbf{x}' = ds$, then the field at point \mathbf{x} with polar coordinates (r, θ) due to an infinitesimal segment ds at the origin (see Fig. 4.8b) is

$$u_{m,n}(\mathbf{x}) = \epsilon_{qjp} b_i C_{ijkl} x_p G_{km,ln}(\mathbf{x}) ds_q. \quad (4.2.4)$$

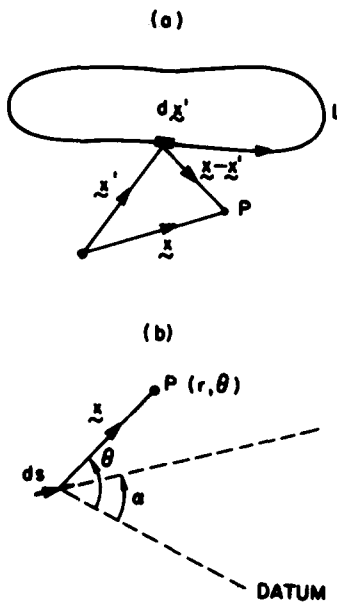


FIG. 4.8. The geometry used in the text to derive the distortion field at P due to an infinitesimal segment. The positive unit normal n is directed out of the plane of the diagram.

We take x and ds to lie in the plane $x_3 = 0$, so that subscripts p and q only take values 1 and 2 with $j = 3$, and then it can be readily shown that

$$\begin{aligned} \epsilon_{qjp} x_p ds_q &= x_1 ds_2 - x_2 ds_1 \\ &= -r \sin(\theta - \alpha) ds, \end{aligned} \quad (4.2.5)$$

where the angle α is defined in Fig. 4.8b. Furthermore, since $G_{ij}(x)$ is homogeneous of degree -1 , eq. (2.4.9) gives

$$G_{ij}(x) = \frac{1}{|x|} g_{ij}, \quad (4.2.6)$$

where g_{ij} is the function describing the orientation-dependence of G_{ij} . Thus, we can write for two dimensions

$$G_{km,ln}(x) = \frac{1}{r^3} h(\theta), \quad (4.2.7)$$

where $h(\theta)$ is a tensor function only of θ and for convenience we omit subscripts. Finally, combining eqs (4.2.4), (4.2.5) and (4.2.7), we can write for the distortion field due to the infinitesimal segment

$$u_{m,n}(r, \theta) = \frac{ds}{r^2} \sin(\theta - \alpha) \Theta(\theta), \quad (4.2.8)$$

where the tensor function

$$\Theta(\theta) = -b_i C_{i3kl} r^3 G_{km,ln}(x) = -b_i C_{i3kl} h(\theta) \quad (4.2.9)$$

and again we omit the explicit insertion of subscripts. It should be noted that although the angles θ and α were implicitly measured from the x_1 axis in the above derivation, it is clear from the final form of eq. (4.2.8) that they can in fact be measured from an arbitrarily-chosen reference axis, as indicated in Fig. 4.8b.

The function $\Theta(\theta)$ is as yet unknown, and Brown deduced its form in the following way. Consider the field at a perpendicular distance d from an infinite straight dislocation line making an angle ϕ with the reference axis (see Fig. 4.9). The field is obtained by integrating the infinitesimal segment field, eq. (4.2.8), along the line with the variable θ having the limits $\theta = \phi$ to $\theta = \phi + \pi$, and it is easily shown that in terms of this variable, r and ds in eq. (4.2.8) are given by

$$r = \frac{d}{\sin(\theta - \phi)}, \quad \frac{ds}{d\theta} = \frac{d}{\sin^2(\theta - \phi)}. \quad (4.2.10)$$

Thus, the distortion field for the infinite line is

$$u_{m,n}(d, \phi) = \frac{1}{d} \int_{\phi}^{\phi + \pi} \sin(\theta - \phi) \Theta(\theta) d\theta, \quad (4.2.11)$$

$$= \frac{1}{d} U_{m,n}(\phi), \quad (4.2.12)$$

where the function $U_{m,n}(\phi)$ defines the orientation-dependent part of the straight-line field; eqs (4.2.11) and (4.2.12) merely confirm the point made in preceding sections that the straight-line field is the product of d^{-1} and a function of the elastic constants and line orientation angle ϕ . To deter-

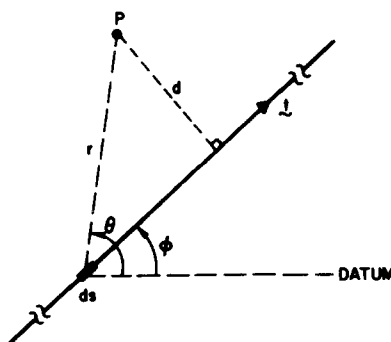


FIG. 4.9. The geometry used in the text to define the field at a distance d from an infinite, straight line.

mine Θ , we differentiate $U_{m,n}$ twice with respect to ϕ :

$$\frac{d}{d\phi} U_{m,n}(\phi) = - \int_{\phi}^{\phi + \pi} \cos(\theta - \phi) \Theta(\theta) d\theta, \quad (4.2.13)$$

$$\frac{d^2}{d\phi^2} U_{m,n}(\phi) = \Theta(\phi + \pi) + \Theta(\phi) - \int_{\phi}^{\phi + \pi} \sin(\theta - \phi) \Theta(\theta) d\theta. \quad (4.2.14)$$

It can be seen that since changing ϕ by π merely reverses the sense of the line integral and leaves the field unchanged, $\Theta(\phi + \pi) = \Theta(\phi)$, and eq. (4.2.14) becomes

$$\frac{d^2}{d\phi^2} U_{m,n}(\phi) = 2\Theta(\phi) - U_{m,n}(\phi). \quad (4.2.15)$$

The function Θ in the field for an infinitesimal segment is, therefore, given by the field for an infinite straight dislocation. Inserting eq. (4.2.15) into eq. (4.2.8) finally yields for the field of the infinitesimal segment shown in Fig. 4.8b:

$$u_{m,n}(r, \theta) = \frac{ds}{2r^2} \sin(\theta - \alpha) \left\{ U_{m,n}(\theta) + \frac{d^2}{d\theta^2} U_{m,n}(\theta) \right\}, \quad (4.2.16)$$

where $U_{m,n}(\theta)$ is defined by eq. (4.2.12).

There are several points which should be noted in relation to eq. (4.2.16). Firstly, it is implicit in the above derivation that the infinite straight line associated with $U_{m,n}(\theta)$ has the same Burgers vector \mathbf{b} as the infinitesimal segment. Secondly, an interesting feature of eq. (4.2.16) is that the orientation of the infinite line is given by the polar angle θ of the field point, *not* the segment orientation angle α . Although the direction of the reference axis from which the polar angles are measured is arbitrary, the most convenient choice for applications in which \mathbf{b} lies in the plane of P and ds is probably the direction of \mathbf{b} . Thirdly, it is clear that, in view of Hooke's law, the derivation given above for the distortion $u_{m,n}$ is also valid for the stress components in a plane containing the segment and for these the field equation is

$$\sigma_{ij}(r, \theta) = \frac{ds}{2r^2} \sin(\theta - \alpha) \{ \Sigma_{ij}(\theta) + \Sigma''_{ij}(\theta) \}, \quad (4.2.17)$$

where " denotes "second derivative of", and $\Sigma_{ij}(\theta) = C_{ijkl} U_{k,l}(\theta)$ is defined as in Section 4.1.1.3 to be such that the in-plane stress field at a distance d from an infinite straight dislocation in the orientation θ is $\Sigma_{ij}(\theta)/d$. (The relationships between $\Sigma_{ij}(\theta)$ and the traction factors $T_i(\theta)$ tabulated in Section 4.1.3 are given in eq. (4.1.59).)

A special case of eq. (4.2.16) arises for self-stress and self-energy problems. If we denote the positive normal to the plane of ds and P by \mathbf{n} ,

then the glide force per unit length due to the infinitesimal segment produced on an element of a dislocation at (r, θ) with the *same* Burgers vector as the segment is $b_i \sigma_{ij}(r, \theta) n_j$. From eq. (4.1.59), the prelogarithmic energy factor for an infinite straight dislocation is $E(\theta) = \frac{1}{2} b_i \Sigma_{ij}(\theta) n_j$. Thus, the glide force per unit length at (r, θ) due to the segment ds is

$$F = \frac{ds}{r^2} \sin(\theta - \alpha) \{E(\theta) + E''(\theta)\}. \quad (4.2.18)$$

The expressions derived above for the field quantities of an infinitesimal segment ds are actually the integrands of line integrals (compare eq. (4.2.3) and eq. (4.2.4)), so that the field of the complete dislocation configuration has to be obtained by integration of the preceding formulae with ds taken around the line. (This was done for the infinite, straight line in eq. (4.2.11).) Some useful alternative forms of these integrals can be obtained by partial integration.⁽⁸¹⁾ Consider the formula for the stress field of an arbitrarily curved planar dislocation loop L

$$\sigma_{ij}^L(\mathbf{x}) = \frac{1}{2} \oint_L \frac{1}{r^2} \{\Sigma_{ij}(\theta) + \Sigma_{ij}''(\theta)\} \sin(\theta - \alpha) ds, \quad (4.2.19)$$

where now $r = |\mathbf{x} - \mathbf{x}'|$. Elementary geometry and calculus yields the relations

$$\frac{dr}{d\theta} = -r \cot(\theta - \alpha), \quad (4.2.20)$$

and

$$d\theta = \frac{1}{r} \sin(\theta - \alpha) ds, \quad (4.2.21)$$

so that eq. (4.2.19) may be rewritten as

$$\sigma_{ij}^L(\mathbf{x}) = \frac{1}{2} \oint_L \frac{1}{r} \{\Sigma_{ij}(\theta) + \Sigma_{ij}''(\theta)\} d\theta. \quad (4.2.22)$$

Integration by parts of the second term of eq. (4.2.22) and use of eq. (4.2.20) shows that

$$\oint_L \frac{1}{r} \Sigma_{ij}''(\theta) d\theta = \left[\frac{1}{r} \Sigma_{ij}'(\theta) \right] - \oint_L \frac{1}{r} \Sigma_{ij}'(\theta) \cot(\theta - \alpha) d\theta. \quad (4.2.23)$$

For integration around the closed loop L , the first term on the right-hand side of eq. (4.2.23) is zero and, thus, from eq. (4.2.21) we see that eq. (4.2.22) becomes

$$\sigma_{ij}^L(\mathbf{x}) = \frac{1}{2} \oint_L \frac{1}{r^2} \{\sin(\theta - \alpha) \Sigma_{ij}(\theta) - \cos(\theta - \alpha) \Sigma_{ij}'(\theta)\} ds. \quad (4.2.24)$$

If L is a smooth, convex planar loop and x is a field point inside L , eq. (4.2.23) may be integrated again to give⁽⁸¹⁾

$$\sigma_{ij}^L(x) = \frac{1}{2} \oint_L \kappa \Sigma_{ij}(\theta) \operatorname{cosec}^3(\theta - \alpha) d\theta, \quad (4.2.25)$$

where κ is the curvature $d\alpha/ds$ of L at x' . Equation (4.2.24) is a useful alternative to eq. (4.2.22) in that it does not involve the second derivative $\Sigma''_{ij}(\theta)$ and eq. (4.2.25) is additionally useful for points inside smooth, convex loops, where $\sin(\theta - \alpha)$ is never zero, for it can be used without knowledge of any of the derivatives. The integrals for $u_{m,n}$ and F can be rewritten in similar ways.

Finally, care has to be exercised with regard to signs whenever equations for stress are required to be used for self- and mutual-interaction force problems, and we have adopted in this section a sign convention consistent with the one used in previous sections. Thus, to calculate the factors $\Sigma_{ij}(\theta)$, $U_{m,n}(\theta)$, etc. from the equations given in Section 4.1, unit vectors m , n , t must be unambiguously defined. The vector n is the positive normal to the plane of L as given by the right-hand screw rule, $t = (x - x')/|x - x'|$ and $m = n \wedge t$, e.g. $\Sigma_{ij}(\theta) \equiv \Sigma_{ij}(m; t)$, where we use this choice for m , n , t in eq. (4.1.20). The Burgers vector b in the equations for the infinite-line factors is that of L . The angles θ , α , etc. which appear in this section must be measured from the reference datum in a positive sense as given by the right-hand screw rule applied to n (see Fig. 4.8). In the case of eq. (4.2.18), the sign of the force F is determined by the sign of $\{E(\theta) + E''(\theta)\}$, which is usually positive (see Section 4.1.3), and the sign of $\sin(\theta - \alpha)$. Reference to the Peach-Koehler formula, eq. (2.6.23), shows that a positive F acts in the direction $n \wedge t'$, whereas a negative F acts in the opposite direction, where t' is the positive direction of the element of dislocation being acted upon by L .^(68,69)

4.2.3. Extension to finite dislocation segments

General expressions for the infinite, straight dislocation field factors which appear in the various field equations derived from Brown's analysis were given in Section 4.1.2, and numerical values for the stress factors for some special cases were presented in Section 4.1.3. It is clear from those sections that in general the integration around the line L has to be undertaken by numerical procedures, even for the isotropic approximation. There are a few special cases, however, for which the line shape is sufficiently simple to allow the infinitesimal segment formulae to be integrated analytically.^(9,82,57,63,68,69,81) One of these relates to field points close to uniformly-curved segments and will be discussed in connection with self-stress problems in Section 4.3. The other case is that of the straight segment. This is particularly useful, for many dislocation configurations have the form of, or can be approximated by, straight finite or

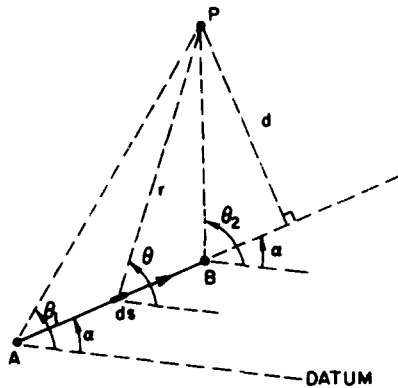


FIG. 4.10. The geometry used in the text to derive the field at P due to a straight segment AB .

semi-infinite segments. The extension of Brown's formula for these segments is presented in the following.

We shall only consider integration of the stress formula, eq. (4.2.19), for the extension to the distortions, eq. (4.2.16), and self-force, eq. (4.2.18), is an obvious one. For the finite, straight, dislocation segment AB shown in Fig. 4.10, substitution of the relations given in eq. (4.2.10) into eq. (4.2.19) gives the following integral form for the field at point P (cf. eq. (4.2.11)):

$$\sigma_{ij} = \frac{1}{2d} \int_{\theta_1}^{\theta_2} \sin(\theta - \alpha) \{ \Sigma_{ij}(\theta) + \Sigma''_{ij}(\theta) \} d\theta. \quad (4.2.26)$$

Integration by parts twice of the term containing Σ''_{ij} yields

$$\sigma_{ij} = \frac{1}{2d} [-\cos(\theta - \alpha) \Sigma_{ij}(\theta) + \sin(\theta - \alpha) \Sigma'_{ij}(\theta)]_{\theta_1}^{\theta_2}. \quad (4.2.27)$$

Hence, the stress field of a segment can be determined without use of the second derivative $\Sigma''_{ij}(\theta)$ and the only data required are the stress factors Σ_{ij} and Σ'_{ij} for infinite, straight lines having the directions of AP and BP . For a semi-infinite dislocation segment terminating at point A as shown in Fig. 4.11, the stress field can be obtained by setting $\theta_1 = 0$ and $\theta_2 = \alpha + \pi$, thus:

$$\sigma_{ij} = \frac{1}{2d} [\Sigma_{ij}(\alpha) + \cos(\theta - \alpha) \Sigma_{ij}(\theta) - \sin(\theta - \alpha) \Sigma'_{ij}(\theta)]. \quad (4.2.28)$$

In the limit as $\theta \rightarrow \alpha$, this expression reduces to the field for an infinite, straight line. Equation (4.2.28) is the basis of the theorem given by Lothe,⁽⁷⁹⁾ which gave rise to Brown's analysis.

Some caution has to be exercised in using equations such as eqs (4.2.17), (4.2.27) and (4.2.28) for terminating dislocation segments. This arises because the field of a dislocation is given by a line integral and any function which is a perfect differential can be added to the integral without

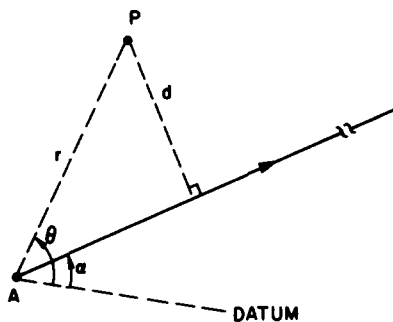


FIG. 4.11. The geometry used in the text to obtain the field at P due to a straight, semi-infinite line terminating at A .

changing the field, provided that the dislocation forms a closed loop, goes to infinity at both ends, or ends at a perfect node at which Burgers vector is conserved. Hence, the field for a terminating segment is not unique⁽⁸³⁾ and the field expressions given above should only be used for combinations of segments which meet these conditions. This is unlikely to create problems for most calculations, for dislocations in real crystals do form loops, perfect nodes or terminate at surfaces, but the reader should be aware of difficulties which can arise either if the segment expressions are used alone or if use is made of combinations of them which have been derived from integrands which are not identical.

To illustrate this point, consider eq. (4.2.24); this is a valid alternative to eq. (4.2.19) for the stress field of a continuous, closed or infinite dislocation, for which the first term on the right-hand side of eq. (4.2.23) vanishes. Applying eq. (4.2.24) to the finite segment of Fig. 4.10, it is easily found that

$$\sigma_{ij} = \frac{1}{2d} [-\cos(\theta - \alpha)\Sigma_{ij}(\theta)]_{\theta_1}^{\theta_2}, \quad (4.2.29)$$

which differs from eq. (4.2.27) by the term containing $\Sigma'_{ij}(\theta)$, a result clearly arising from the neglect of the Σ' term in eq. (4.2.23). In the same way, the field of a semi-infinite line would not contain the Σ' term of eq. (4.2.28) if obtained from eq. (4.2.24). For a continuous dislocation composed of straight segments, the field is the same whether it is obtained by adding segment contributions using eq. (4.2.27) or eq. (4.2.29), since the terms containing Σ' cancel. For configurations with terminations, however, the stresses obtained from eqs (4.2.27) and (4.2.29) would differ by the $(1/r)\Sigma'$ term in eq. (4.2.23).

Equation (4.2.29) appears at first sight to be a more useful formula for a segment field than eq. (4.2.27), for it implies that the field of a closed, polygonal configuration can be determined without knowledge of the angular derivatives of $\Sigma_{ij}(\theta)$. This is important for computations, for, as shown by Bacon and Scattergood^(68,69) and discussed in Section 4.1.3,

values of Σ_{ij} can be obtained to a much higher accuracy—typically one or two orders of magnitude better—than can those for Σ'_{ij} and Σ''_{ij} from the same number of Fourier coefficients or steps in the numerical integration for these factors. (Alternatively, they can be obtained in a much shorter time for a given accuracy.) Thus, eq. (4.2.29) is to be preferred for general use. There is one situation, however, where the field does depend on Σ' ; this arises when the field point is collinear with a segment. For example, setting $r_1 = d/\sin(\theta_1 - \alpha)$ and $r_2 = d/\sin(\theta_2 - \alpha)$ in eq. (4.2.27), and then letting θ_1 and θ_2 tend to α so that P becomes collinear with A and B in Fig. 4.10, it is found that the stress given by that formula is zero, whereas the contribution given by eq. (4.2.29) is

$$\sigma_{ij}(\theta_1 = \theta_2 = \alpha) = \frac{1}{2} \left(\frac{1}{r_1} - \frac{1}{r_2} \right) \Sigma'_{ij}(\alpha). \quad (4.2.30)$$

Some useful extensions of these segment expressions have been given by Asaro and Barnett.⁽⁸¹⁾ For the in-plane stress field of the angular dislocation shown in Fig. 4.12, eq. (4.2.27) leads to

$$\sigma_{ij} = \frac{1}{2r} [\operatorname{cosec}(\theta - \alpha) \Sigma_{ij}(\alpha) + \cot(\theta - \alpha) \Sigma_{ij}(\theta)]_{x_1}^{x_2}. \quad (4.2.31)$$

As expected from the preceding discussion, this is independent of Σ'_{ij} except when P is collinear with one of the arms, i.e. $\theta = \alpha_1 + \pi$ or $\alpha_2 + \pi$, for which eq. (4.2.31) reduces to that for the semi-infinite arm not collinear with P , eq. (4.2.28). The in-plane field of a planar polygon having N sides and vertices has a particularly simple form, which can easily be deduced from eq. (4.2.29). Let the vector from the m^{th} vertex to the field point be R_m , the direction of which makes an angle θ_m with a fixed reference direction, and let the discontinuity in angle between the reference direction and the tangent to the polygon at the m^{th} vertex be $\Delta\alpha_m = \alpha_m^+ - \alpha_m^-$. Then the field of the loop is given by

$$\sigma_{ij} = \frac{1}{2} \sum_{m=1}^N \frac{1}{R_m} \sin \Delta\alpha_m \operatorname{cosec}(\theta_m - \alpha_m^+) \operatorname{cosec}(\theta_m - \alpha_m^-) \Sigma_{ij}(\theta_m). \quad (4.2.32)$$

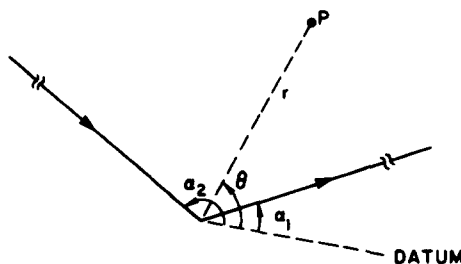


FIG. 4.12. The geometry used in the text to define the in-plane field at P due to an angular dislocation.

Equation (4.2.32) shows that for points inside a convex polygonal loop, the field may be computed without knowledge of the angular derivatives of Σ_{ij} , as first noticed by Brown.⁽⁸²⁾ (This will also be true for curved loops which can be satisfactorily approximated by a series of straight segments; for these cases, numerical integration of the derivatives of field factors will, therefore, not be required.) For points outside a polygonal loop or for points inside a re-entrant polygon, the field point may happen to be collinear with a segment, and then eq. (4.2.32) should be modified, as indicated in eq. (4.2.30). If the point is collinear with the s^{th} and $(s+1)^{\text{th}}$ vertices, then $\theta_s = \theta_{s+1}$ and the stress is given by omitting the terms $m = s$ and $s+1$ from the summation of eq. (4.2.32) and adding the terms

$$\frac{1}{2} \left\{ \frac{1}{R_s} \cot \omega_s + \frac{1}{R_{s+1}} \cot \omega_{s+1} \right\} \Sigma_{ij}(\theta_s) + \frac{1}{2} \left(\frac{1}{R_s} - \frac{1}{R_{s+1}} \right) \Sigma'_{ij}(\theta_s),$$

where ω_s and ω_{s+1} are the interior angles of the polygon at the s^{th} and $(s+1)^{\text{th}}$ vertices. (The term in this expression involving $\Sigma'_{ij}(\theta_s)$ was omitted by Asaro and Barnett.⁽⁸¹⁾)

4.2.4. Considerations in applying the two-dimensional formulae

We have described the geometrical formulae derived in Sections 4.2.2. and 4.2.3. as being applicable to two-dimensional problems and, indeed, the derivation of Brown's theorem for the integrand of the line integral for the field of an arbitrary, planar line assumed the field point to be in the plane of the line. The extent to which the three-dimensional formula of Indenbom and Orlov, eq. (4.2.54), can be partially integrated for polygonal dislocations and other special configurations has still to be investigated. However, there is a wide class of three-dimensional problems for which some of the two-dimensional formulae can be used. These are problems in which the dislocations are polygonal in form. For these cases, eq. (4.2.27) is appropriate for the field contribution arising from a straight segment, the angles θ and α being measured in the plane containing the segment and the field point.⁽¹⁶²⁾ To see that this partially-integrated form is valid for three dimensions, consider a part of a polygonal dislocation shown schematically in Fig. 4.13a; the segments AB , BC , CD , ... need not be coplanar. For the field at an arbitrary point P , we can consider the line to be constructed from the segments AB , BC , ..., plus pairs of semi-infinite lines of equal Burgers vector and opposite line sense collinear with the lines PA , PB , PC , ... and terminating at the vertices A , B , C , ..., as indicated in the figure. Thus, the line can be thought of as being composed of bi-angular dislocations of the form shown in Fig. 4.13b. The field at P due to this bi-angular dislocation with side-arms collinear with P is given by eq. (4.2.27). This is also one of the forms for the field of the segment BC , because the semi-infinite side-arms make zero contribution to the field at P when the integrand in eq. (4.2.26) is used. Since the bi-angular dislocation contains no terminations, eq. (4.2.27) is complete

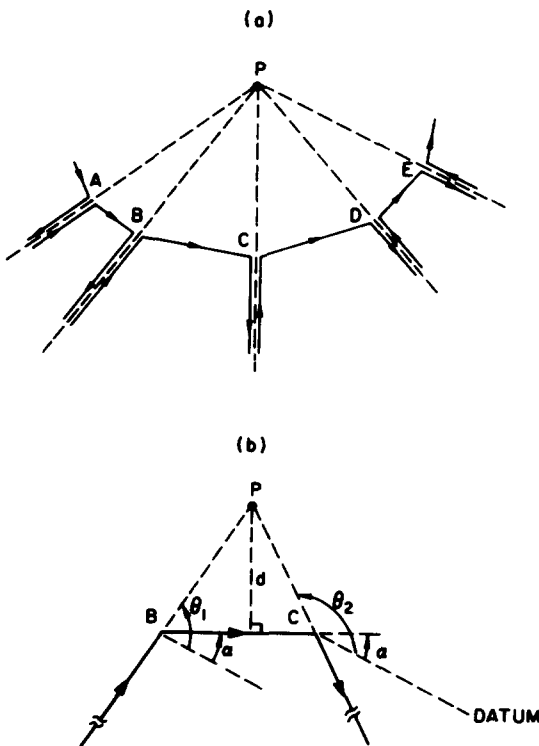


FIG. 4.13. (a) Schematic diagram of the construction of the field at P due to the polygonal dislocation ... $A\ B\ C\ D\ E\dots$ from bi-angular dislocations. (b) The geometry for describing the field of the biangular used in (a).

and it is, therefore, a suitable equation to use for the field of a segment in a three-dimensional problem. Curvilinear configurations can often be approximated sufficiently well for numerical purposes by series of piece-wise straight segments and so eq. (4.2.27) should also be useful for three-dimensional problems involving those dislocations. The field at points collinear with BC in Fig. 4.13(b) is zero and it will not be necessary, therefore, to require higher-order derivatives of the field factors than the first for most applications.

The equations derived above for infinitesimal and finite segments and polygonal lines are ideally suited to applications in which data for infinite, straight-line fields are available in a form not requiring extensive computation. It was shown in Section 4.1.3 that these data for most metals have already been compiled for a special class of two-dimensional problems, namely, one in which the infinite-line rays in the geometrical formulae lie on $\{111\}$ planes for fcc, $\{110\}$ or $\{112\}$ for bcc, or $\{10\bar{1}0\}$ or $\{10\bar{1}1\}$ for hcp metals. For such cases, very little effort is required to use the formulae. For more general situations, however, the data have not yet been determined and additional computations would therefore have to

be performed to obtain the infinite-ray fields which enter the expressions. These can be obtained in a number of ways, but the most straightforward is the one using the integral equations derived in Section 4.1.2. The integrals can be evaluated to a prescribed accuracy and do not contain any singularities. Furthermore, they do not suffer from degeneracy problems associated with isotropy or line symmetry, and the elastic constants and vector components are conveniently referred to an arbitrary reference frame, which will usually be chosen to be the crystal axes. The integrals for the angular derivatives of the fields are lengthy expressions, but may be evaluated easily. In comparison with this, the alternative approach involving numerical solution for the roots of a sextic equation does not appear to be as convenient to use. The sextic expressions⁽²⁷⁾ for the field data to be used in the geometrical formulae are not as easy to handle as their integral counterparts and the sextic method suffers from inherent degeneracy problems, for which special care has to be taken. However, the method of inserting infinite-line field data into the geometrical formulae is perhaps not the best way of determining the fields of polygonal and curvilinear dislocations by the sextic formalism, and a more convenient set of equations for segments and loops was derived by Willis.⁽⁸⁰⁾ They have been used in a number of applications (Section 4.3) and will be briefly described in the following.

The equations derived by Willis⁽⁸⁰⁾ require a solution to be found for the roots of a sextic polynomial, but, unlike the earlier methods of Eshelby *et al.*⁽⁴⁾ and Stroh,⁽⁵⁾ do not require the solution of a set of linear algebraic equations. They also have the convenient feature of containing components referred to an arbitrary reference frame. The equations were obtained by inserting the triple-integral expression for the Green's function in terms of its Fourier transform into the Volterra or Mura equations for the fields of dislocations, eqs (2.5.3) and (2.5.5), and partially reducing the resulting five- or four-dimensional integrals analytically. We have already seen in Section 2.5.2 one direct (alternative) way in which this can be done for the distortions due to an infinite, straight line and for this special case the expressions so derived simply contain a single integral, eq. (2.5.15). As discussed by Barnett and Swanger,⁽⁴²⁾ the integral can be treated as a contour integral around the unit circle in a complex plane and can then be evaluated by Cauchy's residue theorem in terms of a sum over the complex roots p_z of the sextic polynomial

$$\| C_{ijkl} k_j k_k \| \equiv D(\mathbf{k}) = 0, \quad (4.2.33)$$

where, in the notation of Section 4.1, $\mathbf{k} = \mathbf{m} + p\mathbf{n}$. The reduction of this kind is the principle of the analysis given by Willis, and he obtained for the infinite, straight line having direction \mathbf{t}

$$u_i(x) = \frac{1}{\pi} b_j C_{lmjk} n_k \mathcal{I} \sum_{z=1}^3 \frac{k_{mx} N_{il}(k_z)}{n_r \partial D(k_z)/\partial k_r} \ln(k_z \cdot x) \quad (4.2.34)$$

and

$$u_{i,p}(x) = -\frac{1}{\pi} \epsilon_{pqk} b_j t_q C_{lmjk} \sum_{z=1}^3 \frac{k_{mz} N_{il}(k_z)}{n_r \partial D(k_z)/\partial k_r} \frac{1}{(k_z \cdot x)}, \quad (4.2.35)$$

where $\mathbf{k} = \mathbf{m} + p_z \mathbf{n}$, $\mathbf{t} = \mathbf{m} \wedge \mathbf{n}$, the matrix $N(\mathbf{k})$ is the adjoint of the matrix formed by $C_{ijkl} k_j k_k$, and p_1 , p_2 and p_3 are the three roots of eq. (4.2.33) with positive imaginary part. The denominator $n_r \partial D(\mathbf{k})/\partial k_r$ can be written as $2n_r C_{rpqk} k_n N_{pq}(\mathbf{k})$, so that once the roots of eq. (4.2.33) have been obtained, the fields are rather easy to evaluate. (Special care has to be taken in cases of degeneracy, for which the roots are not all distinct.) Mura⁽⁴³⁾ has shown explicitly that eqs (4.2.34) and (4.2.35) are identical to those obtained in the integral formalism, viz. eqs (4.1.16) and (4.1.25).

Willis also reduced the general line integral expression for the field of a straight dislocation segment to a single summation. For the field at P due to segment AB , as shown in Fig. 4.14, he obtained

$$u_{i,p} = \frac{i}{2\pi d} \epsilon_{pqk} b_j C_{lmjk} t_q \left\{ \sum_{z=1}^3 \frac{k_z^B N_{il}(k_z^B)}{n_r \partial D(k_z^B)/\partial k_r} - \sum_{z=1}^3 \frac{k_z^A N_{il}(k_z^A)}{n_r \partial D(k_z^A)/\partial k_r} \right\}, \quad (4.2.36)$$

where

$$k_z^A = \mathbf{m}^A + p_z \mathbf{n}, \quad k_z^B = \mathbf{m}^B + p_z \mathbf{n},$$

$\mathbf{t} = \mathbf{AB}/|\mathbf{AB}|$, \mathbf{n} is the unit vector normal to plane ABP in the direction of $\mathbf{t}^A \wedge \mathbf{t}^B$, $\mathbf{t}^A = \mathbf{PA}/|\mathbf{PA}|$, $\mathbf{t}^B = \mathbf{PB}/|\mathbf{PB}|$, $\mathbf{m}^A = \mathbf{n} \wedge \mathbf{t}^A$ and $\mathbf{m}^B = \mathbf{n} \wedge \mathbf{t}^B$. Equation (4.2.36) is again straightforward to evaluate once the complex roots of $D(\mathbf{k}^A) = 0$ and $D(\mathbf{k}^B) = 0$ have been determined. There is, of course, a similarity between eq. (4.2.36) and the geometrical formula for a segment, eq. (4.2.27), in that it is given by the difference of two functions of the rays PA and PB . The similarity is made explicit if, following Mura

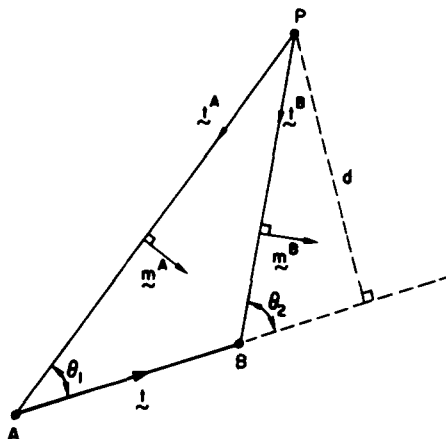


FIG. 4.14. The geometry used by Willis⁽⁸⁰⁾ to obtain the field of a straight, finite segment AB .

and Mori,⁽⁸⁴⁾ we substitute for t in the first term of eq. (4.2.36)

$$t = -t^A \cos \theta_1 + m^A \sin \theta_1 = -t^A \cos \theta_1 + \frac{dt^A}{d\theta_1} \sin \theta_1 \quad (4.2.37)$$

and in the second term

$$t = -t^B \cos \theta_2 + m^B \sin \theta_2 = -t^B \cos \theta_2 + \frac{dt^B}{d\theta_2} \sin \theta_2. \quad (4.2.38)$$

Reference to eq. (4.2.35) for $u_{i,p}$ for the infinite, straight line then shows that the terms involving t^A and t^B are the fields of infinite, straight lines with directions t^A and t^B , respectively, and, from a comparison with eq. (4.2.27), we can, therefore, expect the terms containing $dt^A/d\theta_1$ and $dt^B/d\theta_2$ to be given by the first derivative of these fields. Mura and Mori⁽⁸⁴⁾ have, in fact, shown formally that this is so by use of the residue theorem.

At first sight, eq. (4.2.36) appears to be much simpler to use than its integral counterpart, namely eq. (4.2.27) with the infinite-line factors replaced by the integral expressions given in Section 4.1.2, for the infinite line field and its first derivative in eq. (4.2.27) are combined in eq. (4.2.36) into a single expression, which is no more complicated than that for the field itself. The lengthy integral expressions are easy to evaluate, however, and it was seen in the preceding section that for a two-dimensional polygonal configuration, the first derivative terms in the geometrical formulae can actually cancel. For most practical purposes, therefore, the geometrical-integral expressions can be evaluated as readily as eq. (4.2.36). The computation times required for both approaches will probably be comparable, one requiring numerical integration and the other solution for the complex roots of a sextic equation with subsequent multiplication of complex components. The integrals are always well-behaved, however, whereas degenerate situations arise in the sextic approach; they require special handling in the computer program and this can be computationally inconvenient. Thus, although there is no hard-and-fast rule for which is the better method to employ, we would recommend the geometrical/integral approach for general use.

*4.2.5. The Indenbom-Orlov formula for three dimensions

Brown's formula for two-dimensional problems has a three-dimensional counterpart which was derived by Indenbom and Orlov.⁽¹⁰⁾ It has not been used, to our knowledge, to the same extent as the segment expressions given above and we have, therefore, devoted less attention to it in this article. Nevertheless, it should find application and the description of it here should be of value. The reader may find the original derivation of Indenbom and Orlov rather difficult to follow and we therefore present an alternative derivation given by Asaro and Barnett.⁽⁸¹⁾

Unlike the Brown and Indenbom-Orlov derivations, which start with eq. (2.5.9) for the line-integral expression for the field of a dislocation,

Asaro and Barnett's procedure starts with the more familiar equation, eq. (2.5.5), first derived by Mura:⁽⁴⁰⁾

$$u_{i,p}(x) = -F_{pjrq} \oint_L G_{ir,q}(x - x') dx'_j, \quad (4.2.39)$$

where

$$F_{pjrq} = \epsilon_{pjw} b_m C_{wmrq}. \quad (4.2.40)$$

The field at z due to an infinite, straight dislocation passing through the origin and having a direction given by the unit vector y such that $x' = ys$ ($-\infty \leq s \leq \infty$) is, therefore,

$$u_{i,p}(z; y) = -F_{pjrq} \frac{\partial}{\partial z_q} \int_{-\infty}^{\infty} G_{ir}(z - ys) y_j ds. \quad (4.2.41)$$

Since

$$\frac{\partial}{\partial z_q} G_{ir}(z - ys) = -\frac{1}{s} \frac{\partial}{\partial y_q} G_{ir}(z - ys) \quad (4.2.42)$$

and

$$G_{ir}(z - ys) = \frac{\text{sgn}(s)}{s} G_{ir}\left(\frac{1}{s} z - y\right), \quad (4.2.43)$$

use can be made of eqs (4.2.42) and (4.2.43) and the substitution $\eta = 1/s$ to rewrite eq. (4.2.41) in the form

$$u_{i,p}(z; y) = F_{pjrq} y_j \left\{ \int_0^z G_{ir}(z\eta - y) d\eta - \int_{-\infty}^0 G_{ir}(z\eta - y) d\eta \right\}. \quad (4.2.44)$$

Making use of the relations

$$z_n \frac{\partial}{\partial y_n} G_{ir}(z\eta - y) = -\frac{\partial}{\partial \eta} G_{ir}(z\eta - y) \quad (4.2.45)$$

and

$$\int_0^z \frac{\partial}{\partial \eta} G_{ir}(z\eta - y) d\eta - \int_{-\infty}^0 \frac{\partial}{\partial \eta} G_{ir}(z\eta - y) d\eta = -2G_{ir}(-y), \quad (4.2.46)$$

we find by operating on both sides of eq. (4.2.44) with the operator $z_n \partial/\partial y_n$ that

$$\begin{aligned} z_n \frac{\partial}{\partial y_n} u_{i,p}(z; y) &= F_{pjrq} \left\{ 2y_j \frac{\partial}{\partial y_q} G_{ir}(-y) + z_j \frac{\partial}{\partial y_q} \right. \\ &\times \left. \left[\int_0^z G_{ir}(z\eta - y) d\eta - \int_{-\infty}^0 G_{ir}(z\eta - y) d\eta \right] \right\}. \end{aligned} \quad (4.2.47)$$

Operating on both sides of eq. (4.2.47) with the operator $z_g \partial/\partial y_g$ and again making use of eqs (4.2.45) and (4.2.46), we obtain

$$\begin{aligned} z_g \frac{\partial}{\partial y_g} z_n \frac{\partial}{\partial y_n} u_{i,p}(z; y) &= F_{pjrq} \left\{ 4z_j \frac{\partial}{\partial y_q} G_{ir}(-y) \right. \\ &\quad \left. + 2y_j z_g \frac{\partial}{\partial y_g} \left[\frac{\partial}{\partial y_q} G_{ir}(-y) \right] \right\}. \end{aligned} \quad (4.2.48)$$

We shall show that the left-hand side of eq. (4.2.48) has a special meaning when integrated around a closed loop in the following way. Consider the dislocation loop L defined parametrically by $\mathbf{x}' = \mathbf{x}'(s)$, where s is arc length; let $\mathbf{y} = \mathbf{x} - \mathbf{x}'$ and let \mathbf{z} be the unit tangent vector to L at \mathbf{x}' , so that

$$z_g \partial/\partial x'_g = d/ds \text{ and } z_j = dx'_j/ds. \quad (4.2.49)$$

In the integral around L , we must interpret $\partial/\partial y_g$ as $\partial/\partial x_g$, since eq. (4.2.48) was derived assuming \mathbf{z} and \mathbf{y} to be independent. Integrating eq. (4.2.48) around L therefore yields

$$\begin{aligned} \oint_L z_g \frac{\partial}{\partial x_g} z_n \frac{\partial}{\partial x_n} u_{i,p}(z; \mathbf{x} - \mathbf{x}') ds \\ = F_{pjrq} \left\{ 4 \oint_L \frac{\partial}{\partial x_q} G_{ir}(\mathbf{x} - \mathbf{x}') dx'_j \right. \\ \left. - 2 \oint_L (x_j - x'_j) \frac{d}{ds} \left[\frac{\partial}{\partial x_q} G_{ir}(\mathbf{x} - \mathbf{x}') \right] ds \right\}, \end{aligned} \quad (4.2.50)$$

where we have used eq. (4.2.49) and the fact that $G_{ir}(-y) = G_{ir}(y)$ and

$$\frac{\partial}{\partial x'_q} G_{ir}(\mathbf{x} - \mathbf{x}') = - \frac{\partial}{\partial x_q} G_{ir}(\mathbf{x} - \mathbf{x}'). \quad (4.2.51)$$

The second integral on the right-hand side of eq. (4.2.50) may be integrated by parts as follows

$$2 \oint_L (x_j - x'_j) \frac{d}{ds} \left[\frac{\partial}{\partial x_q} G_{ir}(\mathbf{x} - \mathbf{x}') \right] ds = 2 \oint_L \frac{\partial}{\partial x_q} G_{ir}(\mathbf{x} - \mathbf{x}') dx'_j, \quad (4.2.52)$$

so that eq. (4.2.50) becomes

$$F_{pjrq} \oint_L \frac{\partial}{\partial x_q} G_{ir}(\mathbf{x} - \mathbf{x}') dx'_j = \frac{1}{2} \oint_L z_g \frac{\partial}{\partial x_g} z_n \frac{\partial}{\partial x_n} u_{i,p}(z; \mathbf{x} - \mathbf{x}') ds. \quad (4.2.53)$$

It can be seen that the left-hand side of eq. (4.2.53) is the Mura line integral for the field of a dislocation, eq. (4.2.39), except for a minus sign. The field of dislocation L can, therefore, be written as

$$u_{i,p}(\mathbf{x}) = -\frac{1}{2} \oint_L t_g t_n \frac{\partial^2}{\partial x_g \partial x_n} u_{i,p}(t; \mathbf{x} - \mathbf{x}') ds, \quad (4.2.54)$$

where we have replaced z by t , the more conventional symbol for the unit vector tangent to L . Equation (4.2.54) is the Indenbom-Orlov theorem. Since $u_{i,p}(t; \mathbf{x} - \mathbf{x}')$ is the field at point $\mathbf{x}' + t$ due to an infinite, straight dislocation passing through the point \mathbf{x}' and lying in the direction $(\mathbf{x} - \mathbf{x}')$, it is seen that, as in the two-dimensional case, the field (distortion or stress) due to an infinitesimal segment is given by the field of an infinite, straight line parallel to the vector from the segment to the field point.

The identity of Brown's formula, eq. (4.2.16), and eq. (4.2.54) for the situation when L is a planar loop is readily demonstrated. For the segment of the loop shown in Fig. 4.8b, $ds = t ds$ and $\mathbf{x}' = 0$ in eq. (4.2.54), and simple calculus gives for two dimensions

$$t_m \frac{\partial}{\partial x_m} = \cos(\theta - \alpha) \frac{\partial}{\partial r} - \frac{1}{r} \sin(\theta - \alpha) \frac{\partial}{\partial \theta}. \quad (4.2.55)$$

The field of an infinite, straight dislocation is inversely proportional to the perpendicular distance from the line to the field point, so that in the notation of Section 4.2.2 and eq. (4.2.54), the field at a point a unit distance from the dislocation along the direction of ds due to an infinite, straight line along \mathbf{x} is

$$u_{i,p}(t; \mathbf{x}) = \frac{-1}{\sin(\theta - \alpha)} U_{i,p}(\theta). \quad (4.2.56)$$

(The factor -1 in eq. (4.2.56) is a consequence of the sign convention described in Section 4.2.2.)

Applying the operator of eq. (4.2.55) twice to eq. (4.2.56) gives

$$-t_g t_n \frac{\partial}{\partial x_g} \frac{\partial}{\partial x_n} u_{i,p}(t; \mathbf{x}) = \frac{1}{r^2} \sin(\theta - \alpha) [U_{i,p}(\theta) + U''_{i,p}(\theta)], \quad (4.2.57)$$

so that the Indenbom and Orlov expression reduces to that of Brown for the planar case.

4.3. Applications to Problems of Dislocations in Infinite, Homogeneous Media

When used with the formulae and/or data presented in Section 4.1, the theory described in Section 4.2 is sufficient to enable many theoretical problems involving dislocations in anisotropic materials to be solved. The application of the equations derived is straightforward and they have already been used in a number of studies. Some of these are reviewed in this section. We also include investigations which, although not using the geometrical theorems of Section 4.2, used methods intimately related to the theme of this article, namely, integration of the Green's function equation or evaluation of Willis' sextic expressions for the field of a dislocation. Economy of space precludes a detailed description of the methods

used and results obtained, and the reader is referred to the original papers for these. Nevertheless, we hope to demonstrate the usefulness of the theoretical development discussed in the preceding sections and the topics selected enable the effects of elastic anisotropy to be assessed for a number of quite different situations in which dislocations are not infinitely long and straight.

4.3.1. *Elastic energy of a rhombus-shaped loop*

The first application of the geometrical theorems of Section 4.2 was by Brown,⁽⁸²⁾ who used an equation equivalent to eq. (4.2.32) to discuss the equilibrium form of large dislocation loops and the factors which control the shape of Frank loops in fcc metals; loop energies were not accurately determined. Theoretical and experimentally-observed shapes were compared for extrinsic Frank loops in copper by Brown *et al.*⁽⁸⁵⁾ and close agreement was found. The first sophisticated treatment of a polygonal dislocation configuration in anisotropic elasticity was by Bacon *et al.*⁽⁸⁶⁾ They considered the rhombus-shaped, prismatic loop, which is a form observed in quenched aluminium, aluminium-magnesium alloys, platinum and stainless steel.^(87,88) The experimental observations suggest that the vacancies responsible for these loops initially nucleate in the form of hexagonal Frank loops on close-packed {111} planes and that at some stage, the loops shear to become perfect with $\mathbf{b} = 1/2 \langle 110 \rangle$. The rhombus shape is attained by the two pure-edge sides being removed by climb and the {111} loop is then glissile in the sense that its sides lie on two other {111} planes and can slip on them. The situation is shown schematically in Fig. 4.15 for the particular case of $\mathbf{b} = 1/2 [011]$ and a glide prism with faces $(1\bar{1}\bar{1})$ and $(\bar{1}1\bar{1})$; the (111) loop plane corresponds to the orientation in which $\phi = 30^\circ$. Since the loop is glissile, it is free to adopt an orientation which minimizes its total energy, provided lattice friction and pinning effects are negligible, and the final orientation should be independent of the initial nucleation process. The observed loops have linear dimensions of between 100 and 1000 Å, and the total energy should be dominated by the linear-elastic contribution. Loop orientations have been determined experimentally,⁽⁸⁷⁾ thereby providing a useful reference from which to check the validity of the linear-elastic approximation and test the importance of the anisotropic terms in the energy. The experimentally-determined orientations are close to {012}, which, for the loop of Fig. 4.15, could arise by a rotation about the [011] axis from (111) to the pure edge (011) orientation ($\phi = 0^\circ$) followed by a rotation about [100]. (Orientation changes of this type have been observed.⁽⁸⁷⁾) A loop would retain a rhombus shape throughout these rotations.

The first calculation of the loop energy as a function of orientation was made by Bullough and Foreman⁽⁴⁵⁾ using isotropic elasticity. They derived an analytic expression for the energy as a function of orientation and loop size, defined by the parameter a in Fig. 4.15. The variation of

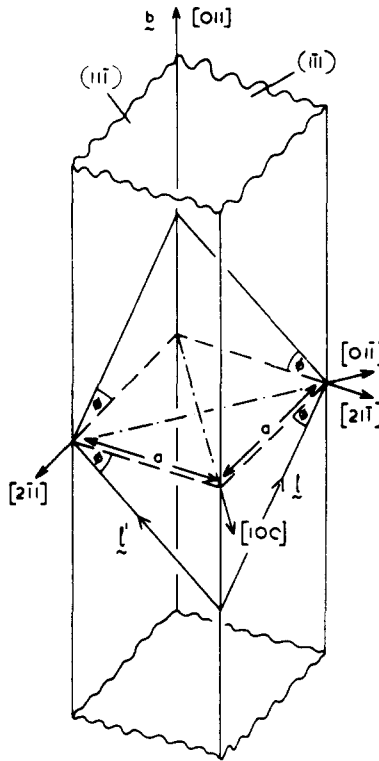


FIG. 4.15. Schematic diagram of a rhombus loop constrained to its glide prism. The figure shows an explicit example, where the prism faces are the $(1\bar{1}\bar{1})$ and $(\bar{1}\bar{1}1)$ planes and its axis (the slip direction) is the $[011]$ direction. ϕ is the angle, measured in the prism faces, defining the rotation of the loop. a is the size of the pure-edge rhombus loop (the right section of the prism) with its adjacent sides along the $[2\bar{1}1]$ and $[2\bar{1}\bar{1}]$ directions. The two possible axes of rotation $[011]$ and $[100]$ are also shown.⁽⁸⁶⁾

energy with orientation for a loop of size $a/r_0 = 50$, where r_0 is the dislocation core radius and a range of v values is shown in Fig. 4.16. (These curves were given by Bacon *et al.*⁽⁸⁶⁾ and the values $v = 0.36$ and 0.44 were chosen to represent aluminium and copper, respectively.) The minima in the curves move closer to (110) as a is increased and, thus, the true minima in the linear, isotropic energy are in the region of (210) , which corresponds to $\phi = 11^\circ$ for the rotation about $[001]$. Despite the apparent agreement between theory and experiment, two problems remain. Firstly, the energy does not decrease continuously from (111) to (210) and it is not clear, therefore, how a loop could make the rotations discussed above. This difficulty was partly answered by Bacon and Crocker,⁽⁸⁹⁾ who showed that if the loop is allowed to adopt a more-general parallelogram shape, rather than being restrained to make rotations in which it is a rhombus, it can follow a path on which the energy always decreases to a minimum

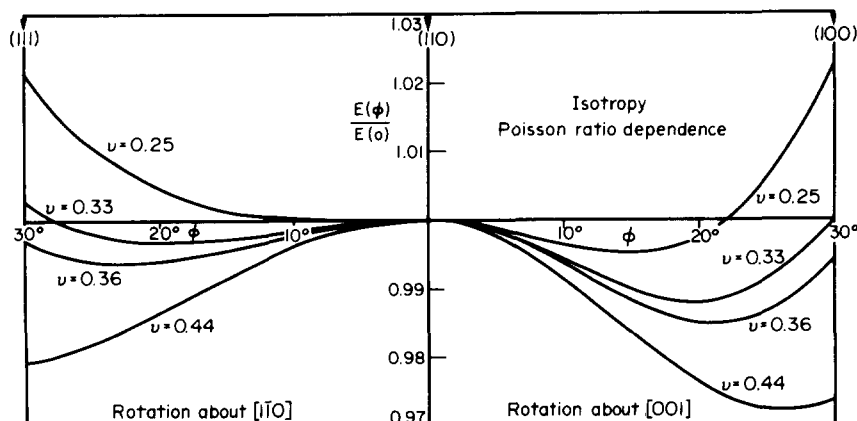


FIG. 4.16. The variation of the elastic energy of the rhombus loop of size $a/r_0 = 50$ in an isotropic body with rotation about either diagonal axis for various values of Poisson's ratio ν . The curves were computed from the analytic result of Bullough and Foreman⁽⁴⁵⁾ and are normalized to the elastic energies of the corresponding pure-edge {110} rhombus loops.⁽⁸⁶⁾

close to (210). Secondly, for both rhombus and parallelogram loops, the reduction in energy from (111) to the stable orientation is small ($\sim 1\%$) and, in view of the possible error associated with the isotropic approximation, the agreement between theory and experiment could be fortuitous. The purpose of the investigation of Bacon *et al.*⁽⁸⁶⁾ was to remove this uncertainty.

They computed the energy of the prismatic rhombus loop using the anisotropic field equations of Willis⁽⁸⁰⁾ (see Section 4.2.4). The energy arising from the integral of the product of stress times displacement over the planar surface enclosed by the loop was obtained by numerical quadrature with the stress at every point due to each side being evaluated from Willis' formula for a straight segment, eq. (4.2.36); this required the solution of a total of four sextic equations for every point. The energy arising from the surface integration over the core surface—the “core-surface traction correction” discussed in Section 2.6.1⁽⁴⁵⁾—was obtained by evaluating the stress and displacement at a point on the core surface of a loop side as though it were an infinite, straight line. This again required the solution of sextic equations for every point (see eqs (4.2.34) and (4.2.35)). With this procedure, evaluation of the energy of a loop required only a few minutes of a computer time, and Bacon *et al.* were able to determine loop energy as a function of both orientation and size in aluminium and copper. Their results for aluminium are shown in Fig. 4.17. The curve for the limiting case of an infinitely large loop was obtained by neglecting interactions between loop sides and assuming each side to have an energy per unit length equal to that of an infinite, straight line.

The curves of Fig. 4.17 for loops of finite size do have a minimum

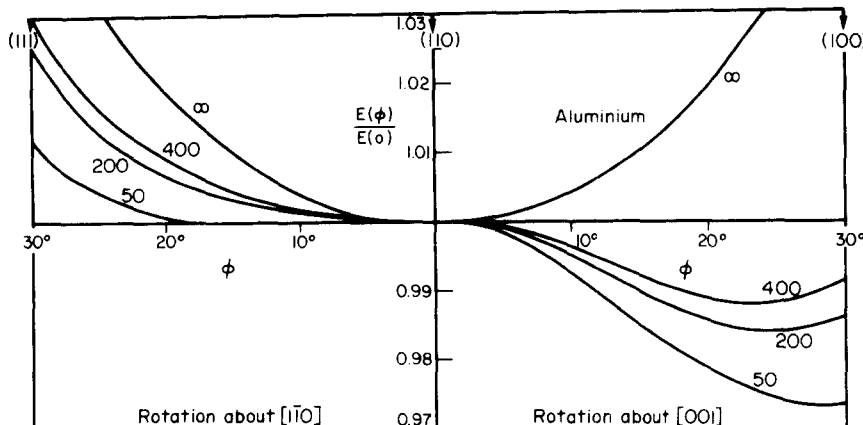


FIG. 4.17. The variation of the elastic energy of the rhombus loop in aluminium for rotation about the diagonal axes. The results are normalized to the elastic energies of the corresponding pure-edge {110} rhombus loops, and the numbers 50, 200, 400 and ∞ refer to the value of the ratio a/r_0 .

between (110) and (100), and in fact the energy decreases continuously from (111), giving a reduction of approximately 4%. Thus, the inclusion of anisotropy actually gives a more satisfactory agreement between theory and experiment than was obtained by Bullough and Foreman. Furthermore, a comparison of the $a/r_0 = 50$ curve with the isotropic curves of Fig. 4.16 reveals that even for aluminium, which has an anisotropy ratio of only 1.21, the anisotropic form cannot be simulated to the accuracy required for this problem by an appropriate choice of Poisson's ratio. This interesting result, which was confirmed by the data for copper, indicates that elastic anisotropy must be included in any calculation in which the important differences in energy (or stress) are of the order of a few percent.

4.3.2. Interactions between dislocations and either dislocations or other defects

The elastic interactions between dislocations and either dislocations or other sources of internal stress are well-known to be of fundamental importance for many of the physical properties of crystalline materials. They govern phenomena such as defect aggregation, high temperature and irradiation-induced creep, and some forms of obstacle-controlled strengthening. The interaction energy between two sources of internal stress A and B in an infinite body is given by

$$\mathcal{E}^I = \iiint_{\text{body}} \sigma_{ij}^A e_{ij}^B dV, \quad (4.3.1)$$

where σ_{ij}^A is the stress field due to A and e_{ij}^B is the strain field of B . For the interaction between a dislocation (A) and a point defect (B) this reduces

to either

$$\mathcal{E}^I = b_i^A \iint_{S_0} \sigma_{ij}^B dS_j, \quad (4.3.2)$$

where S_0 is an arbitrary open surface bounded by the dislocation or

$$\mathcal{E}^I = - \oint_V u_i^A f_i^B dV, \quad (4.3.3)$$

where f^B is the distribution of body force which describes the defect contained in V . To first order, eq. (4.3.3) was shown in Section 2.7.2 to be

$$\mathcal{E}^I = -e_{ij}^A P_{ij}^B, \quad (4.3.4)$$

where P_{ij}^B are the dipole moments of the defect and e_{ij}^A is evaluated at its centre. As was mentioned in Section 2.7.2, eqs (4.3.2) and (4.3.4) are easily shown to be identical, for from eq. (2.7.7)

$$\sigma_{ij}^B = -C_{ijkl} P_{mn}^B G_{km,ln}(x), \quad (4.3.5)$$

so that after substituting eq. (4.3.5) into eq. (4.3.2) and using Volterra's formula, eq. (2.5.4), for the strain field of a dislocation, eq. (4.3.2) is transformed into eq. (4.3.4). The elastic anisotropy of the host medium enters \mathcal{E}^I through the form of the stiffness constants C_{ijkl} , whereas the microscopic anisotropy of the defect, i.e. the symmetry of the defect site and the associated force distribution, enters through the moments P_{ij} . For a spherically symmetric (cubic) defect (cf. Fig. 2.10 and eq. (2.7.8))

$$P_{ij} = \pm P \delta_{ij} \quad (4.3.6)$$

and eq. (4.3.4) reveals the well-known result that \mathcal{E}^I depends only on the hydrostatic field of A . Since an infinitesimal dislocation loop dS^B can be represented by an appropriate combination of force dipoles (see Section 2.7.1), eq. (4.3.4) is also valid for the interaction between a dislocation and an infinitesimal loop, for which it reduces to the obvious form

$$\mathcal{E}^I = b_i^B \sigma_{ij}^A dS_j^B. \quad (4.3.7)$$

Equation (4.3.4) can be evaluated by expressing e_{ij}^A as a line integral, eq. (2.5.5), the integrand of which will itself have to be evaluated either by integration, eq. (2.4.29), or by solving for the roots of a sextic polynomial.⁽⁸⁰⁾ (The additional integral which appears to occur in eq. (4.3.2) is eliminated by the application of Stokes' theorem, as in the reduction of Volterra's surface integral to Mura's line integral equation, see Section 2.5.1.) For polygonal dislocations, the evaluation is further simplified by use of the geometrical formulae of Section 4.2.3, and \mathcal{E}^I is then given by the sum of one-dimensional integrals. Clearly, the evaluation of \mathcal{E}^I requires little computational effort for most situations.

Some influences of elastic anisotropy on the relatively simple interaction between an infinite, straight line of mixed orientation and a centre of

dilatation are demonstrated by the results of Goodman and Sines.⁽⁹⁰⁾ (Results for perfect edge dislocations in cubic crystals and the dissociated edge dislocation in copper were given by Goodman and Sines⁽⁹¹⁾ and Navi *et al.*,⁽⁹²⁾ respectively.) Equation (4.3.2) was evaluated for straight dislocation of arbitrary orientation in a number of cubic crystals. The geometry considered is shown in Fig. 4.18a, where the line lies in a direction \mathbf{t} at an angle ψ to \mathbf{b} , and the centre of dilatation is at a radial distance R from the line and a vertical distance $R \sin \eta$ above the slip plane. For the isotropic case, ε^I has the well-known form

$$\varepsilon^I = \varepsilon_{\max}^I \sin \eta \sin \psi, \quad (4.3.8)$$

where ε_{\max}^I is the maximum value of ε^I for the defect at the distance R from an edge dislocation. The form of ε^I for this case is shown in Fig. 4.18b, where the ε^I values have been normalized by ε_{\max}^I . Results for ε^I

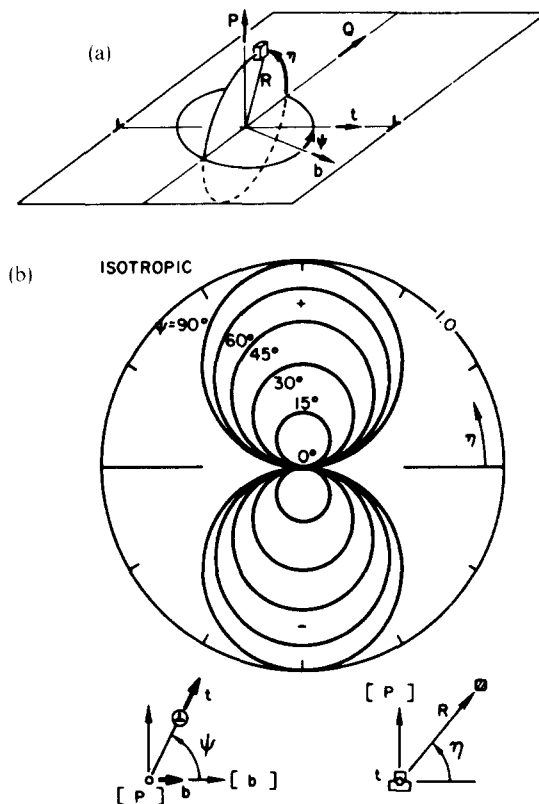


FIG. 4.18. (a) Vector geometry of mixed, glissile dislocation and point-defect interaction. Vector \mathbf{t} is the positive dislocation direction, \mathbf{b} is the Burgers vector, \mathbf{P} is the normal to the slip plane and R is the distance from the dislocation to the point defect. (b) Isoenergetic plots of normalized interaction energy for mixed dislocations and a symmetric point defect in an isotropic crystal.⁽⁹⁰⁾

for the $1/2 \langle 1\bar{1}0 \rangle \{111\}$ systems of Al and Cu, the $1/2 \langle 111 \rangle \{1\bar{1}0\}$ system of α -Fe and the $1/2 \langle 110 \rangle \{1\bar{1}0\}$ system of LiF are shown in Figs 4.19a-d, respectively. (The values are normalized with respect to a suitably-defined isotropic average of δ_{\max}^I .⁽⁹⁰⁾) It can be seen that the effects of anisotropy can be marked for even this simple case. For example, the maximum interaction need not occur at 90° from the slip plane and the contours

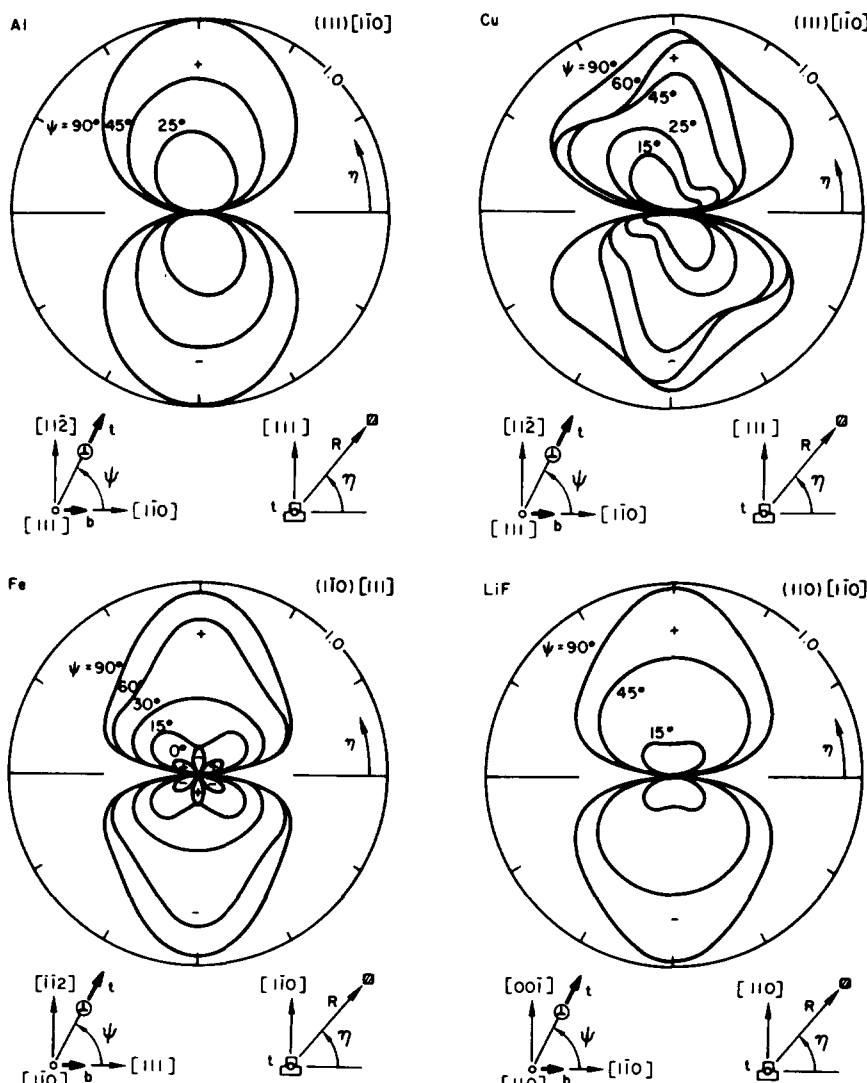


FIG. 4.19. Interaction energy between a symmetric point defect and (a) $1/2 \langle 1\bar{1}0 \rangle \{111\}$ dislocations in aluminium, (b) $1/2 \langle 1\bar{1}0 \rangle \{111\}$ dislocations in copper, (c) $1/2 \langle 111 \rangle \{1\bar{1}0\}$ dislocations in iron and (d) $1/2 \langle 110 \rangle \{1\bar{1}0\}$ dislocations in lithium fluoride.⁽⁹⁰⁾

can be quite irregular for a given value of ψ . In addition, regions of negative interaction energy may exist above the slip plane with the converse below. Several other intriguing effects of anisotropy on the fields of infinite straight dislocations have been discussed by Steeds and Willis.⁽⁹³⁾

Many defects do not, of course, exhibit spherical symmetry, and then the combined effects of defect asymmetry and elastic anisotropy may give results bearing little resemblance to those given by the symmetric-defect/isotropic-elasticity model. This was revealed by the investigation of the interaction between a circular edge dislocation loop and a self-interstitial atom in copper by Meissner *et al.*⁽⁹⁴⁾ The motivation was to determine the influence of anisotropy on the interaction between interstitial loops and interstitial atoms and to see if it enhances the preferential attraction for interstitials as compared with vacancies, which is a basic feature of theories of void growth in neutron-irradiated metals. The interstitial was considered to be in a $\langle 100 \rangle$ dumbbell configuration; the forces on, and displacements of, the atoms neighbouring this defect were calculated by the lattice-statics method by Bullough and Tewary⁽⁹⁵⁾ and, thus, the dipole moments are known. Meissner *et al.* evaluated \mathcal{E}^I directly from eq. (4.3.4) using the following levels of approximation. (a) The medium was assumed to be elastically isotropic with constants given by the Voigt average for copper, and the loop field e_{ij} was calculated from the isotropic distortion formula obtained by combining eqs (2.4.21) and (2.5.5).⁽¹²⁾ The interstitial was modelled by a spherical inclusion with strength P given by the average value of the true dipole moments. Results in the form of isointeraction-energy contour plots are shown in Fig. 4.20; the interstitial loop of radius r_L lies on the (111) plane and is centred on the lower left-hand corner of the diagram, which is a quadrant of the (112) plane. There is, of course, complete axial symmetry about the loop normal for this case. (b) The influence of defect asymmetry was considered by computing the interaction energy between the dumbbell interstitial with axis along [100] and the loop; isotropic elasticity was assumed. The resulting contours on the orthogonal (112) and (110) planes, which pass through the centre of the loop, are shown in Figs 4.21a and b, respectively. (The loop is at the centre of these figures, as shown.) (c) Results for the interaction between the [100] interstitial and the (111) loop in anisotropically-elastic copper were obtained by computing the strain field of the loop from an equation derived by Willis;⁽⁸⁰⁾ special numerical procedures were employed to avoid singularities which arise in his sextic analysis. The equipotential contours on the (112) and (110) planes are reproduced in Figs 4.22a and b. (d) The interstitial in a crystal can adopt any of the three $\langle 100 \rangle$ orientations and the contours which result when the dumbbell orientation having the lowest value of \mathcal{E}^I at any point is chosen are shown in Fig. 4.23.

The marked effects of anisotropy in the defect symmetry and elastic response of the host crystal are self-evident in these results. They show

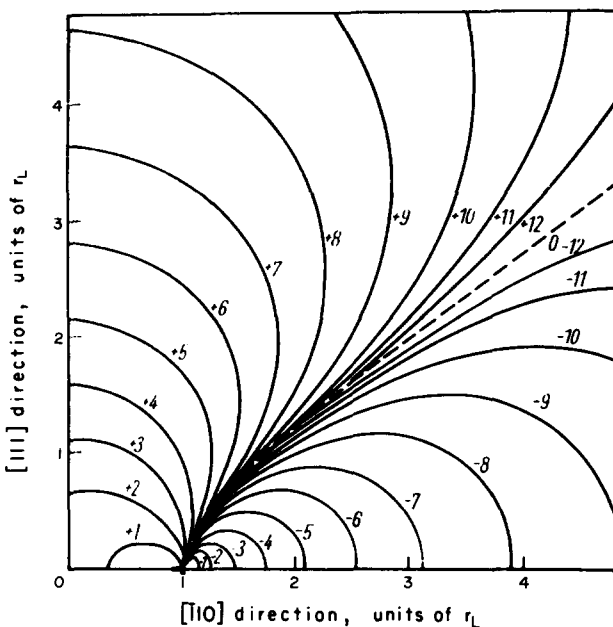


FIG. 4.20. The iso-interaction energy contours between an isotropic, interstitial point defect and the interstitial, pure-edge dislocation loop in a quadrant of the (112) plane through the centre of the loop. The cross-section through the perimeter of the loop is indicated by the usual dislocation symbol. The number $\pm n$ ($n = 1 \dots 12$) on each contour indicates an energy of $\pm 0.4 \times 2^{1-n}$ eV for that contour; the $n = 0$ contour (---) means zero interaction energy.⁽⁹⁴⁾

clearly that both features can change the isotropic results in qualitative as well as quantitative ways. The effects are unpredictable in the sense that choosing different values of μ and v for the isotropic case will not reproduce the anisotropic results. Meissner *et al.*⁽⁹⁴⁾ conclude that the important effect of anisotropy in the present example is that it actually reduces the length of the drift path an interstitial would have to take to reach the loop, and it thus enhances the capture efficiency of interstitials at interstitial loops.

An extensive study of the interaction between dislocation loops and either other loops or point defects in α -uranium was carried out using anisotropic elasticity by Meissner.⁽³⁰⁾ This metal has orthorhombic symmetry and, therefore, nine independent elastic constants. As a result of irradiation by high-energy neutrons, it undergoes dimensional changes, which are believed to arise from the preferential nucleation, growth and coalescence of coplanar vacancy loops on {100} planes and similarly of interstitial loops on {010} planes. Hudson⁽⁹⁶⁾ has observed sheets of coplanar loops on these planes. The aim of Meissner's work was to investigate the role of elastic anisotropy in these processes. His results for the interaction of dislocation loops and point defects, which were assumed

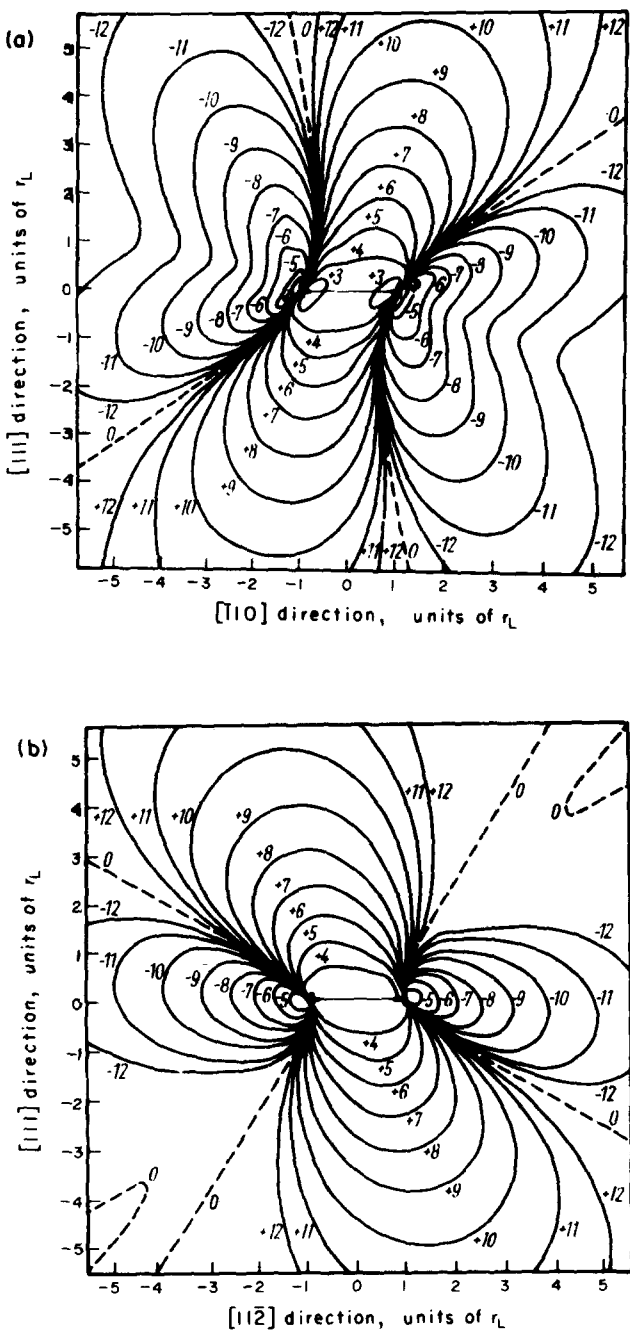


FIG. 4.21. The iso-interaction energy contours between a [100] dumbbell interstitial and a (111) pure-edge, interstitial loop in an isotropic body in (a) the {112} plane and (b) the {110} plane through the centre of the loop. Other details are specified in the caption to Fig. 4.20.⁽⁹⁴⁾

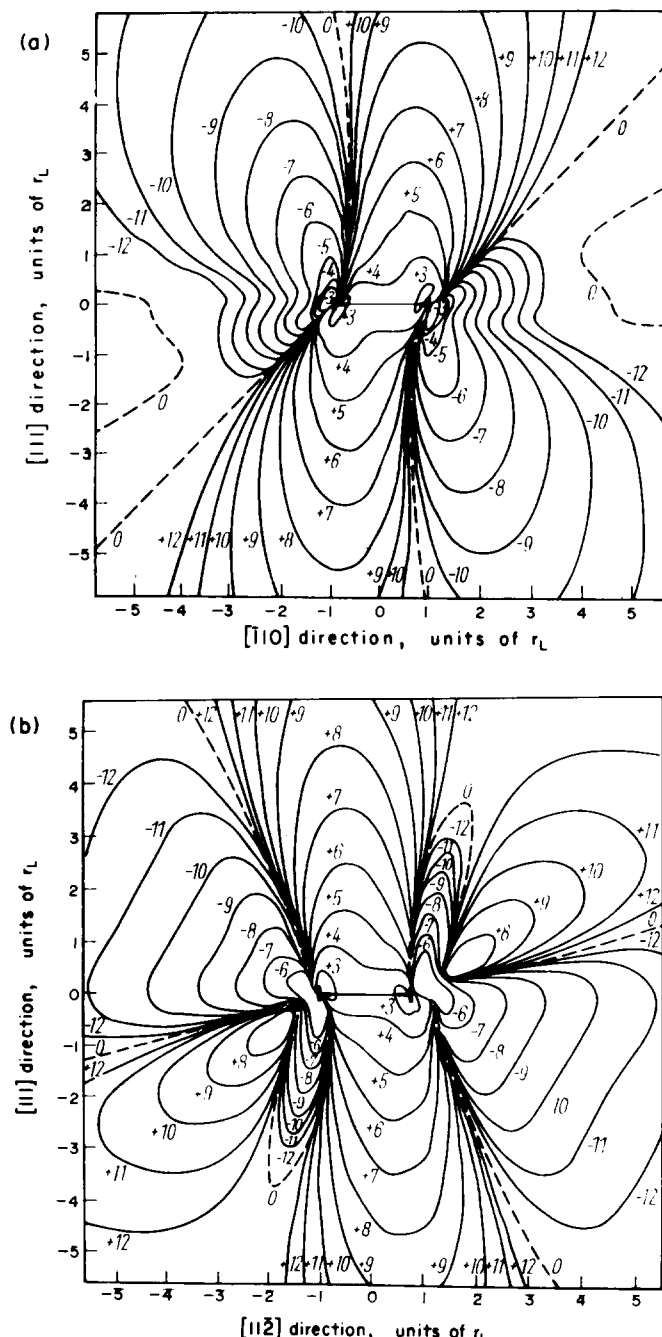


FIG. 4.22. The iso-interaction energy contours between a [100] dumbbell interstitial and a (111) pure-edge, interstitial loop in copper in (a) the $[11\bar{2}]$ plane and (b) the $[1\bar{1}0]$ plane through the centre of the loop. Other details are specified in the caption to Fig. 4.20.⁽⁹⁴⁾

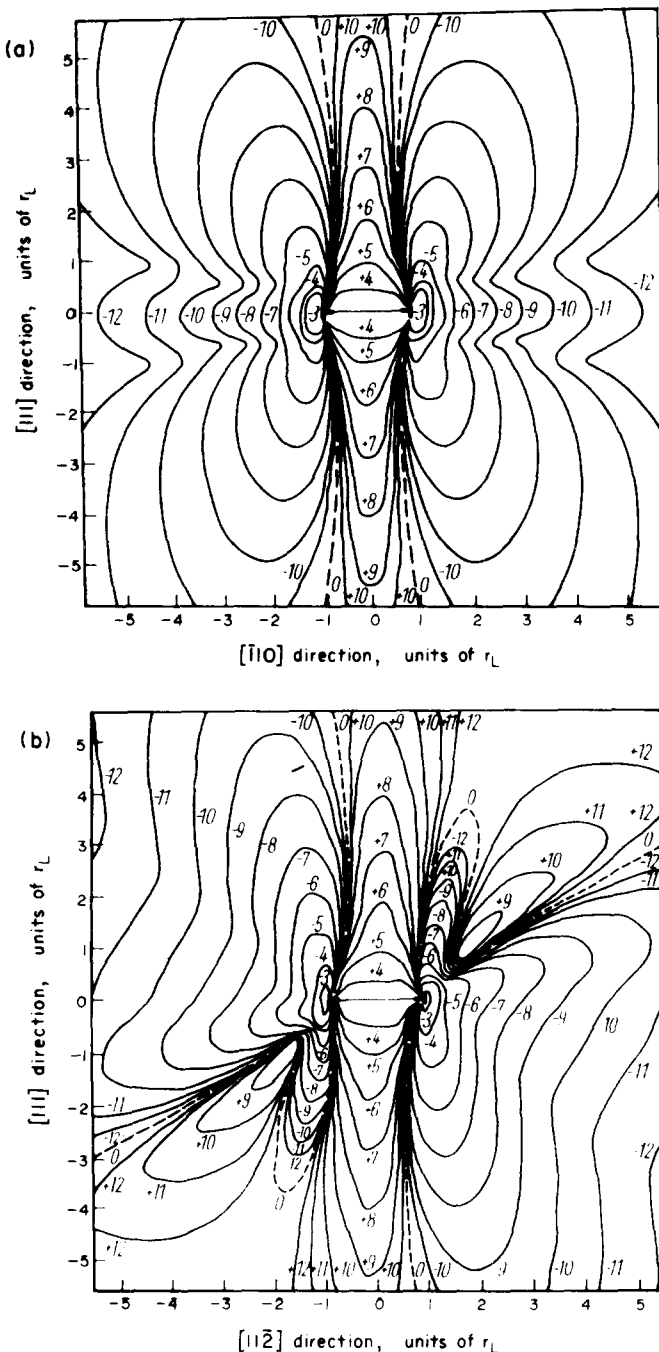


FIG. 4.23 The iso-interaction energy contours between the $\langle 100 \rangle$ dumbbell interstitial which has the lowest interaction energy and a (111) pure-edge, interstitial loop in copper in (a) the $\{11\bar{2}\}$ plane and (b) the $\{1\bar{1}0\}$ plane through the centre of the loop. Other details are specified in the caption to Fig. 4.20.⁽⁹⁴⁾

to be spherically symmetric, show strong effects due to anisotropy, as in the copper study described above, and are reported to confirm the preferential growth model. (Full details are given by Meissner.⁽³⁰⁾) In order to determine if elastic interactions can cause loops to glide prismatically into planar configurations, Meissner computed ϵ^I for loops constrained to move in this way. He considered interactions between two vacancy loops, two interstitial loops, and vacancy and interstitial loops, but, for brevity, we shall mention only one case here. Consider two vacancy edge loops on {100} planes, as shown schematically in Fig. 4.24. The loops are circles of radius R and loop A is considered fixed with loop B being free to glide on a cylinder whose [100] axis is a distance D from the centre of A. Meissner⁽³⁰⁾ calculated ϵ^I by numerically integrating eq. (4.3.7) over the planar surface contained within B; the field of A was obtained from field equations given by Willis.⁽⁸⁰⁾ In the limit when $D \gg 2R$, both loops can be assumed to be infinitesimal and integration of eq. (4.3.7) is not required. Meissner obtained ϵ^I for this approximation by evaluating the second derivative of the Green's function in σ_{ij}^A from the integral expression given in eq. (2.4.29). His results for the variation of ϵ^I with X for loops of $R = 50 \text{ \AA}$ and $D = 3R$ and $2.5R$ are shown in Figs 4.25a and b, respectively; the curves labelled a, b and c indicate, respectively, ϵ^I for two finite loops in α -U, two infinitesimal loops in α -U and two infinitesimal loops in an isotropic medium. The vertical arrows indicate the positions of the energy minima. The isotropic interaction between infinitesimal loops was considered by Hudson⁽⁹⁶⁾ and the results of Fig. 4.25 reveal that the inclusion of anisotropy actually predicts equilibrium positions which are more nearly coplanar. Consideration of the finite size of the loops (curve a) enhances this effect. Furthermore, as the ratio of loop size to separation increases, the degree of planarity, as measured by the ratio of X to D at the energy minimum, increases. Thus, the incorporation of anisotropy

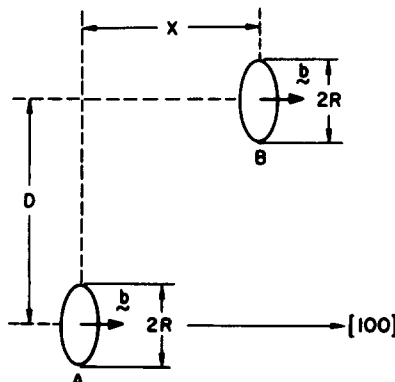


FIG. 4.24. Schematic diagram of two circular (100) vacancy loops in α -uranium; the loops are pure-edge in character. X is the [100] component of the separation of the loops.

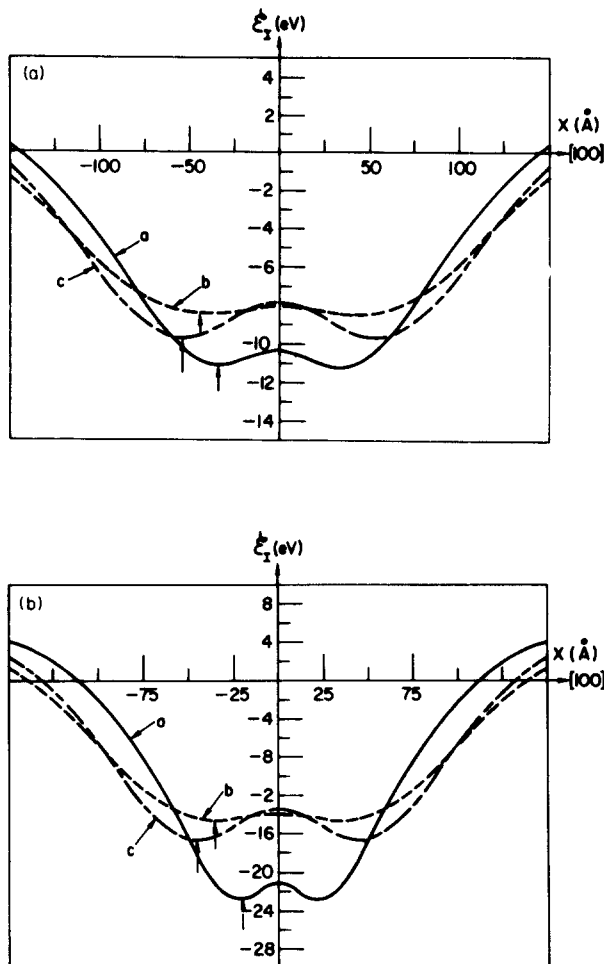


FIG. 4.25. The variation of interaction energy with X of two (100) vacancy loops of radius $R = 50 \text{ \AA}$ in x -uranium; the value of D specified in Fig. 4.24 is (a) $3R$ and (b) $2.5R$.⁽³⁰⁾

and finite size into the analysis gives the growth and coalescence model a more satisfactory theoretical basis, a result which could not be predicted beforehand. Meissner reported similar effects for the other interactions considered.

The results of this section show the extent to which the theoretical developments of Section 4.2 enable elastic anisotropy to be considered in the interactions between dislocations and sources of internal stress in crystals. They lead us to conclude that the use of anisotropy is probably essential in any theory which depends on the quantitative details of these interactions.

4.3.3. Orowan mechanism in anisotropic crystals

The equilibrium shape of a dislocation bowing against a periodic row of impenetrable obstacles (Orowan bypassing mechanism) under the action of a constant applied stress σ was investigated by Scattergood and Bacon⁽⁹⁷⁾ for various anisotropic metals. These authors used the geometry shown in Fig. 4.26 and they calculated the equilibrium shapes of the bowing dislocation at increasing values of σ up to a critical value beyond which no further stable equilibrium shapes could be found. This last stable configuration gives the Orowan stress for the particular choice of crystal and obstacle-dislocation geometry. In addition to the elastic anisotropy of the host crystal, it should be clear that for this problem the dislocation self interactions also play a vital role and, therefore, the line tension approximation is not appropriate. The two dislocation branches tangent to each obstacle (Fig. 4.26) will interact with each other as a result of the dislocation stress field, particularly at stresses near the Orowan stress where the bowout is large and the branches assume a dipole-like configuration. In order to take into account the combined effects of dislocation self-interaction and elastic anisotropy, the authors used the self-stress method outlined in Section 2.6.2 to obtain the equilibrium configurations. To include elastic anisotropy, they evaluated the self stress by means of Brown's theorem in conjunction with the requisite infinite straight dislocation field data obtained by the integral formalism discussed in Section 4.1.

Scattergood and Bacon did not use the prescription embodied in eq. (2.6.28) for their self stress evaluation. Instead, they calculated the self stress at a point P on the dislocation line L by integrating Brown's geometric theorem over L up to a point ρ_0 away from P , i.e. a length $2\rho_0$ of line at P was omitted. In the isotropic case this procedure is consistent with a self energy evaluation, wherein the energy is obtained from a double line integral (see Section 2.6.1) taken over two coincident configurations L under the restriction that elements on the line closer together than ρ_0 make a zero contribution.^(98,6) Arguments can be made⁽⁹⁸⁾ to show that the cutoff parameter ρ_0 has the identification $\rho_0 = r_0/2$, where r_0 is the conventional core radius already mentioned. In the case of anisotropy, there is no analogous double line integral representation and, hence,

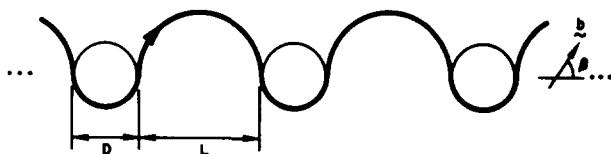


FIG. 4.26. Schematic diagram of the dislocation-obstacle geometry used for the investigation of the Orowan mechanism. The diagram shows several obstacles and bowing loops from an infinite periodic row. The obstacle diameter is D , the interobstacle spacing is L and the Burgers vector orientation β is measured as shown.⁽⁹⁷⁾

the procedure used by Scattergood and Bacon must be considered an approximate extension.

The method of integration used by Scattergood and Bacon to compute the self stress at P was as follows: the dislocation configuration is approximated by a set of finite dislocation segments such that the segment containing P is a circular arc—a circular arc gives the first-order approximation to the curvature at P in the sense of the osculating circle limit—and the rest of the segments are straight, as is shown schematically in Fig. 4.27. The self stress contribution τ^{ARC} at P due to the arc is obtained by integrating eq. (4.2.18) over a finite circular arc, using the ρ_0 cutoff procedure already mentioned. The contribution τ^{SEG} to the self stress at P due to the remaining straight segments is obtained by summing the contributions given by eq. (4.2.27) over all segments. When developing their segment formulae, Scattergood and Bacon inserted a Fourier series representation of the energy or stress factors into Brown's theorem prior to integrating over the segments and, thus, the final expressions were given in terms of the Fourier coefficients displayed in Table 4.3. In this manner, the anisotropic cases could be treated as simply as the isotropic cases merely by changing the coefficients. The total self stress τ^L at P is obtained as $\tau^L = \tau^{ARC} + \tau^{SEG}$. Since the τ^{ARC} expression derived by the authors does not follow a completely consistent energy evaluation method, we shall not reproduce this segment expression here. We would suggest instead that in future studies a similar evaluation method for τ^L be used, but with a τ^{ARC} expression derived on the basis of the prescription given in eq. (2.6.28).

Despite the lack of consistency in their τ^{ARC} expression, the results of Scattergood and Bacon should be accurate to within some small numerical error. This follows because their τ^{ARC} expression does contain a dominant term logarithmically singular in r_0^{-1} and premultiplied by the line tension factor $E + E''$ of the tangent dislocation at P . The self-stress method described in Section 2.6.2 should also produce an expression of this form. The differences will be manifest primarily in the non-logarithmic part of the τ^{ARC} term and, while these differences are rather difficult to evaluate analytically, we would not expect them to be very significant. Neglect of the core traction term (see Appendix) and uncertainties in the precise

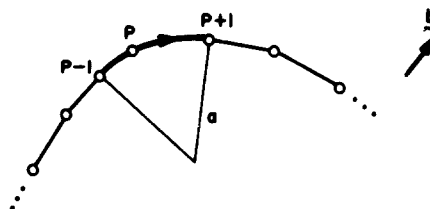


FIG. 4.27. Schematic diagram of the finite segment dislocation geometry used to calculate the self stress τ_{SELF} at the point P on the dislocation. The segment containing P is a circular arc through P and the two neighbouring segments, as shown in the figure, while the remaining segments are straight.

value of r_0 also contribute in effect to a non-logarithmic τ^{ARC} term, so there is an inherent degree of uncertainty in this part of τ^L in any event. The remainder of the procedure used by Scattergood and Bacon, viz. the τ^{SEG} evaluation, stands unchanged, and, hence, the "non-local" part of the self stress is properly included (non-local in the sense that it does not explicitly depend on the curvature at P , whereas the τ^{ARC} contribution is proportional to it). The non-local contribution to τ^L is perhaps the most interesting aspect of the self stress method since this part of the dislocation self interaction cannot be captured in a line tension approximation.

Scattergood and Bacon used an algorithm based on curvature adjustment for relaxing the dislocation into its equilibrium configuration. For the class of problems considered by the authors, the algorithm converged quickly and smoothly to the equilibrium configurations. The use of the geometric-theorem-based methods, in conjunction with an efficient relaxation algorithm, allowed the authors to obtain the equilibrium configurations for rather complex curvilinear dislocation geometry with only a very moderate expenditure of computer time. The elastic anisotropy was, of course, very easily included in the calculations by means of the Fourier coefficients. The reader is referred to the original paper⁽⁹⁷⁾ for details of the relaxation method.

Figure 4.28 shows typical equilibrium shapes of bowing dislocation loops obtained by Scattergood and Bacon for various metals. The pair of obstacles for each set of loops represents one pair in the periodic row and the increasing bowouts correspond to increasing values of σ up to the Orowan stress. The marked differences in loop shapes between the various metals clearly reflects the influence of the elastic anisotropy on the bowing process.

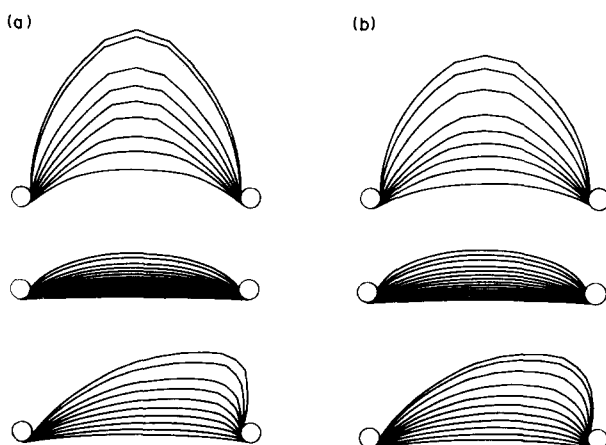


FIG. 4.28(a) and (b).

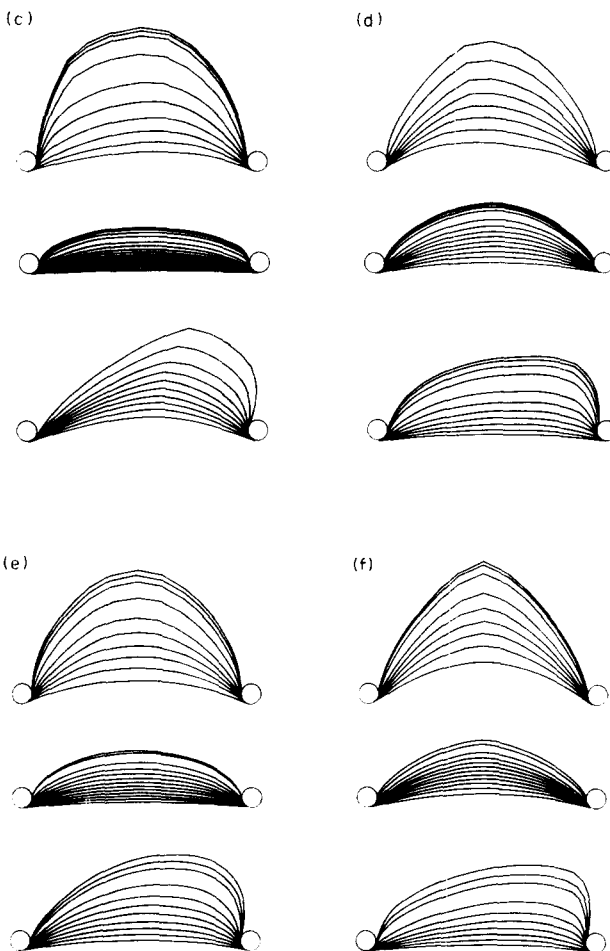


FIG. 4.28. Equilibrium shapes for $D = 100r_0$, $L = 1000r_0$. The successive shapes for each obstacle pair correspond to increasing values of the applied stress up to the Orowan stress; the obstacle pair represents one out of the periodic row shown in Fig. 4.26. The crystals are: (a) Au, (b) Cu, (c) Fe, (d) Nb, (e) Ni and (f) Zn; with reference to Table 4.1, the slip systems are: Au, Cu, Ni-fcc1; Fe, Nb-bcc1; Zn-hept. For the three sets of shapes for a given metal, the Burgers vector orientation angle β (see Fig. 4.26) equals 90° for the top set, 0° for the middle set and 45° for the bottom set.⁽⁹⁷⁾

In analyzing their results, the authors addressed the question as to how the elastic anisotropy can be characterized for the Orowan mechanism and, in particular, if an "effective" isotropic shear modulus μ_A and Poisson ratio ν_A can be defined; there are numerous methods for defining average elastic constants (Voigt or Reuss averages, for example) and they may differ by factors of two or more, but it is not *a priori* obvious if any of these averages are appropriate for the Orowan problem. In addition,

the authors sought a simple means whereby the complicated influence of the dislocation self interaction could be characterized. Based on a heuristic line tension argument, which views the Orowan mechanism as a dipole extension process for the critical (unstable) configuration, the authors found, as shown in Fig. 4.29, that their Orowan stress values could be accurately described by the formulae

$$\tau_{\text{EDGE}}^{\text{OROWAN}} = \frac{\mu_A b}{2\pi L} \left(\ln \frac{\bar{D}}{r_0} + 0.65 \right), \quad (4.3.9)$$

$$\tau_{\text{SCREW}}^{\text{OROWAN}} = \frac{\mu_A b}{2\pi L(1 - v_A)} \left(\ln \frac{\bar{D}}{r_0} + 0.65 \right). \quad (4.3.10)$$

with

$$\bar{D} \equiv (D^{-1} + L^{-1})^{-1}, \quad (4.3.11)$$

where D and L are defined as shown in Fig. 4.26,

$$\mu_A \equiv \frac{4\pi E_{\text{SCREW}}}{b^2}, \quad (4.3.12)$$

$$v_A \equiv 1 - \frac{E_{\text{SCREW}}}{E_{\text{EDGE}}}, \quad (4.3.13)$$

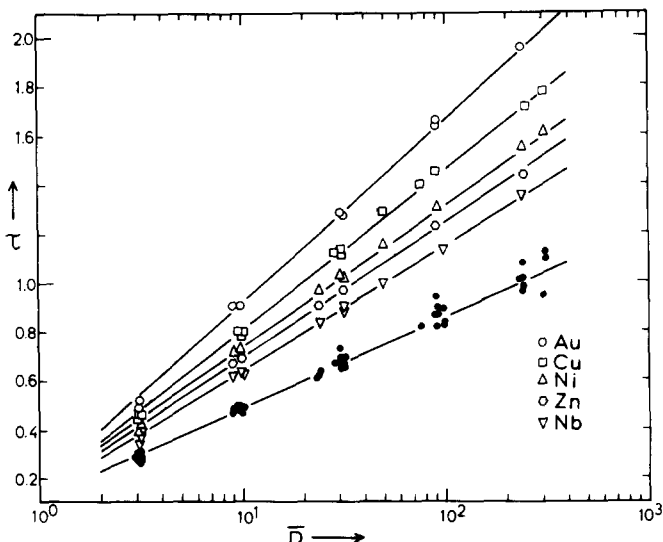


FIG. 4.29. Orowan stress values in units of $\mu_A b / L$ vs. $\ln(\bar{D}/r_0)$ for the crystals shown. The slip systems are as given in Fig. 4.28. The open symbols are for screws while the filled circles are for all edge cases. The straight lines through the data points have the slopes required by eqs (4.3.9) and (4.3.10) in the text.

Each cluster of points for the edges contains values for all crystals.⁽⁹⁷⁾

and where EDGE and SCREW in eqs (4.3.9) and (4.3.10) correspond to $\beta = 90^\circ$ and 0° , respectively, in Fig. 4.26 and E_{EDGE} and E_{SCREW} denote the prelogarithmic energy factors for infinite straight edge and screw dislocations, as discussed in Section 4.1.1.5. The similarity between the form of eqs (4.3.9) and (4.3.10) and the conventional isotropic line tension formulae should be apparent, and one should note that these equations also hold in the isotropic case; μ_A and v_A then reduce to the conventional isotropic values. For this complicated dislocation problem, it is perhaps surprising that the influence of elastic anisotropy can be captured in the two simple parameters μ_A and v_A , while the effects of self interaction can be manifest in the single logarithmic parameter \bar{D} (the harmonic mean of D and L). The reader is referred to the original paper of Scattergood and Bacon⁽⁹⁷⁾ for a more detailed discussion of the results and their interpretation. The main point to be made here is that without the full anisotropic elastic self-stress calculation, simple, widely-used formulae like eqs (4.3.9) and (4.3.10) cannot be properly justified, nor can the elastic constants be properly identified. Using the geometric theorems and related methods discussed in this review, Scattergood and Bacon were able to incorporate elastic anisotropy into their calculations with almost no more effort than that required for isotropy.

4.3.4. Dislocation shear loops in anisotropic crystals

Scattergood and Bacon⁽⁹⁹⁾ used the methods described previously in Section 4.3.3 to investigate the (unstable) equilibrium configurations of dislocation shear loops in anisotropic crystals acted upon by a constant applied stress σ . This problem is the anisotropic elastic self-stress counterpart of the well-known anisotropic line tension calculations performed by de Wit and Koehler,⁽⁵¹⁾ and it provides an interesting basis upon which line tension results can be directly compared to the self-stress results.

Figure 4.30 shows typical equilibrium shear loop shapes obtained by Scattergood and Bacon.⁽⁹⁹⁾ As was already mentioned, their method accounts for the combined effects of elastic anisotropy and dislocation self-interaction. The influence of elastic anisotropy on the loop shapes in various metals is evident from Fig. 4.30; for isotropy, the loops are very close to true ellipses. The authors found that for a given stress σ , the loop size could be accurately related to the stress by the relation,

$$\sigma = \frac{\mu_A b}{2\pi l} \left(\ln \frac{l}{r_0} + 1.56 \right), \quad (4.3.14)$$

where l represents the minor axis of the loop and μ_A is the same as that defined in eq. (4.3.12). The axial ratio (major/minor axis) was found to be as shown in Fig. 4.31 and, in the limit of large loop size, the ratio approaches $(1 - v_A)^{-1}$, where v_A is given by eq. (4.3.13). The axial ratio $(1 - v_A)^{-1}$ is predicted by the line tension approximation calculations of de Wit and Koehler⁽⁵¹⁾ (independent of loop size), whereas Fig. 4.31 shows

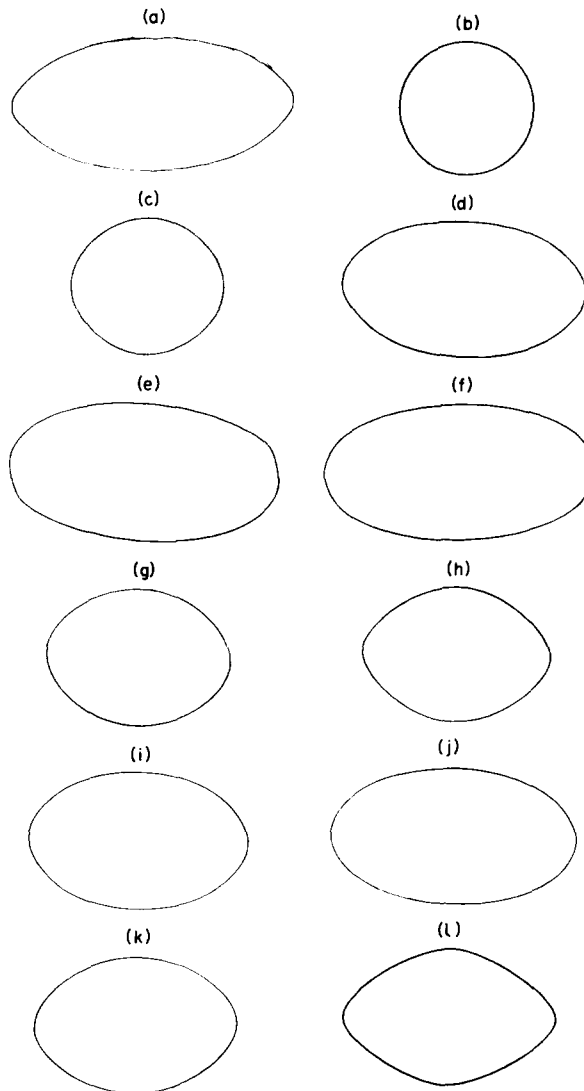


FIG. 4.30. Equilibrium shear loop shapes. The Burgers vector lies along the major (horizontal) axis. The crystals are: (a) Au, (b) Be, (c) Cr, (d) Cu, (e) Fe (bcc1), (f) Fe, (g) Mo, (h) Nb, (i) Ni, (j) Ta, (k) V, (l) Zn. With reference to Table 4.1, the slip systems are (except where noted otherwise): Au, Cu, Ni—fcc1; Cr, Fe, No, Nb, Ta, V—bcc2; Be, Zn—hcp1.⁽⁹⁹⁾

that the true ratios may deviate somewhat from this value, especially at small loop sizes or large eccentricities. For a given applied stress σ , eq. (4.3.14) gives the loop size l/r_0 and, to within the approximation displayed in Fig. 4.31, we may assume this to be a loop with axial ratio $(1 - v_A)^{-1}$. One should note that eq. (4.3.14) is a familiar form, which can be derived within the framework of the line-tension approximation,

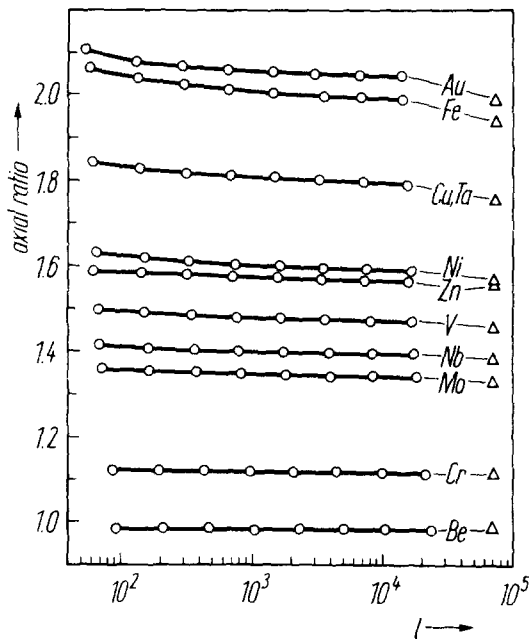


FIG. 4.31. Axial ratio (major:minor axis) vs. $\ln(l/r_0)$ for the crystals shown in Fig. 4.30.⁽⁹⁹⁾ The triangles indicate the values corresponding to the line tension calculations of de Wit and Koehler.⁽⁵¹⁾

although with line tension, the logarithmic term is completely arbitrary. The results of Scattergood and Bacon, therefore, show that the conventional line tension results can be applied to the shear-loop problem; the parameters μ_A and v_A account for the elastic anisotropy, while the logarithmic term in eq. (4.3.14) accounts for the self interaction. As was also the case for the Orowan problem discussed in the last section, the use of familiar, line-tension formulae, along with what appear to be isotropic elastic constants, cannot be justified until the full anisotropic elastic self-stress calculations have been made. The reader is referred to the paper of Scattergood and Bacon⁽⁹⁹⁾ for a detailed discussion of the shear loop results.

We must remark here that Li and Liu⁽¹⁰⁰⁾ questioned the validity of the self-stress method. Their criticism was based on the isotropic self-stress shear loop calculations of Mitchell and Smialek,⁽¹⁰¹⁾ who reported a limiting axial ratio of $((1 + v)/(1 - 2v))^{-1/3}$. On the other hand, Li and Liu used a direct energy evaluation scheme to find equilibrium shapes and they obtained a limiting ratio of $(1 - v)^{-1}$. Scattergood and Bacon⁽⁹⁹⁾ also made isotropic self-stress calculations and their limiting axial ratios were in good agreement with those of Li and Liu. The latter authors applied various core traction corrections to their energy evaluations, whereas Scattergood and Bacon did not (Section 2.6.1), and therefore at

small loop sizes the results may differ somewhat in detail; however, at large loop sizes the core traction terms become a negligible contribution so that the limiting ratios must be comparable. The discrepancy here appears to be in the *a priori* assumption of elliptical shapes made by Mitchell and Smialek; Scattergood and Bacon made no such assumptions in their calculations. It appears that care must be exercised in carrying out self-stress calculations to ensure that artificial constraints are not imposed on the relaxation of the dislocation configurations into their equilibrium positions. When properly applied, the self-stress method does correspond to a proper energy minimization, as should be evident from the analysis given in Section 2.6.2.

4.3.5. Stacking-fault nodes in anisotropic crystals

As a final example of the application of the anisotropic theory to rather complex, curvilinear dislocation problems, we shall review symmetric stacking-fault nodes in fcc metals. The planar, three-fold symmetric stacking-fault node geometry is shown schematically in Fig. 4.32, where θ is the node orientation, b denotes the Burgers vector of the Shockley partial dislocation and the radius W of the inscribed circle is used as a measure of the node size. It should be clear from the geometry shown that the combined effects of elastic anisotropy and dislocation self-interaction are quite important in determining the equilibrium node configurations.

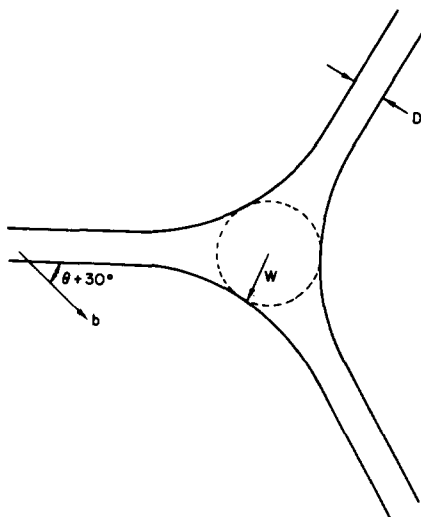


FIG. 4.32. Schematic diagram of the planar, symmetric three-fold node geometry. The three node branches consist of Shockley partial dislocations bounding a stacking fault in fcc crystals. The node size W is as shown and the Burgers vector orientation θ of a node branch is measured as shown. At large distances from the node centre, the spacing D of the sidearm asymptotes is assumed to be that for an infinite, straight dislocation in the given crystal.⁽¹⁰²⁾

Brown⁽⁵⁰⁾ first computed the equilibrium node configurations on a reasonable basis using an isotropic self-stress method. Later, Scattergood and Bacon⁽¹⁰²⁾ reexamined the problem using the anisotropic self-stress method discussed in Section 4.3.3. For the node problem, the angular part of the in-plane tractions and their derivatives for infinite straight dislocations are required (rather than just the energy factors), because the Burgers vector orientation differs for the three branches (Fig. 4.32). The tractions are needed for the calculation of the dislocation interactions between different node branches. As was shown by Scattergood and Bacon,⁽¹⁰²⁾ the incorporation of this feature into the calculations is quite straightforward when the methods follow those outlined in Section 4.2; the basic steps are identical to those discussed in Section 4.3.3, except that the Fourier series representations must be extended to include the in-plane tractions of the partial dislocations and this was done by the authors. Including elastic anisotropy required little more effort than isotropy once the infinite, straight dislocation field data were available.

Figure 4.33 shows typical equilibrium node configurations in silver obtained by Scattergood and Bacon,⁽¹⁰²⁾ while Fig. 4.34 shows the node size W vs. θ relationship; both figures pertain to fixed γ with $r_0 = b$. The anisotropic curve (solid) in Fig. 4.34 is plotted along with an "isotropic" counterpart (broken), which was obtained using the v_A and μ_A values defined by eqs (4.3.12) and (4.3.13). Relative to the cases covered in Sections 4.3.3 and 4.3.4, this choice of effective isotropic elastic constants is more difficult to rationalize; nevertheless, the use of μ_A and v_A gives a good overall approximation to the anisotropic results, the differ-

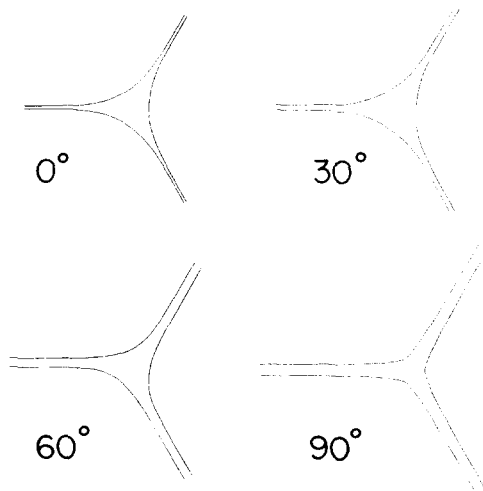


FIG. 4.33. Equilibrium node shapes in silver with $r_0 = b$ and a stacking-fault energy per unit area $\gamma = 2000/\mu_A b$. The orientation θ for each node shape is shown.⁽¹⁰²⁾

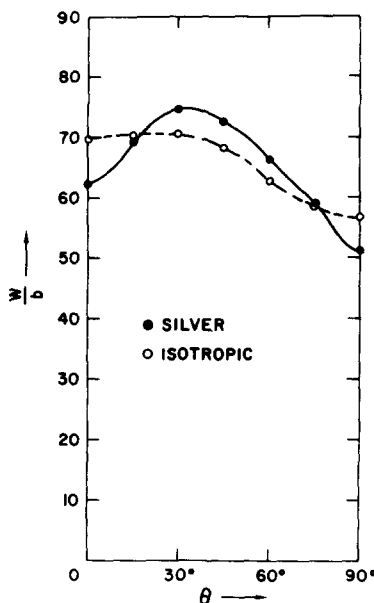


FIG. 4.34. Node size W as a function of θ for silver (solid) and isotropy (broken) using the isotropic elastic constants μ_A and v_A appropriate for silver, as defined in the text. For these curves, $r_0 = b$ and $\gamma = 4000/\mu_A b^{(102)}$.

ences being about 15 to 20% in the worst case. The distinct maximum which appears in the anisotropic curve in Fig. 4.34 is a direct manifestation of the elastic anisotropy. No such maximum appeared in any isotropic curve over the whole range of $0 \leq v \leq \frac{1}{2}$. The maximum can be rationalized by a corresponding maximum in the anisotropic line tension curve $E + E''$ vs. Burgers vector orientation ϕ for the partial dislocation in silver, as is shown (solid) in Fig. 4.35. When the line tension in the central portion of a node branch is large, its "stiffness" is large; hence it resists inward bending and the node size W must be relatively large (Fig. 4.32). For isotropy (shown broken in the figure for the appropriate μ_A and v_A values), such maxima will never occur. The reader is referred to the paper of Scattergood and Bacon⁽¹⁰²⁾ for a complete discussion and interpretation of the node results. The authors also give a quantitative correlation relating γ and r_0 to W and θ for the full anisotropic elastic self-stress node results.

In this and the two previous sections, we have seen that the effective shear modulus and Poisson ratio defined by eqs (4.3.12) and (4.3.13) are useful in many dislocation problems. It appears that other kinds of problems will also display similar dependencies, e.g. void strengthening.⁽¹⁰³⁾ The values of μ_A and v_A appropriate to various metals are easily found from eqs (4.3.12) and (4.3.13) used in conjunction with the tabulations discussed in Section 4.1.3. A selected compilation of these effective elastic constants may also be found in several papers of Scattergood and

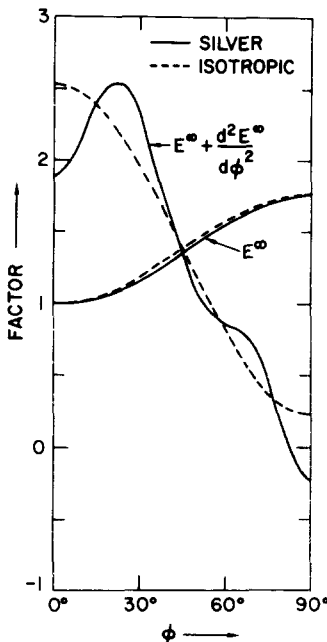


FIG. 4.35. The line tension $E + E''$ and energy E factors for infinite straight Shockley partial dislocations in silver (solid) and isotropy (broken) in arbitrary units vs. the Burgers vector orientation ϕ . The isotropic curve uses the constants μ_A and v_A appropriate for silver, as defined in the text. The angle ϕ is measured between the Burgers vector and the line direction.⁽¹⁰²⁾

Bacon^(99,97,102) and in the work of Kocks *et al.*⁽⁴⁸⁾ Effective values for dissociated dislocations in f.c.c. metals have also been discussed recently by Bacon.⁽¹⁶³⁾

4.3.6. Other problems

The investigations reviewed above demonstrate the applicability of the theoretical developments described in Sections 4.1 and 4.2 and, in addition, give an indication of the possible consequences of anisotropy in a number of areas. There have been other applications, for which limitations of space preclude a detailed discussion. For example, Asaro and Hirth⁽⁶⁷⁾ derived the integral expressions for the in-plane tractions of infinite, straight dislocations which were used to obtain the data presented in Section 4.1.4 and applied them to the study of straight dislocation nodes and networks in α -iron. These configurations arise from dislocation reactions of the form $1/2 [111] + 1/2 [\bar{1}\bar{1}1] \rightarrow [001]$ and the angle between the $1/2 \langle 111 \rangle$ arms is found experimentally to be 91° .⁽¹⁰⁴⁾ Using the semi-infinite and finite segment formulae of Section 4.2.3, Asaro and Hirth showed that the theoretically-predicted equilibrium angle is in excellent agreement with this value, in contrast to the result obtained in the isotropic approximation. As another example, Scattergood and Kocks⁽¹⁰⁵⁾ have analyzed the line-tension forces acting on point obstacles when dislocations

bow between them under stress. Plots of force vs. dislocation cusp angle for anisotropic crystals reveal features which cannot be reasonably approximated by the isotropic formula.

There are a number of other areas in which the theory of anisotropic elasticity may be expected to find increasing application. Computer simulation of images produced by transmission-electron microscopy is a particular example. It is a powerful technique for the identification of defects,⁽¹⁰⁶⁾ but one in which the effects of anisotropy have only been allowed for to date for straight dislocations. The results of Ohr⁽¹⁰⁷⁾ indicate that these effects should be important for the accurate identification of small loops and other defects. By analytically reducing to a double integral the Volterra formula, eq. (2.5.3), with the Green's function given as a Fourier integral, Ohr obtained by numerical integration the displacements around a circular dislocation loop in some cubic metals. His contour plots show features due to anisotropy which would clearly be manifested in a TEM image. Although the image of a defect can be obtained from its displacement field, the simple geometrical formulae of Section 4.2 do not apply to displacements and so a considerable amount of computing is required to obtain them from the Volterra surface integral. The transmitted electron intensities can be calculated, however, from the first derivative of the displacement⁽¹⁰⁸⁾ and so the geometrical formulae can, in fact, be used to compute the image contrast in a straightforward manner. In the same area, the integral formalism of Section 4.1 has an additional use. McConnell⁽¹⁰⁹⁾ has considered the conditions under which the simulated image of a straight dislocation in an anisotropic crystal can be matched to an image of an actual dislocation, such that its Burgers vector is uniquely determined. He finds that if a set of vectors, which are simple functions of S and B defined in Section 3.6 and the diffraction vector, are not co-planar, then a single match is sufficient. If not, it may be necessary to match two or three micrographs, depending on the vectors. A computer program to determine S and B , and hence the sufficiency conditions, can easily be written. Similar conditions are found for grain-boundary dislocations and the analysis has recently been extended to "nuclei of strain" such as force dipoles and infinitesimal loops.⁽¹¹⁰⁾

All the studies referred to in the preceding sections highlight the fact that for some applications the use of anisotropic elasticity is essential if quantitative results are required, whereas in other cases a judicious choice of effective shear modulus and Poisson's ratio may enable the isotropic approximation to suffice. Even in the latter situations, the appropriate values for μ and ν are not usually *a priori* self-evident, so that a limited number of anisotropic calculations are generally required. Fortunately, the geometrical formulae of Section 4.2 and the integral expressions of Section 4.1 often enable the anisotropic calculations to be performed with little extra effort. This is particularly true when the Fourier coefficients in the infinite-line fields have been obtained by a separate calculation.

4.4. Straight Dislocations in Inhomogeneous Anisotropic Media

The Stroh and the integral formalisms may be used to study straight dislocations in certain simple inhomogeneous anisotropic media. Three such problems which may be investigated are:

- (i) a straight dislocation parallel to the boundary of an anisotropic half-space,
- (ii) a straight dislocation at the interface between two dissimilar anisotropic half-spaces which have been welded together,
- (iii) a straight dislocation situated wholly in one of two dissimilar anisotropic half-spaces which have been welded together.

It is well-known that the presence of a dissimilar second phase introduces certain image forces on dislocations. As we shall see, the rotational invariance of the Stroh eigenvectors is reflected in some rather interesting physical invariances of the dislocation energies and image forces associated with problems (i) to (iii).

In connection with the above mentioned problems it turns out to be useful to introduce the matrix M_{zi} by⁽⁸⁾

$$\sum_{z=1}^3 L_{jz} M_{zi} = \delta_{ij}, \quad (4.4.1)$$

i.e. M is the inverse of L . Completeness requires that

$$M_{zi} L_{ip} = \delta_{zp} (\alpha, \beta = 1, 2, 3). \quad (4.4.2)$$

Since the Stroh eigenvector L_{ip} is rotationally invariant it follows that $\partial M_{zi}/\partial\omega = 0$, where ω is the polar angle fixing the basis (m, n) in the plane normal to t , i.e. M_{zi} depends only on t and the elastic constants (and the velocity v if we are considering problems of uniform motion). Using the Stroh orthogonality relation eq. (3.4.14) and the completeness relations eqs (3.4.21) and (3.4.22) one may deduce the following relations:

$$M_{\beta i}^* L_{iz} + L_{ip}^* M_{zi} = 0 (\alpha, \beta = 1, 2, 3), \quad (4.4.3)$$

$$\sum_{z=1}^6 M_{zi} M_{zs} = 0, \quad (4.4.4)$$

$$\sum_{z=1}^3 (M_{zi} A_{sz} + M_{zs}^* A_{iz}^*) = 0, \quad (4.4.5)$$

$$\sum_{z=1}^3 (M_{zi} A_{sz} + M_{zs} A_{iz}) = \sum_{z=1}^3 M_{zi} M_{zs}, \quad (4.4.6)$$

where

$$M_{z+3,i} = M_{zi}^* \quad (\alpha = 1, 2, 3) \quad (4.4.7)$$

for both static and uniform motion problems if we consider only velocities below the limiting dislocation velocity v_L . The matrix M_{xi} always exists except when $||L_{iz}|| = 0$, which is precisely the condition determining the Rayleigh velocity for surface waves in an anisotropic half-space.^(8,66,62) Thus, for static problems or for uniform motion problems at velocities other than the Rayleigh velocity in question, M_{xi} is well-defined.

4.4.1. The straight dislocation parallel to a planar free surface

Consider an infinite straight dislocation (line direction \mathbf{t} and Burgers vector \mathbf{b}) parallel to the free surface of an anisotropic half-space and situated a distance h beneath the free surface (Fig. 4.36). This problem has been studied by Tucker and Crocker,⁽¹¹¹⁾ and Barnett and Lothe.⁽¹¹²⁾ If one computes the total energy (strain energy) per unit length of dislocation, the total “image force” on the dislocation induced by the presence of the free surface may be found by computing the negative derivative of the energy with respect to h . This image force is normal to the free surface (translation symmetry precludes the existence of an image force parallel to the free surface) and is considered positive if the free surface tends to attract the dislocation. The image force per unit length of dislocation is given by

$$F = \frac{E}{h} = B_{ij} b_i b_j / h, \quad (4.4.8)$$

where E is the pre-logarithmic energy factor of the same dislocation in the infinite medium whose elastic constants are identical to those of the half-space. Since E and \mathbf{B} depend only on \mathbf{t} , C_{ijkl} and \mathbf{b} , any plane free surface parallel to a fixed crystal dislocation (fixed \mathbf{t} and \mathbf{b}) a distance h from the surface induces the same magnitude of image force on the dislocation; the direction of the image force is always normal to the free surface. This result is somewhat surprising in view of the fact that all planes parallel to the dislocation line are not crystallographically equivalent in an elastic medium of general anisotropy. Data for E to be used in eq. (4.4.8) have been presented in Section 4.1.3 for the common cubic and hexagonal metals.

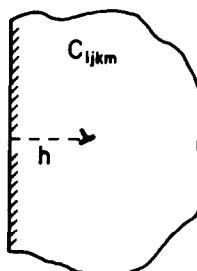


FIG. 4.36. A straight dislocation parallel to the free boundary of an elastic half-space.

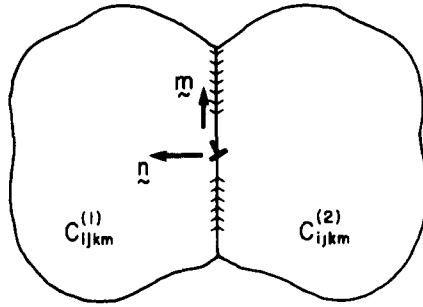


FIG. 4.37. A straight dislocation in the interface between two joined dissimilar anisotropic half-spaces.

4.4.2. The interfacial dislocation

Consider an infinite straight dislocation (line direction t , Burgers vector b) situated at the interface between two dissimilar anisotropic half-spaces welded together (Fig. 4.37). The elastic constants of the two media are $C_{ijkm}^{(1)}$ and $C_{ijkm}^{(2)}$. This problem has been studied by Gemperlova and Saxl,⁽¹¹³⁾ Clements,⁽¹¹⁴⁾ Willis,⁽¹¹⁵⁾ Nakahara and Willis,⁽¹¹⁶⁾ and Barnett and Lothe.⁽¹¹²⁾ The total energy per unit length of the interfacial dislocation is given by

$$\mathcal{E}^{int} = E^{1-2} \ln \frac{R}{r_0}, \quad (4.4.9)$$

where⁽¹¹²⁾

$$E^{1-2} = -\frac{1}{2\pi i} G_{js} b_j b_s \quad (4.4.10)$$

and G is the inverse of the matrix F , whose elements are

$$F_{si} = \sum_{\beta=1}^3 (A_{s\beta}^{(1)} M_{\beta i}^{(1)} + A_{i\beta}^{(2)} M_{\beta s}^{(2)}). \quad (4.4.11)$$

Obviously E^{1-2} , the prelogarithmic energy factor for the interfacial dislocation, depends only on the elastic constants of each medium and the crystallographic components of b and t relative to each medium, since the Stroh matrices A and M depend only on these quantities. For a fixed dislocation (fixed b and t relative to each medium), the interfacial dislocation energy is the same for all interface planes whose zonal axis is the dislocation line. In terms of the matrices B and S associated with the integral formalism Barnett and Lothe⁽¹¹²⁾ have shown that

$$E^{1-2} = 2b \cdot B(2) \cdot N^{-1} \cdot B(1) \cdot b, \quad (4.4.12)$$

where

$$\begin{aligned} N = & \{ [B(1) + B(2)] + [S^T(1) \cdot B(2) + B(1) \cdot S(2)] \\ & \times [B(1) + B(2)]^{-1} [S^T(1) \cdot B(2) + B(1) \cdot S(2)] \}. \end{aligned} \quad (4.4.13)$$

If each half-space is isotropic, then

$$E^{1-2} = \frac{b^2}{2\pi} \mu_1 \mu_2 \frac{[\mu_2(k_1 + 1) + \mu_1(k_2 + 1)]}{(\mu_2 k_1 + \mu_1)(\mu_1 k_2 + \mu_2)} \text{ (edge),} \quad (4.4.14)$$

$$E^{1-2} = \frac{b^2}{2\pi} \frac{\mu_1 \mu_2}{\mu_1 + \mu_2} \text{ (screw),} \quad (4.4.15)$$

where

$$k_i = 3 - 4v_i$$

and (μ_1, v_1) and (μ_2, v_2) are the respective shear moduli and Poisson's ratio for the media.

For completeness we note that the interfacial dislocation displacement field in medium 1 is given by

$$\begin{aligned} u_i^{(1)} = & \frac{1}{2\pi i} \sum_{s=1}^3 A_{iz}^{(1)} M_{sk}^{(1)} G_{ks} b_s \ln \{ \mathbf{m} \cdot \mathbf{x} + p_z^{(1)} \mathbf{n} \cdot \mathbf{x} \} \\ & + \frac{1}{2\pi i} \sum_{s=4}^6 A_{iz}^{(1)} M_{sk}^{(1)} G_{sk} b_s \ln \{ \mathbf{m} \cdot \mathbf{x} + p_z^{(1)} \mathbf{n} \cdot \mathbf{x} \}, \end{aligned} \quad (4.4.16)$$

where \mathbf{n} is the unit inner normal to medium 1 at the interface and $\mathbf{m} = \mathbf{n} \wedge \mathbf{t}$. Equation (4.4.16) gives the displacement field in medium 2 if we replace the superscript 1 by 2 everywhere and if G_{sk} replaces G_{ks} and vice versa.

4.4.3. The image force theorem

Consider an infinite straight dislocation (line direction \mathbf{t} and Burgers vector \mathbf{b}) situated a distance h from the interface of two dissimilar anisotropic half-spaces which have been welded together (Fig. 4.38). The elastic constants of the two media are $C_{ijklm}^{(1)}$ and $C_{ijklm}^{(2)}$, respectively, and we assume the dislocation lies wholly in medium 1. The image force induced on the

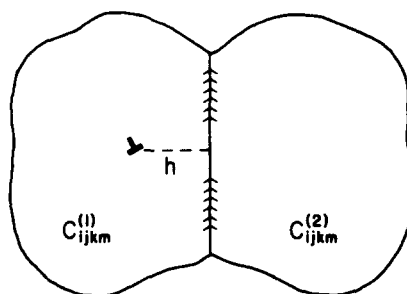


FIG. 4.38. A straight dislocation near the interface of two joined, dissimilar half-spaces.

dislocation per unit length is⁽¹¹²⁾

$$F = \frac{E^{(1)} - E^{1-2}}{h}, \quad (4.4.17)$$

where $E^{(1)}$ is the prelogarithmic energy factor for the dislocation when it exists in an infinite medium elastically identical to medium 1, and E^{1-2} is the prelogarithmic energy factor for the dislocation when it is situated at the interface between the two half-spaces. The image force is normal to the interface and is positive if the dislocation is attracted to the interface.

The results of the previous two sections show that for a fixed crystal dislocation (fixed t and b relative to each medium), all interfaces parallel to the dislocation induce the same magnitude of image force on the dislocation. The interface orientation independence of the magnitude of the image force is a reflection of the rotational invariance of the Stroh eigenvectors. Tucker⁽¹¹⁷⁾ first deduced this orientation independence of the magnitude of F , even though the rotational invariance of the Stroh eigenvectors was not known at the time. In addition, Tucker⁽¹¹⁷⁾ has treated the case of a dislocation separated from the interface of two joined dissimilar half-spaces when the interface is incapable of supporting shear tractions, i.e. a slipping interface.

4.4.4. The straight dislocation emergent at a planar free surface

There is another situation involving a dislocation in an inhomogeneous anisotropic medium for which the induced force acting on the dislocation has a simple form. It is shown schematically in Fig. 4.39 and involves a straight dislocation emerging at the planar free surface of an anisotropic, semi-infinite medium. The dislocation is at an angle α to the inward normal to the surface and the Burgers vector makes an angle β with this normal. The dislocation will in general experience a force induced by the presence of the free surface and Lothe⁽¹¹⁸⁾ has shown that the force per unit length is distributed according to the law

$$F = \frac{1}{\lambda} \left[E(\alpha - \beta) \tan \alpha + \frac{dE}{dx} (\alpha - \beta) \right], \quad (4.4.18)$$

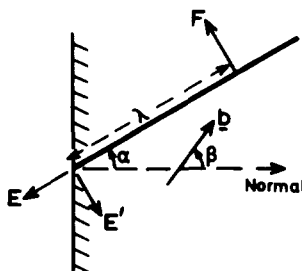


FIG. 4.39. A straight dislocation emergent at a planar free surface.

where λ is the distance from the surface and $E(\alpha - \beta)$ is the energy factor for an infinite straight dislocation in the orientation α with Burgers vector \mathbf{b} . Values of this force for the common cubic and hexagonal metals can easily be computed from the data for $T_1 (= E/b)$ presented in Section 4.1.3. For other materials, data for E and E' can be obtained from the formulae of Section 4.1.2.

It can be seen from eq. (4.4.18) that there are some orientations of the dislocation for which F is zero along the line, and for these angles of incidence it can remain straight. They occur when α satisfies the relation

$$E(\alpha - \beta) \sin \alpha + E'(\alpha - \beta) \cos \alpha = 0; \quad (4.4.19)$$

the values of α for which this is so are in general non-zero. This is illustrated for the case of isotropy (with $\nu = 1/3$), copper, niobium and zinc in Fig. 4.40, where values of α satisfying eq. (4.4.19) are plotted as a function of β . The Burgers vector and slip plane, i.e. plane of diagram in Fig. 4.40, for the three metals are $1/2\langle 110 \rangle \{ \bar{1}11 \}$ for Cu, $1/2\langle 111 \rangle \{ 11\bar{2} \}$ for Nb and $1/3\langle 11\bar{2}0 \rangle \{ 1\bar{1}00 \}$ for Zn, and the data for these cases were calculated directly from the coefficients for T_1 in Table 4.3. It can be seen that the dislocation can remain in equilibrium with angles of incidence some 20° to 30° away from the surface normal for some orientations of the Burgers vector. The changes in α from metal to metal for a given value of β are quite large and features arising from elastic anisotropy are clearly seen in the curves. The shape of the curve for zinc at small α and β values arises from the fact that E is not a minimum in the screw orientation for the hcpl system of this metal.

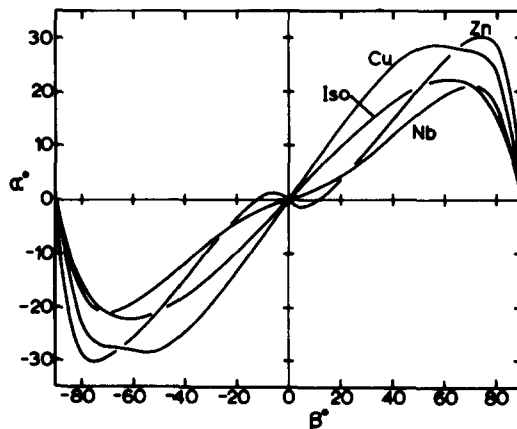


FIG. 4.40. The variation of α with β for equilibrium orientations of the dislocation shown in Fig. 4.39. The isotropic curve is for Poisson's ratio $\nu = 1/3$, and the data for Cu(fcc1), Nb (bcc2) and Zn(hcp1) used in eq. (4.4.19) were obtained from Table 4.3.

The form of eq. (4.4.19) has a rather simple interpretation in the line-tension model of a dislocation. At the termination point, two forces act on the end of the dislocation to keep it in equilibrium.^(72,74) One acts along the line and is proportional to E , and the other acts normal to the line and is proportional to E' (see Fig. 4.39). In the absence of any other forces on the dislocation at the surface—due, say, to a surface step with a non-zero surface energy—these “tension” and “torque” terms must resolve to give zero net force in the surface. This requirement leads to eq. (4.4.19).

The dislocation core energy will modify the shape of the line close to the surface. Lothe⁽¹¹⁸⁾ has argued that curvature due to this effect will be short ranged, however, since any stresses associated with it must decrease at least as fast as λ^{-2} . Any deviation from the angle given by eq. (4.4.19) should, therefore, not be significant beyond about $50b$ from the surface.

5. OTHER DEFECTS

5.1. Point Defects

In this section we shall review various models for point defects in an infinite, homogeneous, anisotropic, elastic body. We consider the field quantities associated with point defects only as they are derived in the continuum approximation and we shall not mention any of the numerous lattice or atomistic models (for further discussion, see e.g. Flocken and Hardy,⁽¹¹⁹⁾ Johnson,⁽¹²⁰⁾ Tewary,⁽¹²¹⁾ Heald⁽¹²²⁾).

The description of point defects within the continuum framework is conveniently given in terms of the Green's function G_{ij} discussed in Section 2.4; recall that $G_{ij}(\mathbf{x} - \mathbf{x}')$ is the displacement along x_i at \mathbf{x} due to a unit point force along x_j at \mathbf{x}' . In the most transparent case, we assume *a priori* that a certain array of self-equilibrated “defect” forces act on the host medium containing the defect. These forces arise from the perturbed interatomic potential and they should be viewed as internal forces, which act over and above the normal interatomic forces in the defect-free state. For such models consisting of prescribed arrays of point forces, the description of the field quantities follows directly from the displacements given by G_{ij} . Another class of continuum models for point defects is possible through use of the elastic inclusion or transformation strain models discussed in Section 5.2. In this case, the point defect would be described as an atomic-sized misfitting or inhomogeneous inclusion inserted into the host matrix such that continuous tractions and displacements are maintained everywhere. The inclusion models are perhaps the most natural ones, insofar as the continuum theory is concerned, but the mathematical development is more difficult than for the simple point force arrays. G_{ij} also plays a role in the inclusion models because, as will be

discussed in Section 5.2, the sequence of conceptual cutting and welding operations by which the inclusion is formed, require the final elimination of a distribution of body force. The application of the elastic inclusion results to point defects is a straightforward one using the methods outlined in Section 5.2. In the present section, we shall focus attention primarily on elementary models of point defects as they are constructed using point force arrays. We shall be concerned primarily with the effects of elastic anisotropy on the intrinsic field properties; the interaction of point defects with dislocations has already been considered in Section 4.3.2.

The most elementary point-force model for a point defect is the centre of dilatation or compression discussed in Section 2.7 and shown schematically in Fig. 2.10. These centres consist of three equal, orthogonal force dipoles of strength P , where compression or dilatation corresponds, respectively, to the case where the forces act toward or away from the array centre at \mathbf{x}' . Note that a compression centre as conventionally defined here actually dilates the host medium and vice versa. Centres of compression or dilatation may be used as elementary models for point defects in situations where the symmetry is appropriate, and in f.c.c. crystals a self-interstitial could be represented by a dilatation centre, while an under-sized defect, such as a vacancy, could be a compression centre. The appropriate value of P has to be obtained from atomistic calculations, such as fitting asymptotic harmonic lattice results to the continuum results.⁽¹¹⁹⁾ In Section 2.7 we derived that for such centres

$$P_{sj} = \pm P\delta_{sj} \quad (5.1.1)$$

with all other multipole tensors identically zero. The associated displacements are

$$u_i(\mathbf{x}) = \mp PG_{ij,j}(\mathbf{x} - \mathbf{x}'), \quad (5.1.2)$$

so that the first derivatives of G_{ij} are the quantities of interest here. The minus sign in eqs (5.1.1) and (5.1.2) corresponds, respectively, to centres of compression and dilatation. Since G_{ij} is homogeneous of degree -1 in $|\mathbf{x} - \mathbf{x}'|$, we see that the displacements decay as $|\mathbf{x} - \mathbf{x}'|^{-2}$. The dilatational strain e is given as

$$e = e_{ii} = u_{i,i}(\mathbf{x}) = PG_{ij,ji}(\mathbf{x} - \mathbf{x}'). \quad (5.1.3)$$

By combining eq. (5.1.1) with eqs (2.7.15) and (2.7.16) the interaction energy between a centre of dilatation or compression and another source of strain such as a dislocation D is

$$\mathcal{E}^D = \mp Pe_{ii}^D, \quad (5.1.4)$$

where e_{ii}^D is the dislocation dilatational strain evaluated at \mathbf{x}' . In addition, the mutual interaction energy between two centres A and B reads

$$\mathcal{E}^{AB} = (\pm P^A)(\pm P^B) G_{ij,ji}(\mathbf{x} - \mathbf{x}').$$

where $\mathbf{x} - \mathbf{x}'$ gives the separation between A and B . For an isotropic medium we can substitute eq. (2.4.21) for G_{ij} into eq. (5.1.2) and thereby derive the familiar properties of the infinite-body fields of compression or dilatation centres in isotropic media.⁽¹⁹⁾ One can easily show that in the isotropic case the displacement field is purely radial, i.e. there is no orientation dependence and, since eq. (2.4.21) gives $G_{ij,ji} \equiv 0$, we have that the dilatational strain e is zero (purely deviatoric stresses) and the mutual interaction energy \mathcal{E}^{AB} is zero. A centre of dilatation or compression is a point source of dilatational strain, because, even though the resultant field is dilatation-free, eq. (5.1.4) shows that the interaction with other defects D results from the dilatational (hydrostatic) part of the D field. In the case of anisotropy, none of the previous simplifications hold and, therefore, a distinct change in the intrinsic behaviour occurs. The displacements in anisotropic media need not be purely radial and, in fact, in cubic crystals such as Cu, a centre of dilatation with dipoles along the cube axes (interstitial) will give rise to outward displacements along the {111} and {110} directions, but inward displacements along the {100} directions;^(26,123) the latter is not an obvious result. Furthermore, since $G_{ij,ji} \neq 0$ for anisotropy, the dilatational strain e and mutual interaction energy \mathcal{E}^{AB} need not be zero. In Fig. 5.1 we show the angular dependence of $G_{ij,ji}$ as computed by Barnett⁽²⁹⁾ for strain centres in Cu, where the dipoles lie along the cube axes. Lie and Koehler⁽²⁶⁾ give an extensive set of results for various features of the fields due to single dipoles and strain centres in cubic crystals; however, Barnett⁽²⁹⁾ has shown that their results may be inaccurate in some instances due to the differentiation of truncated Fourier series which were fitted to the computed values of G_{ij} (see Fig. 5.1). Using the method of Lie and Koehler,⁽²⁶⁾ Bullough *et al.*⁽¹²⁴⁾ have given the full three-dimensional form of G_{ij} for Cu; however, one should exercise caution when using these results to obtain derivatives. The earlier mentioned integral results in Chap. 2 for G_{ij} and its derivatives do not suffer from these disadvantages. (See also note added in proof on p. 81.)

When spherical symmetry can no longer be assumed, we can modify the results for compression or dilatation centres and make the three force dipoles (Fig. 2.10) of unequal strength. If we let one of the dipoles be of strength $P + \Delta P$, while the other two are of strength P , we obtain a model of a defect possessing tetragonal symmetry. This kind of simple dipole model could be applied to, say, dumbbell interstitials in face-centered cubic crystals or single interstitials in body-centered cubic crystals such as C in Fe. If the dipole of strength $P + \Delta P$ lies along the x_3 axis, superposing the additional ΔP field on the symmetric field gives

$$P_{sj} = \pm(P\delta_{sj} + \Delta P\delta_{s3}\delta_{j3}) \quad (5.1.5)$$

and the displacements read

$$u_i(\mathbf{x}) = \mp(PG_{ij,j}(\mathbf{x} - \mathbf{x}') + \Delta PG_{i3,3}(\mathbf{x} - \mathbf{x}')). \quad (5.1.6)$$

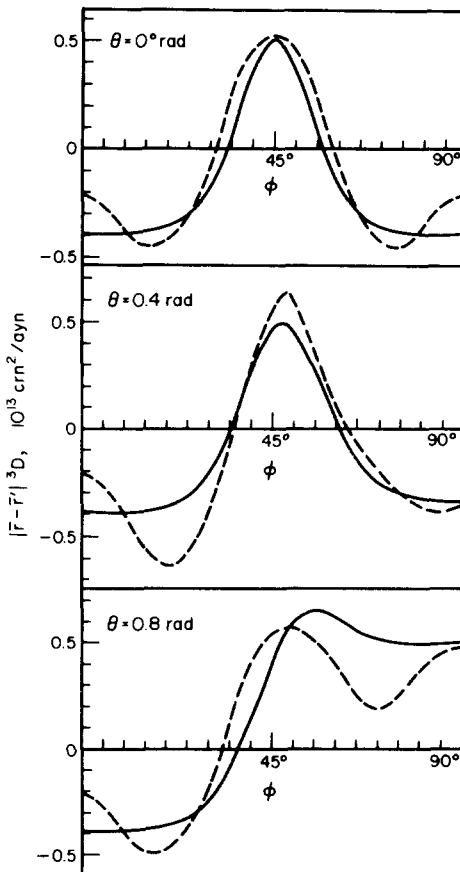


FIG. 5.1. Angular dependence of $D = G_{ij,ii}$ for compression or dilatation centres in Cu. The dipoles are oriented along the cube directions and the angles ϕ and θ are the angular spherical polar coordinates with respect to the cube axes. Solid line: Barnett,⁽²⁹⁾ broken line: Lie and Koehler.⁽²⁶⁾

In the case of isotropy, the properties of this field can be readily investigated by substituting eq. (2.4.21) for G_{ij} into the previous equation for $u_i(\mathbf{x})$. As is well known,^(125,19) the addition of tetragonal symmetry through the ΔP field causes a significant change from the original spherically symmetric field. (Bacon⁽¹²⁶⁾ has given an estimate of the values of P and ΔP for C in Fe.) The tetragonal defect field is not purely radial; it has a dilatational component e and the mutual interaction energy ϵ^{AB} is not zero. Furthermore, the interaction with other defects D is

$$\epsilon^D = \mp(Pe_{ii}^D + \Delta Pe_{33}^D), \quad (5.1.7)$$

so that a non-zero interaction occurs even when the D field has no dilatational component; this latter feature can be important in point defect-dislocation interactions. Introducing the tetragonal symmetry thus compli-

cates even the isotropic results for the infinite-body field. Introducing anisotropy will further modify the results and, although the anisotropy is easily incorporated using the results of Chap. 2, detailed numerical evaluations have not been reported.

Up to this point, we have focussed attention primarily on the "misfit" nature of point defects, as they are described by force dipole arrangements. The misfit arises from the fact that the defect fits imperfectly into the host lattice site and, therefore, gives rise to additional "defect forces", whose magnitude is expressed by the constant dipole strength P . On the other hand, it is possible that the point defect fits perfectly into the lattice, but displays different elastic constants from the host medium, i.e. it is a region of inhomogeneity within the matrix. It is clear that many point defects (a vacancy, for example) could display a combination of both misfit and inhomogeneity properties. Later we will mention one means of dealing with inhomogeneity effects, which is accomplished by treating the point defects as finite elastic inclusions. Within the framework of the simpler dipole models, Kröner⁽¹²⁷⁾ has stressed the analogy between electrostatics and elasticity. In this context, a pure inhomogeneity would be represented by an "induced" dipole tensor P_{ij} , where P_{ij} is proportional to the existing small strains e_{ij} through a fourth-order elastic polarizability tensor χ_{ijkp} . Kröner develops certain concepts along these lines, including the analog of a Clausius-Mosotti formula for the elastostatic case, but explicit results are obtained only for isotropy.

It should be clear that the force dipole models lack any real information on the atomistic nature of point defects in crystals and, therefore, they should be applicable mainly to a description of the far field properties. In an effort to capture the discrete nature of point defects within the continuum approximation, Bullough *et al.*⁽¹²⁴⁾ proposed a model wherein an array of finitely-spaced, single point forces are arranged in a balanced fashion at the atom positions surrounding the defect centre. Such a point force array is shown schematically in Fig. 2.8 and has been discussed in Section 2.7. These finitely-spaced point force arrays were called "non-local" continuum models by the authors. The displacement field due to the point force array was given in eq. (2.7.3) as the multipole expansion

$$u_i(\mathbf{x}) = \sum_{n=0}^N \frac{(-1)^n}{n!} P_{s_1 \dots s_n j} G_{ij, s_1 \dots s_n} (\mathbf{x} - \mathbf{x}'),$$

where

$$P_{s_1 \dots s_n j} = \sum_{\alpha=1}^N F_j^\alpha a_{s_1}^\alpha \dots a_{s_n}^\alpha \quad (5.1.8)$$

and for the balanced distribution $P_i = 0$, $P_{ij} = P_{ji}$. Because of the finite spacings, the multipole tensors of higher order than dipole must be retained and it is these terms which must then account for the discrete nature of the defect. As was mentioned in Section 2.7, only the dipole

terms survive in the limit of the far field. Bullough *et al.* obtained results for a dipole force model (compression centre), a non-local second nearest neighbour force model and a harmonic lattice model for the case of a vacancy in Cu. The main results are shown in Fig. 5.2, which gives the angular factor in the displacement field at various atom neighbour positions around the defect for increasing distances r from the defect centre. If the medium is isotropic, this factor would be constant for the dipole model, as has already been mentioned, and would be asymptotic to a constant value in the remaining two models. The strong fluctuations evident in Fig. 5.2 are thus a direct manifestation of the complex effect of elastic anisotropy on the displacements. The results for the dipole and non-local force models approach each other in the limit of large r , as the multipole expansion formula indicates they must. The non-local force model gives a better representation of the near-field behaviour, although the simple dipole model yields acceptable results. Siems⁽⁵²⁾ has given a good discussion of the connection between the lattice models and the non-local force model and he develops a number of interesting results for isotropy. A notable feature of the non-local force model is that the mutual interaction energy \mathcal{E}^{AB} between two cubically symmetric force arrays in an isotropic medium (see eq. (2.7.16)) displays a $|x - x'|^{-5}$ dependence, which is in agreement with harmonic lattice models. If one recalls that the force dipole model gives $\mathcal{E}^{AB} = 0$ for this case and notes that the isotropic inhomogeneity mutual interaction displays a $|x - x'|^{-6}$ dependence,⁽¹⁹⁾ then it is clear that the discreteness introduces first order effects. Also note that a non-local force model was used to obtain some of the point defect-dislocation interaction results reviewed in Section 4.3.2.

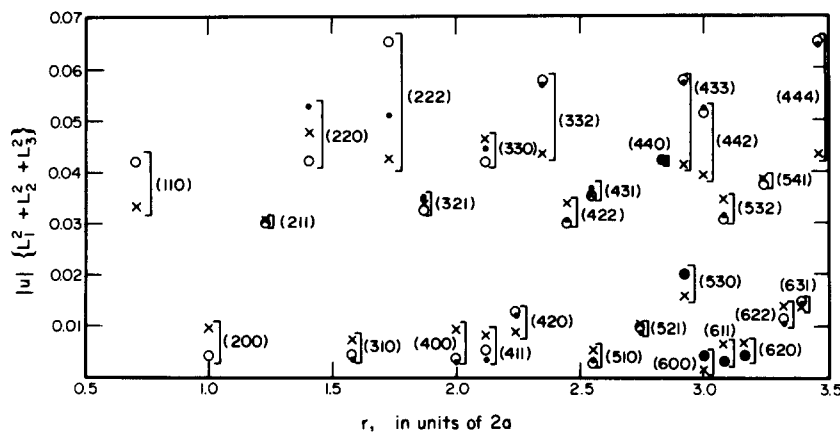


FIG. 5.2. The angular factor $|u|/(L_1^2 + L_2^2 + L_3^2)$ in the displacement u evaluated at the positions $(L_1, L_2, L_3) a$ around a vacancy in Cu. The displacement and distance r from the vacancy are in units of the cell size $2a$. O: dipole model, ●: second nearest neighbour non-local force model, ×: harmonic lattice model. All displacements are inward, except at the (200), (400) and (600) positions, which are outward.⁽¹²⁴⁾

Finally, as was already mentioned, models for point defects can be constructed using the transformation strain techniques discussed in Section 5.2 for finite elastic inclusions embedded in an infinite matrix. In this context, the point defect would be modelled as a finite, misfitting, spherical (or ellipsoidal) inclusion of atomic size in an infinite matrix of the same elastic material; the parameters describing the degree of misfit must be obtained from separate physical considerations. As will be shown in Section 5.2, the displacement or distortion field solution for a misfitting inclusion can be regarded as that due to a self-equilibrated distribution of body force and the Green's tensor G_{ij} again plays an important role in the description of the field quantities; when the inclusion is ellipsoidal, the field properties interior to the inclusion take a very simple form and in fact are uniform for a uniform transformation strain. The results of the inclusion models for point defects in isotropic media are well known and the details need not be repeated here.^(12,122) In the case of isotropy, the field due to a misfitting spherical inclusion having a uniform dilatational transformation strain corresponds exactly to that for a force dipole centre of compression or dilatation (Fig. 2.10) of appropriate strength P ; thus, all the earlier mentioned results for compression or dilatation centres hold for this special transformation strain model as well. For anisotropic bodies, this correspondence does not hold, except for the far field.⁽¹²⁸⁾ In Section 5.2, we review some results for uniform dilatational transformation strain inclusions of ellipsoidal shape in anisotropic media and the results are compared to the isotropic case.

The transformation strain solutions for homogeneous misfitting inclusions can also be applied to the case of inhomogeneous inclusions, i.e. inclusions with different elastic constants from the matrix; again, the parameters describing the degree of inhomogeneity must be obtained from separate physical considerations (bulk elastic constants are generally used). The details of the "equivalent inclusion" technique are outlined in Section 5.2 and this technique offers one of the most convenient methods available for treating the elastic interactions between inhomogeneities (foreign solute atoms, vacancies, etc.) and other sources of stress such as dislocations. An interesting application of these techniques in isotropic media is the so-called "induced" interaction between vacancies or interstitials (both of which may be regarded as elastic inhomogeneities) and a dislocation in the presence of an applied stress.⁽¹²⁹⁾ The interaction arises because the work done by the external tractions is modified by the combined presence of the point defects and the dislocation, and the transformation strain technique provides a convenient method for describing the rather complicated elastic interaction energy. As yet, the induced interaction has been investigated only in isotropic media.

We must remark here that the content of Section 5.2 deals with the elastic field inside an inclusion; this field is generally all that is needed for calculating self energy and the interaction energies with other sources

of stress such as dislocations. In some situations, however, the field exterior to the inclusion may be of interest as well, e.g. if one wishes to compute the mutual interaction ε^{AB} between two inclusions (point defects) in an anisotropic body. At the end of Section 2.7.3 we have outlined one method whereby the exterior field may be calculated for uniform transformation strain models in anisotropic media.

5.2. Inclusion Problems

One of the few soluble, fully three-dimensional elasticity problems is the "transformation strain" problem associated with an ellipsoidal inclusion or inhomogeneity treated by Eshelby.^(11,12) Eshelby's remarkable solution has found a wide range of applications in metallurgical circles and has been invaluable in the calculation of energy changes associated with phase transformations, thermal stresses and fracture instabilities. Eshelby considered the following two classes of problems:

- (i) the *transformation* problem: a region (the "inclusion") in an infinite homogeneous elastic medium undergoes a permanent change of form which, in the absence of the constraint imposed by its surroundings (the "matrix"), would be a prescribed uniform strain e_{ij}^T ; find the elastic field in both matrix and inclusion;
- (ii) the *inhomogeneity* problem: a region in an otherwise homogeneous elastic medium has elastic constants differing from those of its surroundings; find how an applied stress, uniform at large distances from the inhomogeneity, is disturbed by the inhomogeneity.

In isotropic elasticity for cases in which the inclusion or the inhomogeneity is an ellipsoid and the "matrix" is infinite in extent, Eshelby⁽¹²⁾ showed the final state of stress and strain inside the ellipsoid is uniform in both problems (i) and (ii). In fact, the solution to (i) can be used to construct very simply the solution to (ii); this method is Eshelby's "equivalent ellipsoidal inclusion technique" discussed in his 1961 monograph (p. 111). It would be impossible to give a detailed reproduction of Eshelby's enlightening analysis in this review. We shall try to give the salient features of the solution and remark on several extensions which have been made since the original analysis. The reader interested in exploiting Eshelby's results and the extensions is encouraged to refer to the articles cited in this section.

Consider problem (i), the transformation strain problem. Eshelby's formulation, which is valid for anisotropic media and an arbitrary compatible symmetric transformation strain e_{ij}^T , proceeds along the following lines. In the undeformed state carve out the "inclusion" so that it is no longer constrained by the surrounding infinite matrix and let it assume the stress-free compatible strain $e_{ij}^T(x)$ (which need not be uniform). At this stage both inclusion and matrix are stress-free, although the inclusion no longer

has its original size and shape. Now elastically strain the inclusion back to its original form by applying tractions $-\sigma_{ij}^T(\mathbf{x}) n_i(\mathbf{x})$ to its boundary and distributing body forces of magnitude $\partial\sigma_{ij}^T(\mathbf{x})/\partial x_i$ throughout its volume. \mathbf{n} is the unit outer normal to the external surface of the inclusion and σ_{ij}^T is the stress related to e_{ij}^T by Hooke's Law, i.e.

$$\sigma_{ij}^T(\mathbf{x}) = C_{ijkl} e_{kl}^T(\mathbf{x}). \quad (5.2.1)$$

At this stage the matrix is still undeformed, and the stress and elastic strain in the inclusion are $-\sigma_{ij}^T(\mathbf{x})$ and $-e_{ij}^T(\mathbf{x})$, respectively. The inclusion now fits back into the region it occupied before it was carved out from the undeformed medium, but it contains a layer of surface tractions distributed over its external boundary as well as a distribution of body forces over its volume. The discontinuity in surface traction across the matrix-inclusion interface and the body force distribution can be removed if both matrix and inclusion take on the displacement field $u_i^C(\mathbf{x})$ given by (see, for example, Asaro and Barnett^(5,6) or eq. (2.7.19))

$$u_i^C(\mathbf{x}) = \iiint_V \sigma_{kj}^T(\mathbf{x}') G_{ik,j'}(\mathbf{x} - \mathbf{x}') dV', \quad (5.2.2)$$

where $G_{ik}(\mathbf{x} - \mathbf{x}')$ is the elastic Green's function for the homogeneous infinite medium and the integral is over the volume of the inclusion. $u_i^C(\mathbf{x})$ is continuous across the inclusion-matrix interface.

The displacement gradients associated with eq. (5.2.2) are given by

$$u_{i,p}^C = - \iiint_V \sigma_{kj}^T(\mathbf{x}') G_{ik,j'p}(\mathbf{x} - \mathbf{x}') dV'. \quad (5.2.3)$$

The final states of stress and elastic strain in the transformed inclusion and the surrounding matrix are given by

$$\left. \begin{aligned} \sigma_{ij}^I &= \sigma_{ij}^C - \sigma_{ij}^T \\ e_{ij}^I &= e_{ij}^C - e_{ij}^T \end{aligned} \right\} \text{in the inclusion,} \quad (5.2.4)$$

$$\left. \begin{aligned} \sigma_{ij}^M &= \sigma_{ij}^C \\ e_{ij}^M &= e_{ij}^C \end{aligned} \right\} \text{in the matrix,} \quad (5.2.5)$$

where the superscripts I and M refer to inclusion and matrix, respectively, and e_{ij}^C and σ_{ij}^C are the strains and stresses derived from eq. (5.2.3). e_{ij}^C and σ_{ij}^C are discontinuous across the inclusion-matrix interface, but the displacements associated with and the tractions given by eqs (5.2.4) and (5.2.5) are continuous across the inclusion-matrix interface.

The strain energy associated with the transformation strain problem is merely^(1,2)

$$\mathcal{E}^T = - \frac{1}{2} \iiint_V \sigma_{ij}^I e_{ij}^T dV, \quad (5.2.6)$$

where the integral is over the volume of the inclusion, so that \mathcal{E}^T may

be computed solely from a knowledge of the stress state inside the inclusion and the transformation strain. If the transformation occurs in the presence of an external applied stress state $\sigma_{ij}^A(x)$, there is an additional "interaction energy" induced which is given by^(1,2)

$$\delta^{INT} = - \iiint_V \sigma_{ij}^A e_{ij}^T dV, \quad (5.2.7)$$

where, again, the integral is over the inclusion. The A -field may be due to either externally applied loads or another internal defect separate from the inclusion. The effect of the applied stress state is to induce continuous fields σ_{ij}^A, e_{ij}^A in both matrix and inclusion in addition to the fields given by eqs (5.2.4) and (5.2.5).

If we consider the case in which the transformation strain $e_{ij}^T(x)$ is a polynomial in x_m of degree M and the inclusion V is an ellipsoid, then the following theorem (the "polynomial" theorem) may be proved.^(5,6)

"If an ellipsoidal region in an infinite, anisotropic, linear elastic medium undergoes, in the absence of its surroundings, a stress-free transformation strain which is a polynomial of degree M in the position coordinates x_m , then the final stress and strain state inside the transformed inclusion, when constrained by its surroundings, is also a polynomial of degree M in x_m ".

For $M = 0$, e_{ij}^T is uniform and so is the final state of stress and strain in the ellipsoid. This is the result deduced by Eshelby⁽¹¹⁾ (p. 384) for isotropic and anisotropic media and by Walpole^(12,8) and Kinoshita and Mura^(13,0) for anisotropic media. In fact, Eshelby⁽¹²⁾ deduced the "polynomial theorem" stated above for isotropic materials. The ellipsoid is a sufficiently general shape and a polynomial form $e_{ij}^T(x)$ is a sufficiently general transformation strain that the theorem allows one to investigate many problems of practical significance. For example, the transformation $e_{ij}^T(x)$ may arise from the misfit introduced when an ellipsoidal precipitate nucleates during a solid state phase transformation. If the ellipsoidal region has thermal expansion coefficients α_{ij}^I differing from those of the matrix, α_{ij}^M , the transformation strain associated with a uniform temperature change, ΔT , of the entire medium is merely

$$e_{ij}^T = (\alpha_{ij}^I - \alpha_{ij}^M) \Delta T.$$

For $M = 0$ (e_{ij}^T uniform) the constrained strains e_{ip}^C inside the ellipsoidal inclusion are constant and are given by

$$e_{ip}^C = D_{ipkj} \sigma_{kj}^T, \quad (5.2.8)$$

where the D_{ipkj} are constants given by^(5,6)

$$D_{ipkj} = \frac{a_1 a_2 a_3}{8\pi} \iint_{|z|=1} \frac{\{z_p z_j (zz)_{ik}^{-1} + z_i z_j (zz)_{pk}^{-1}\}}{\{a_1^2 z_1^2 + a_2^2 z_2^2 + a_3^2 z_3^2\}^{3/2}} dS; \quad (5.2.9)$$

a_1, a_2, a_3 are the lengths of the semi-major axes of the ellipsoid and

the integral is over the unit sphere, i.e. in spherical polar coordinates,

$$dS = \sin \varphi d\varphi d\theta.$$

\mathbf{z} is a unit vector whose components along the three semi-major axes of the ellipsoid are given by

$$z_1 = \sin \varphi \cos \theta,$$

$$z_2 = \sin \varphi \sin \theta,$$

$$z_3 = \cos \varphi$$

and $(zz)^{-1}$ is the inverse of (zz) , which is defined by the usual relation

$$(zz)_{jk} = z_i C_{ijkm} z_m. \quad (5.2.10)$$

Eshelby has given a relation similar to eq. (5.2.8) for isotropic media; he relates e_{ip}^C to e_{kj}^T rather than σ_{kj}^T . For isotropy eq. (5.2.9) reduces to elliptic integrals; Kneer⁽¹³¹⁾ has numerically evaluated formulae similar to eq. (5.2.9) for spherical inclusions in cubic and hexagonal metals. Equation (5.2.9) is easily evaluated by numerical integration for any medium and any ellipsoid.

From eq. (5.2.9) it is clear that D_{ipkj} is symmetric in i and p ; furthermore, eq. (5.2.8) shows that we are interested only in the part of D_{ipkj} , which is symmetric in k and j , since σ_{kj}^T is a symmetric tensor. Thus, we may also write

$$e_{ip}^C = \bar{D}_{ipkj} \sigma_{kj}^T \quad (5.2.11)$$

where

$$\bar{D}_{ipkj} = \frac{1}{2}(D_{ipkj} + D_{ipjk}). \quad (5.2.12)$$

Since (zz) and $(zz)^{-1}$ are symmetric matrices, one may easily verify that D_{ipkj} possesses the same symmetry properties as an elastic constant tensor, namely

$$\bar{D}_{ipkj} = \bar{D}_{pikj} = \bar{D}_{ipjk} = \bar{D}_{kji p}. \quad (5.2.13)$$

Thus, \mathbf{D} is probably better suited for computational work than is \mathbf{D} , particularly for computations which require the inverse of the tensor \mathbf{D} .

Walpole⁽¹²⁸⁾ and Kinoshita and Mura⁽¹³⁰⁾ have shown how one can obtain a closed form solution for D_{ipkj} when the ellipsoid is a disc, i.e. when $a_3 \rightarrow 0$. In this instance the denominator explicitly shown in the integrand in eq. (5.2.9) has a delta function character and eq. (5.2.9) reduces to

$$D_{ipkj}(\text{DISC}) = t_p t_j (tt)_{ik}^{-1} + t_i t_j (tt)_{pk}^{-1}, \quad (5.2.14)$$

where \mathbf{t} is the unit vector normal to the plane of the disc. All quantities in eq. (5.2.14) are known *explicitly*.

For an elliptical cylinder ($a_3 \rightarrow \infty$) one may deduce that

$$D_{ipkj}(\text{CYLINDER}) = \frac{a_1 a_2}{4\pi} \int_0^{2\pi} d\theta \frac{\{T_p T_j (TT)_{ik}^{-1} + T_i T_j (TT)_{pk}^{-1}\}}{\{a_1^2 \cos^2 \theta + a_2^2 \sin^2 \theta\}}, \quad (5.2.15)$$

where \mathbf{T} is a unit vector normal to the cylinder axis such that its components along the semi-major axes of the elliptical cross-section are

$$T_1 = \cos \theta; T_2 = \sin \theta.$$

For a spherical inclusion eq. (5.2.9) reduces to

$$D_{ipkj}(\text{SPHERE}) = \frac{1}{8\pi} \oint_{|z|=1} \{z_p z_j (zz)_{ik}^{-1} + z_i z_j (zz)_{pk}^{-1}\} dS, \quad (5.2.16)$$

which is similar in form to a related tensor whose elements were evaluated numerically for cubic and hexagonal media by Kneer.⁽¹³¹⁾

If one considers the polynomial theorem for $M = 1$, so that

$$\sigma_{kj}^T(x) = A_{kjm} x_m,$$

a result similar to eq. (5.2.8) may be obtained. Asaro and Barnett⁽⁵⁶⁾ have given an integral representation of the appropriate connection coefficients D_{ipkj} corresponding to $M = 1$.

The previous results have been obtained assuming that the ellipsoidal inclusion has the same elastic constants as the infinite matrix in which it is imbedded. Eshelby⁽¹²⁾ has shown how the transformation strain problem associated with an ellipsoid whose elastic constants differ from those of the matrix may be easily obtained when the transformation strain is uniform. We first solve the problem for a constant transformation strain e_{ij}^T and an ellipsoid E with elastic constants C_{ijkm} identical to those of the matrix. Consider a second ellipsoid E^* with elastic constants C_{ijkm}^* , which initially is identical to E in shape and size. Let E^* undergo a uniform stress-free strain e_{ij}^{T*} and then apply surface tractions to E^* so as to produce an interior elastic strain $e_{ij}^C - e_{ij}^{T*}$, where e_{ij}^C is constant and is related to e_{ij}^T by eq. (5.2.8). E^* is now identical in shape and size to the transformed ellipsoid E in its final state. If E^* happens to be in the same stress state as E , E may be replaced by E^* without upsetting continuity in tractions and displacement across the matrix-inclusion interface. This is always possible if inside the ellipsoid E

$$\sigma_{ij}^T = C_{ijkm}^*(e_{km}^C - e_{km}^{T*}),$$

i.e. if

$$C_{ijkm}(e_{km}^C - e_{km}^T) = C_{ijkm}^*(e_{km}^C - e_{km}^{T*}). \quad (5.2.17)$$

Since e_{km}^C is related to σ_{kj}^T (and thus e_{kj}^T) by eq. (5.2.8), eq. (5.2.17) represents six algebraic equations for e_{km}^T in terms of e_{km}^{T*} (which would be known

or prescribed). Equation (5.2.17) may be written in the form

$$\begin{aligned} \{C_{ijkm} - C_{ijkm}^*\}\bar{D}_{kmrs} - \frac{1}{2}(\delta_{ir}\delta_{js} + \delta_{is}\delta_{jr})\sigma_{rs}^T \\ = -C_{ijkm}^*e_{km}^{T*} = -\sigma_{ij}^{T*}, \end{aligned} \quad (5.2.18)$$

where σ_{rs}^T and \bar{D}_{kmrs} are calculated from eqs (5.2.1) and (5.2.12) using the matrix elastic constants C_{ijkm} . Equation (5.2.18) is easily solved for σ_{rs}^T using matrix inversion and e_{ij}^T is obtained from

$$e_{ij}^T = S_{ijkm}\sigma_{km}^T,$$

where the compliances S_{ijkm} satisfy

$$C_{ijkm}S_{kmrs} = \frac{1}{2}(\delta_{ir}\delta_{js} + \delta_{is}\delta_{jr}). \quad (5.2.19)$$

The strain energy associated with the transforming inhomogeneity E^* is given by eq. (5.2.6) with e_{ij}^T replaced by e_{ij}^{T*} . As Eshelby⁽¹²⁾ notes, this technique is applicable for a constant e_{ij}^{T*} , since the final stress and strain state in both E and E^* is uniform. The polynomial theorem indicates that the replacement of E by E^* is always possible for any transformation strain e_{ij}^{T*} which is a polynomial of degree M in x_m , since e_{ij}^C and e_{ij}^T will also be polynomials of degree M inside the ellipsoid.

If the final stress state in the transformed, homogeneous, ellipsoidal inclusion is hydrostatic pressure, i.e. if

$$\sigma_{ij}^T = -p\delta_{ij},$$

the transformation strain solution corresponds to the problem of an ellipsoidal cavity containing a fluid (at pressure p) in a matrix with no far-field stresses. The appropriate transformation strain e_{ij}^T is chosen as the solution to

$$C_{ijkm}(e_{km}^C - e_{km}^T) = -p\delta_{ij}$$

or

$$\{C_{ijkm}\bar{D}_{kmrs} - \frac{1}{2}(\delta_{ir}\delta_{js} + \delta_{is}\delta_{jr})\}\sigma_{rs}^T = -p\delta_{ij}. \quad (5.2.20)$$

which is easily solved by matrix inversion.

If the transformation strain occurs in the presence of a uniform applied stress σ_{ij}^A , the final state of stress in the homogeneous transformed ellipsoid is

$$\sigma_{ij}^T = C_{ijkm}(e_{ij}^C - e_{ij}^T) + \sigma_{ij}^A. \quad (5.2.21)$$

We can make σ_{ij}^T vanish identically by choosing e_{ij}^T so that σ_{rs}^T satisfies eq. (5.2.20) with $-p\delta_{ij}$ replaced by $-\sigma_{ij}^A$. This solution then corresponds to the problem of an ellipsoidal cavity in an infinite matrix subjected to the uniform far-field stress σ_{ij}^A . Using eqs (5.2.6) and (5.2.7), the decrease in total energy of deformation when the cavity forms in the presence of

the uniform stress σ_{ij}^A is⁽¹²⁾

$$\varepsilon^A = -\frac{1}{2}\sigma_{ij}^A e_{ij}^T V, \quad (5.2.22)$$

where V is the cavity volume. ε^A is a quantity of considerable interest in linear elastic fracture mechanics. If we consider an applied stress state $\sigma_{ij}^A = E_{ijk}x_k$, we may use the same method to force σ_{ij}^I to vanish everywhere inside the ellipsoid (e_{ij}^T and e_{ij}^C will be linear functions of x_k due to the polynomial theorem); one then has constructed the solution for an ellipsoidal cavity in a medium subjected to far-field bending and torsion.

Finally, problem (ii), Eshelby's "inhomogeneity problem" is easily soluble when the inhomogeneity is an ellipsoid with elastic constants C_{ijkm}^* . Consider an homogeneous ellipsoid E with elastic constants C_{ijkm} identical to those of its infinite surrounding matrix. Let E undergo a stress-free uniform strain e_{ij}^T . If the transformation occurs in the presence of a uniform stress σ_{ij}^A , the final stress and elastic strain states inside E are

$$e_{ij}^I = e_{ij}^C - e_{ij}^T + e_{ij}^A, \quad (5.2.23a)$$

$$\sigma_{ij}^I = C_{ijkm}(e_{ij}^C - e_{ij}^T) + \sigma_{ij}^A, \quad (5.2.23b)$$

where

$$e_{ij}^A = S_{ijkm}\sigma_{km}^A.$$

The total strain within the transformed inclusion E is given by eq. (5.2.23a) and the stress-free (plastic) strain e_{ij}^T , i.e. the total strain within E is $e_{ij}^C + e_{ij}^A$. Now consider the ellipsoid E^* , which is identical to E in shape and size and whose elastic constants are C_{ijkm}^* . Give E^* the uniform elastic strain $e_{ij}^C + e_{ij}^A$, so that the corresponding stress state within E^* is

$$\sigma_{ij}^{I*} = C_{ijkm}^*(e_{km}^C + e_{km}^A). \quad (5.2.24)$$

In this deformed state E^* has the same shape and size as the transformed ellipsoid E , since both have acquired the same total strain, namely, $e_{ij}^C + e_{ij}^A$. If we pick e_{ij}^T so that $\sigma_{ij}^{I*} = \sigma_{ij}^I$, we may replace E by E^* without disturbing continuity in displacements and tractions across the matrix-inclusion interface. This condition is satisfied if e_{ij}^T is a solution to

$$C_{ijkm}(e_{km}^C - e_{km}^T) + \sigma_{ij}^A = C_{ijkm}^*(e_{km}^C + e_{km}^A), \quad (5.2.25)$$

which may be rewritten in the form

$$\begin{aligned} & \{(C_{ijkm} - C_{ijkm}^*)\bar{D}_{kmrs} - \frac{1}{2}(\delta_{ir}\delta_{js} + \delta_{is}\delta_{jr})\}\sigma_{rs}^T \\ & = (C_{ijkm}^* - C_{ijkm})e_{km}^A. \end{aligned} \quad (5.2.26)$$

σ_{rs}^T (and, hence, e_{rs}^T) is easily obtained from eq. (5.2.26) by matrix inversion. We remark that in computing \bar{D}_{kmrs} , one uses the elastic constants C_{ijkm} . The solution thus generated solves the problem of an ellipsoidal inhomogeneity perturbing a prescribed uniform far-field stress state.

The same method suffices to solve the problem of an ellipsoidal inhomogeneity

geneity perturbing a prescribed far-field stress state which is a polynomial of degree M in x_m ; the polynomial theorem guarantees that eq. (5.2.25) can still be satisfied at every point within E and E^* since σ_{ij}^A , e_{ij}^C and e_{ij}^T will be polynomials of degree M in x_m .

The utility of the Eshelby solution for the transformation strain problem is apparent from eqs (5.2.6) and (5.2.7). The energy of deformation is determined solely from a knowledge of the stress and strain state within the inclusion. For an ellipsoid and a polynomial transformation strain, the interior elastic state is a simple one. The elastic state exterior to the ellipsoid is quite complex, but, in most metallurgical applications, the exterior solution is never needed. We remark that outside the inclusion the constrained strains e_{ij}^C are also given by eq. (5.2.8) when e_{ij}^T is uniform; however, outside the inclusion the connection coefficients D_{ipkj} are complex functions of position.

Space limitations do not permit a more extensive referencing of the literature associated with this interesting class of problems. The interested reader is referred to the bibliography given in Eshelby⁽¹²⁾ and Sternberg.⁽¹³²⁾

An interesting application of the analyses associated with Eshelby's transformation strain problem has been presented by Lee *et al.*⁽¹³³⁾ These authors considered the strain energy associated with transformed precipitates of ellipsoidal shape (ellipsoids of revolution) in metal matrices of cubic symmetry as a function of the ellipsoid aspect ratio β . The transformation strain was taken to be a pure dilatation (i.e. $e_{ij}^{T*} = \epsilon \delta_{ij}$); precipitates of cubic, tetragonal and hexagonal symmetry were considered for the seven orientations listed in the Table 5.1.

Figures 5.3 and 5.4 depict results for the normalized strain energy per unit volume of precipitate, W/W_0 , as a function of aspect ratio β for niobium and tin precipitates in a copper matrix for the seven orientations listed in the table. W_0 is the strain energy per unit volume of precipitate as predicted by homogeneous, isotropic, elasticity theory, namely

$$W_0 = 2\mu \frac{1 + v}{1 - v} \epsilon^2,$$

Table 5.1. Orientation Relationships Examined

No.	a	Ellipsoid axes		
		b	c	
1	[100] <i>m</i> [100] <i>i</i>	[010] <i>m</i> [010] <i>i</i>	[001] <i>m</i> [001] <i>i</i>	
2	[101] <i>m</i> [100] <i>i</i>	[121] <i>m</i> [010] <i>i</i>	[111] <i>m</i> [001] <i>i</i>	
3	[121] <i>m</i> [010] <i>i</i>	[111] <i>m</i> [001] <i>i</i>	[101] <i>m</i> [100] <i>i</i>	
4	[101] <i>m</i> [111] <i>i</i>	[121] <i>m</i> [101] <i>i</i>	[111] <i>m</i> [121] <i>i</i>	
5	[121] <i>m</i> [101] <i>i</i>	[111] <i>m</i> [121] <i>i</i>	[101] <i>m</i> [111] <i>i</i>	
6	[101] <i>m</i> [101] <i>i</i>	[121] <i>m</i> [121] <i>i</i>	[111] <i>m</i> [111] <i>i</i>	
7	[101] <i>m</i> [332] <i>i</i>	[121] <i>m</i> [113] <i>i</i>	[111] <i>m</i> [110] <i>i</i>	

m = matrix phase.

i = ellipsoidal precipitate phase.

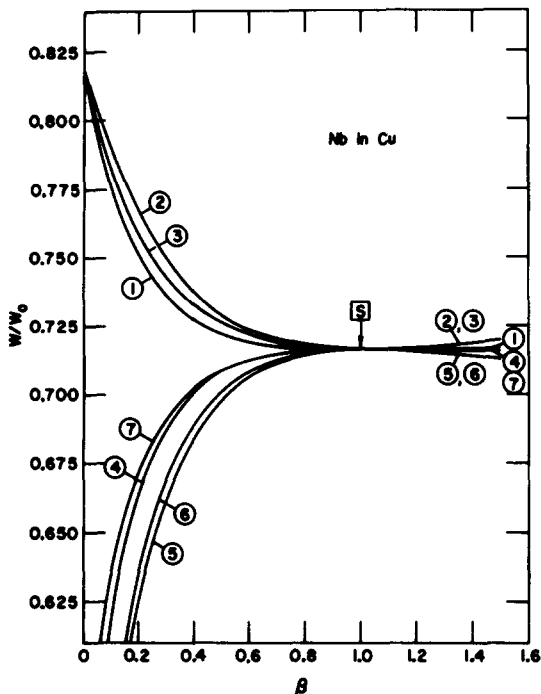


FIG. 5.3. Normalized strain energy of a Nb precipitate in a Cu matrix vs. aspect ratio.⁽¹³³⁾

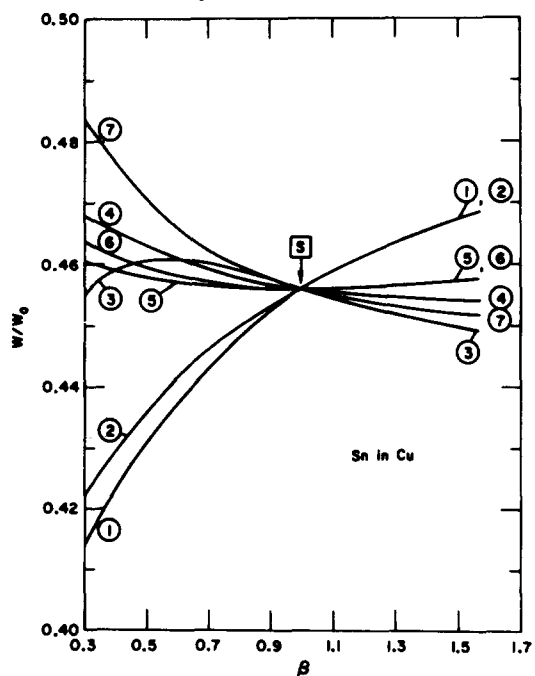


FIG. 5.4. Normalized strain energy of a Sn precipitate in a Cu matrix vs. aspect ratio.⁽¹³³⁾

$$\mu = C_{44}, \nu = \frac{C_{12}}{2(C_{12} + C_{44})}$$

and the elastic constants are taken to be those of the matrix. The results for niobium precipitates are typical of those obtained for precipitates of cubic symmetry, i.e. a spherical precipitate ($\beta = 1$) always yields an extremum (either a maximum or a minimum) in the W/W_0 vs. β curve. This is not the case for tin precipitates and this body of results indicates that elastic anisotropy can have a marked influence on the morphology and crystallographic orientations (of the precipitate relative to the matrix) associated with solid-state phase transformations.

5.3. Fracture Mechanics

Fracture mechanics, the contemporary theory of instabilities associated with crack propagation, is a branch of applied mathematics with an extensive literature of its own. We shall give only a brief discussion of the fracture mechanics of slit-cracks in anisotropic linear elastic solids insofar as it relates to the formalisms we have developed for straight dislocations. Bilby and Eshelby⁽¹³⁴⁾ and Rice⁽¹³⁵⁾ have presented excellent in-depth treatments of modern fracture mechanics from the points of view of both dislocation mechanics and more conventional applied mechanics.

Consider the plane problem of an infinite, anisotropic, linear elastic medium containing a slit-like crack of length $2c$ (Fig. 5.5). The unit inner normal to the upper crack face is n , the crack fronts are parallel to the unit vector t and the unit normal to the leading crack edge is $m = n \wedge t$. The stress field far from the crack is a uniform applied stress state σ_{ij}^A and the upper and lower crack faces are loaded by equal and opposite self-equilibrating tractions R_i . The crack is the region $n \cdot x = 0$, $-c \leq m \cdot x \leq c$ and the tractions R_i are arbitrary functions of $s = m \cdot x$

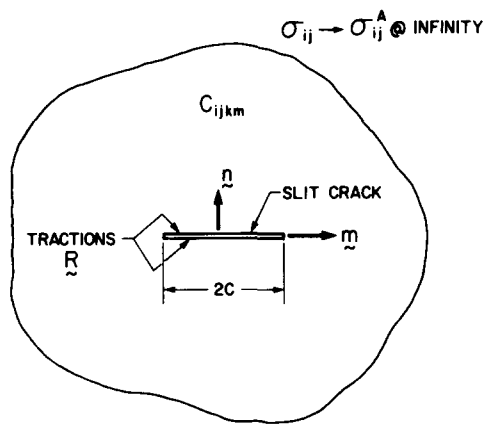


FIG. 5.5 A slit-crack of length $2c$ in an infinite anisotropic medium.

only. Since the crack is infinitely long in the direction parallel to \mathbf{t} , the problem is one of plane elastostatics and may be treated using the formalism developed in Chap. 3 and 4. This problem has been investigated by Stroh,⁽⁵⁾ Heald⁽¹³⁶⁾ and Barnett and Asaro⁽¹³⁷⁾ using dislocation methods. We shall develop the method of Barnett and Asaro⁽¹³⁷⁾ because of its close relation to the dislocation formalism presented in Chap. 4.

Bilby and Eshelby⁽¹³⁴⁾ have shown that, in general, the solution to this problem may be written as the sum of two fields, an "A" field due to the uniform applied stress σ_{ij}^A and a "D" field due to some arrangement of infinite straight dislocations parallel to \mathbf{t} and distributed over the region occupied by the slit crack. Thus,

$$\begin{aligned} u_i &= u_i^A + u_i^D, \\ v_{ij} &= v_{ij}^A + v_{ij}^D, \\ \sigma_{ij} &= \sigma_{ij}^A + \sigma_{ij}^D. \end{aligned} \quad (5.3.1)$$

Since the "A" fields and the fields of any single straight dislocation are admissible solutions to the compatibility and equilibrium equations of elasticity theory, and since the stress field of a single dislocation vanishes in the far field, we can guarantee that eq. (5.3.1) is the required solution by arranging to distribute the dislocations so as to satisfy the traction conditions on the crack faces. This requires that on $\mathbf{n} \cdot \mathbf{x} = 0$

$$\sigma_{ij} n_i = -R_i(s = \mathbf{m} \cdot \mathbf{x}) = (\sigma_{ij}^A + \sigma_{ij}^D) n_i; |s| \leq c. \quad (5.3.2)$$

Now on $\mathbf{n} \cdot \mathbf{x} = 0$ eq. (4.1.22) shows that the in-plane tractions at s due to a *single* straight dislocation of Burgers vector \mathbf{b} located at $\mathbf{n} \cdot \mathbf{x} = 0$, $\mathbf{m} \cdot \mathbf{x} = y$ are given by

$$\sigma_{ij} n_i = \frac{2}{s - y} B_{ji} b_i. \quad (5.3.3)$$

Thus, for Burgers vectors $b_i(y)$ distributed over $|s| < c$, on $\mathbf{n} \cdot \mathbf{x} = 0$

$$\sigma_{ij}^D n_i = 2B_{ji} \int_{-c}^c \frac{b_i(y) dy}{s - y}. \quad (5.3.4)$$

Calling

$$\sigma_{ij}^A n_i = T_i^A, \quad (5.3.5)$$

where T^A is the traction induced on $\mathbf{n} \cdot \mathbf{x} = 0$ by the applied stresses, the boundary condition eq. (5.3.2) may be recast as the singular integral equation

$$\int_{-c}^c \frac{b_i(y) dy}{s - y} = -\frac{1}{2} B_{im}^{-1} \{ T_m^A + R_m(s) \}; |s| \leq c. \quad (5.3.6)$$

The singular integral in eq. (5.3.6) is defined by its Cauchy principal value,⁽¹³⁴⁾ as are all singular integrals discussed in this section.

The singular integral equation is easily solved for $b_i(y)$ once one specifies how the solution should behave as $s \rightarrow \pm c$. If there is no displacement discontinuity across the crack faces at $s = \pm c$ (i.e. if there is no net dislocation content within the crack) then

$$\int_{-c}^c b_i(y) dy = 0. \quad (5.3.7)$$

For cracks with stress singularities at $s = \pm c$, the appropriate solution to eq. (5.3.6) satisfying eq. (5.3.7) is

$$b_i(y) = B_{im}^{-1} \left\{ \frac{T_m^A y}{\pi(c^2 - y^2)^{1/2}} - \frac{1}{\pi^2(c^2 - y^2)^{1/2}} \int_{-c}^c \frac{R_m(s)(c^2 - s^2)^{1/2} ds}{s - y} \right\}. \quad (5.3.8)$$

For "equilibrium cracks"⁽¹³⁸⁾ which have no associated stress singularities,

$$b_i(y) = -\frac{1}{\pi^2} B_{im}^{-1} (c^2 - y^2)^{1/2} \int_{-c}^c \frac{R_m(s) ds}{(c^2 - s^2)^{1/2}(s - y)} \quad (5.3.9)$$

provided that the subsidiary condition

$$\int_{-c}^c \frac{R_m(s) ds}{(c^2 - s^2)^{1/2}} = -\pi T_i^A \quad (5.3.10)$$

is satisfied. Equation (5.3.10) determines the length of the "equilibrium crack" as a function of the loading state.

Equations (5.3.8) and (5.3.9) show that the quantity $B_{mi}b_i(y)$ depends only on c , T^A and R , but does not depend on the elastic constants (i.e. the anisotropy) of the medium. Since the tractions in the crack plane ahead of the crack are calculated from eq. (5.3.4) with $|s| > c$, the tractions and stress concentrations in the crack plane ahead of the crack depend only on c , T^A and R and are *independent* of C_{ijkm} . This result was first deduced by Stroh.⁽⁵⁾

The stress intensity factor vector \mathbf{k} is defined by considering the crack plane tractions near the crack tips and is given by

$$k_j(s = \pm c) = \lim_{\begin{array}{l} \mathbf{m} \cdot \mathbf{x} \rightarrow \pm c \\ \mathbf{n} \cdot \mathbf{x} = 0 \end{array}} \sigma_{ij} n_i (2\pi r)^{1/2},$$

where $r = |\mathbf{m} \cdot \mathbf{x}| - c$. For equilibrium cracks $\mathbf{k} = 0$; otherwise⁽¹³⁷⁾

$$k_i(\pm c) = T_i^A (\pi c)^{1/2} + (\pi c)^{-1/2} \int_{-c}^c R_i(s) \left\{ \frac{c \pm s}{c \mp s} \right\}^{1/2} ds. \quad (5.3.11)$$

Thus \mathbf{k} is independent of C_{ijkm} and material anisotropy. i.e. the stress intensity factors are the same as those computed in isotropic elasticity. The complete stress field about the slit-like crack has been given by Sоловьев⁽¹³⁹⁾ using the Stroh⁽⁸⁾ sextic formalism.

If we consider the extension of one edge of the crack by an amount dc , Barnett and Asaro⁽¹³⁷⁾ have shown that the crack extension force G is given by

$$G = -\frac{dE}{dc} = \frac{1}{8\pi} k_i k_m B_{im}^{-1}, \quad (5.3.12)$$

where E is the total energy of deformation of the stressed cracked solid. The Griffith criterion for brittle fracture is $G = 2\gamma$, where γ is the specific surface energy for the plane $\mathbf{n} \cdot \mathbf{x} = 0$. The crack extension force depends on anisotropy only through the matrix B^{-1} , which is essentially the inverse of the pre-logarithmic energy factor matrix for a straight dislocation parallel to the crack front. The formalism of Chap. 3 indicates that B^{-1} is independent of the direction of the crack front, \mathbf{m} , in the plane of the problem.

For isotropic media with the x_3 direction parallel to \mathbf{t}

$$B_{11}^{-1} = B_{22}^{-1} = \frac{4\pi(1-v)}{\mu}; B_{33}^{-1} = \frac{4\pi}{\mu},$$

so that the well-known isotropic Griffith fracture criterion deduced from eq. (5.3.12) is

$$(k_1^2 + k_2^2)(1-v) + k_3^2 = 4\mu\gamma.$$

Sinclair and Hirth⁽¹⁴⁰⁾ have used the method described above to study the interaction of a crack and a line of force in an anisotropic solid. Asaro⁽¹⁴¹⁾ has studied the interaction between a semi-infinite, freely-slipping slit-crack ($\mathbf{T}^A = 0; \mathbf{R} = 0$) and a straight dislocation, whose polar coordinates relative to the crack tip are (r, θ) . Asaro reports the interesting result that in a general anisotropic medium the image force on the dislocation in the radial direction induced by the crack-dislocation interaction is merely

$$F_r = -\frac{B_{ij} b_i b_j}{r} = -\frac{E}{r}, \quad (5.3.13)$$

where E is the pre-logarithmic energy factor for the dislocation in the uncracked solid. F_r is *independent* of θ , a result which is intimately related to the image force results discussed in Section 4.3. Rice and Thomson⁽¹⁴²⁾ derived eq. (5.3.13) for isotropic media. Data for E to be used in eq. (5.3.13) have been presented in Section 4.1.3 for the common cubic and hexagonal metals.

Willis⁽¹¹⁵⁾ and Clements⁽¹¹⁴⁾ have treated the slit-crack along the interface between two dissimilar anisotropic half-spaces. Willis' most elegant analysis even accounts for an interfacial crack moving with a uniform velocity.

5.4. Line Force Solutions in Infinite Media

In Chap. 4 the displacement field solution for a line of force of uniform strength f per unit length was given in the Stroh representation as (see eq. 4.1.13)

$$u_i = -\frac{1}{2\pi i} \sum_{z=1}^6 \pm A_{iz} A_{sz} f_s \ln (\mathbf{m} \cdot \mathbf{x} + p_z \mathbf{n} \cdot \mathbf{x}). \quad (5.4.1)$$

The line of force is parallel to $\mathbf{t} = \mathbf{m} \wedge \mathbf{n}$. The associated displacement gradients are

$$u_{i,p} = -\frac{1}{2\pi i} \sum_{z=1}^6 \pm A_{iz} A_{sz} f_s \frac{m_p + p_z n_p}{\mathbf{m} \cdot \mathbf{x} + p_z \mathbf{n} \cdot \mathbf{x}}. \quad (5.4.2)$$

We now resort to the same method used to deduce the displacement gradients in the “integral representation”, namely, we choose \mathbf{m} and \mathbf{n} such that $\mathbf{m} \cdot \mathbf{x} = |\mathbf{x}|$, $\mathbf{n} \cdot \mathbf{x} = 0$. Equation (5.4.2) may be written in the form

$$u_{i,p} = -(2\pi i |\mathbf{x}|)^{-1} f_s \left\{ m_p \sum_{z=1}^6 \pm A_{iz} A_{sz} + n_p \sum_{z=1}^6 \pm p_z A_{iz} A_{sz} \right\}. \quad (5.4.3)$$

Using eq. (3.6.4) and the sum rule eq. (3.6.25), the expression for the displacement gradients becomes

$$\begin{aligned} u_{i,p} &= (2\pi |\mathbf{x}|)^{-1} f_s \{ m_p Q_{is} \\ &\quad - n_p (nn)_{ij}^{-1} \{ S_{sj} + (nm)_{jk} Q_{ks} \} \}. \end{aligned} \quad (5.4.4)$$

The same reasoning which led to eq. (4.1.25) may be used to deduce that the displacement field given by eq. (5.4.1) has the integral representation

$$\begin{aligned} u_i(|\mathbf{x}|, \omega) &= \frac{1}{2\pi} f_s \left\{ Q_{is} \ln |\mathbf{x}| \right. \\ &\quad \left. - Q_{ks} \int_0^\omega (nn)_{ij}^{-1} (nm)_{jk} d\omega - S_{sj} \int_0^\omega (nn)_{ij}^{-1} d\omega \right\}, \end{aligned} \quad (5.4.5)$$

where ω is the angle measured counter clockwise from a fixed datum in the plane to \mathbf{x} .

The stresses obtained from eq. (5.4.4) using Hooke's law are

$$\begin{aligned} \sigma_{mn} &= (2\pi |\mathbf{x}|)^{-1} f_s C_{mnip} \{ m_p Q_{is} \\ &\quad - n_p (nn)_{ij}^{-1} \{ S_{sj} + (nm)_{jk} Q_{ks} \} \}, \end{aligned} \quad (5.4.6)$$

from which it follows that

$$\begin{aligned} \sigma_{mn} m_m &= (2\pi |\mathbf{x}|)^{-1} f_s \{ (mm)_m Q_{is} \\ &\quad - (mn)_m (nn)_{ij}^{-1} \{ S_{sj} + (nm)_{jk} Q_{ks} \} \} \end{aligned} \quad (5.4.7)$$

and

$$\sigma_{mn}n_m = -(2\pi|x|)^{-1}f_s S_{sn}. \quad (5.4.8)$$

Thus, we have shown that the complete field of the line force is expressible solely in terms of real variables and the matrices \mathbf{Q} and \mathbf{S} of the integral formalism. The other matrices in eq. (5.4.7) are known explicitly.

The total energy of deformation associated with the line of force is

$$\mathcal{E}^{TOT} = \frac{1}{2} \iiint_V \sigma_{ij} u_{i,j} dV - \frac{1}{2} \iiint_V f_i u_i dV. \quad (5.4.9)$$

Using the divergence theorem, \mathcal{E} , the energy per unit length along \mathbf{t} , is (we note that u_i given by eq. (5.4.1) is everywhere continuous)

$$\mathcal{E} = \frac{1}{2} \oint_{|\mathbf{x}|=R} \sigma_{ij} u_j N_i ds - \frac{1}{2} \oint_{|\mathbf{x}|=r_0} \sigma_{ij} u_j N_i ds \quad (5.4.10)$$

where the integrals are over two concentric circles of radii R and r_0 , respectively, and ds is an element of circular arc whose unit normal is N . For the line of force

$$\oint_c \sigma_{ij} N_i ds = -f_j \quad (5.4.11)$$

for any circle enclosing the defect line. Only the portion of u_i dependent on $\ln|\mathbf{x}|$ (see eq. (5.4.5)) contributes to the energy computed from eq. (5.4.10) and the result is

$$\mathcal{E} = -\frac{1}{4\pi} Q_{is} f_i f_s \ln \frac{R}{r_0}. \quad (5.4.12)$$

\mathcal{E} must always be positive, so that \mathbf{Q} is always a negative definite matrix.

All of these results hold for a line of force moving with a uniform velocity \mathbf{v} ($|\mathbf{v}| < v_L$) normal to \mathbf{t} , if we replace the static elastic constants by their "dynamic" counterparts C'_{ijklm} defined in eq. (3.7.7) and if we replace \mathcal{E} in eq. (5.4.12) by $-\mathcal{L}$, the negative Lagrangian per unit length.

It is useful to have available the solution for the elastic field of a line force dipole. Let the constant tensor dipole strength per unit length be $P_{sp} = P_{ps}$ (so that no net moment is associated with the dipole). The element P_{sp} refers to two line forces of strengths f_s and $-f_s$ separated by an amount Δx_p so that (see Section 2.7)

$$P_{sp} = \lim_{\substack{f_s \rightarrow s \\ \Delta x_p \rightarrow 0}} f_s \Delta x_p$$

remains finite, i.e. the dipole displacement field U_i is given by

$$U_i = \lim_{\substack{f_s \rightarrow s \\ \Delta x_p \rightarrow 0}} \Delta x_p u_{i,p},$$

where $u_{i,p}$ is obtained from either eq. (5.4.3) or eq. (5.4.4).

Thus, the dipole displacement field is given by either

$$U_i = -\frac{P_{sp}}{2\pi i} \sum_{z=1}^6 \pm A_{iz} A_{sz} \frac{m_p + p_z n_p}{\mathbf{m} \cdot \mathbf{x} + p_z \mathbf{n} \cdot \mathbf{x}} \quad (5.4.13)$$

or

$$\begin{aligned} U_i &= (2\pi|\mathbf{x}|)^{-1} P_{sp} \{ m_p Q_{is} \\ &\quad - n_p (nn)_{ij}^{-1} (S_{sj} + (nm)_{jk} Q_{ks}) \}, \end{aligned} \quad (5.4.14)$$

where in eq. (5.4.14) we have chosen (\mathbf{m}, \mathbf{n}) so that $\mathbf{m} \cdot \mathbf{x} = |\mathbf{x}|$ and $\mathbf{n} \cdot \mathbf{x} = 0$. The dipole displacement gradients obtained from eq. (5.4.13) are

$$U_{i,r} = \frac{1}{2\pi i} P_{sp} \sum_{z=1}^6 \pm A_{iz} A_{sz} \frac{(m_p + p_z n_p)(m_r + p_z n_r)}{(\mathbf{m} \cdot \mathbf{x} + p_z \mathbf{n} \cdot \mathbf{x})^2}. \quad (5.4.15)$$

Choosing \mathbf{m} along \mathbf{x} , we may rewrite $U_{i,r}$ as

$$\begin{aligned} U_{i,r} &= \frac{1}{2\pi|\mathbf{x}|^2} P_{sp} \left\{ -m_p m_r Q_{is} \right. \\ &\quad + (m_p n_r + m_r n_p) (nn)_{ij}^{-1} (S_{sj} + (nm)_{jk} Q_{ks}) \\ &\quad \left. - i n_p n_r \sum_{z=1}^6 \pm p_z^2 A_{iz} A_{sz} \right\}. \end{aligned} \quad (5.4.16)$$

The explicit sum in eq. (5.4.16) may be found by differentiating the sum rule eq. (3.6.25) with respect to ω , noting that the Stroh eigenvectors are independent of ω and using the relations (3.5.7), (3.5.9) and (3.5.27). The result is the sum rule

$$\begin{aligned} \sum_{z=1}^6 \pm p_z^2 A_{wz} A_{sz} &= i(nn)_{wj}^{-1} \left\{ (mm)_{jk} Q_{ks} \right. \\ &\quad \left. - [(mn)_{jk} + (nm)_{jk}] (nn)_{km}^{-1} [S_{sm} + (nm)_{mp} Q_{ps}] \right\}. \end{aligned} \quad (5.4.17)$$

Hence $U_{i,r}$ has a representation in the integral formalism which involves only \mathbf{Q} , \mathbf{S} and matrices which are known explicitly.

The line force and line dipole solutions may be convenient for use in computer simulations of dislocations in discrete crystal lattices. It has been found that certain non-linearities associated with the near field of a dislocation may be accounted for adequately by appropriately superimposing the above fields on those of the linear elastic fields of a straight dislocation.⁽¹⁴³⁾ In a certain sense the line dipole solution is the continuum analogue of a linear arrangement of "misfitting point defects". Choosing $P_{sp} = \delta_{sp}$ yields the solution for a row of three orthogonal sets of like double forces (an anisotropic "dilatation" centre) distributed uniformly

along a line parallel to \mathbf{t} . Such a solution may be of use in computing electron diffraction contrast produced by segregation at stacking faults (J. Warren and J. Hren, private communication).

5.5. Two- and Three-Dimensional Surface Green's Functions

Similar to the manner in which one defines elastic Green's functions for infinite media, one may define "surface Green's functions" for elastic half-spaces. The two-dimensional surface Green's function is merely the displacement at \mathbf{x} due to a line of force applied on the plane boundary of an anisotropic elastic half-space. If the direction of the defect line is parallel to \mathbf{t} and if the strength of the line force per unit length is f_s , the two-dimensional surface Green's function is given by⁽⁶⁰⁾

$$u_i = -\frac{1}{2\pi i} \sum_{z=1}^6 \pm A_{iz} M_{zs} f_s \ln \{ \mathbf{m} \cdot \mathbf{x} + p_z \mathbf{n} \cdot \mathbf{x} \}, \quad (5.5.1)$$

where \mathbf{m} and \mathbf{n} are any two orthogonal unit vectors normal to \mathbf{t} , and \mathbf{x} is the radius vector from a point on the line of force to a point in the plane containing \mathbf{m} and \mathbf{n} . Barnett and Lothe⁽⁶⁰⁾ have shown that the solution given by eq. (5.5.1) is valid for all half-plane boundaries parallel to \mathbf{t} , due to the rotational invariance of the Stroh eigenvectors. Using the sum rules⁽⁶⁰⁾

$$\sum_{z=1}^6 \pm A_{iz} M_{zs} = \frac{i}{2\pi} B_{is}^{-1}, \quad (5.5.2)$$

$$\sum_{z=1}^6 \pm p_z A_{iz} M_{zs} = -\frac{i}{2\pi} (nn)_{ij}^{-1} (nm)_{jk} B_{ks}^{-1}, \quad (5.5.3)$$

the displacement gradients derived from eq. (5.5.1) may be given the integral representation

$$u_{i,p} = -(4\pi^2 |\mathbf{x}|)^{-1} B_{ks}^{-1} f_s [m_p \delta_{ik} - n_p (nn)_{ij}^{-1} (nm)_{jk}], \quad (5.5.4)$$

where we have chosen \mathbf{m} and \mathbf{n} so that $\mathbf{m} \cdot \mathbf{x} = |\mathbf{x}|$ and $\mathbf{n} \cdot \mathbf{x} = 0$. One may use eq. (5.5.4) to verify that for $\mathbf{x} \neq 0$

$$\sigma_{ng} n_n = 0,$$

so that all radial planes containing the line of force are traction-free. Using linear superposition, the displacement field due to an arbitrary distribution of parallel lines of force of varying strength $f_s(\lambda)$ on the half-space boundary is merely

$$u_i = -\frac{1}{2\pi i} \sum_{z=1}^6 \pm A_{iz} M_{zs} \int_{-\infty}^{\infty} d\lambda f_s(\lambda) \ln \{ \mathbf{m} \cdot \mathbf{x} + p_z \mathbf{n} \cdot \mathbf{x} - \lambda \}, \quad (5.5.5)$$

where we choose \mathbf{n} to be the unit outer normal to the half-space boundary; λ is the distance along the boundary in the direction of $\mathbf{m} = \mathbf{n} \wedge \mathbf{t}$.

The three-dimensional surface Green's function $G_{km}(\mathbf{x})$ is defined to be the displacement in the x_k direction at \mathbf{x} due to a unit point force applied in the x_m direction *on* the boundary of an elastic half-space. The origin of coordinates is taken at the point of application of the unit force. Let \mathbf{Y} be the unit inner normal to the half-space boundary so that

$$\mathbf{x} = \mathbf{X} + \zeta \mathbf{Y} \quad (5.5.6)$$

where ζ measures depth into the half-space and \mathbf{X} lies in the half-space boundary. The boundary Fourier transform of G_{km} , namely g_{km} , is defined to be^(161,60)

$$g_{km} = \int \int'_{-\infty} d^2 \mathbf{X} G_{km}(\mathbf{x}) \exp(iK \mathbf{z} \cdot \mathbf{X}), \quad (5.5.7)$$

where the integral is over the boundary and the Fourier wave vector \mathbf{K} is given by

$$\mathbf{K} = K \mathbf{z}; |z| = 1;$$

\mathbf{z} is parallel to the half-space boundary, so that $\mathbf{z} \cdot \mathbf{Y} = 0$. The solution for g_{km} is⁽⁶⁰⁾

$$g_{km} = \frac{i}{K} \sum_{z=1}^3 A_{kz}^* M_{zm}^* \exp(-iK p_z^* \zeta). \quad (5.5.8)$$

The Stroh eigenvectors appearing in eq. (5.5.8) are those associated with the solution of plane elastostatic problems for the plane whose normal is $\mathbf{t} = \mathbf{z} \times \mathbf{Y}$.

If we take $\zeta = 0$ we may invert eq. (5.5.8) to compute $G_{km}(\mathbf{X})$, i.e. the displacement along the half-space boundary. The result is⁽⁶⁰⁾

$$G_{km}(\mathbf{X}) = (8\pi^2 |\mathbf{X}|)^{-1} \left\{ B_{km}^{-1}(\theta_0) + \frac{1}{\pi} P \int_0^\pi B_{kj}^{-1}(\theta) S_{mj}(\theta) \csc(\theta - \theta_0) d\theta \right\}, \quad (5.5.9)$$

where P indicates the Cauchy principal value of the integral. θ is the polar angle measured counter-clockwise from a fixed datum in the boundary plane to any point \mathbf{R} in the boundary. θ_0 is the value of θ corresponding to $\mathbf{R} = \mathbf{X}$. A quantity such as

$$B_{kj}^{-1}(\theta)$$

refers to the matrix \mathbf{B} calculated for a two-dimensional plane problem, in which \mathbf{R} is normal to the plane of the problem, i.e. \mathbf{t} is parallel to \mathbf{R} . The first term in eq. (5.5.9) is symmetric in the indices k and m ; the integral in eq. (5.5.9) is anti-symmetric in these indices. Thus, unlike the infinite space elastic Green's functions, the surface Green's function contain both a symmetric and an anti-symmetric part.

These two- and three-dimensional surface Green's function represen-

tations are of utility when one wishes to investigate the effect of free surfaces upon defect stress fields. We have given the Fourier transform of G_{km} , eq. (5.5.8), because this quantity is often of more utility than G_{km} itself (see, for example, Willis⁽¹⁶¹⁾).

APPENDIX

A Recent Development in the Theory of the Self-Force on a Plane Dislocation Loop

Recent work by S. D. Gavazza⁽¹⁴⁴⁾ presents some results relevant to the problem of determining the self-force on a plane dislocation loop in an infinite anisotropic linear elastic medium. The results appear to be of sufficient importance to be included in this review. We omit the involved analysis leading to these results and refer the reader to Gavazza's thesis and some subsequent publications^(46,145) for details.

Consider a circular loop L of dislocation of Burgers vector \mathbf{b} and radius a . The infinite-body stresses in the plane of the loop are given, according to Brown's^(9,82) theorem, by (see Section 4.2)

$$\sigma_{ij}^L(\mathbf{x}) = \frac{1}{2} \oint_L \frac{\Sigma_{ij}(\theta) + (\partial^2/\partial\theta^2)\Sigma_{ij}(\theta)}{|\mathbf{x} - \mathbf{x}'|} d\theta, \quad (\text{A.1})$$

where \mathbf{x}' is a point on the loop,

$$d\theta = ds' \frac{\sin(\theta - \alpha)}{|\mathbf{x} - \mathbf{x}'|}$$

and the $\Sigma_{ij}(\theta)$ are the in-plane angular stress factors for an infinite straight dislocation whose line direction is specified by θ , eq. (4.2.22). We wish to find the dominant (singular) contributions to eq. (A.1) when \mathbf{x} as measured from the centre of the loop is such that

$$|\mathbf{x}| = a \pm \epsilon; \epsilon > 0$$

and ϵ tends to zero, i.e. we wish to extract the singular nature of the in-plane dislocation stresses as we approach a point on the loop from within and from the exterior along the local normal to the loop.

Simple geometric considerations show that

$$\sigma_{ij}^L(|\mathbf{x}| = a - \epsilon) = \frac{1}{a(1 - k^2)} \int_{-\pi/2}^{\pi/2} \{\Sigma_{ij} + \Sigma''_{ij}\} (1 - k^2 \sin^2 \theta)^{1/2} d\theta, \quad (\text{A.2})$$

$$\sigma_{ij}^L(|\mathbf{x}| = a + \epsilon) = \frac{1}{a(1 - p^2)} \int_{-\theta_0}^{\theta_0} \{\Sigma_{ij} + \Sigma''_{ij}\} (1 - p^2 \sin^2 \theta)^{1/2} d\theta, \quad (\text{A.3})$$

where

$$\begin{aligned} k &= 1 - \frac{\epsilon}{a} < 1, \\ p &= 1 + \frac{\epsilon}{a} > 1, \\ \theta_0 &= \sin^{-1}(1/p). \end{aligned} \quad (\text{A.4})$$

A detailed analysis shows that as $\epsilon \rightarrow 0$

$$\sigma_{ij}^L(|x| = a \mp \epsilon) \simeq \pm \frac{\Sigma_{ij}(t)}{\epsilon} + \frac{1}{2a} \left\{ \Sigma_{ij}(t) + \frac{\epsilon^2}{c x^2} \Sigma_{ij}(t) \right\} \ln \frac{8a}{\epsilon} + O(1), \quad (\text{A.5})$$

where the plus sign is used inside the loop and the minus sign is used outside the loop. The angular stress factors $\Sigma_{ij}(t)$ are those for an infinite straight dislocation tangent to the loop at x as $\epsilon \rightarrow 0$, and x fixes the direction of this tangent t in the plane. Hence, the singular behaviour of the in-plane stresses near a circular loop is of two types: the first term in eq. (A.5) is merely the singular behaviour of an infinite straight dislocation tangent to the loop at the point in question; the second term in eq. (A.5) is logarithmically divergent as $\epsilon \rightarrow 0$ and arises solely from the curvature of the loop, since this term vanishes as $a \rightarrow \infty$.

Gavazza has extended the analysis to prove that the singular behaviour of the stresses in the plane of a loop of arbitrary shape is the same as that for the osculating circle to the loop at the point in question. Thus, eq. (A.5) is valid for any plane loop if a is taken to be the radius of curvature of the loop at x ! (A rigorous derivation has been provided by Barnett.⁽¹⁴⁵⁾)

Gavazza defines the self-force F^L at a point P on a plane dislocation loop in the following manner. The self-energy of the loop in an infinite medium is defined to be the total strain energy outside a small tube of radius ϵ surrounding the dislocation loop L . Neglecting for the moment any possible contribution to the energy from a surface integral over the tube (we shall discuss this contribution later) the usual expression for the self-energy is, eq. (2.6.17).

$$\mathcal{E}^L = \frac{1}{2} \iint_{S_0(\epsilon)} \sigma_{ij}^L b_i n_j dS,$$

where the integral is over the cut S_0 bounded by L and the integral is taken only to within a distance ϵ of L , as was discussed in Section 2.6.1; to simplify the notation, we use ϵ here rather than r_0 and the reader should be aware that a finite value of ϵ must be retained in the energy expressions. During a plane virtual motion δr of each point of L (δr is everywhere normal to L , but may vary in magnitude along L) the loop assumes the configuration L' and the associated energy variation is

$$\delta\mathcal{E}^L = \frac{1}{2} \int_{L'} \sigma_{ij}^{L'} b_i n_j \delta r ds_\epsilon + \frac{1}{2} \iint_{S_0(\epsilon)} (\sigma_{ij}^{L'} - \sigma_{ij}^L) b_i n_j dS. \quad (\text{A.6})$$

ds_ϵ is an elemental arc of L_ϵ and L_ϵ is the bounding curve of $S_0(\epsilon)$. The first integral on the right side of eq. (A.6) accounts for the new slipped region swept out as L_ϵ moves to the configuration L'_ϵ during the virtual motion δr ; the remaining integral accounts for the change in the stress field of L during the variation.

Now $\sigma^{L'} - \sigma^L$ is merely the stress field of the dislocations L and $-L$ (i.e. L with its sense reversed) so that the second integral in eq. (A.6) is merely half the interaction energy of the dislocation “loop” $L' - L$ with the slipped region $S_0(\epsilon)$. This is identical with half the interaction energy between L_ϵ and the slipped region between L' and $-L$, so that

$$\iint_{S_0(\epsilon)} (\sigma_{ij}^{L'} - \sigma_{ij}^L) b_i n_j dS = \iint_{S' - S} \sigma_{ij}^{L'} b_i n_j dS$$

where S' and S are the cuts associated with L' and L , respectively. Since

$$\iint_{S' - S} \sigma_{ij}^{L'} b_i n_j dS = \oint_L \sigma_{ij}^{L'} b_i n_j \delta r ds,$$

where ds is an elemental arc of L , we obtain for eq. (A.6) the symmetric form

$$\delta \mathcal{E}^L = \frac{1}{2} \int_{L_\epsilon} \sigma_{ij}^L b_i n_j \delta r ds_\epsilon + \frac{1}{2} \int_L \sigma_{ij}^{L'} b_i n_j \delta r ds. \quad (\text{A.7})$$

We can use eq (A.5) with the upper and lower signs to evaluate σ_{ij}^L on L_ϵ and $\sigma_{ij}^{L'}$ on L , respectively. Noting that if L_ϵ lies within L ,

$$ds_\epsilon = \left(1 - \frac{\epsilon}{a}\right) ds,$$

where a is the local radius of curvature ($a = 1/\kappa$ where κ is the curvature) at two corresponding points on L_ϵ and L , eq. (A.7) reduces to (as $\epsilon \rightarrow 0$)

$$\delta \mathcal{E}^L = - \int_L F^L \delta r ds,$$

where F^L is by definition the self force per unit length at a point P on L given by

$$F^L = + \frac{1}{a} \left(E(t) - \left\{ E(t) + \frac{\partial^2}{\partial \alpha^2} E(t) \right\} \ln \frac{8a}{\epsilon} \right) - J[L]. \quad (\text{A.8})$$

t is the unit local tangent to L at P and $E(t)$ is the pre-logarithmic energy factor for an infinite straight dislocation parallel to t , i.e.

$$\mathcal{E}^\infty(t) = E(t) \ln \frac{R}{\epsilon} = \frac{1}{2} \Sigma_{ij}(t) b_i n_j \ln \frac{R}{\epsilon}.$$

The quantity $J[L]$ in eq (A.8) comes from the term $O(1)$ in eq (A.5) and depends on the global shape of the loop. For a straight dislocation

($a \rightarrow \infty$), $J[L]$ and F^L vanish identically. Using eq. (A.5) to take the average of the stresses in the plane of L at a normal distance ϵ on either side of L shows that eq. (A.8) is equivalent to

$$F^L = +\frac{1}{a} E(t) - \frac{1}{2} \{ \sigma_{ij}^L|_{a+\epsilon} + \sigma_{ij}^L|_{a-\epsilon} \} b_i n_j. \quad (\text{A.9})$$

Gavazza's derivation is unequivocal and self-consistent in the sense that he began by considering variations in the self-energy outside a tube of radius ϵ surrounding the loop L ; this is the same ϵ appearing in eqs (A.8) and (A.9). An earlier prescription given by Brown⁽⁵⁰⁾ was ambiguous in this respect.

Brown had defined the self-force to be merely the average of the in-plane resolved stresses near the dislocation loop, i.e.

$$F^{\text{Brown}} = -\frac{1}{2} \{ \sigma_{ij}^L|_{a+\epsilon} + \sigma_{ij}^L|_{a-\epsilon} \} b_i n_j,$$

but, as Brown noted, there exists a discrepancy between the self-energy release rate calculated from his definition of F^L and the correct self-energy release rate expressions for known dislocation solutions. The discrepancy is due precisely to the omission of the term $1/a E(t)$ in Brown's definition of F^L .

To illustrate that eqs (A.8) and (A.9) produce a correct result for a case in which Brown's definition of F^L does not, consider the uniform in-plane expansion of a circular edge loop of radius a in an isotropic medium. The problem has been studied by Kroupa.⁽¹⁴⁶⁾ Careful consideration of Kroupa's equations (20) and (21) shows that the term corresponding to $J(L)$ in eq. (A.8) vanishes and that the self-energy \mathcal{E}^L of the loop is given by

$$\mathcal{E}^L = \frac{\mu b^2}{2(1-v)} a \left\{ \ln \frac{8a}{\epsilon} - 2 \right\}. \quad (\text{A.10})$$

Since during a uniform in-plane expansion the virtual displacement $\delta r = \delta a$, the self-force per unit length is

$$\begin{aligned} F^L &= -\frac{1}{2\pi a} \frac{\partial \mathcal{E}^L}{\partial a} \\ &= -\frac{\mu b^2}{4\pi(1-v)a} \left\{ \ln \frac{8a}{\epsilon} - 1 \right\}. \end{aligned} \quad (\text{A.11})$$

For the circular edge loop in an isotropic medium

$$E(t) = \frac{\mu b^2}{4\pi(1-v)}; \frac{\partial^2}{\partial x^2} E(t) = 0$$

so that F^L calculated from eq. (A.8) is

$$F^L = +\frac{\mu b^2}{4\pi(1-v)a} - \frac{\mu b^2}{4\pi(1-v)a} \ln \frac{8a}{\epsilon}$$

in agreement with eq. (A.11). Had we followed Brown's prescription for the self-force we would have obtained

$$F^{\text{Brown}} = -\frac{\mu b^2}{4\pi(1-v)a} \ln \frac{8a}{\epsilon},$$

which does not agree with eq. (A.11). A careful analysis of the circular shear loop in an isotropic medium shows that the definition of self-force in eqs (A.8) and (A.9) is consistent with the known energy release rate, whereas Brown's prescription is not.

Gavazza has also pointed out that eqs (A.8) and (A.9) do not yield the complete distributed self-force on a rational dislocation element because there exists an additional contribution to the self-energy release rate from the tractions acting over a small tube of radius ϵ surrounding the dislocation loop. Bullough and Foreman⁽⁴⁵⁾ first pointed out this core traction contribution and noted that the tube integral is, in fact, dependent on the cut surface used to render the dislocation displacement field single-valued. The tube contribution to the self-energy is merely

$$\begin{aligned} \mathcal{E}^{\text{TUBE}} &= \frac{1}{2} \oint_{\text{TUBE}} \sigma_{ij}^L u_i n_j dS \\ &= \frac{1}{2} \oint_L ds \int_0^{2\pi} \sigma_{ij}^L u_i n_j \epsilon d\omega, \end{aligned} \quad (\text{A.12})$$

where n is the unit inner normal to the tube and ω is the polar angle about the dislocation in any plane cross-section of the tube. Bullough and Foreman⁽⁴⁵⁾ have asserted that as $\epsilon \rightarrow 0$ the inner integral in eq. (A.12) may be evaluated using only the fields of a straight dislocation tangent to the loop element ds . This assertion is probably correct, although a rigorous proof must await further investigation. Adopting the Bullough Foreman assumption it is not difficult to show that

$$\mathcal{E}^{\text{TUBE}} = \oint_L ds H(\alpha), \quad (\text{A.13})$$

where

$$\begin{aligned} H(\alpha) &= -\frac{1}{2} \int_0^{2\pi} \frac{\partial \phi_i}{\partial \omega} u_i d\omega \\ &= \frac{1}{2} \int_0^{2\pi} \phi_i \frac{\partial u_i}{\partial \omega} d\omega, \end{aligned} \quad (\text{A.14})$$

where the cut $\omega = 0$ corresponds to $\phi_i = 0$. ϕ_i is the vector Airy stress function of Stroh⁽⁸⁾ for the infinite straight dislocation tangent to the loop at ds . For a given cut H is independent of ϵ and depends only upon α , the direction of the local tangent to the loop at ds .

Gavazza showed that for an arbitrary in-plane virtual normal displacement δr of the loop the variation of eq. (A.13), i.e. the tube energy release rate, is

$$\delta\mathcal{E}^{\text{TUBE}} = \int_L \frac{1}{a} \left\{ H(\alpha) + \frac{\partial^2 H}{\partial \alpha^2} \right\} \delta r \, ds, \quad (\text{A.15})$$

where a is the local radius of curvature of the loop at ds . Thus, there exists in addition to the self-force given by eqs (A.8) and (A.9) an additional distributed self-force

$$F^{\text{TUBE}} = -\frac{1}{a} \left\{ H(\alpha) + \frac{\partial^2 H}{\partial \alpha^2} \right\}. \quad (\text{A.16})$$

We note that eq. (A.16) vanishes for an infinite straight dislocation ($a \rightarrow \infty$), as it must, since the contribution of the tube to the total self-energy is cancelled by a corresponding negative contribution from a tube "at infinity" (e.g. see Chap. 4).

Thus, the complete distributed self-force at a point on a plane dislocation loop whose local radius of curvature is a is given by

$$F^L = \frac{1}{a} \left\{ E(t) - \left(E(t) + \frac{\partial^2}{\partial \alpha^2} E(t) \right) \ln \frac{8a}{\epsilon} - \left(H(\alpha) + \frac{\partial^2 H}{\partial \alpha^2} \right) \right\} - J(L) \quad (\text{A.17})$$

$$= \frac{1}{a} \left\{ E(t) - H(\alpha) - \frac{\partial^2}{\partial \alpha^2} H(\alpha) \right\} - \frac{1}{2} \{ \sigma_{ij}^L|_{a+\epsilon} + \sigma_{ij}^L|_{a-\epsilon} \} b_i n_j. \quad (\text{A.18})$$

As Bullough and Foreman have pointed out, the self-energy expression which yielded eq. (A.8) and the tube self-energy contribution eq. (A.13), which yielded eq. (A.16) are separately sensitive functions of the choice of cut used to define the dislocation loop. The sum of these two contributions to the total self-energy, which is in fact the total strain energy outside the tube of radius ϵ , is invariant to the choice of cut. Since eqs (A.8) and (A.9) were computed by taking a cut in the plane of the loop, eqs (A.17) and (A.18) should be evaluated by computing $H(\alpha)$ using the same planar cut.

Equation (A.17) points out that the total distributed self-force on a dislocation element can be easily determined from a knowledge of the local curvature and the tangent straight dislocation data $E(t)$, $E(t) + E''(t)$ (which can be computed using the methods of Chap. 4), and $H(\alpha) + H''(\alpha)$. $J[L]$ is not difficult to compute since eq. (A.5) has indicated how to "subtract out" the singular contribution to eq. (A.1); however, for computational purposes eq. (A.18) should be easier to use than eq. (A.17) since the use of eq. (A.18) does not require a direct evaluation of $J[L]$.

In deriving the equations for the glide component of the self force in this Appendix, we have, for simplicity, restricted the derivation to the

scalar quantity F^L , which gives the magnitude of the force as a signed quantity. A more detailed, but less transparent, analysis can be made which permits the derivation of the vector force. The latter analysis allows us to give a self-consistent interpretation to the sign of F^L and we give here the convention which allows the direction of F^L in the glide plane to be unambiguously established using the sign of F^L . Consider a planar loop L as shown in Fig. A.1, and denote the glide plane normal by \mathbf{n} , where the positive direction of \mathbf{n} follows from a right-hand screw rule taken with respect to the arbitrarily chosen positive direction of L . Let \mathbf{t} be the unit tangent vector to L such that \mathbf{t} points along the positive direction. The in-plane curvature vector $\boldsymbol{\kappa} = \kappa \mathbf{m} = d\mathbf{t}/ds$, where κ is the curvature (always considered positive) and s is the arc length, which increases along the positive direction.⁽¹⁴⁷⁾ The curvature $\kappa = 1/a$, where a is the radius of curvature. The unit vector \mathbf{m} is directed along $\pm \mathbf{n} \wedge \mathbf{t}$, where $\mathbf{n} \wedge \mathbf{t}$ is the in-plane unit normal to L . For example, the loop shown in Fig. A.1 is such that κ is the same at points A and B , \mathbf{t} and $\mathbf{n} \wedge \mathbf{t}$ are the same, but $\mathbf{m} = +\mathbf{n} \wedge \mathbf{t}$ at A and $\mathbf{m} = -\mathbf{n} \wedge \mathbf{t}$ at B . The unit normal \mathbf{m} defining the direction of the curvature vector allows us to determine the direction of F^L according to the following rule: if F^L obtained from eq. (A.17) or eq. (A.18) (or one of their simplified forms without the tube integral correction) is positive, then the self force acts along $-\mathbf{m}$, whereas if the force is negative, it acts along $+\mathbf{m}$.

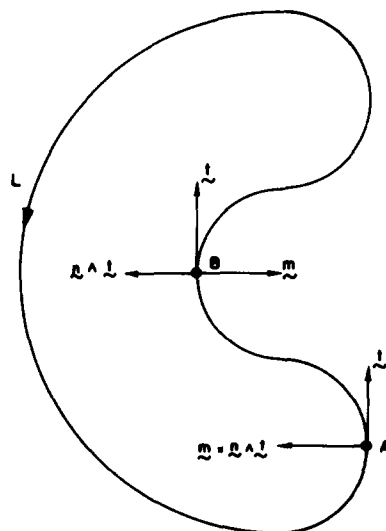


FIG. A.1. Schematic diagram of the planar dislocation loop L mentioned in the text. \mathbf{t} is the unit tangent vector and the unit normal \mathbf{n} to the plane of the loop is directed out of the diagram (as given by a right-hand screw rule taken with respect to the arbitrarily chosen positive sense for L). Note that the curvature or principal normal \mathbf{m} changes direction at the points A and B , whereas the normal vector $\mathbf{n} \wedge \mathbf{t}$ remains unchanged.

ACKNOWLEDGEMENTS

The authors acknowledge for their assistance and valuable discussions Drs A. K. Head, S. Gavazza and W. H. McConnell, and Dr. U. F. Kocks and other members of the Mechanical Properties Group at the Argonne National Laboratory. In addition, some errors and significant omissions in the original manuscript were kindly brought to the attention of the authors by Profs. J. D. Eshelby and E. Kröner and Dr. R. Bauer. The review was written with support from the U.S. Department of Energy, the U.S. National Science Foundation through the Materials Research Laboratory Program, Centre for Materials Research, Stanford University and the U.K. Science Research Council. Finally, the care and effort taken with the typing of the manuscript by Betty Heramb and Robin Sharon is gratefully acknowledged.

REFERENCES

1. V. VOLTERRA, *Annls Scient. Ec. Norm. Sup. Paris* **24** (1907) 401.
2. R. DE WIT, *Solid St. Phys.* **10** (1960) 249.
3. T. MURA, *Advances in Materials Research* (edited by H. Herman), Wiley, **3** (1968) 1.
4. J. D. ESHELBY, W. T. READ and W. SHOCKLEY, *Acta Metall.* **1** (1953) 251.
5. A. N. STROH, *Phil. Mag.* **3** (1958) 625.
6. J. P. HIRTH and J. LOTHE, *Theory of Dislocations* (1968) McGraw-Hill, New York.
7. J. SIEHLDS, *Introduction to Anisotropic Elasticity Theory of Dislocations* (1973) Oxford University Press.
8. A. N. STROH, *J. Math. Phys.* **41** (1962) 77.
9. L. M. BROWN, *Phil. Mag.* **15** (1967) 363.
10. V. L. INDENBOM and S. S. ORLOV, *Soviet Phys. JETP* **6** (1967) 274.
11. J. D. ESHELBY, *Proc. R. Soc. A* **241** (1957) 376.
12. J. D. ESHELBY, *Progress in Solid Mechanics* 2 (edited by I. Sneddon and R. Hill), p. 89 (1961) North Holland, Amsterdam.
13. J. F. NEL, *Physical Properties of Crystals* (1960) Oxford University Press.
14. Y. C. FUNG, *Foundations of Solid Mechanics* (1965) Prentice-Hall.
15. R. E. COLLINS, *Mathematical Methods for Physicists and Engineers* (1968) Reinhold.
16. I. M. GEL'FAND and G. E. SHILOV, *Generalized Functions*, Vol. I (1964) Academic Press.
17. R. DE WIT, *J. Res. Natn. Bur. of Stand* **77A**, **1** (1973) 49.
18. A. E. H. LOVE, *The Mathematical Theory of Elasticity* (1944) Dover.
19. J. D. ESHELBY, *Solid St. Phys.* **3** (1956) 79.
20. N. P. SUH and A. P. L. TURNER, *Elements of the Mechanical Behavior of Solids* (1975) McGraw-Hill.
21. A. H. COUTRILL, *The Mechanical Properties of Matter*, Chap. 4 (1964) Wiley.
22. R. A. FRAZER, W. J. DUNCAN and A. R. COLLAR, *Elementary Matrices* (1938) Cambridge University Press.
23. R. W. LARDNER, *Mathematical Theory of Dislocations and Fracture*, Math. Expositions No. **17** (1974) Univ. of Toronto Press.
24. G. LEIBFRIED, *Z. Phys.* **135** (1953) 23.
25. E. MANN, R. V. JAN and A. SEEGER, *Phys. Status Solidi* **1** (1961) 17.
26. K. H. C. LIU and J. S. KOEHLER, *Adv. Phys.* **17** (1968) 421.
27. K. MALÉN, *Phys. Status Solidi* **38** (1970) 259.
28. J. L. SYNGE, *The Hypercircle in Mathematical Physics* (1957) Cambridge University Press.
29. D. M. BARNETT, *Phys. Status Solidi* (b) **49** (1972) 741.
30. N. MEISSNER, Ph.D. Thesis, University of Surrey (In Harwell report T. P. 556) (1973).
31. I. M. GEL'FAND, M. I. GRAEV and N. YA. VILENKIN, *Generalized Functions*, Vol. 5 (1966) Academic Press.
32. E. H. YOFFE, *Phil. Mag.* **30** (1974) 923.

33. J. R. WILLIS, *Q. Jl Mech. appl. Math.* **18** (1965) 419.
34. J. R. WILLIS, *J. Mech. Phys. Solids* **23** (1975) 129.
35. F. R. N. NABARRO, *Phil. Mag.* **42** (1951) 1224.
36. F. R. N. NABARRO, *Theory of Crystal Dislocations* (1967) Oxford University Press.
37. J. FRIEDEL, *Dislocations* (1964) Pergamon.
38. A. H. COTTRELL, *Dislocations and Plastic Flow in Crystals* (1953) Oxford University Press.
39. B. A. BILBY, R. BULLOUGH and E. SMITH, *Proc. R. Soc. A* **231** (1955) 263.
40. T. MURA, *Phil. Mag.* **8** (1963) 843.
41. R. J. ASARO, Tech. Report DMR-720-3023 A06/94, Mat. Res. Lab., Brown Univ., Providence, R.I. (1975).
42. D. M. BARNETT and L. A. SWANGER, *Phys. Status Solidi (b)* **48** (1971) 419.
43. T. MURA, *Phys. Status Solidi (b)* **70** (1975) K1.
44. R. J. ASARO, J. P. HIRTH, D. M. BARNETT and J. LOTHE, *Phys. Status Solidi (b)* **60** (1973) 261.
45. R. BULLOUGH and A. J. E. FOREMAN, *Phil. Mag.* **9** (1964) 351.
46. S. D. GAVAZZA and D. M. BARNETT, *J. Mech. Phys. Solids* **24** (1976) 171.
47. M. PEACH and J. S. KOEHLER, *Phys. Rev.* **80** (1950) 436.
48. U. F. KOCKS, A. S. ARGON and M. F. ASHBY, *Thermodynamics and Kinetics of Slip*. *Prog. mater. Sci.* **19** (1975).
49. S. D. GAVAZZA and D. M. BARNETT, *Scripta Metall.* **9** (1975) 1263.
50. L. M. BROWN, *Phil. Mag.* **10** (1964) 441.
51. G. DE WIT and J. S. KOEHLER, *Phys. Rev.* **116** (1959) 1113.
52. R. SIEMS, *Phys. Status Solidi* **30** (1968) 645.
53. P. A. FLINN and A. A. MARADUDIN, *Ann. Phys.* **18** (1962) 81.
54. P. M. MORSE and H. FESHBACH, *Methods of Theoretical Physics* (1953) McGraw-Hill.
55. P. P. GROVES and D. J. BACON, *J. appl. Phys.* **40** (1969) 4207.
56. R. J. ASARO and D. M. BARNETT, *J. Mech. Phys. Solids* **23** (1975) 77.
57. K. MALÉN and J. LOTHE, *Phys. Status Solidi* **39** (1970) 287.
58. K. NISHIOKA and J. LOTHE, *Phys. Status Solidi (b)* **51** (1972) 645.
59. D. M. BARNETT and J. LOTHE, *Physica Norvegica* **7** (1973) 13.
60. D. M. BARNETT and J. LOTHE, *Physica Norvegica* **8** (1975) 13.
61. K. MALÉN, *Fundamental Aspects of Dislocation Theory* (edited by J. Simmons, R. de Wit and R. Bullough), N.B.S. pub. 317, p. 23 (1970).
62. D. M. BARNETT and J. LOTHE, *J. Phys. F: Metal Phys.* **4** (1974) 671.
63. D. M. BARNETT, R. J. ASARO, S. D. GAVAZZA, D. J. BACON and R. O. SCATTERGOOD, *J. Phys. F: Metal Phys.* **2** (1972) 854.
64. R. J. ASARO and D. M. BARNETT, *J. Phys. F: Metal Phys.* **4** (1974) L103.
65. R. J. BELTZ, T. L. DAVIS and K. MALÉN, *Phys. Status Solidi* **26** (1968) 621.
66. D. M. BARNETT, J. LOTHE, K. NISHIOKA and R. J. ASARO, *J. Phys. F: Metal Phys.* **3** (1973) 1083.
67. R. J. ASARO and J. P. HIRTH, *J. Phys. F: Metal Phys.* **3** (1973) 1659.
68. D. J. BACON and R. O. SCATTERGOOD, *J. Phys. F: Metal Phys.* **4** (1974) 2126.
69. D. J. BACON and R. O. SCATTERGOOD, *J. Phys. F: Metal Phys.* **5** (1975) 193.
70. A. K. HEAD, *Phys. Status Solidi* **19** (1967) 185.
71. L. M. CLAREBROUGH and A. K. HEAD, *Phys. Status Solidi* **33** (1969) 431.
72. Y. T. CHOU and J. D. ESHELBY, *J. Mech. Phys. Solids* **10** (1962) 27.
73. F. C. FRANK and W. T. READ, *Symposium on Plastic Deformation of Crystalline Solids* (1950) p. 44. Carnegie Inst. of Tech., Pittsburgh.
74. L. M. BROWN and R. K. HAM, *Strengthening Methods in Crystals* (edited by A. Kelly and R. B. Nicholson) (1971) p. 9, Elsevier.
75. F. R. N. NABARRO, Z. S. BASINSKI and D. B. HOLT, *Adv. Phys.* **13** (1964) 192.
76. A. J. E. FOREMAN and M. J. MAKIN, *Phil. Mag.* **14** (1966) 911.
77. R. J. ARSENault and T. CADMAN, *Rate Processes in Plastic Deformation of Materials* (edited by J. C. M. Li and A. K. Mukherjee), p. 102 (1975) Amer. Soc. for Metals.
78. K. HANSON, S. ALTINTAS and J. W. MORRIS, *Computer Simulation for Materials Applications* (edited by R. J. Arsenault, J. R. Beeler, Jr. and J. A. Simmons), *Nuclear Metallurgy* **20** (part 2) (1976) 917.
79. J. LOTHE, *Phil. Mag.* **15** (1967) 353.
80. J. R. WILLIS, *Phil. Mag.* **21** (1970) 931.

81. R. J. ASARO and D. M. BARNETT, *Computer Simulation for Materials Applications* (edited by R. J. Arsenault, J. R. Beeler, Jr. and J. A. Simmons), *Nucl. Metallurgy* **20** (part 2) (1976) 313.
82. L. M. BROWN, *Can. J. Phys.* **45** (1967) 893.
83. J. D. ESHELBY and T. LAUB, *Can. J. Phys.* **45** (1967) 887.
84. T. MURA and T. MORI, *Phil. Mag.* **33** (1976) 1021.
85. L. M. BROWN, M. S. SPRING and M. IPOHORSKI, *Phil. Mag.* **24** (1971) 1495.
86. D. J. BACON, R. BULLOUGH and J. R. WILLIS, *Phil. Mag.* **22** (1970) 31.
87. M. J. MAKIN and B. HUDDSON, *Phil. Mag.* **8** (1963) 447.
88. B. HUDDSON and M. J. MAKIN, *Phil. Mag.* **11** (1965) 423.
89. D. J. BACON and A. G. CROCKER, *Phil. Mag.* **13** (1966) 217.
90. J. W. GOODMAN and G. SINAS, *J. appl. Phys.* **43** (1972) 2086.
91. J. W. GOODMAN and G. SINAS, *Scripta Metall.* **5** (1971) 631.
92. P. NAVI, J. W. GOODMAN and G. SINAS, *Scripta Metall.* **6** (1972) 71.
93. J. W. STEEDS and J. R. WILLIS, to be published in *Dislocations in Solids* (edited by F. R. N. Nabarro), Vol. I (in the press) North-Holland.
94. N. MEISSNER, E. J. SAVINO, J. R. WILLIS and R. BULLOUGH, *Phys. Status Solidi* (b) **63** (1974) 139.
95. R. BULLOUGH and V. K. TEWARY, *Interatomic Potentials and Simulation of Lattice Defects* (edited by P. C. Gehlen, J. R. Beeler, Jr. and R. I. Jaffee) (1972) p. 155. Plenum Press.
96. B. HUDDSON, *Phil. Mag.* **10** (1964) 949.
97. R. O. SCATTERGOOD and D. J. BACON, *Phil. Mag.* **31** (1975) 179.
98. E. KRÖNER, *Kontinuumstheorie der Versetzungen und Eigenspannungen* Erg. Ang. Math. **5** (1958) Springer-Verlag.
99. R. O. SCATTERGOOD and D. J. BACON, *Phys. Status Solidi* (a) **25** (1974) 395.
100. J. C. M. LI and G. C. T. LIOU, *Trans. Japan Inst. Metals* **9** (1968) 20.
101. T. E. MITCHELL and R. L. SMIALEK, *Chicago Work Hardening Symposium* (edited by J. P. Hirth and J. Weertman) (1967) p. 365. Gordon and Breach, New York.
102. R. O. SCATTERGOOD and D. J. BACON, *Acta Metall.* **24** (1976) 705.
103. R. O. SCATTERGOOD and D. J. BACON, unpublished work.
104. S. M. OHRE and D. N. BISHERS, *Phil. Mag.* **8** (1963) 1343.
105. R. O. SCATTERGOOD and U. F. KOCKS, unpublished work.
106. A. K. HEAD, P. HUMBLE, L. M. CLAREBROUGH, A. J. MORTON and C. T. FORWOOD, *Computed Electron Micrographs and Defect Identification* (1973) North-Holland.
107. S. M. OHRE, *Phys. Status Solidi* (b) **64** (1974) 317.
108. P. B. HIRSCH, A. HOWIE, R. B. NICHOLSON, D. W. PASHLEY and M. J. WHELAN, *Electron Microscopy of Thin Crystals* (1965) Butterworths.
109. W. H. MCCONNELL, *Phil. Mag.* **33** (1976) 863.
110. W. H. MCCONNELL and D. M. BARNETT, *Phil. Mag.* **35**, 4 (1977) 1037.
111. M. O. TUCKER and A. G. CROCKER, *Mechanics of Generalized Continua* (edited by E. Kröner) (1968) p. 286. Springer-Verlag, Berlin.
112. D. M. BARNETT and J. LOTHE, *J. Phys. F: Metal Phys.* **4** (1974) 1618.
113. J. GEMPERLOVA and I. SAXL, *Czech. J. Phys.* **B18** (1968) 1085.
114. D. L. CLEMENTS, *Int. J. Engng. Sci.* **9** (1971) 256.
115. J. R. WILLIS, *J. Mech. Phys. Solids* **19** (1971) 353.
116. S. NAKAHARA and J. R. WILLIS, *J. Phys. F: Metal Phys.* **3** (1973) L249.
117. M. O. TUCKER, *Phil. Mag.* **19** (1969) 1141.
118. J. LOTHE, *Fundamental Aspects of Dislocation Theory* (edited by J. A. Simmons, R. de Wit and R. Bullough), N.B.S. pub. 317, p. 11 (1970).
119. J. W. FLOCKEN and J. R. HARDY, *Fundamental Aspects of Dislocation Theory* (edited by J. A. Simmons, R. de Wit and R. Bullough), N.B.S. pub. 317, p. 219 (1969).
120. R. A. JOHNSON, *J. Phys. F: Metal Phys.* **3** (1973) 295.
121. V. K. TEWARY, *Adv. Physics* **22** (1973) 757.
122. P. T. HEALD, *Proc. Conf. Point Defect Behaviour and Diffusional Processes* (edited by J. E. Harris and R. F. Smallman) (1976) p. 11, Metals Soc., London.
123. J. W. FLOCKEN and J. R. HARDY, *Phys. Rev. B1* (1970) 2447.
124. R. BULLOUGH, M. J. NORGETT and S. WEBB, *J. Phys. F: Metal Phys.* **1** (1971) 345.
125. A. W. COCHARDT, G. SCHOECK and H. WIEDERSICH, *Acta metall.* **3** (1955) 533.
126. D. J. BACON, *Scripta Metall.* **3** (1969) 735.

127. E. KRÖNER, *Theory of Crystal Defects* (edited by B. Gruber) (1966) p. 215, Academia, Prague.
128. L. J. WALPOLE, *Proc. R. Soc. A* **300** (1967) 270.
129. R. BULLOUGH and J. R. WILLIS, *Phil. Mag.* **31** (1975) 855.
130. N. KINOSHITA and T. MURA, *Phys. Status Solidi (a)* **5** (1971) 759.
131. G. KNEER, *Phys. Status Solidi* **9** (1965) 825.
132. E. STERNBERG, *Appl. Mech. Rev.* **11** (1958) 1.
133. J. K. LEE, D. M. BARNETT and H. I. AARONSON, *Trans. AIME* **8A** (1977) 963.
134. B. A. BILBY and J. D. ESHELBY, *Fracture: An Advanced Treatise* (edited by H. Liebowitz), Vol. 1 (1968) p. 29, Academic Press, New York and London.
135. J. R. RICH, *Fracture: An Advanced Treatise* (edited by H. Liebowitz), Vol. 2 (1968) p. 191, Academic Press, New York and London.
136. P. T. HEALD, *Bull. Acad. Pol. Sci.* **6** (1970) 211.
137. D. M. BARNETT and R. J. ASARO, *J. Mech. Phys. Solids* **20** (1972) 353.
138. G. I. BARENBLATT, *Problems in Continuum Mechanics*, SIAM, Philadelphia (1961) 21.
139. V. A. SOLOVEV, *Phys. Status Solidi (b)* **65** (1974) 857.
140. J. E. SINCLAIR and J. P. HIRTH, *J. Phys. F: Metal Phys.* **5** (1975) 236.
141. R. J. ASARO, *Int. J. Engng Sci.* **13** (1975) 217.
142. J. R. RICE and R. THOMSON, *Phil. Mag.* **29** (1974) 73.
143. P. C. GEHLEN, J. P. HIRTH, R. G. HOAGLAND and M. F. KANNINEN, *J. appl. Phys.* **43** (1972) 3921.
144. S. D. GAVAZZA, *Energy Release Rates and Associated Forces on Singular Dislocations* (Ph.D. Thesis, Department of Applied Mechanics, Stanford University; July, 1975).
145. D. M. BARNETT, *Phys. Status Solidi (a)* **38** (1976) 637.
146. F. KROUPA, *Czech J. Phys.* **10B** (1960) 284.
147. J. G. COFFIN, *Vector Analysis* (1959) Wiley.
148. G. SIMMONS and H. WANG, *Single Crystal Elastic Constants and Calculated Aggregate Properties: A Handbook* (1971) M.I.T. Press (Cambridge, Mass.)
149. R. E. MACFARLANE, J. A. RANE and C. K. JONES, *Phys. Lett.* **20** (1966) 234.
150. H. C. NASH and C. S. SMITH, *Physics Chem. Solids* **9** (1959) 113.
151. J. A. RAYNE, *Phys. Rev.* **118** (1960) 1545.
152. R. E. MACFARLANE, J. A. RAYNE and C. K. JONES, *Phys. Lett.* **18** (1965) 91.
153. J. F. SMITH and C. L. ARBOGAST, *J. appl. Phys.* **31** (1960) 99.
154. C. W. GARLAND and J. SILVERMAN, *Phys. Rev.* **127** (1962) 2287.
155. E. S. FISHER and C. J. RENKEN, *Phys. Rev.* **135A** (1964) 482.
156. A. R. WAZZAN and L. B. ROBINSON, *Phys. Rev.* **155** (1967) 586.
157. G. A. ALERS and J. R. NEIGHBOURS, *Physics Chem. Solids* **7** (1958) 58.
158. D. M. BARNETT and J. LOTHE, *Phys. Status Solidi (b)* **67** (1974) 105.
159. A. SEEGER, *Handb. Phys.* **7/1** (1955) 383.
160. J. R. WILLIS, *Int. J. Engng Sci.* **5** (1968) 171.
161. J. R. WILLIS, *J. Mech. Phys. Solids* **14** (1966) 163.
162. D. J. BACON, D. M. BARNETT and R. O. SCATTERGOOD, *Phil. Mag.* (in the press).
163. D. J. BACON, *Phil. Mag.* **38** (1978) 333.
164. Y. T. CHOU and J. D. ESHELBY, *J. Mech. Phys. Solids* **12** (1964) 68.
165. E. KRÖNER, *Z. Phys.* **136** (1953) 402.
166. N. ZEILON, *Ark. Math.* **6** (1911) 23.
167. T. MURA and N. KINOSHITA, *Phys. Status Solidi (b)* **47** (1971) 607.
168. A. SEEGER, E. MANN and R. V. JAN, *J. Physics Chem. Solids* **23** (1962) 639.
169. G. SCHOTTKY, A. SEEGER and G. SCHMID, *Phys. Status Solidi* **4** (1964) 439.
170. H. E. SCHÄFER and H. KRONMÜLLER, *Phys. Status Solidi (b)* **67** (1975) 63.
171. R. K. LEUTZ, doctoral thesis, Universität Stuttgart (1978).
172. R. K. LEUTZ and R. BAUER, *Computer Physics Comm.* **11** (1976) 339.
173. W. VOIGT, *Lehrbuch der Kristalphysik* (1910) Teubner, Leipzig.
174. J. D. ESHELBY, *Phil. Mag.* **40** (1949) 903.
175. P. CHADWICK and G. D. SMITH, *Adv. Appl. Mechanics* **17** (1977) 303.
176. A. J. MORTON and A. K. HEAD, *Phys. Status Solidi* **37** (1970) 317.
177. R. C. CRAWFORD, I. L. F. RAY and D. J. H. COCKAYNE, *Phil. Mag.* **27** (1973) 1.
178. R. BULLOUGH and B. A. BILBY, *Proc. Phys. Soc. (Lond.)* **B67** (1954) 615.
179. A. W. SÁENZ, *J. Rat. Mech. Analysis* **2** (1953) 83.